

Generation Of Diverse Molecular Complexity From Cyclooctatetraene

Mohamed Fawzy El Mansy
Marquette University

Recommended Citation

El Mansy, Mohamed Fawzy, "Generation Of Diverse Molecular Complexity From Cyclooctatetraene" (2014). *Dissertations (2009 -)*. Paper 343.
http://epublications.marquette.edu/dissertations_mu/343

GENERATION OF DIVERSE MOLECULAR COMPLEXITY
FROM CYCLOOCTATETRAENE

By

Mohamed F. El Mansy, B.Sc., M.Sc.

A Dissertation submitted to the Faculty of the Graduate School,
Marquette University,
in Partial Fulfillment of the Requirements for
the Degree of Doctor of Philosophy

Milwaukee, Wisconsin

May 2014

ABSTRACT
GENERATION OF DIVERSE MOLECULAR COMPLEXITY
FROM CYCLOOCTATETRAENE

Mohamed F. El Mansy, B.Sc, M.Sc.

Marquette University, 2014

The use of simple hydrocarbons as starting materials for the synthesis of complex molecules relies on efficient methods for oxidation, functionalization or rearrangement. For example, various researchers have explored cyclopentadiene or cycloheptatriene as precursors for the preparation of a wide variety of drug candidates, natural products and synthetic products. The purpose of this research is to explore methods to transform the simple hydrocarbon, cyclooctatetraene (COT) into complex target molecules.

Tricarbonyl (cyclooctatetraene)iron, readily prepared from COT, reacts with a variety of electrophiles to form (dienyl)iron cations. These steps may be regarded as branching pathways in diversity oriented synthesis. Reaction of these cations with a variety of nucleophiles, followed by oxidative decomplexation gave the corresponding racemic polyenes. Further manipulation of the generated polyenes can be effected by cycloaddition, oxidation, oxidative cleavage, rearrangement or reduction.

Utilizing these reactions, a variety of stereochemically diverse polyhydroxy aminocycloalkanes (“aminocyclitols”) have been prepared. The inhibitory activity of these aminocyclitols against β -glucosidase (from almonds) was reported. Conversely, ring-rearrangement metathesis of the polyenes containing a pendant olefin tether leads to a variety of carbocycles and heterocycles by what can be considered folding pathways in diversity oriented synthesis. This strategy has lead to a number of biologically active or natural product-line structures from the simple hydrocarbon cyclooctatetraene in a short number of steps.

ACKNOWLEDGEMENTS

Mohamed F. El Mansy, B.Sc, M.Sc.

I would like to express my gratitude to Allah (God) for his guidance and his blessings that have been showered on me not only in my Ph.D. study but in my entire life.

I would like to extend my heartfelt gratitude to Professor William A. Donaldson who helped in every step of the way and for his superb supervision, guidance, constructive comments and encouragement. I was very fortunate to learn from him how to conduct a high quality research and how to analyze the research problems. He stimulated me to work hard and he gave me a great degree of freedom to approach the obstacles in my research to develop some sort of being independent. Not only Dr. Donaldson is a great teacher and a real king in his research field, he treated me in a very friendly way, we shared personal experiences. Professor Donaldson influenced me a lot not only academic wise, but also personality wise.

I would also like to thank my Professor Daniel S. Sem for being my first supervisor and for introducing me to the biology world. Dr. Sem and his student Kelsey were so nice and very helpful during testing my compounds against commercial glycosidase.

I would also like to thank my committee member, Professor Chae S. Yi for his comments and suggestions during personal interactions. Moreover, I enjoyed taking organometallic course with him and I learnt many things in catalysis research area.

Furthermore, I would like to express my appreciation to Professor Christopher Dockendorff for his valuable support, constructive ideas based on his rich research experience. I also benefited significantly from the involvement and cooperation in his group meetings where we used to discuss the different research problems and draw the reaction mechanisms on the board.

I am extremely appreciative of the financial assistance and the research assistantship given by Marquette University which provided me with more time to focus on my research.

Sincere thanks go to Vaughn Ausman and Linda Davis for their unreserved support and sincere advices. My gratefulness to the countless technical support from Dr. Sergey Lindeman for providing single crystal diffraction analysis data and Dr. Sheng Cai for his support and his help running special NMR studies. I am also grateful to all the faculty and staff members in Chemistry Department and my current and previous lab colleagues for their support and friendship. Also, I would like to thank the Graduate School and all of the Marquette University administration.

Finally, my deepest gratitude and appreciation goes to my beloved parents for their endless love, prayers and encouragement. I would like to thank my wife and my Yasmina for supporting me, taking the responsibility of raising our sons Youssef and Omar and for giving me the wings to fly and to pursue my dreams. Also not forgetting my twin sister Enas and my younger brother Ahmed for their support and encouragement.

DEDICATION

I dedicate this work to my parents, wife and sons for their patience and support.

Thank you for your understanding and your love.

TABLE OF CONTENTS

ABSTRACT.....	i
ACKNOWLEDGMENTS.....	ii
DEDICATION.....	iv
LIST OF TABLES.....	vii
LIST OF SCHEMES.....	viii
LIST OF FIGURES.....	xi
LIST OF EQUATIONS.....	xiii
I-INTRODUCTION..	1
General introduction.....	1
The development of DOS approach	2
Aminocyclicpolyols	6
Medicinal chemistry of aminocyclitols.....	9
Implementation of organoiron approach in DOS.....	15
Exploring the expanded homologs of aminocyclitols.....	19
Eight-membered ring aminocyclitols.....	25
Bicycliccyclitols.....	28
Cyclooctatetraene as a simple starting material.....	31
II-RESULTS & DISCUSSION.....	41
Generation of molecular complexity using dienyliron approach	41
Synthesis of racemic and optically active aminocycloheptitols.....	49
Preparation of bicyclo[5.1.0]octane derivatives of cyclitols.....	58

Evaluation of potential β -glycosidase inhibitors.....	84
III- SUMMARY.....	91
IV- CONCLUSIONS AND RECOMMENDATIONS.....	98
V- EXPERIMENTAL	101
VI- REFERENCES.....	157
VII- APPENDIX.....	166

LIST OF TABLES

Table II-1.....	87
-----------------	----

LIST OF SCHEMES

SCHEME I-1.....	3
SCHEME I-2.....	4
SCHEME I-3.....	4
SCHEME I-4.....	6
SCHEME I-5.....	7
SCHEME I-6.....	16
SCHEME I-7.....	17
SCHEME I-8.....	18
SCHEME I-9.....	19
SCHEME I-10.....	21
SCHEME I-11.....	22
SCHEME I-12.....	23
SCHEME I-13.....	25
SCHEME I-14.....	26
SCHEME I-15.....	26
SCHEME I-16.....	28
SCHEME I-17.....	29
SCHEME I-18.....	31
SCHEME I-19.....	33
SCHEME I-20.....	34
SCHEME I-21.....	35

SCHEME I-22.....	36
SCHEME I-23.....	37
SCHEME I-24.....	38
SCHEME I-25.....	39
SCHEME I-26.....	39
SCHEME I-27.....	40
SCHEME II-1.....	41
SCHEME II-2.....	43
SCHEME II-3.....	44
SCHEME II-4.....	46
SCHEME II-5.....	47
SCHEME II-6.....	48
SCHEME II-7.....	50
SCHEME II-8.....	52
SCHEME II-9.....	54
SCHEME II-10.....	55
SCHEME II-11.....	56
SCHEME II-12.....	64
SCHEME II-13.....	66
SCHEME II-14.....	67
SCHEME II-15.....	73
SCHEME II-16.....	74
SCHEME II-17.....	79

SCHEME II-18.....	83
SCHEME II-19.....	89
SCHEME III-1.....	91
SCHEME III-2.....	93
SCHEME III-3.....	94
SCHEME III-4.....	95
SCHEME III-5.....	96
SCHEME III-6.....	97
SCHEME IV-1.....	99

LIST OF FIGURES

FIGURE I-1.....	5
FIGURE I-2.....	7
FIGURE I-3.....	8
FIGURE I-4.....	10
FIGURE I-5.....	11
FIGURE I-6.....	12
FIGURE I-7.....	13
FIGURE I-8.....	14
FIGURE I-9.....	15
FIGURE I-10.....	20
FIGURE I-11.....	32
FIGURE II-1.....	53
FIGURE II-2.....	57
FIGURE II-3.....	59
FIGURE II-4.....	60
FIGURE II-5.....	61
FIGURE II-6.....	62
FIGURE II-7.....	64
FIGURE II-8.....	66
FIGURE II-9.....	68
FIGURE II-10.....	69

FIGURE II-11.....	70
FIGURE II-12.....	71
FIGURE II-13.....	72
FIGURE II-14.....	75
FIGURE II-15.....	77
FIGURE II-16.....	78
FIGURE II-17.....	79
FIGURE II-18.....	80
FIGURE II-19.....	81
FIGURE II-20.....	82
FIGURE II-21.....	85
FIGURE II-22.....	86
FIGURE II-23.....	90

LIST OF EQUATIONS

EQUATION II-1.....	42
EQUATION II-2.....	49
EQUATION II-3.....	51
EQUATION II-4.....	58
EQUATION II-5.....	59
EQUATION II-6.....	61
EQUATION II-7.....	62
EQUATION II-8.....	63
EQUATION II-9.....	65
EQUATION II-10.....	69
EQUATION II-11.....	70
EQUATION II-12.....	74
EQUATION II-13.....	75
EQUATION II-14.....	76
EQUATION II-15.....	76
EQUATION II-16.....	77
EQUATION II-17.....	78
EQUATION II-18.....	80
EQUATION II-19.....	81
EQUATION II-20.....	84

I- INTRODUCTION

I.1. General Introduction:

The ability of small molecules to interact with biological systems and perturb their function has emerged as a powerful tool for the study of complex biological systems.^{1,2} Small molecules that modulate crucial cell signaling pathways have been identified via the screening of large libraries of diverse small molecules.^{3,4} Traditionally, high-throughput screening (HTS) of large libraries of compounds has been employed to identify chemical probes of biological function and as a consequence, lead compounds for drug development.⁵ HTS can be used in a “chemical genetic” approach with phenotypic assays to identify compounds which promote a particular biological effect.⁶

Although current small molecule libraries can lead to identification of effective modulators of certain targets, the focus has primarily been on a relatively narrow region of chemical structure space, the so-called ‘drug-like’ compounds.⁷ To address the important need for modulation of so-called “undruggable” targets, diversity-oriented synthesis (DOS) has emerged as a promising approach to generating libraries that explore untapped or underrepresented regions of chemical structure space.⁸

In contrast to target-oriented synthesis, which aims to prepare a specific target compound, the goal of DOS is the facile preparation of collections of structurally complex and diverse compounds from simple starting materials.⁹

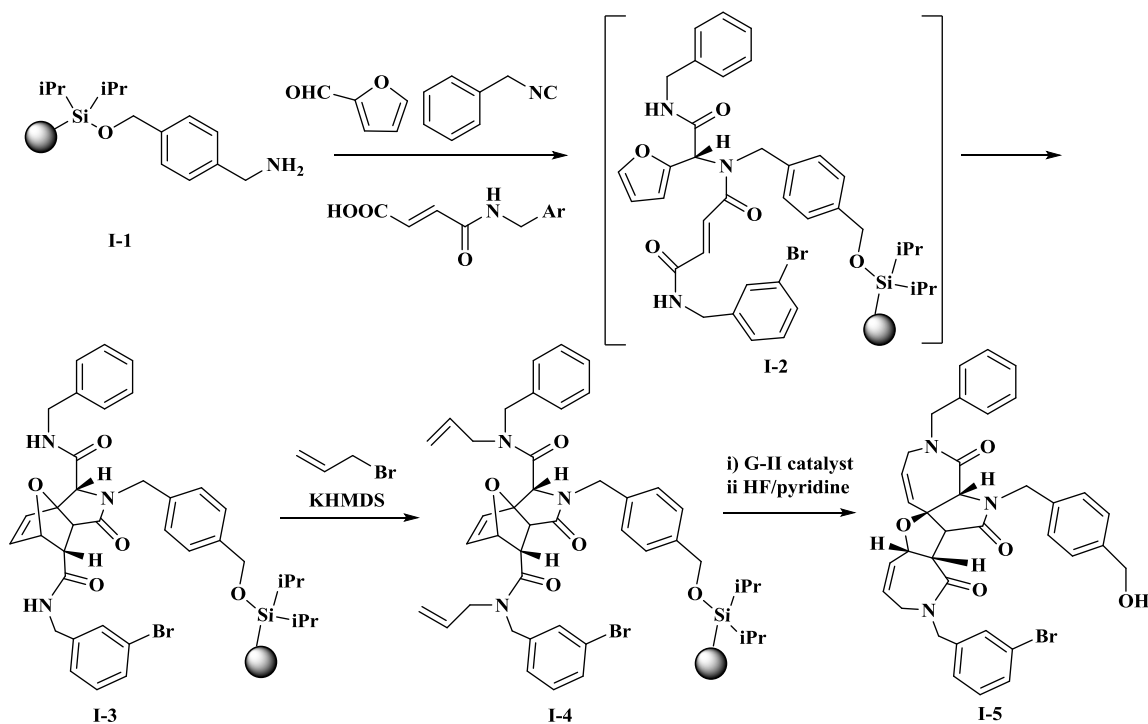
Structural diversity can be achieved via different ways; incorporation of diverse building blocks,¹⁰ incorporation of a variety of functional groups,¹¹ synthesis of

stereoisomeric products¹² and branching reaction pathways that result in structures with widely varying connectivity.¹³

I.2. The development of DOS approach

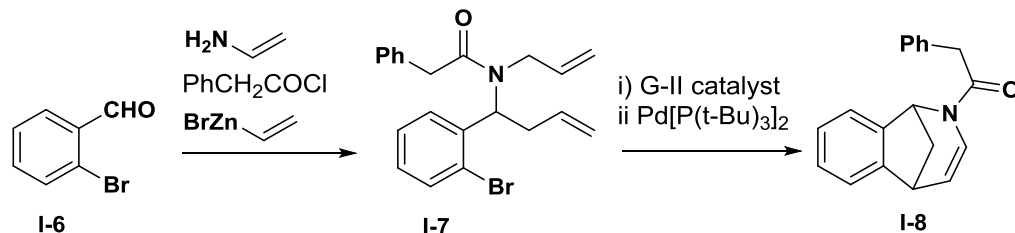
The early examples of DOS chemistry were mainly focused on showing the ability to synthesize complex molecules within few synthetic steps. This Structural complexity can be efficiently generated in diversity-oriented synthesis through the use of tandem reactions, processes involving reactions in which the product is a substrate for the next step.^{14,15}

A classic example of generating complex molecules was reported by Schreiber and coworkers¹⁶ where they used tandem reactions in an iterative manner is an especially powerful concept that enabled the efficient conversion of simple starting materials into complex products. For example, The Ugi four component condensation^{17,18} of the amine **I-1** to give intermediate **I-2** followed by intramolecular Diels Alder reaction¹⁹ generates complexity by formation of a alkene within a five-membered ring **I-3**. After addition of two allyl groups to provide **I-4**, Schreiber and coworkers introduced additional complexity through a subsequent ring-opening/ring closing metathesis reaction, thus forming a complex product **I-5** containing two five membered and two seven-membered rings (Scheme-I-1).¹⁶



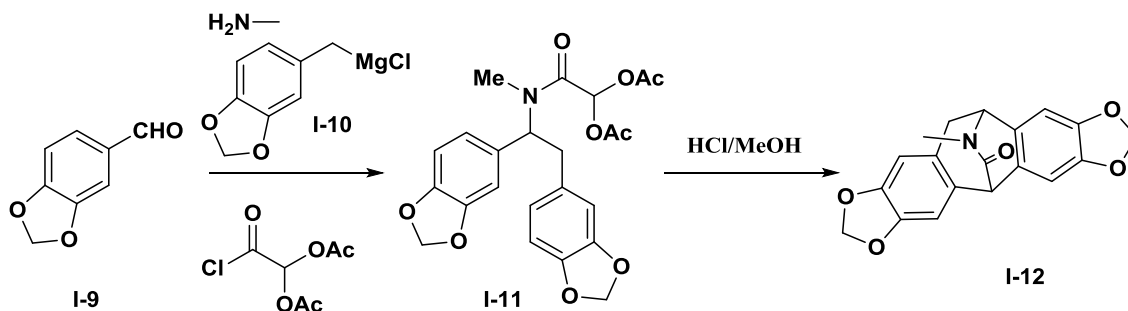
Scheme I-1. Tandem Ugi-Diels-Alder-Ring Opening/Closing Metathesis.

More recent DOS approach is directed to rapidly make complex molecules that have useful biological applications or share the structural features with other natural products.^{20,21} In an attempt to use DOS chemistry to make natural product like compounds, Martin and coworkers reported the synthesis of diverse heterocyclic cyclic scaffolds via sequential reactions.²² A one-pot multicomponent reaction of *o*-bromobenzaldehyde **I-6** with allylamine followed by attack of allylzinc nucleophile gave allylamine derivative **I-7** (Scheme I-2). Ring closing metathesis of **I-7** followed by Heck cyclization reaction gave the corresponding bridged azabicyclic structure **I-8** which has a framework similar to that in naturally occurring methylated morphine (also known as codeine) which has analgesic, antitussive, antidiarrheal, antihypertensive, anxiolytic, antidepressant, sedative and hypnotic properties.²³



Scheme I-2. Sequential ring closing metathesis/Heck cyclization.

The same research group presented the synthesis of compounds containing isopavine skeleton which has interesting biological activities.²⁴ Condensation reaction of methyl amine with piperonal **I-9** followed by reaction with Grignard reagent **I-10** then diacetoxyacetyl chloride gave amide **I-11** which upon treatment with HCl and methanol afforded roelactamine **I-12** in a good yield (Scheme I-3).²²



Scheme I-3. Preparation of isopavine containing structure.

A high-throughput screening campaign of about 12,000 diverse chemical compounds containing pure natural products and DOS libraries was conducted to search for antimalarial agents with potential new mechanisms using a phenotypic growth inhibition assay against the blood-stage parasite of malaria.²⁵⁻²⁷ This search led to the identification of the lead racemic spiroazepineindole^{28,29} **I-13** with moderate potency in

both wild type (NF54) and chloroquine resistant (K1) of IC₅₀ in nanomolar scale (Figure I-1).

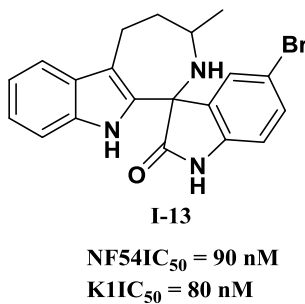
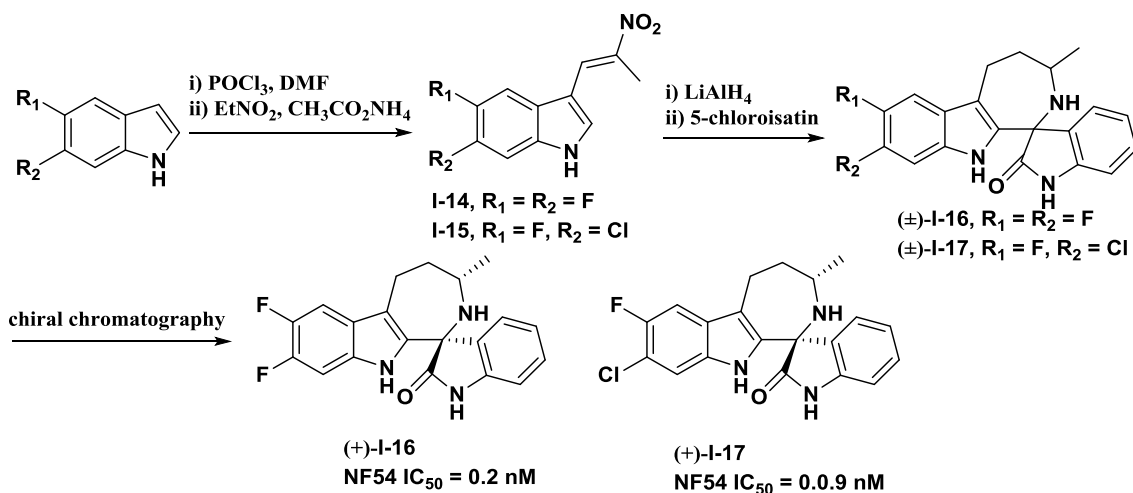


Figure I-1. Discovery of spiroazepineindole **I-13**.

This discovery of **I-13** initiated structure activity relationship studies to optimize its potency and in vivo activity. Yeung and coworkers³⁰ reported the synthesis of new derivatives which are more potent than **I-13**. Vilsmeier–Haack formylation³¹ of the indole followed by condensation with nitroethane gave the corresponding nitroalkenes **I-14** and **I-15** (Scheme I-4). Reduction **I-14** followed by condensation with 5-chloroisatin provided racemic **I-16** and **I-17**. The 1*R*,3*S* and 1*S*,3*R* enantiomers were then resolved by chiral chromatography to give (+)-**I-16** and (+)-**I-17**.



Scheme I-4. Preparation of isopavine containing structure.

I.3. Aminocyclicpolyols

Polyhydroxyl aminocyclic compounds are important synthetic targets and attractive candidates for diversity-oriented synthesis. Polyhydroxyl aminocyclohexanes, best known as “aminocyclitols” are reported to be glycosidase inhibitors and they are also present as aglycon units of numerous aminoglycoside antibiotics, e.g., streptomycin and fortimycin, which possess inhibitory activity against various glycosidases.¹⁰

The glycosidic bond, shown in (Figure I-2), is the exocyclic ether linkage between two sugar units. This bond is known to be very stable towards hydrolysis; in particular, the linkage between two sugar residues is known to be the most stable within naturally occurring biopolymers which include polypeptides and nucleic acids.

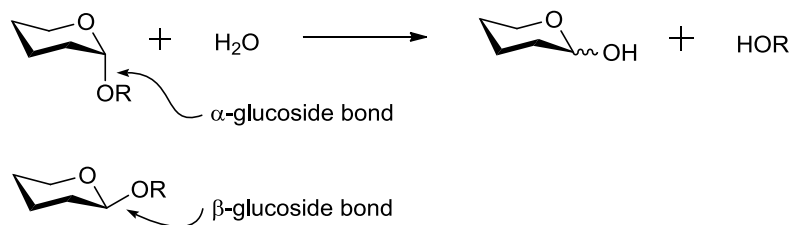
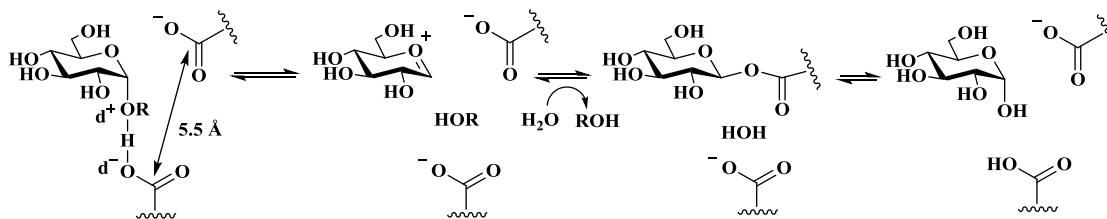


Figure I-2. Glycosidic bond between two sugar residues.

Enzymes that cleave glycosidic bonds are called "glycoside hydrolases" or "glycosidases". The mechanisms of the glycosidic bond hydrolysis have been extensively studied.³²⁻³⁴ Hydrolysis can be achieved with retention of configuration at the anomeric carbon as shown in scheme I-5, where the enzyme active site involves two carboxylic acidic residues $\sim 5.5 \text{ \AA}$ apart. The hydrolysis starts with one of the acidic residue which acts as a general acid catalyst that protonates the glycosidic oxygen followed by bond cleavage forming the oxocarbenium ion. Stabilization of the generated oxocarbenium ion is achieved by forming a covalent glycosyl-enzyme bond with the other acid residue in the enzyme active site. Eventually in the presence of a water molecule attack takes place at the anomeric center facilitated by the carboxylate general base.³⁴



Scheme I-5. Mechanism of the hydrolysis of glycosidic bond with retention of configuration at anomeric carbon.

Researchers extensively studied the transition-state of glycosidase inhibitors and proposed different intermediate compounds that mimic both *exo* and *endo* positively charged oxygen intermediate in the enzyme active sites.^{34,35} To mimic the positive charge that developed during this mechanism, many researchers showed cyclitols containing amine group at $\text{pH} < 5$ will be protonated and form the analogue of the positively charged oxygen in the enzyme active site.³⁶

Alternatively, other glycosidases proceed via a different mechanism with inversion at the anomeric center as illustrated in figure I-3. In this mechanism the hydrolysis starts with enhancing the nucleophilicity of water molecule by an enzymic general base. The hydroxyl anion attacks the anomeric center leading to departure of the aglycon and is assisted by a general-acid catalytic group on the enzyme active site.³⁷

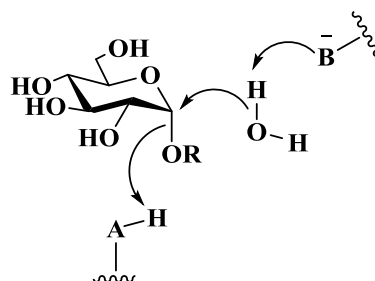


Figure I-3. Mechanism of the hydrolysis of glycosidic bond with inversion of configuration at the anomeric carbon.

Due to the importance of aminocyclitols, several attempts to synthesize them and their derivatives have been reported. For example synthesis of quercitols (deoxyinositols)^{38,39} from inositols where they start from a single optically active cyclitol and selectively converting it by deoxygenation⁴⁰ to amine functionality to give two

diastereomeric aminocyclitols. Also carbohydrates have been used to synthesize aminocyclitols using Ferrier carbocyclic ring-closure,^{41,42} from oximes through 6-exo radical cyclization of carbohydrates,⁴³ and from chiral 1,7-octadienes via ring closing metathesis have been reported.^{44,45}

I.4. Medicinal chemistry of aminocyclitols

Aminocyclitols show a variety of biological effects including antibiotic, antiviral, anticancer activities.⁴⁶ The aminoglycoside antibiotics are a family of natural products in which diaminocyclitols are connected to different sugar units.⁴⁷ The 1,3-diaminocyclitols are the most common scaffold in this class of compounds which possess antibacterial activity. It was found that most of the 1,3-diaminocyclitols contain 2-deoxystreptamine as part of their structures.⁴⁸ Neomycin,⁴⁹ kanamycin,⁵⁰ gentamicin,⁵¹ tobramycin,⁵² sisomicin,⁵³ verdamicine⁵⁴ and lividomycin⁵⁵ are representative examples of 2-deoxystreptamine-containing aminoglycosides (Figure I-4).

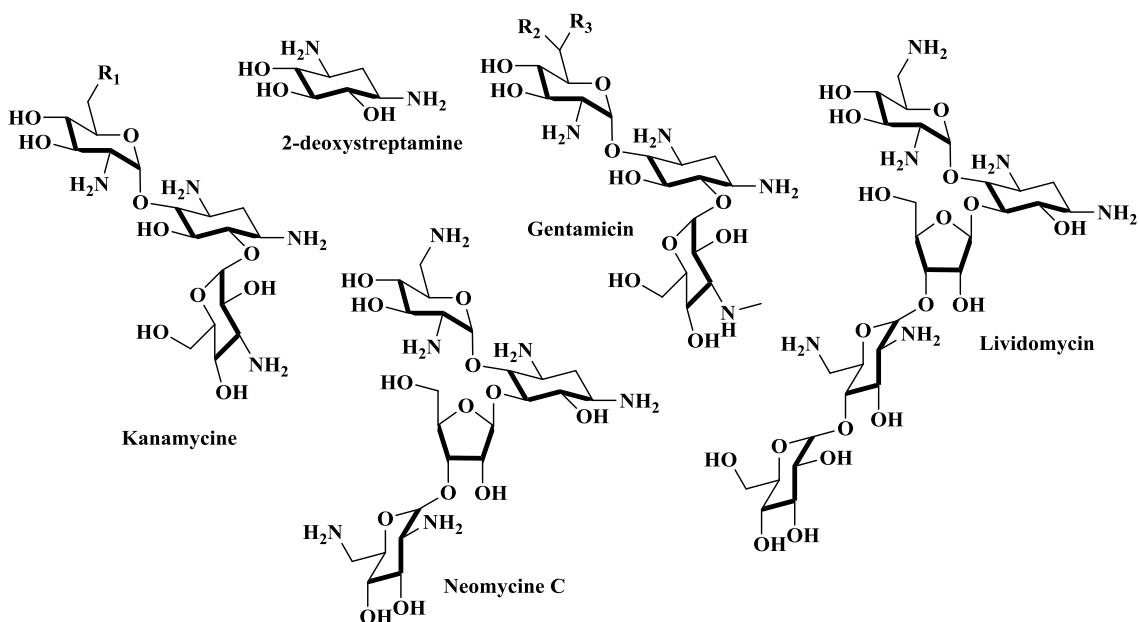


Figure I-4. Representative structures of 2-deoxystreptamine-containing aminoglycosides.

While 1,3-diaminocyclitols show activity against both gram positive and gram negative bacteria, 1,2-diaminocyclitols also show interesting biological activity. 1,2-The diaminocyclohexitol oseltamivir, (Tamiflu®) which is a very potent inhibitor of influenza neuraminidase.⁵⁶ Llebaria's research group discovered the new 1,2-diaminocyclitol **I-18**, a β -glucocerebrosidase inhibitor and with potential therapeutic applications for Gaucher disease (Figure I-5).⁵⁷

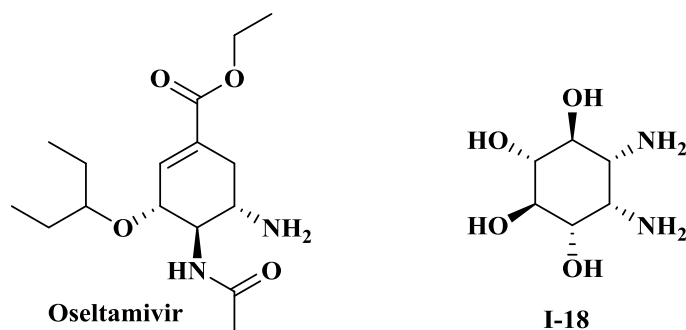


Figure I-5. Representative structures of 1,2-diaminocyclohexitols.

Aminocyclohexitols have been extensively studied as glycohydrolase inhibitors, due to the ability of aminocyclohexitols to mimic the protonation of the exocyclic oxygen intermediate in glycosidic bond hydrolysis.³⁴

Similar to 2-deoxystreptamine (Figure I-4) a building unit for 1,3-diaminocyclitols, valienamine (Figure I-6), was first isolated from the microbial degradation of validoxylamine A with *Pseudomonas denitrificans*,^{58,59} is an essential component in many glycosidase inhibitors.⁶⁰ Valiolamine and validamine, which were isolated from the fermentation broth of *Streptomyces hygroscopicus subsp*, inhibit α -glucosidases and combat bacterial diseases in rice plants.⁶¹ Hydroxyvalidamine⁶² also exhibits glycosidase inhibition activity while validamycin A is used to treat sheath blight disease in rice.^{63,64} Acarbose, which was discovered in a target-directed screening from the culture broth of *Actinoplanes spec*,⁶⁵ is currently used for the treatment of type II insulin-independent diabetes.⁶⁶

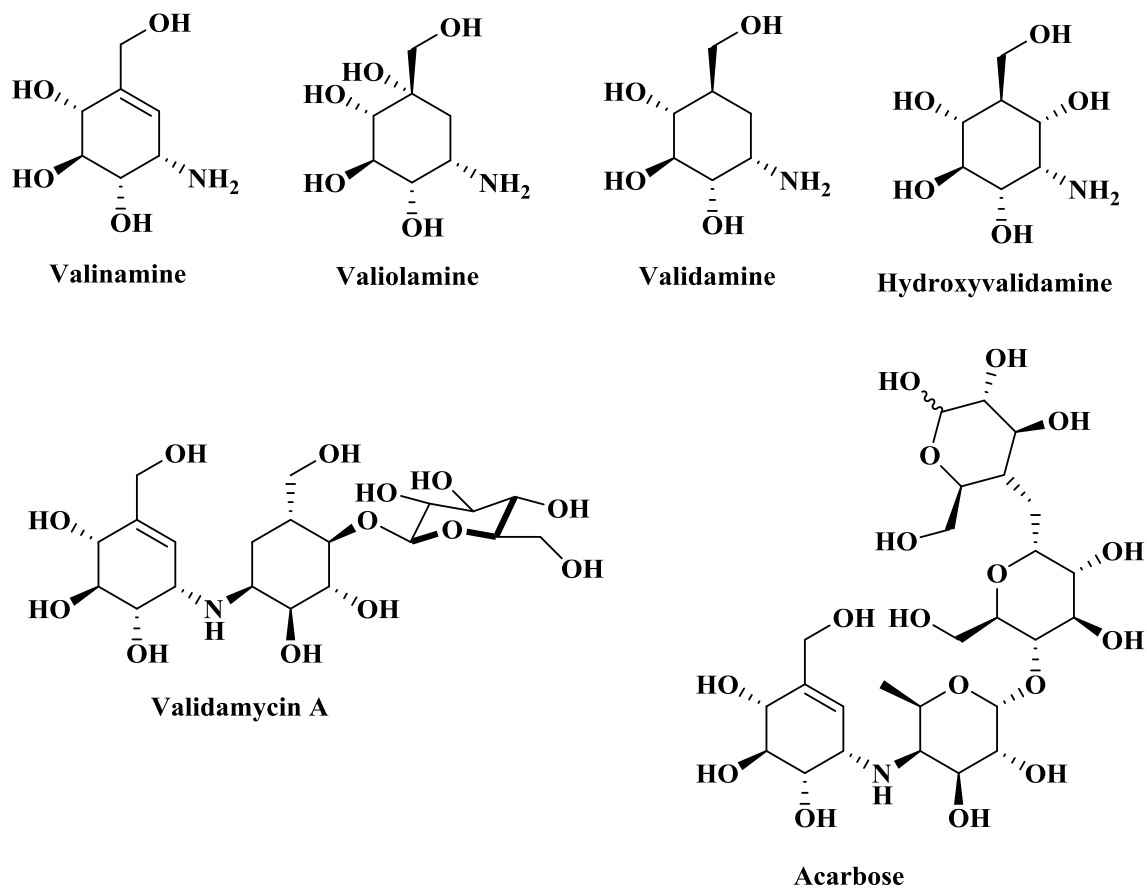


Figure I-6. Representative examples of valienamine based structures.

Ogawa and coworkers synthesized dimeric compounds derived from validamine, validamine or valioline (Figure I-7), which exhibit trehalase inhibitory activity.⁶⁷⁻⁶⁹

The same group also reported the synthesis of new α -glucosidase inhibitors **I-19** in which valinamine is linked to a sugar moiety containing a 1,6-anhydrobridge.⁷⁰

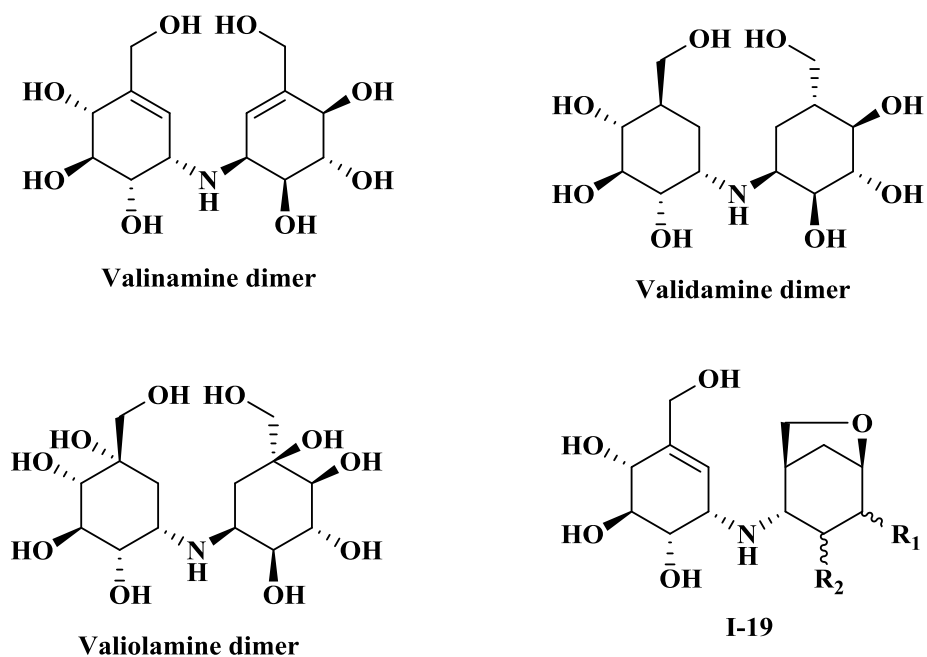


Figure I-7. Trehalase inhibitors incorporating dimeric aminocyclohexitols and α -glucosidase inhibitors.

Due to the potent inhibition that was observed for valioamine against sucrase ($IC_{50} = 49 \text{ nM}$),⁶¹ several medicinal chemistry studies were carried out that led to voglibose, a therapeutically useful antidiabetic agent (Figure I-8).⁷¹ Structurally related compounds were synthesized but they showed less potency towards glycosidase inhibition.⁷²

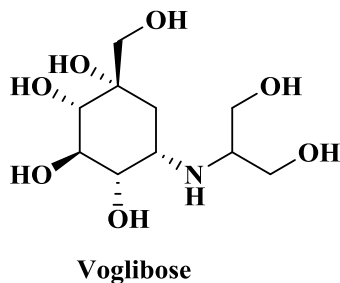


Figure I-8. Volibose, antidiabetic agent.

Synthesis of β -valienamine and β -validamine also led to the discovery of a new series of glycosidases inhibitors. For example, compound **I-20** showed to be potent and selective GlcCer β -glucosidase inhibitors for both *E* and *Z* isomers with IC_{50} values 0.3 μ M and 0.1 μ M respectively.⁷³ Modification of *N*-substituent in β -valienamine to *N*-octyl to give *N*-octyl- β -valienamine (NOV) which turned out to be the most potent inhibitor of GlcCer β -glucosidase with $IC_{50} = 0.03 \mu$ M⁷⁴ and also as pharmacological chaperone for Gaucher disease.⁷⁵ Further studies on NOV led to discovery of *N*-octyl-4-epi- β -valienamine (NOEV) which was found to be potent inhibitor for lysosomal β -galactosidase and potential pharmacological chaperone Morquio B disease (Figure I-9).⁷⁶

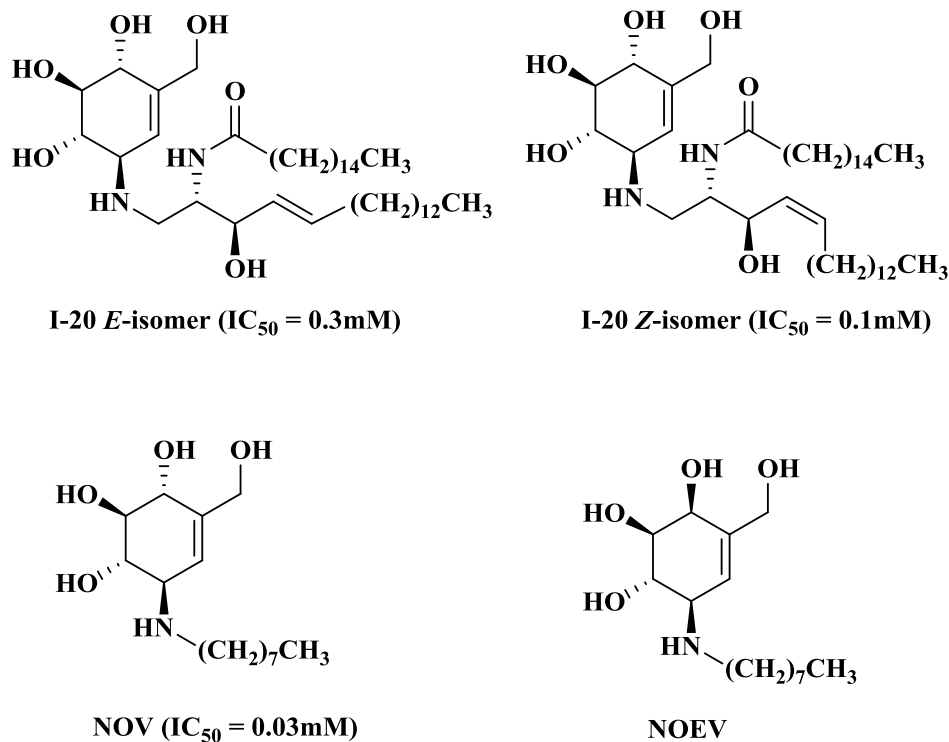
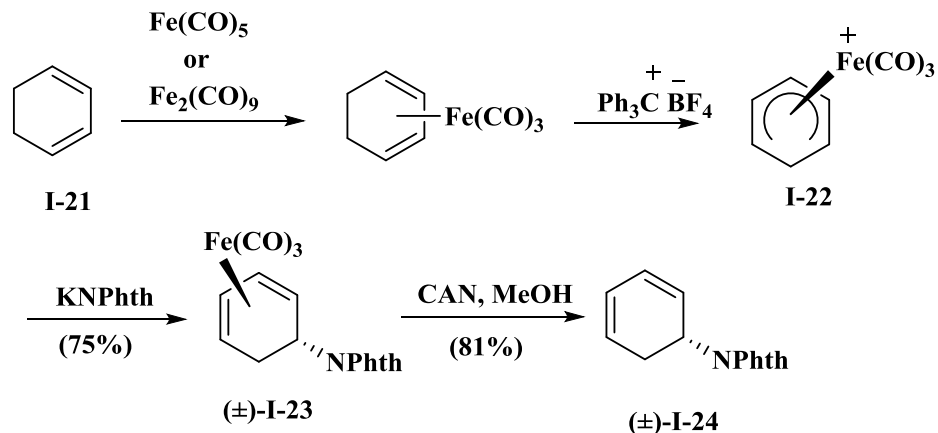


Figure I-9. Examples of GlcCer β -glucosidase and lysosomal β -galactosidase inhibitors.

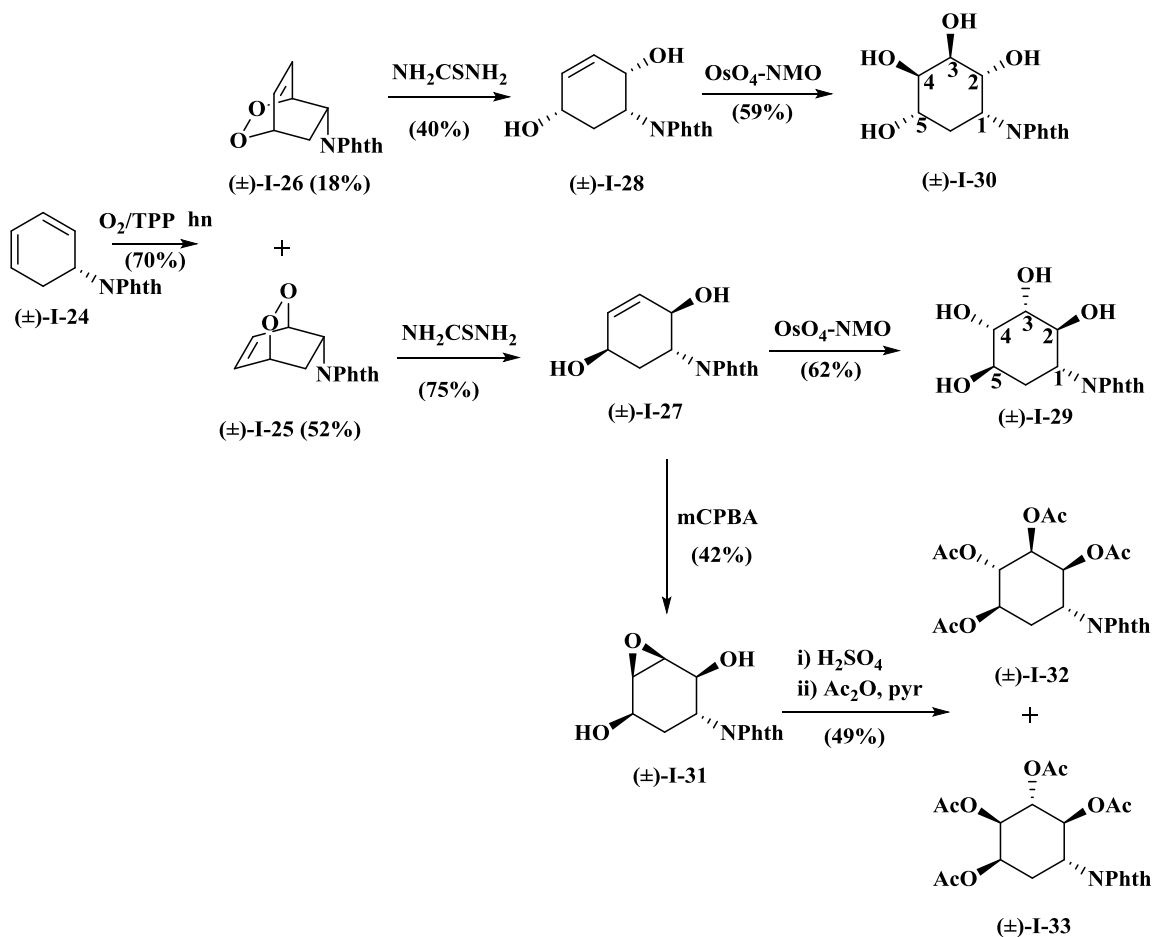
I.5. Implementation of an organoiron approach to DOS

Recently, Donaldson's group was the first to report the synthesis of a family of diverse stereoisomeric aminocyclitols using an organoiron approach.⁷⁷ $[(\eta^5\text{-Cyclohexadienyl)Fe(CO)}_3]^+$ cation **I-22** was easily prepared from 1,3-cyclohexadiene **I-21**⁷⁸⁻⁸⁰ followed by nucleophilic attack of potassium phthalimide (KNPhth) at the diene terminus of the symmetric cation **I-22** to give (\pm) -**I-23**. Oxidative decomplexation of (\pm) -**I-23** using CAN/MeOH gave the free diene (\pm) -**I-24** (Scheme I-6).⁷⁷



Scheme I-6. Synthesis of (Cyclohexadienyl)phthalimide (\pm) **I-24**.

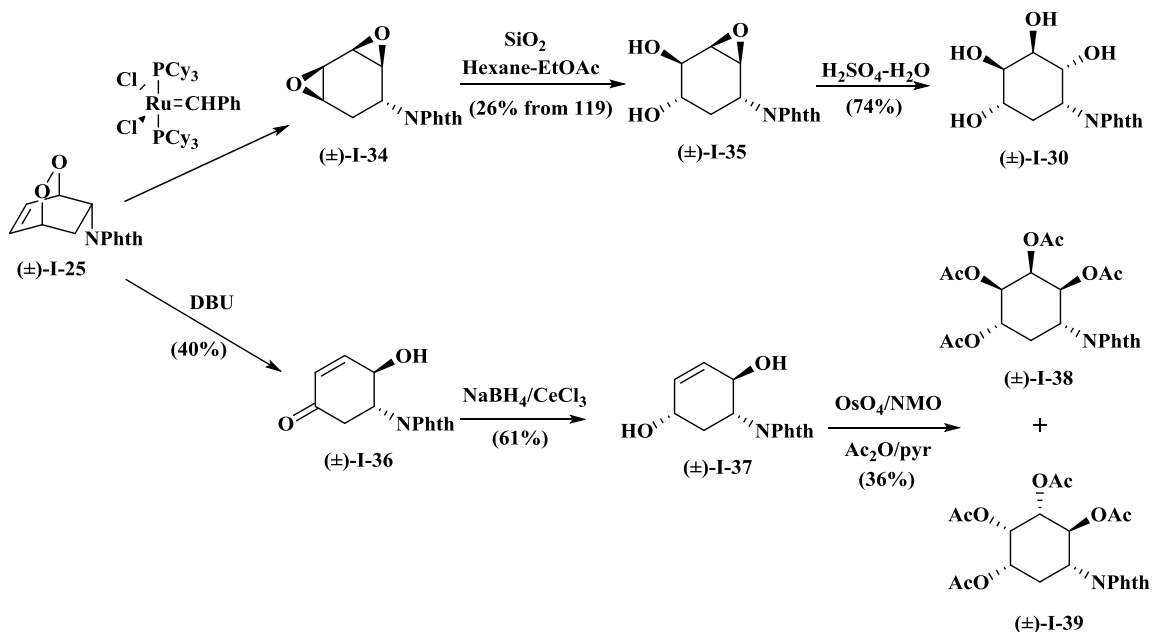
Singlet oxygen cycloaddition of (\pm)-**I-24** resulted in a separable mixture of endoperoxides (\pm)-**I-25** and (\pm) **I-26**, which upon reduction with thiourea gave (\pm)-**I-27** or (\pm)-**I-28** respectively. The OsO_4 catalyzed dihydroxylation of (\pm)-**I-28** afforded (\pm)-**I-30** while for (\pm)-**I-27** dihydroxylation gave (\pm)-**I-29**. Epoxidation of (\pm)-**I-27** using *meta*-chloroperbenzoic acid produced (\pm)-**I-31** which undergoes epoxide ring opening under acidic conditions followed by acetylation to give a mixture of diastereomeric tetraacetates (\pm)-**I-32** and (\pm)-**I-33** (Scheme I-7).⁷⁷



Scheme I-7. Synthesis of diverse stereoisomeric aminocyclitols from endoperoxide compounds.

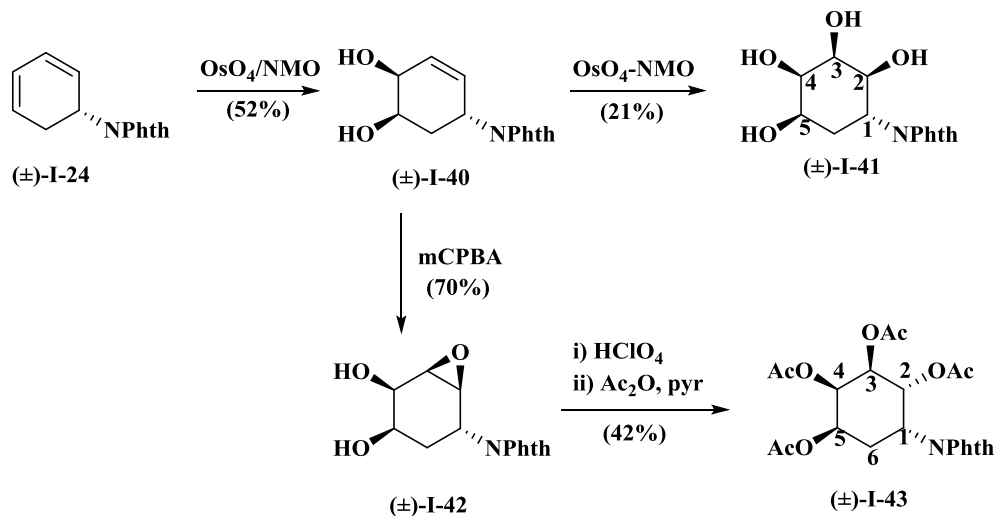
The metal-mediated rearrangement^{81–83} of endoperoxide compound (±)-I-25 using Grubbs' (II) catalyst through inner sphere radical mechanism yielded the corresponding bisepoxide compound (±)-I-34 which on hydrolysis gave (±)-I-30 (Scheme I-8). Kornblum DeLaMare rearrangement⁸⁴ of (±)-I-25 gave compound (±)-I-36 as the major product along with a mixture of two other rearrangement regioisomers in lesser yield. Reduction of (±)-I-36 under Luche conditions⁸⁵ gave (±)-I-37 followed by

osmium catalyzed dihydroxylation then acetylation where a mixture of two diastereomeric tetraacetates, (\pm)-**I-38** and (\pm)-**I-39** is obtained.⁷⁷



Scheme I-8. Utilizing rearrangement reactions to generate stereochemically diverse of aminocyclitols.

Brief dihydroxylation of (\pm)-**I-24** gave the diol (\pm)-**I-40** which was again treated with osmium tetroxide to provide (\pm)-**I-41**, while the epoxidation of (\pm)-**I-40** gave the monoepoxide derivative (\pm)-**I-42** (Scheme I-9). Notably, stereochemical outcome of this transformation follows Henbest's model⁸⁶ in which the allylic hydroxyl group directs peroxide mediated epoxidation onto the same face of the olefin. Epoxide ring opening of (\pm)-**I-42** followed by acetylation gave (\pm)-**I-43**.⁷⁷



Scheme I-9. Synthesis of aminocyclitols using dihydroxylation and epoxidation reactions.

I.6. Exploring the expanded homologs of aminocyclitols

The interesting biological activity of aminocyclitols, motivated chemists to explore the preparation of expanded aminocyclic polyols. The synthesis of the 7-membered carbocycles (**I-44**, **I-45**, **I-46**, **I-47**) shown in Figure I-10 has been reported by the groups of Casiraghi⁸⁷ and Landais.⁸⁸

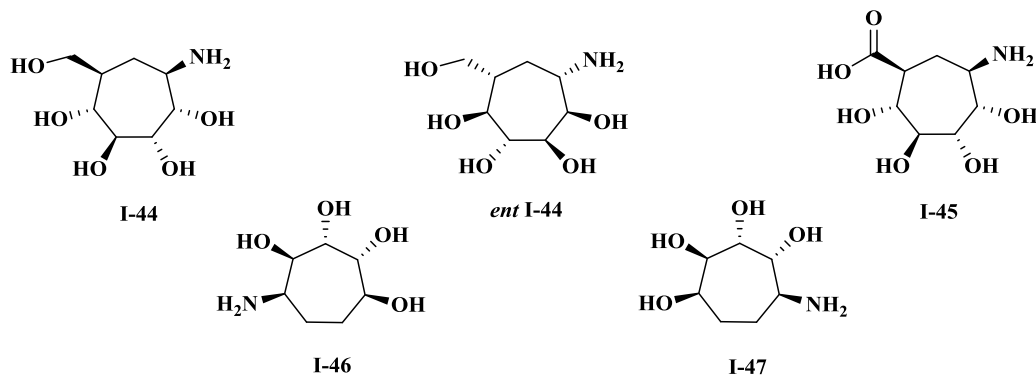
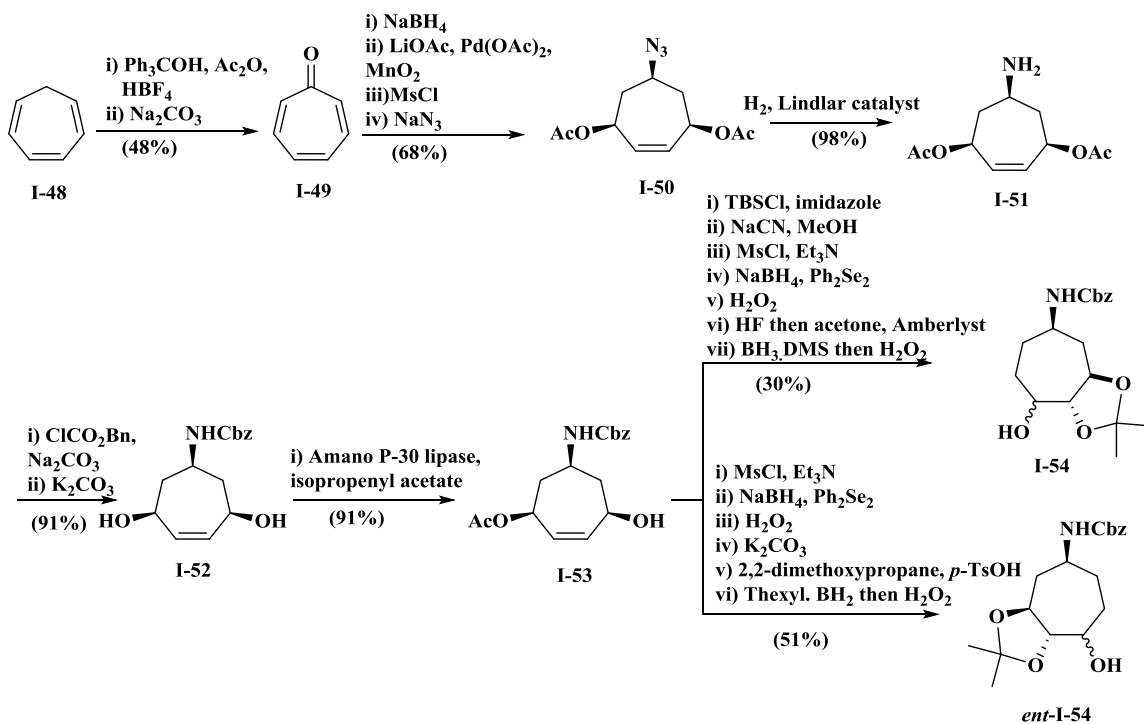


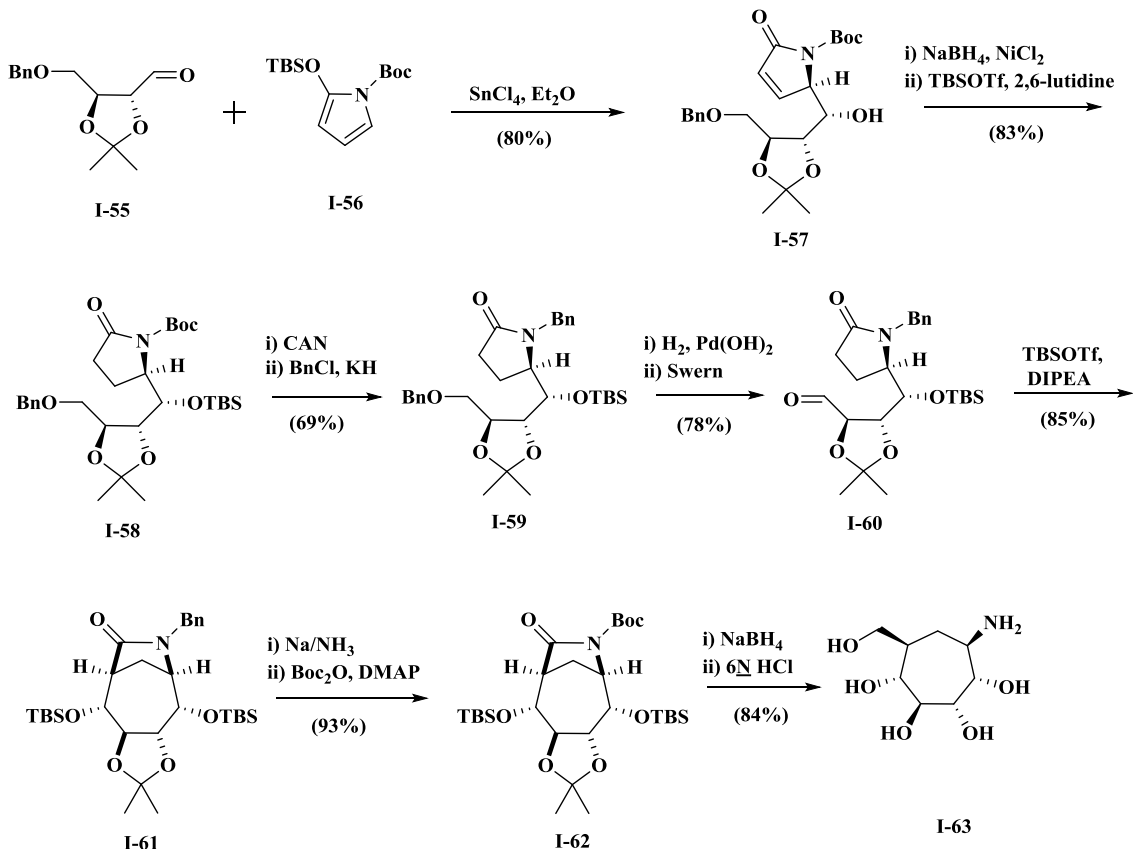
Figure I-10. Partial list of recently synthesized seven-membered carbasugars.

Johnson *et al*⁸⁹ reported the synthesis of aminoheptatriols **I-54** and *ent*-**I-54** starting from cycloheptatriene **I-48** which was oxidized to tropone **I-49** according to the literature⁹⁰ (Scheme I-10). Reduction of tropone with sodium borohydride, diacetoxylation utilizing procedure developed by Backval1,⁹¹ protection of the alcohol as mesylate followed by displacement of mesylate using NaN₃ to give azide derivative **I-50**. Chemoselective reduction by hydrogenolysis of **I-50** to unsaturated amine **I-51** using Lindelar catalyst^{92,93} then protection of the resultant amine as carbamate derivative **I-52**. Enzymatic asymmetric acetylation of **I-52** with Amano P-30 lipase in presence of isopropenyl acetate gave the corresponding monoacetate derivative **I-53** in very high enantiomeric excess (>98% ee). Conversion of **I-53** to the corresponding enantiomers of protected diols followed by hydroboration-oxidation to give the desired products **I-54** and *ent*-**I-54**.



Scheme I-10. Synthesis of aminoheptatriols from cycloheptatriene.

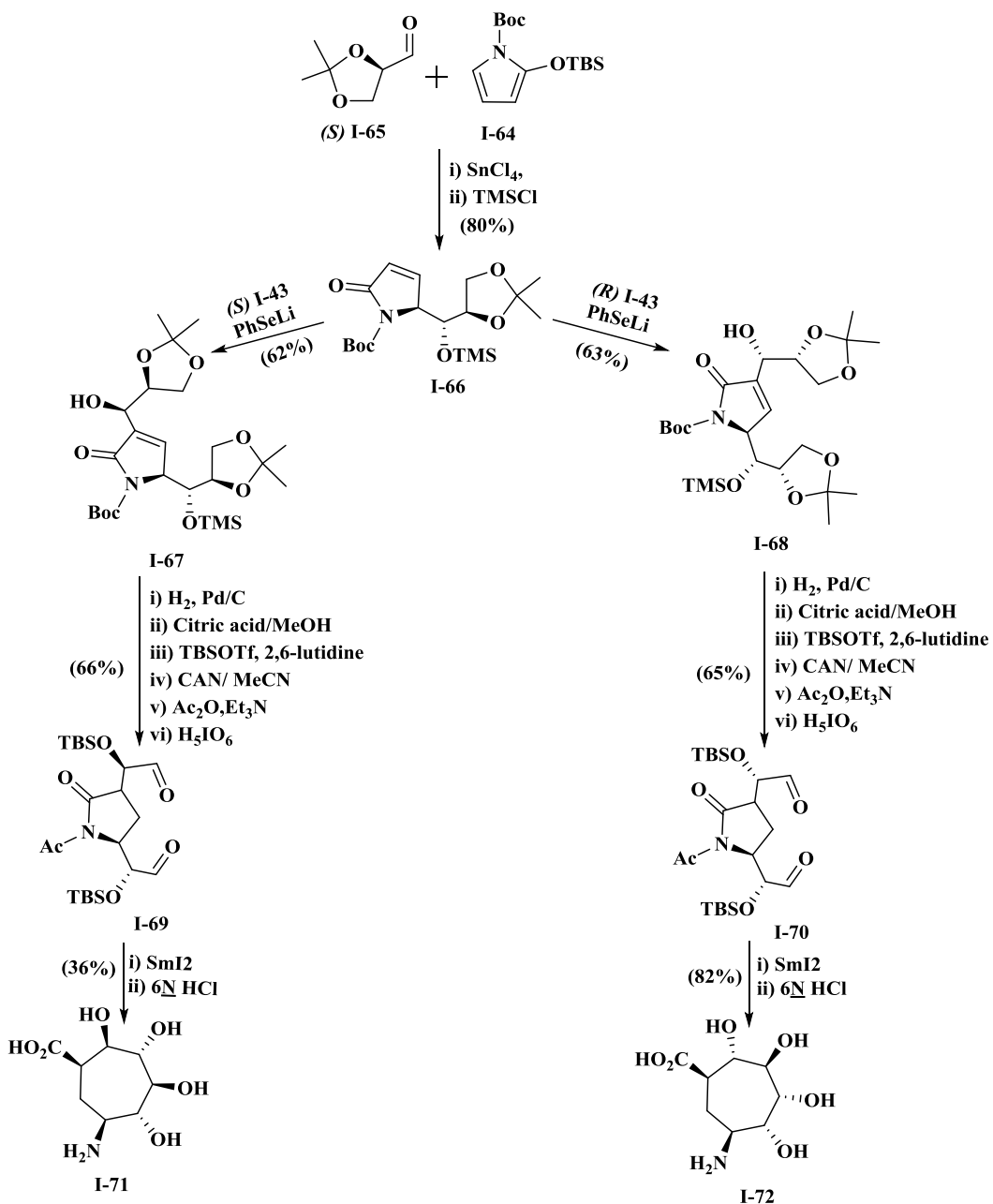
Casiraghi reported aldol-type condensation catalyzed by Lewis acid between aldehyde **I-55** (prepared from (+)-tartrate) and pyrrole derivative **I-56** afforded the unsaturated lactam **I-57** as a single diastereomer (Scheme I-11). Nickel catalysed 1,4 reduction of the α,β -unsaturated lactam followed by protection of the hydroxyl group gave **I-58**. Exchange of the *N*-protecting group then selective deprotection followed by Swern oxidation afforded the aldehyde **I-60**. Intramolecular aldol condensation of **I-60** followed by protecting the resultant hydroxyl group as a silyl ether gave compound **I-61** as a single diastereoisomer. Swapping the protection of *N*-protecting group from a benzyl to a *t*-butylcarbonate group followed by reductive cleavage of the amide bond and acid hydrolysis afforded the aminocycloheptitol **I-63**.⁹⁴



Scheme I-11. Synthesis of aminocycloheptitol **I-63** from (+)-tartrate.

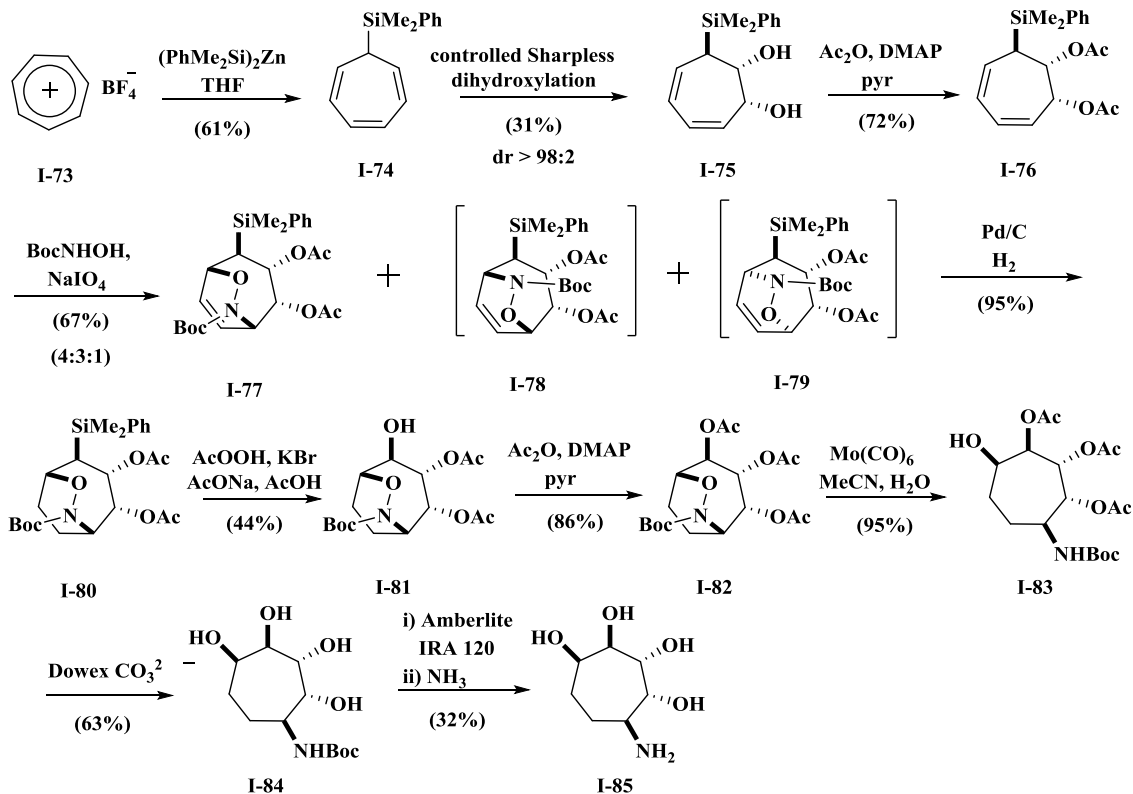
Casiraghi's group also reported the synthesis of densely hydroxylated cycloheptane amino acids **I-71** and **I-72** via succession of a vinylogous Mukaiyama aldol reaction (VMAR)⁹⁵ by reaction of pyrrole-based dienoxysilane **I-64** and (*S*)-protected glyceraldehyde (*S*) **I-65** using SnCl_4 as Lewis acid gave **I-66** as a single diastereoisomer (Scheme I-12). Installation of a second polyol appendage at the α -position of the lactam moiety was achieved via Morita-Baylis-Hillman reaction⁹⁶ upon treatment with both (*S*) and (*R*) glyceraldehyde derivatives leading to the major products **I-67** and **I-68** respectively. Several steps involving reduction of the double bond using hydrogenation in presence of palladium as a catalyst, protection of the hydroxyl group, exchange of the N-

protecting group to an acetyl followed by diol cleavage afforded the dialdehydes **I-67** and **I-70**. Separate intramolecular pinacol coupling of either **I-69** or **I-70** followed by hydrolysis and deprotection provided amino acids polyols **I-71** or **I-72** respectively.⁸⁷



Scheme I-12. Synthesis of **I-49** and **I-50** from pyrrole-based dienoxysilane.

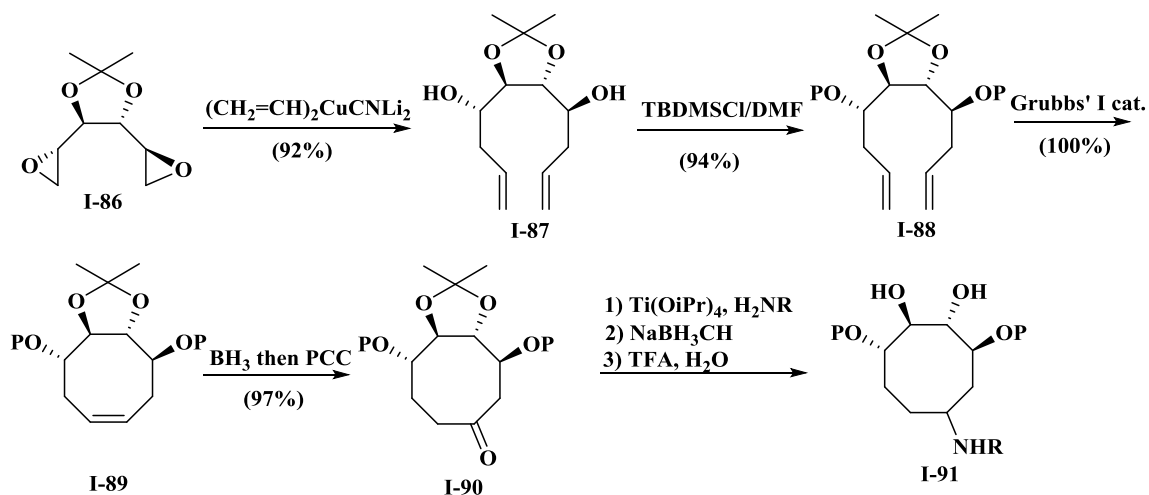
The Landais's research group managed to desymmetrize 7-(dimethyl)phenylsilylcycloheptatriene and through consecutive dihydroxylation and acyl-nitrosocycloaddition to synthesize new aminocycloheptitols. They converted tropylium fluoroborate **I-73** into cycloheptatriene **I-74** using a bis-silyl zinc reagent (Scheme I-13). Sharpless asymmetric dihydroxylation using a modified AD-mix containing quinuclidine as the chiral ligand followed by protection of the diol with acetyl groups to give **I-76**. Diels-Alder cycloaddition of the diene **I-76** with an acyl-nitroso as dienophile afforded three isomers **I-77**, **I-78** and **I-79**. Hydrogenation of the major cycloaddition adduct **I-77** then C-Si oxidation under Felming conditions⁹⁷ followed by acetylation of the resultant hydroxyl group yielded **I-82**. N-O reductive cleavage using Mo(CO)₆ of **I-82** followed by deprotection of the amine group gave the final product **I-85**.⁸⁸



Scheme I-13. Synthesis of **I-63** from commercially available tropylium fluoroborate.

I.7. Eight-membered ring aminocyclitols

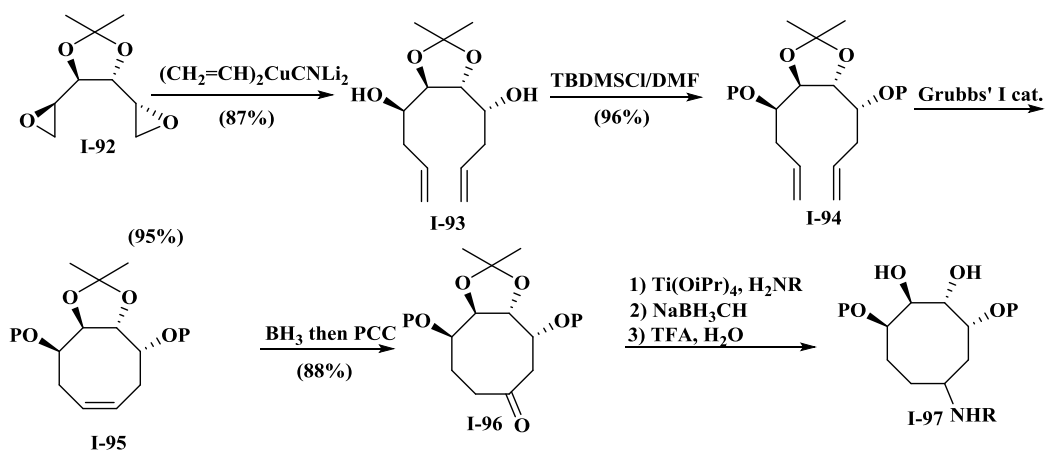
Andriuzzi and others⁹⁸ reported the synthesis of aminocyclooctitols starting from 3,4-o-methylethylidene-L-ido-bisepoxide **I-86**.⁹⁹ Double epoxide ring opening using excess of lithium divinylcyanocuprate¹⁰⁰ led to the formation of the free diol compound **I-87** (Scheme I-14). Silylation of **I-87** gave the corresponding protected compound **I-88**. Ring closing metathesis using Grubbs' I catalyst afforded the corresponding cyclooctenes **I-89**. Hydroboration of **I-89** followed by in situ oxidation¹⁰¹ to give **I-90**. Reductive amination of **I-90** followed by hydrolysis gave the aminocyclooctitol **I-91**.



Scheme I-14. Synthesis of aminocyclooctitol **I-91** from L-ido-bisepoxide.

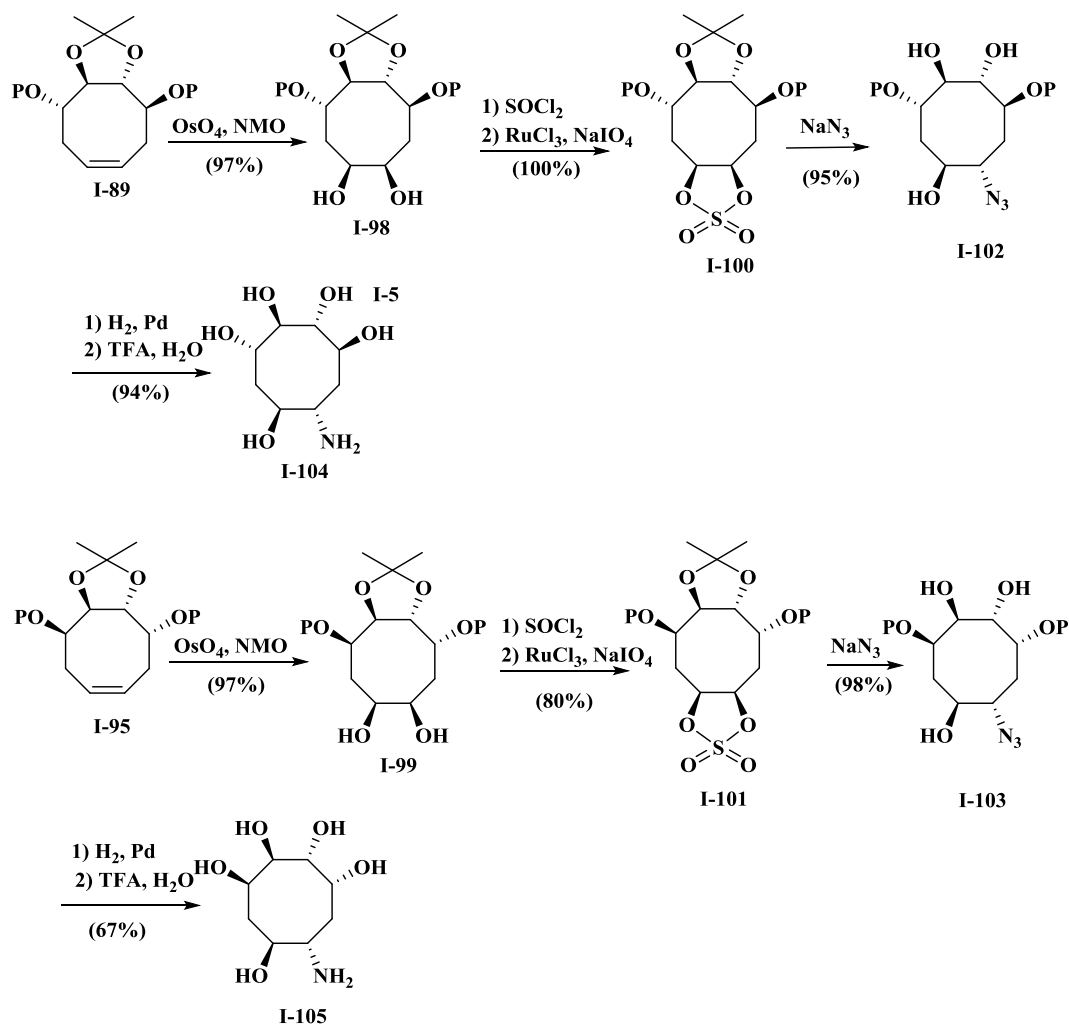
In the same study⁹⁸ they used D-manno bisepoxide **I-92** as starting material.

Similarly, double epoxide ring opening, protection, ring closing metathesis, hydroboration then oxidation followed by reductive amination and finally deprotection resulted in aminocyclooctitol **I-97** (Scheme I-15).



Scheme I-15. Synthesis of aminocyclooctitol **I-97** from D-manno bisepoxide.

In the same year the same research group reported the synthesis of new aminocyclooctitols.¹⁰² Catalytic dihydroxylation of compounds **I-89** and **I-95** gave cis diol compounds **I-98** and **I-99** respectively (Scheme I-16). Treatment of **I-98** and **I-99** with thionyl chloride in the presence of triethyl amine followed by oxidation with sodium periodate in the presence of ruthenium trichloride gave the corresponding cyclic sulfates **I-100** and **I-101**. Nucleophilic opening of these sulfates followed by acidic hydrolysis gave the corresponding azido alcohols **I-102** and **I-103**. Reduction of the azide functionality in both **I-102** and **I-103**, using hydrogen in the presence of palladium black generated the desired amino derivatives which upon hydrolysis provided the aminocyclooctitols **I-104** and **I-105**.

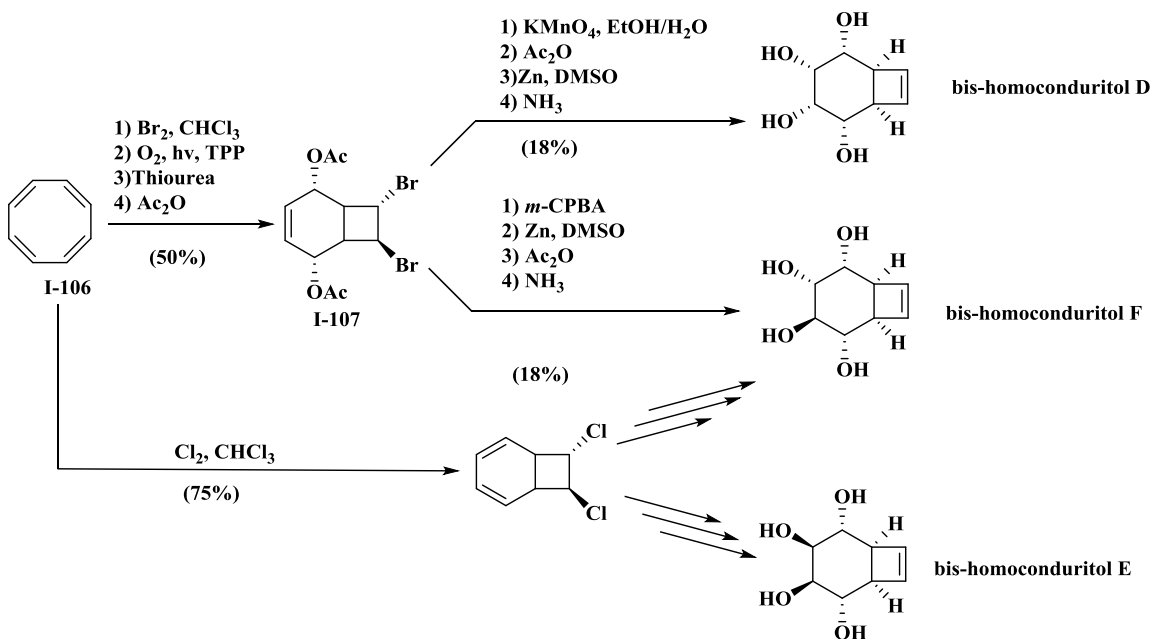


Scheme I-16. Synthesis of aminocyclitol **I-104** and **I-105**.

I.6. Bicyclic cyclitols

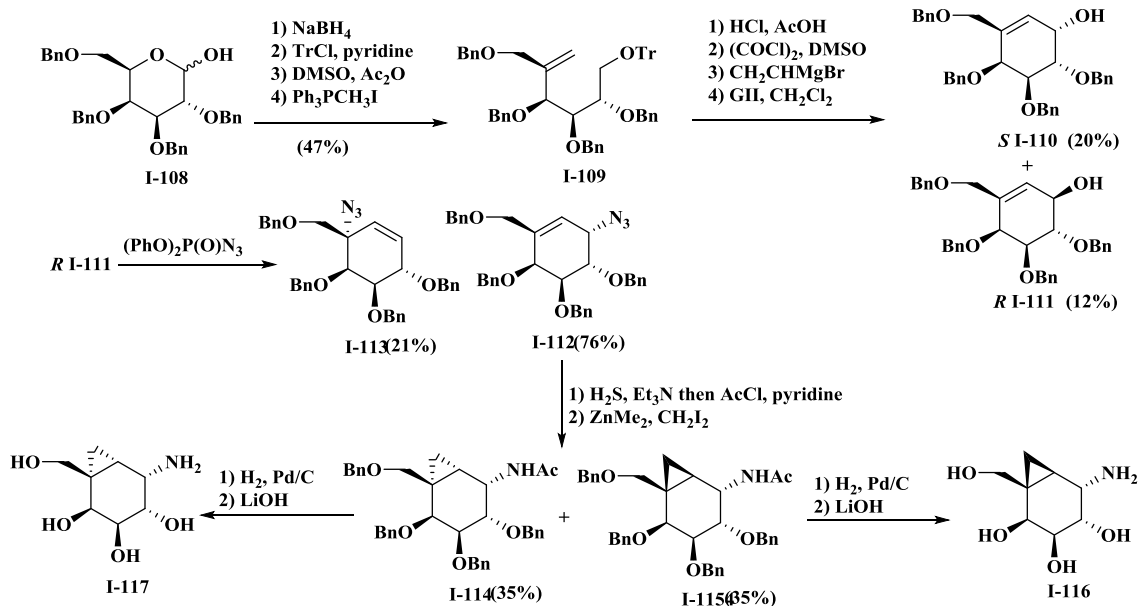
A survey of the literature identified only a few examples for bicyclic cyclitols, all of which contain a 6-membered ring fused either to a 3- or 4-membered ring. Balci's group accomplished the synthesis of a new class of bicyclic compounds named as bis-homoconduritol D, E and F.¹⁰³ Starting from cyclooctatetraene **I-106** (Scheme I-17),

dibromide **I-107** was prepared followed by singlet oxygen cycloaddition, endoperoxide reduction using thiourea and subsequent acetylation to give the diacetate **I-107**. *Syn* dihydroxylation and acetyl protection followed by Zn-reductive elimination reaction and eventually deprotection afforded bis-homoconduritol D. The bicyclic diacetate compound **I-107** underwent epoxidation followed by Zn-reductive elimination of the dibromide, acetylation and finally deprotection to give bis-homoconduritol F. To obtain bis-homoconduritol E, chlorination was used instead of bromination because it was presumed that the endo-oriented bromine atom in **I-107** determines the stereoselectivity of hydroxylation and epoxidation reactions. In a similar fashion to the synthesis of bis-homoconduritol D, bis-homoconduritol E was prepared in a 1:1 ratio.¹⁰³



Scheme I-17. Synthesis of bis-homoconduritol D, E and F.

Bennet and coworkers¹⁰⁴ reported the synthesis of two bicyclic aminocyclitols; one of these was a potent inhibitor of α -galactosidase (Scheme I-18). They started the synthesis with D-galactose derivative **I-108** which can be made in two steps from methyl α -D-galactopyranoside. Reduction of hemiacetal **I-08**, selective protection of the primary alcohol as the trityl ether then Swern oxidation followed by Wittig olefination gave olefin **I-109**. Deprotection of the primary alcohol, Swern oxidation followed by Grignard reaction with vinylmagnesium bromide gave an equimolar mixture of R and S diastereomers. This mixture undergoes ring closure metathesis reaction with Grubbs' II catalyst to give a mixture of cyclohexene diastereomers that were separated using radial chromatography.¹⁰⁵ Conversion of the minor allylic alcohol *R* **I-111** into an allylazide functionality proceeded with inversion of configuration to give allylic azide **I-112** along with small amount of S_N2' product **I-113**. Cyclopropanation of **I-112** using a Furukawa¹⁰⁶ modification of the Simmons-Smith reaction gave a separable mixture cyclopropyl isomers **I-114** and **I-115** with over all yield 88%. Deprotection of the benzyl groups by hydrogenation and hydrolysis of the amide groups gave the final bicyclic aminocyclitols **I-116** and **I-117**.¹⁰⁴



Scheme I-18. Synthesis of bicyclic aminocyclitols **I-116** and **I-117**.

I.7. Cyclooctatetraene as a simple starting material

As part of our long term interest to extend the organoiron approach to the preparation of aminocycloheptitols, we considered the use of cyclooctatetraene as a starting material. A literature survey showed that many research groups have used cyclooctatetraene **I-105**, which is a simple hydrocarbon readily made from acetylene by Ni-catalyzed cyclotetramerization.^{107–109} Different complex molecules, for example aminocyclohexitols,¹¹⁰ bis-homoconduritols (*vide supra*),¹⁰³ bis-homoinositol,¹¹¹ and cyclooctitols¹¹² (Figure I-11) have been synthesized from cyclooctatetraene **I-106**.

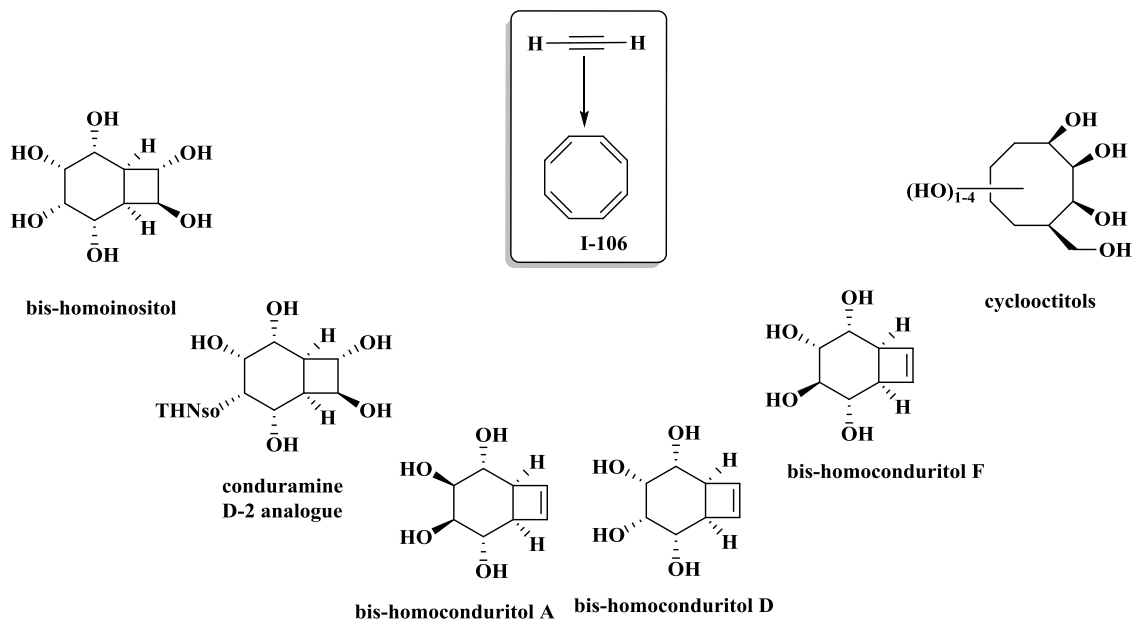
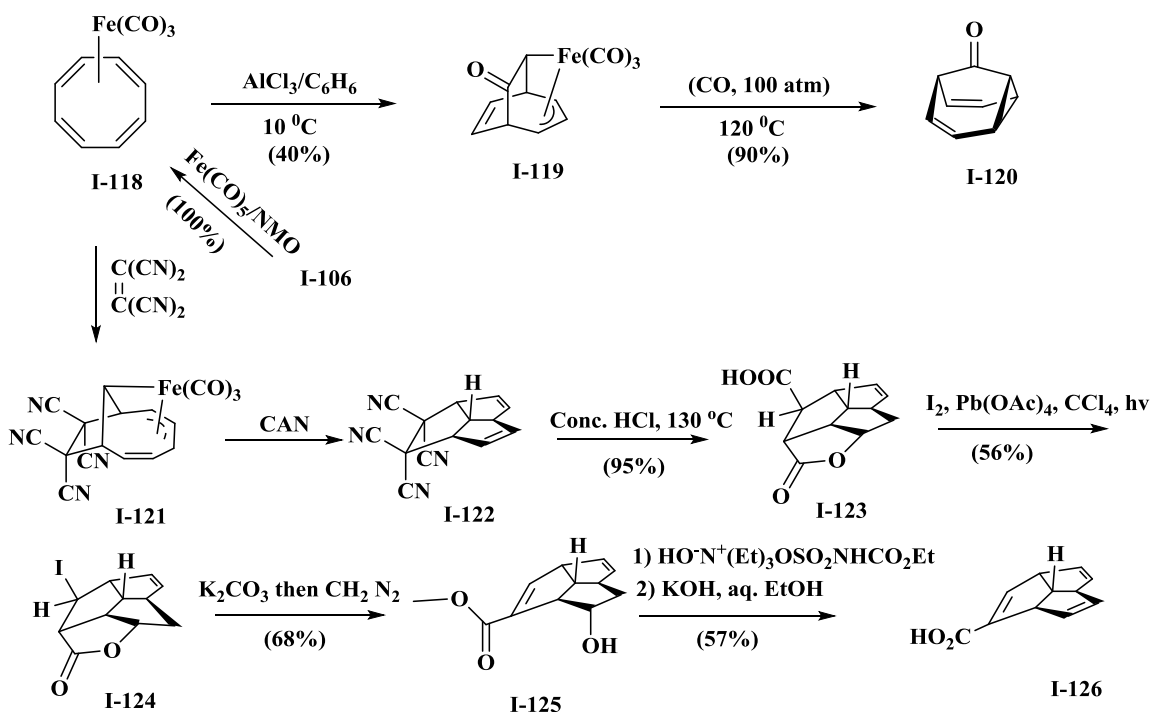


Figure I-11. Synthesis of cyclooctatetraene and target recently prepared from this hydrocarbon.

The complexation of iron pentacarbonyl with cyclooctatetraene **I-106** gives tricarbonyl(cyclooctatetraene)iron **I-118** $[(\text{COT})\text{Fe}(\text{CO})_3]$ in a quantitative yield (Scheme I-19).¹¹³ The number of publications that report on reactions of **I-118** are very small. For instance, upon treatment of **I-118** with a Lewis acid (AlCl_3) it rearranges to form a σ -alkyl- π -allyl complex **I-119** which undergoes decomplexation followed by carbonyl insertion in the presence of a high pressure of CO to give barbaralone **I-120**.¹¹⁴ Paquette and coworkers showed that reaction of **I-118** with tetracyanoethylene afforded bicyclic σ -alkyl- π -allyl complex **I-121** which undergoes oxidative decomplexation using ceric ammonium nitrate (CAN) and further rearranges to form tricyclo[5.2.1.0^{4,10}]deca-2,5-diene **I-122**. Hydrolysis of the tetranitrile **I-122** using conc. HCl gave the acid lactone **I-123** followed by reaction of lead tetraacetate and iodine while irradiated with 250-W

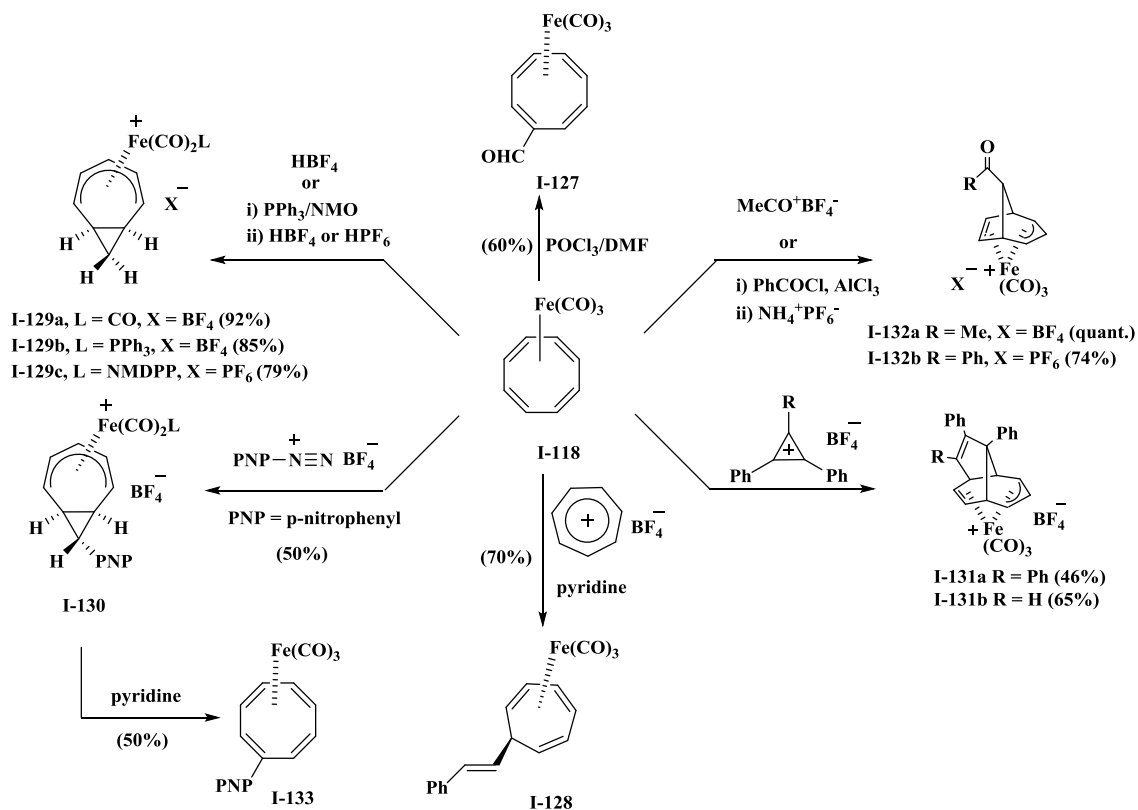
tungsten lamp to give **I-124**. Mild hydrolysis and dehydroiodination of **I-124** gave a carboxylic acid which upon reaction with diazomethane afforded the methyl ester **I-125**. The third double bond was introduced by dehydration of **I-125** followed by saponification using KOH gave the final product (-)-triquinacene-2-carboxylic acid **I-126**.¹¹⁵⁻¹¹⁷



Scheme I-19. Preparation of (COT)Fe(CO)₃ and previous synthetic applications.

Interestingly enough, **I-118** behaves differently with different electrophiles. The electrophilic iminium cation which is generated from the Vilsmeier-Haack formylation reaction³¹ of the dimethyl formamide with phosphorus oxychloride is attacked by the electron rich complex **I-118** to give **I-127** (Scheme I-20).¹¹⁸ In a similar fashion

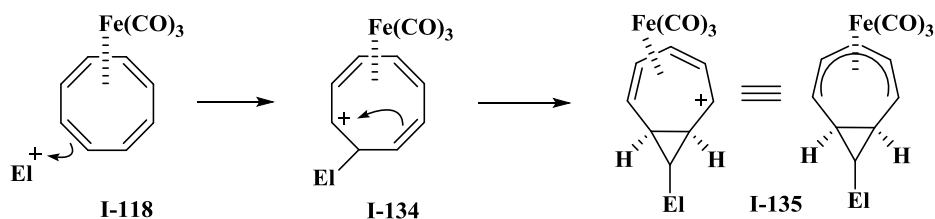
tropylium cation reacts with **I-118** in the presence of one equivalent of pyridine to give styrylcycloheptatriene complex **I-87**. Reaction of complex **I-118** with H^+ or p-nitrophenyldiazonium ion gave [5.1.0] bicyclic structures (**I-129**, **I-130**) and reaction of **I-118** with cyclopropenyl cation afforded polycyclic structures (**I-131 a,b**) while with acylium cation electrophiles gave [3.2.1] bicyclic compounds (**I-132a,b**).^{119–124}



Scheme I-20. Reactions of **I-118** with electrophiles to generate cationic and neutral compounds.

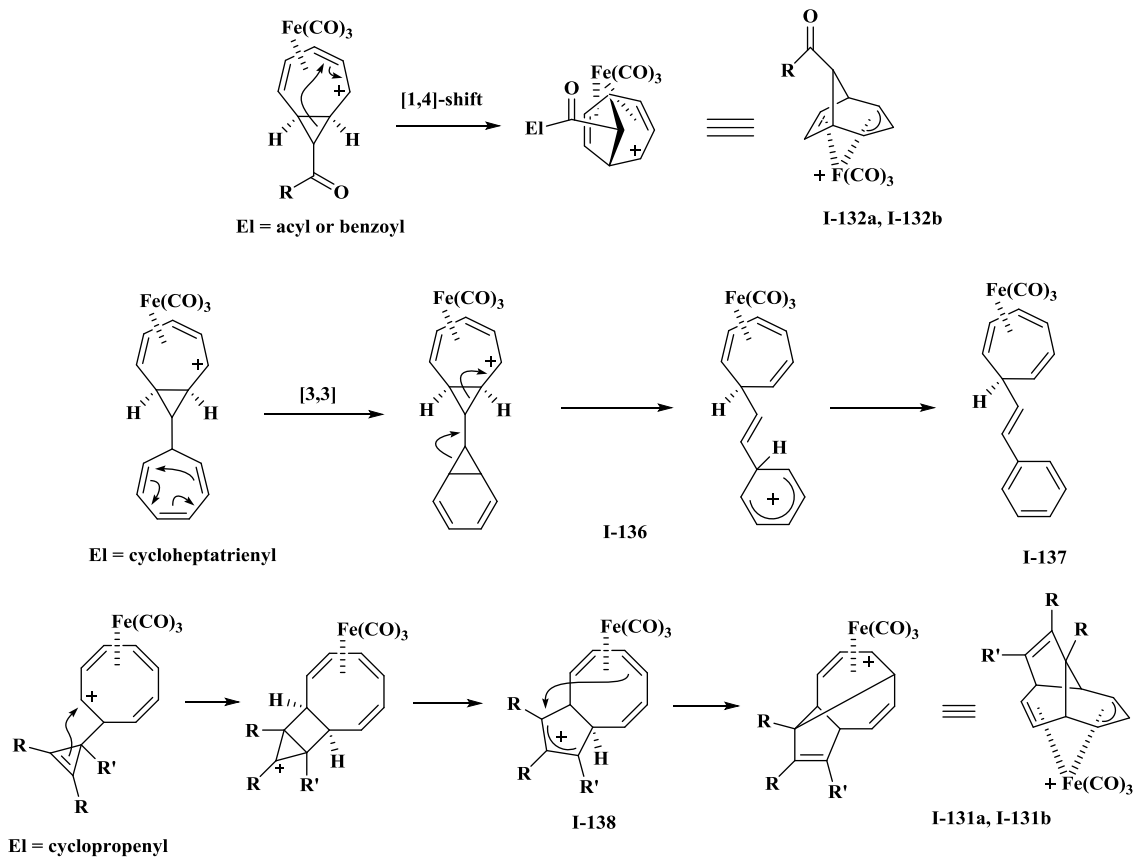
A mechanistic rationale for the formation of these rearranged structures has been proposed by Connelly and co-workers. Upon the addition of an electrophile to a non-coordinated olefin of **I-118** produces cation **I-134** (Scheme I-21); which further

rearranges into a cyclopropylcarbinyl cation of structure **I-135**. In case of H^+ or *p*-nitrophenyl⁺, the bicyclo[5.1.0]octadienyl cation **I-135** was stable and isolable (i.e. products **I-129/ I-130**).^{120–122}



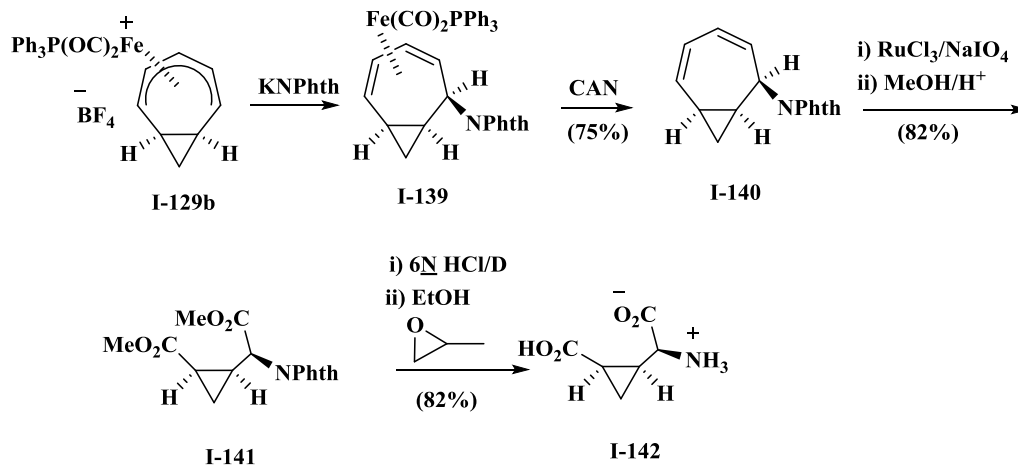
Scheme I-21. Generic attack of electrophile on $(COT)Fe(CO)_3$.

If the electrophile is an acylium cation, the acyl group present at C7 of **I-135** weakens the adjacent cyclopropane bond leading to a [1,4]-shift to relieve the strain of the cyclopropane ring and to form the bicyclo[3.2.1]octadienyl cation **I-132a,b** (Scheme I-22).^{123,124} If the electrophile is the tropylium cation, **I-135** undergoes a [3,3] Cope rearrangement to generate the norcaradiene intermediate **I-136**; in order to re-attain the aromaticity it loses one proton to give the styrylcycloheptatriene complex **I-137**.¹¹⁹ Finally, for cyclopropenyl cation as electrophile, **I-134** rearranges to a bicyclo[6.3.0]nonatetraenyl cation **I-138** followed by transformation into a tricyclic cation **I-131a,b** through an intramolecular bond formation.



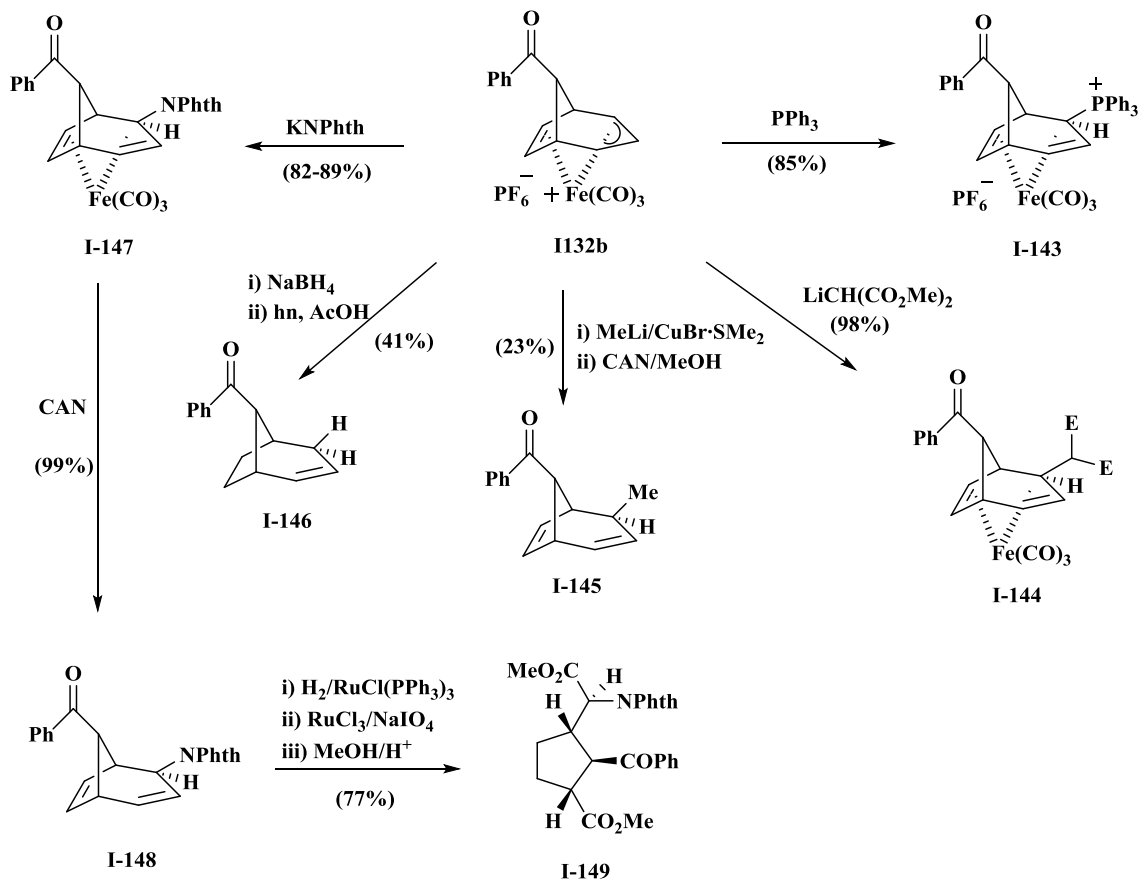
Scheme I-22. Proposed mechanism for the generation of the skeletal rearranged products.

Donaldson's group reported the synthesis of (\pm)-*cis*-2-(2'-carboxycyclopropyl)glycine **I-142** through the nucleophilic attack of phthalimide anion on the cationic compound **I-129b** at the terminal carbon to give complex **I-139**, followed by oxidative decomplexation to give the free diene **I-140**. Catalytic Sharpless oxidation using sodium periodate as oxidant in excess amount and esterification yielded **I-141**. Hydrolysis of **I-141** followed by free base generation provided the desired final product (\pm)-*cis*-2-(2'-carboxycyclopropyl)glycine **I-142** (Scheme I-23).¹²⁵



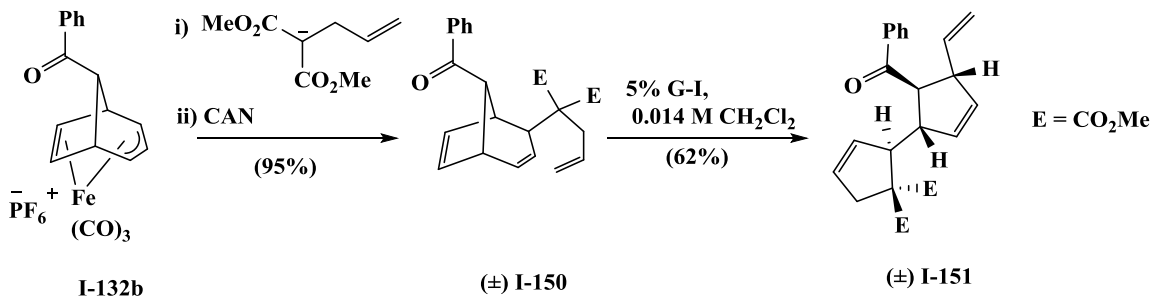
Scheme I-23. Synthesis of (±)-cis-2-(2'-carboxycyclopropyl)glycine from **I-129b**.

The nucleophilic attack of triphenyl phosphine on **I-132b** gave the corresponding triphenylphosphonium cation **I-143** while reaction of **I-132b** with lithium dimethylmalonate gave compound **I-144** (Scheme I-24). Methyl nucleophile also attacks **I-132b** which undergoes oxidative decomplexation to give **I-145**. Nucleophilic attack of hydride anion gave the olefin **I-146**. In a similar fashion phthalimide anion attacks **I-132b** to give the corresponding phthalimide derivative **I-147** followed by decomplexation to give the free diene **I-147**. Chemoselective double bond hydrogenation then cleavage of the remaining double bond and finally Fisher esterification afforded **I-149**.¹²⁶



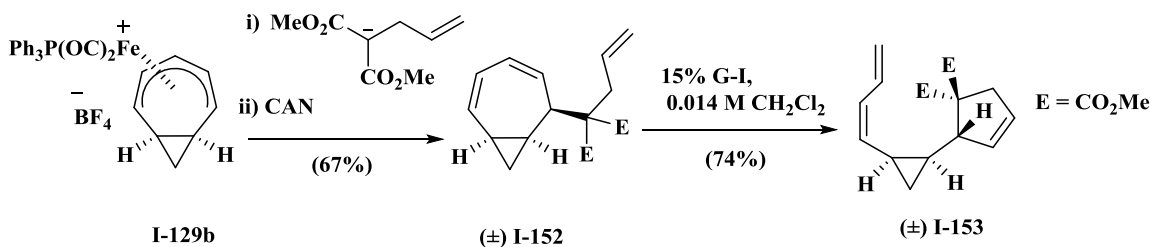
Scheme I-24. Reactivity of **I-132b** with various nucleophiles and synthesis of protected amino acid analog **I-149**.

In order to create more structural diversity of cyclooctatetraene, recently Donaldson's research group studied the reactivity of compounds **I-128**, **I-129b** and **I-132b** towards allylmalonate nucleophile. Nucleophilic attack of allylmalonate on cation **I-132b** followed by oxidative decomplexation afforded **I-150**. Ring rearrangement metathesis reaction of **I-150** with Grubbs' 1st generation catalyst gave **I-151** (Scheme I-25).¹²⁷



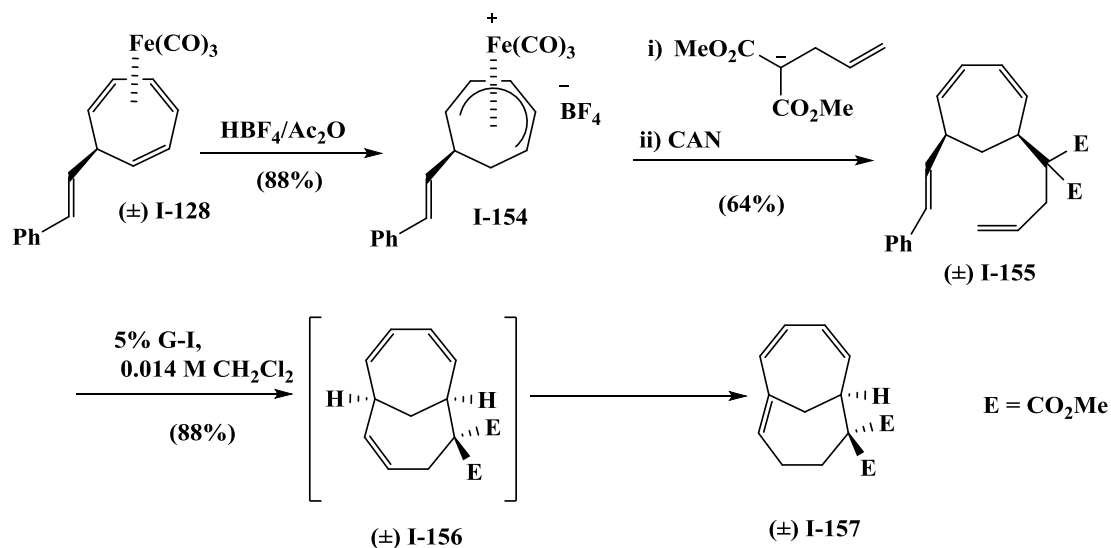
Scheme I-25. Ring rearrangement metathesis reaction of **I-150**.

Reaction of **I-129b** with allylmalonate nucleophile then decomplexation using CAN gives (\pm) **I-152**. Treatment with Grubbs' 1st generation catalyst produces ring rearrangement product (\pm) **I-153** (Scheme I-26).¹²⁸



Scheme I-26. Ring rearrangement metathesis reaction of (\pm) **I-152**.

Finally reaction of **I-28** with tetrafluoroboric acid gave the corresponding cation **I-154** which reacts with allylmalonate nucleophile followed by oxidative decomplexation to generate free tetraene compound (\pm) **I-155**. Ring closure metathesis reaction with Grubbs' I catalyst gives bicyclic triene intermediate (\pm) **I-156** that undergoes olefin isomerization to produce the final compound (\pm) **I-157** as shown in scheme I-27.¹²⁹



Scheme I-27. Ring rearrangement metathesis reaction of (±) I-155.

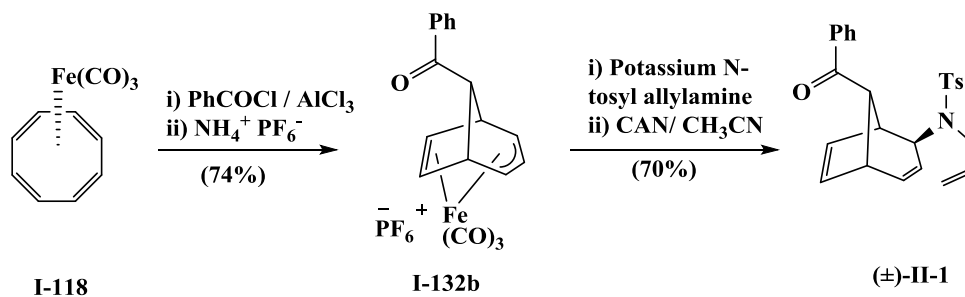
In this introduction part we showed some representative examples of the different synthetic approaches for making aminocyclitols where the major limitation in all these methods is the limited number of aminocyclitols which can be obtained using each synthetic route. Another disadvantage is the use of starting materials which in certain cases are expensive or difficult to make.

In this work we aim to further generate molecular complexity and structural diversity from cyclooctatetraene and to provide more examples of aminocycloheptitols. It is also planned to access the here-to-fore unknown bicycle[5.1.0] aminopolyols as a new class of compounds using organoiron chemistry. These latter compounds will be tested for their inhibition towards a commercially available glucosidase.

II- RESULTS AND DISCUSSION

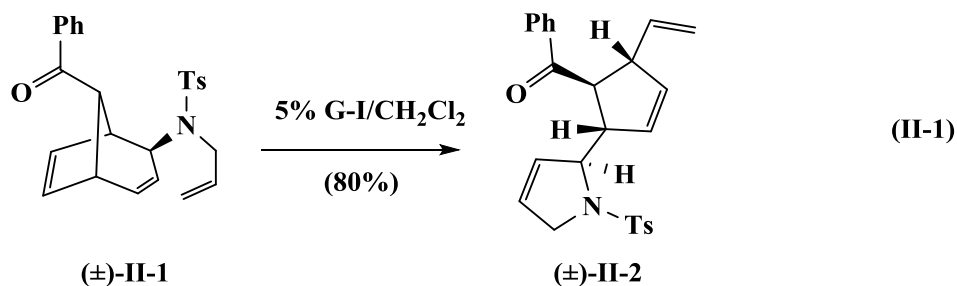
II.1. Generation of diverse molecular complexity using dienyron approach

Electrophilic addition of the phenacylium cation (generated from reaction of aluminum chloride and phenacyl chloride) to tricarbonyl(cyclooctatetraene)iron **I-118** according to prior literature led to the formation of (dienyl)iron cation **I-132b**.¹²³ Reaction of this cation (\pm)-**I-132b** with the potassium salt of (allyl)tosylamine followed by oxidative decomplexation using cerium ammonium nitrate gave benzoylbicyclooctadienyl-*N*-tosylamine (\pm)-**II-1** (Scheme II-1). The ¹H NMR spectrum of the free ligand shows a signal characteristic for the methyl protons of the tosyl group at δ 2.43 ppm (3H) and the diastereotopic methylene protons of the *N*-tosyl allylamine appeared at δ 3.98 ppm (1H) and 4.13 ppm (1H) along with 9 aromatic protons. In the ¹³C NMR spectrum of (\pm)-**II-1**, characteristic peaks for the sulfonamide appear at δ 143.6 ppm and for the ketone at δ 199.4 ppm.



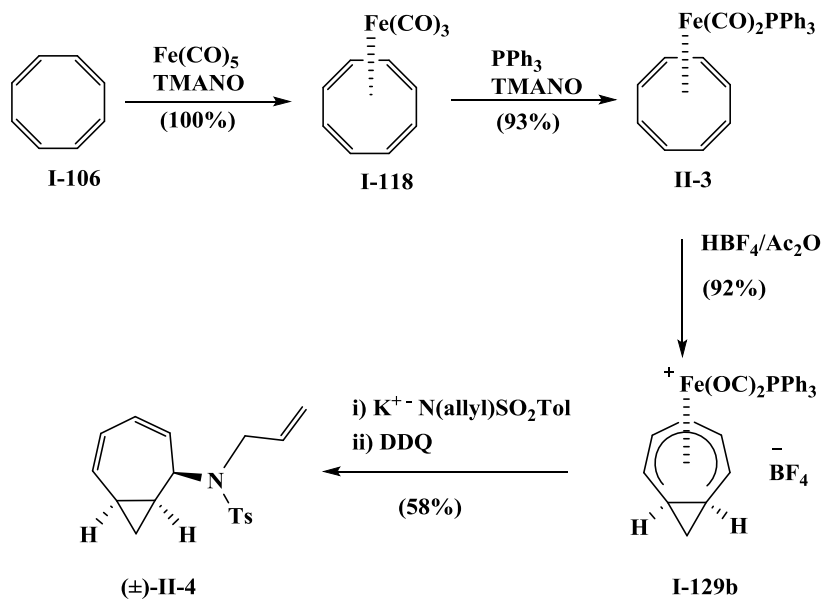
Scheme II-1. Preparation of free ligand (\pm)-**II-1**.

The reaction of (\pm)-**II-1** with Grubbs' 1st generation catalyst led to the ring rearrangement metathesis (RRM) product (\pm)-**II-2** (eqn. II-1). The NMR spectral data for (\pm)-**II-2** supports the proposed structure, particularly the signal at δ 3.39-3.46 ppm which is characteristic for the allylic proton of the cyclopentene ring and the protons at range of δ 4.02-4.10 ppm (2H) which are characteristic for the dihydropyrrole ring at position 5.¹³⁰



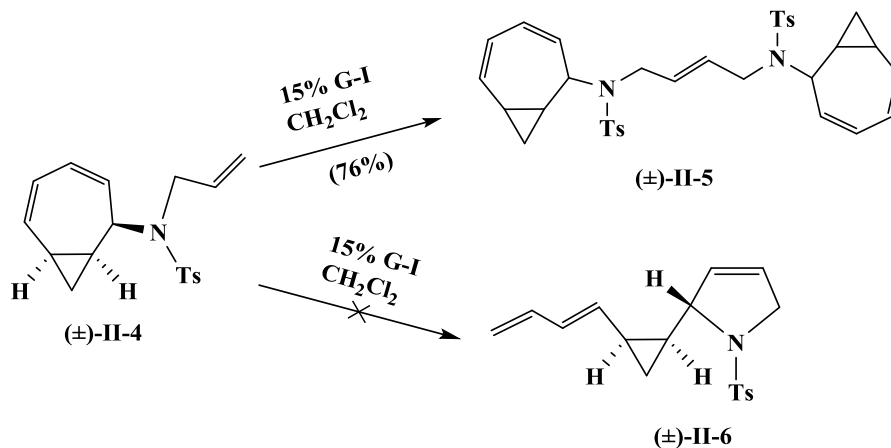
The synthesis of bicyclo-N-tosyl allylamine (\pm)-**II-4** was achieved by reaction of cyclooctatetraene **I-106** with iron pentacarbonyl to afford tricarbonyl ligated iron complex **I-118** (Scheme II-2). This complex **I-118** underwent ligand exchange with triphenylphosphine to give the corresponding monosubstituted triphenylphosphine iron complex **II-3** which was treated with a cold solution of aqueous tetrafluoroboric acid in acetic anhydride to afford bicyclooctadienyl iron cation **I-129b**. The NMR spectral data and melting points for **II-3** and **I-129b** were consistent with the literature values.¹²⁵ This freshly prepared cation **I-129b**, was allowed to react with the potassium salt of N-tosyl allylamine¹³¹ in water-saturated ether; the crude product underwent oxidative decomplexation after treatment with 2,3-dichloro-5,6-dicyano-1,4-benzoquinone to give bicyclooctadienyl-N-allylamine derivative (\pm)-**II-4**. The structural assignments for (\pm)-**II-4** were based on its ¹H NMR spectral data. The characteristic signals for the

diastereotopic methylene protons of the N-tosyl allylamine appear at δ 3.75 ppm (1H) and 3.95 ppm (1H) and the methyl protons of the tosyl group at δ 2.35 ppm (3H), along with the methylene protons of the cyclopropane ring at 0.77 and 1.15 ppm (1H each).



Scheme II-2. Synthesis of the bicyclic free ligand (\pm)-II-4.

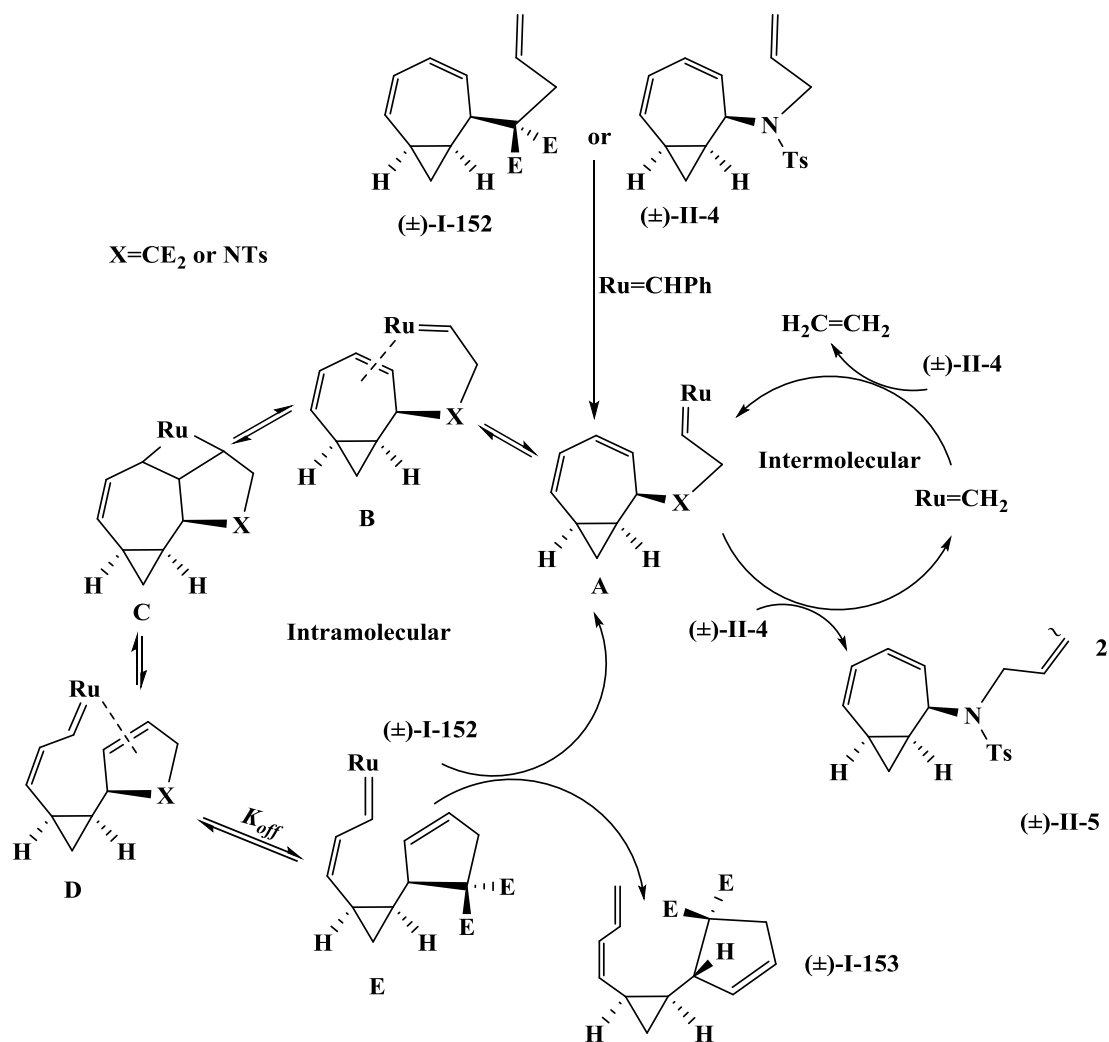
Reaction of the free ligand (\pm)-II-4 with Grubbs' I catalyst gave only the self-metathesis dimer (\pm)-II-5 as a mixture of diastereomers instead of the expected ring rearrangement product (\pm)-II-6 (Scheme II-3). The structure of the dimer (\pm)-II-5 was assigned on the basis of its NMR spectral data, absence of signals corresponding to a mono-substituted olefin and the appearance of a narrow multiplet at δ 5.80–5.85 (2H) corresponding to the new 1,2-disubstituted double bond. In addition, the presence of a signal at δ 130.5 ppm in the ^{13}C NMR spectrum of dimer (\pm)-II-5 (instead of a signal at ca. δ 117–119 ppm) indicated the presence of the self-metathesis olefin.



Scheme II-3. Formation of dimer (±)-II-5 via metathesis reaction of (±)-II-4.

The difference in reactivity between (±)-I-152 and (±)-II-4 toward G-I catalyst may be rationalized on the basis of the allylmalonate group of (±)-I-152 compared to the (allyl)tosylamine group of (±)-II-4. Two possible explanation for this different behavior; Throp-Ingold effect¹³² where increasing the size of the two geminal substituents on a tetrahedral center increases both the rate and equilibrium constants of cyclization reactions. In this case the rate of attaching the ruthenium metal to the allylmalonate compound is faster than it for (allyl)tosylamine derivative. The other explanation is proposed by Hoye and co-workers whom have previously noted that the allylmalonate group is particularly effective as an activator for initiating relay ring closing metathesis (RRCM).¹³³ These authors suggested that the rate-determining step in some RRCM reactions is the decomplexation of the product olefin (i.e. a cyclopentene ring), and that this decomplexation was more rapid for a cyclopentene ring with a sterically bulky dicarboxylate substitution pattern which encounters a steric repulsion with ruthenium ligand sphere. In the present case initiation generates the Ru-carbene A (Scheme 4). Two

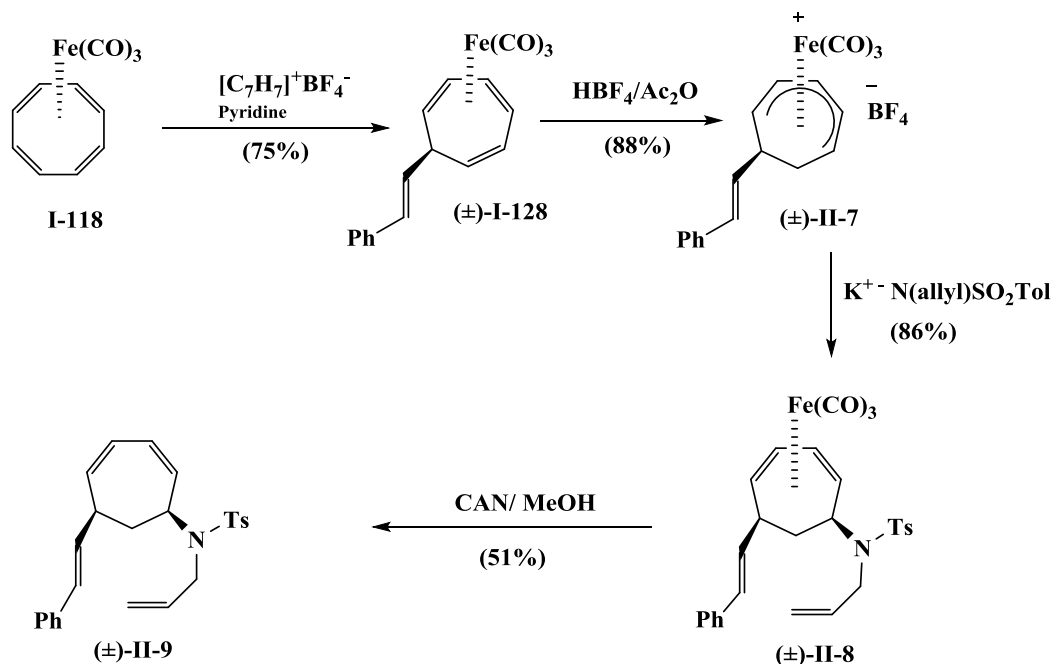
pathways are available to this intermediate: either reversible intramolecular equilibration to afford intermediate E, or irreversible self-metathesis dimerization. According to Hoye's proposal, the rate of decomplexation of D [$X = C(CO_2Me)_2$] is rapid (i.e. k_{off} is fast), and thus E reacts with (\pm)-**I-152** to give the ring rearranged product **I-153** and regenerate intermediate A. Conversely, intermediate D [$X = NTs$] undergoes decomplexation at a slower rate leading to the eventual irreversible self metathesis and concomitant formation of ethylene via the methylene carbene complex $[(Cy_3P)Cl_2Ru=CH_2]$.



Scheme II-4. Mechanistic rationale for the reactivity difference of (±)-I-152 and (±)-II-4 toward G-I catalyst.

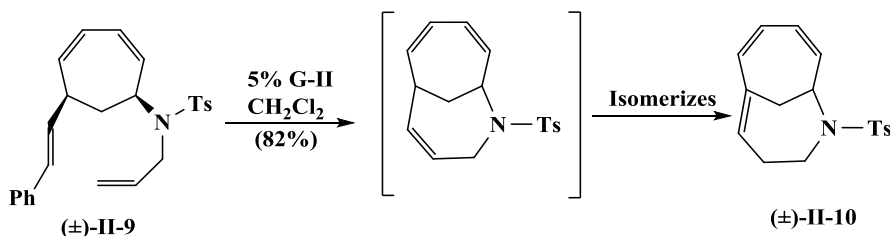
Reaction of (cyclooctatetraene)Fe(CO)₃ **I-118** with tropylium tetrafluoroborate in presence of pyridine as a base provided styrylcycloheptatriene complex (±)-I-128 (Scheme II-5). The reported yield in the literature was only modest (41%).¹³⁴ The yield of this product could be improved by using one equivalent of pyridine and running the reaction for 8 hours, which increased the yield to (75%). Treatment of (±)-I-128 with tetrafluoroboric acid gave the corresponding cation (±)-II-7; the NMR spectral data for

(±)-**I-128** and (±)-**II-7** are consistent with the literature values.¹²⁹ Nucleophilic attack of the potassium salt of tosyl allylamine at this cation led to styryl-cycloheptadienyl tosyl allylamine complex (±)-**II-8**; which undergoes oxidative decomplexation using cerium ammonium nitrate to give styryl cycloheptadienyl tosyl allylamine (±)-**II-9**. The ¹H NMR spectra of the free ligand (±)-**II-9** contained signals characteristic for the styryl olefinic proton at δ 6.39 (d, 1H), methyl protons of the tosyl group at δ 2.42 ppm (3H) and diastereotopic methylene protons of the N-tosyl allylamine at δ 3.73 (1H) and δ 3.85 ppm (1H).



Scheme II-5. Preparation of styryl cycloheptadienyl tosyl allylamine (±)-**II-9**.

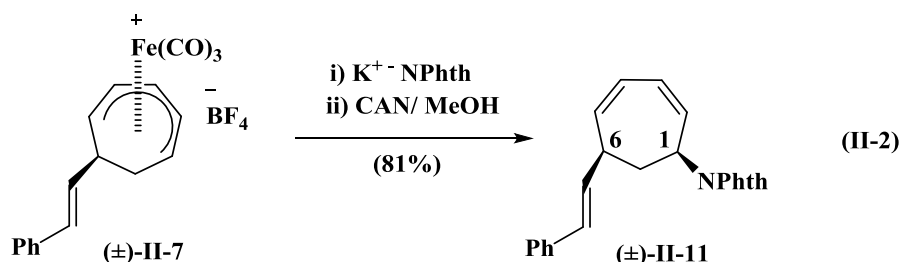
The substrate (\pm)-**II-9** has a number of potential sites for olefin metathesis. Exposure of free ligand (\pm)-**II-9** to Grubbs' first generation catalyst gave a complex mixture of products; use of Grubbs' second generation catalyst led to a ring-closed product. This product was found to isomerize to give 2-azabicyclo[4.4.1]undeca-5,7,9-triene (\pm)-**II-10** (Scheme II-6). The structural assignment for this isomer is based on its NMR spectral data. In particular, the ^1H NMR of (\pm)-**II-10** integrates to 19 Hs; five of which are olefinic. Furthermore, the ^{13}C NMR spectrum of (\pm)-**II-10** consisted of 15 signals with seven aryl/alkenyl methine carbons and three quaternary aryl/alkenyl carbons.



Scheme II-6. Formation of ring closure product (\pm)-**II-10**.

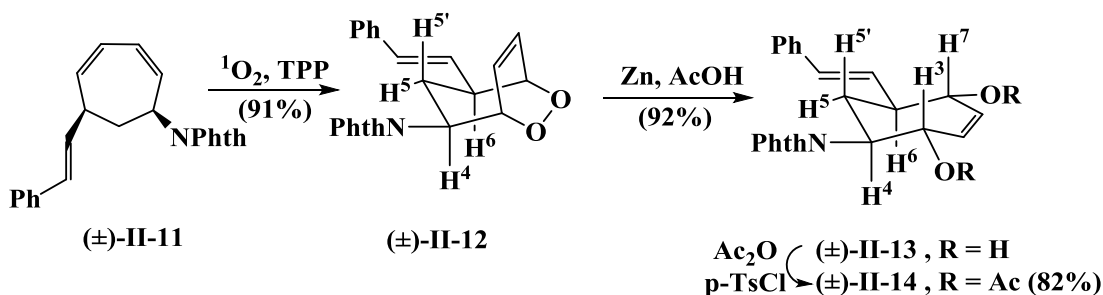
II.2. Synthesis of racemic and optically active aminocycloheptitols

As had reported by a previous graduate student¹²⁹ in our group, styrenylcycloheptadiene derivative (\pm)-**II-11** was prepared by nucleophilic attack of phthalimide anion at C-1 of the cation (\pm)-**II-7** to afford the corresponding phthalimidocycloheptadiene complex which undergoes oxidative decomplexation to give phthalimidocycloheptadiene free ligand (\pm)-**II-11** (eqn. II-2).



Cycloaddition of (\pm)-**II-11** with singlet oxygen gave (\pm)-**II-12** as a single diastereomer (Scheme II-7). Cycloaddition occurs on the diene face opposite to the *syn*-C¹/C⁶ substituents. Similar facial selectivity was also observed for substituted cycloheptadiene systems by the groups of Pearson and Seitz.⁵⁴ Initial attempts to reduce the generated endoperoxide (\pm)-**II-12** were done using thiourea but the yield was low with a long reaction time.¹²⁹ The yield and reproducibility of the reduction reaction was improved using activated zinc and glacial acetic acid to afford the diol derivative (\pm)-**II-13**. Acetylation of (\pm)-**II-13** in acetic anhydride and p-toluenesulfonyl chloride in catalytic amount provided the diacetate derivative (\pm)-**II-14**. The relative stereochemistries of (\pm)-**II-12**, (\pm)-**II-13**, and (\pm)-**II-14** were assigned based on their ¹H

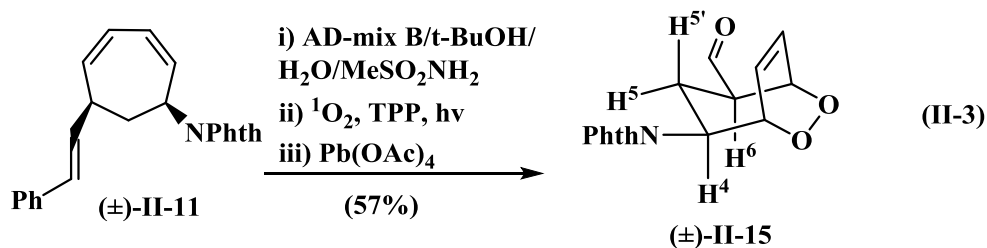
NMR spectral data. In particular the signal for H-5' of (\pm)-**II-12** appears at δ 2.11 (q, J = 10.1 Hz)ppm, while the comparable signal for H-5' of (\pm)-**II-13** and (\pm)-**II-14** appear at δ 2.73 (td, J = 11.8, 14.0 Hz) and 2.85 (q, J=12.8 Hz) ppm respectively. The relative upfield shift for H-5' of (\pm)-**II-12** (compared to H-5' of (\pm)-**II-13**/ \pm)-**II-14**) may be attributed to the anisotropic effects of the proximal C6-C7 olefin. In addition, the signal for H-4 of (\pm)-**II-14** appears as a broad triplet at δ 4.42 ppm (J = 10.8 Hz); these two large coupling constants are due to axial-axial couplings to both H-5' and H-3, thus indicating that H-3 occupies an axial orientation in (\pm)-**II-14**.



Scheme II-7. Singlet oxygen cycloaddition of (\pm)-**II-11** followed by reduction.

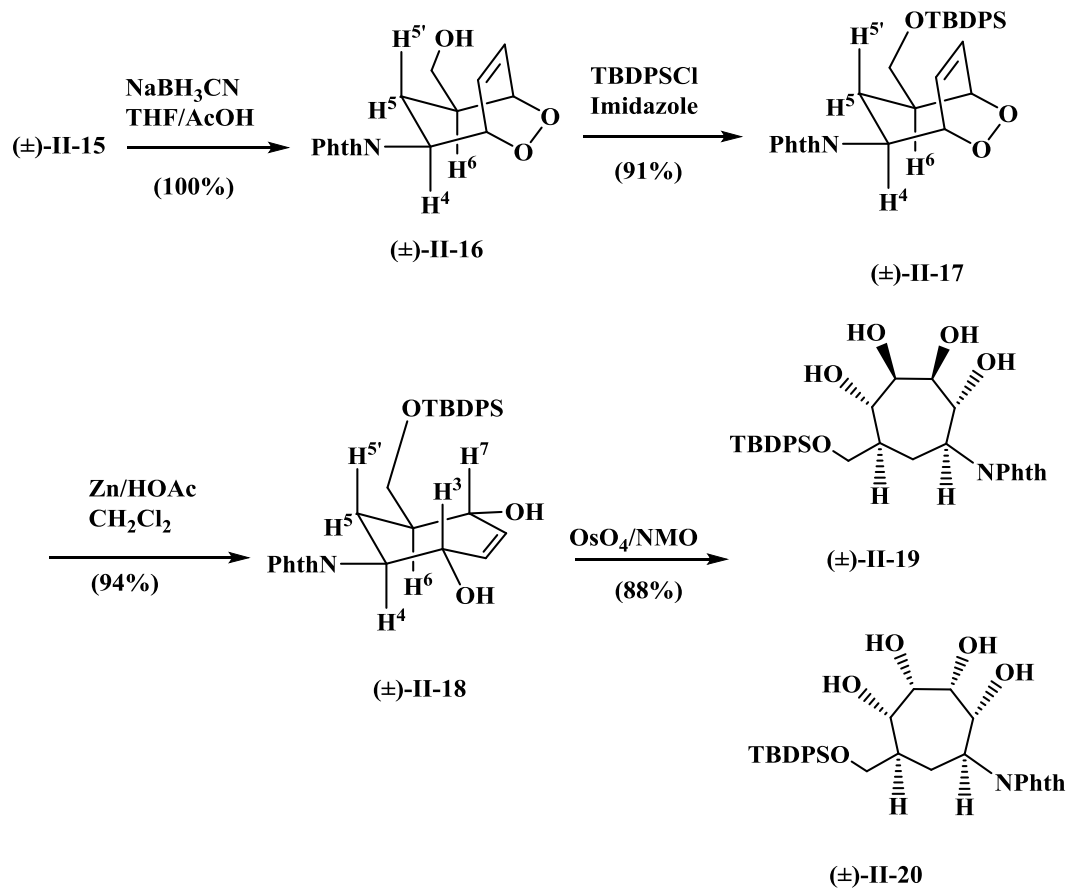
Truncation of the styrenyl group present on (\pm)-**II-11** into a hydroxymethyl substituent was achieved in the following fashion (eqn. II-3). Sharpless asymmetric dihydroxylation of (\pm)-**II-11** with commercially available AD-mix β^{135} gave a mixture of diastereomeric diols. The dihydroxylation exclusively took place on the styrene double bond in a stereofacial fashion leaving the diene olefins intact because it favors the reaction with *trans* double bonds more than *cis* double bonds. Notably, the “binding pocket” of the phthalazine ligands in the AD-mix is well suited to accommodate olefins

with flat, aromatic substituents. Phthalazine ligands are also recommended for the 1,1- and 1,2-*trans*-disubstituted as well as the trisubstituted classes of olefins.¹³⁵ Singlet oxygen cycloaddition to the diol mixture gave a mixture of diastereomeric endoperoxide diols, which undergo diol cleavage with lead tetraacetate to give a single racemic endoperoxide aldehyde (\pm)-**II-15**. The presence of the aldehyde group was confirmed by a singlet in ^1H NMR spectrum for one proton at δ 9.65 ppm while in the ^{13}C NMR spectrum an aldehydic carbonyl was observed at δ 199.0 ppm.



Reduction of only the aldehyde functionality in the presence of the endoperoxide proved to be challenging, however this was eventually accomplished by using $\text{NaBH}_3\text{CN}/\text{AcOH}$ to afford (\pm)-**II-16** in quantitative yield (Scheme II-8). Protection of (\pm)-**II-16** via reaction with *t*-butylchlorodiphenylsilane gave the corresponding silyl ether (\pm)-**II-17**. Reduction of the endoperoxide moiety with zinc and glacial acetic acid gave the diol (\pm)-**II-18**. The relative stereochemistry of **II-15** to **II-18** were assigned by comparison of their ^1H NMR spectral data with that for **II-12** to **II-14**. In particular the signals for H-3' of **II-15**, **II-16** and **II-17** appear relatively upfield at δ 2.11, 1.84 and 1.78 ppm respectively. The signal for H-4 of **II-18** appears as doublet of doublet of doublets at δ 4.14 ppm ($J=2.4, 10.0$ and 12.4 Hz); the two larger coupling constants are

due to axial-axial couplings to H-5' and H-3. Dihydroxylation of (\pm)-**II-18** with catalytic OsO₄ led to a mixture of diastereomeric tetraols (\pm)-**II-19** and (\pm)-**II-20** (ca. 6:1). The relative stereochemistry of the major compound (\pm)-**II-19** was tentatively assigned on the basis of facial selectivity noted by Kishi, *et al.*,^{136,137} for dihydroxylation of an allylic alcohol opposite to the adjacent hydroxyl groups. In this fashion, the racemic protected cycloheptitol was prepared from (cyclooctatetraene)Fe(CO)₃ (\pm)-**I-77** in 11 steps and 17% overall yield.



Scheme II-8. Synthesis of final tetraols (\pm)-**II-19** and (\pm)-**II-20**.

In Kishi's empirical model, the substrate reacts in a conformation that minimizes steric repulsion of the oxygen lone pairs with OsO₄ the reagent comes in from the face opposite the oxygen substituent (Figure II-1).^{136,137}

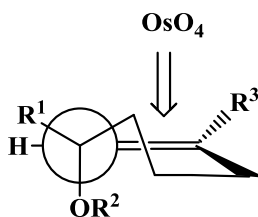
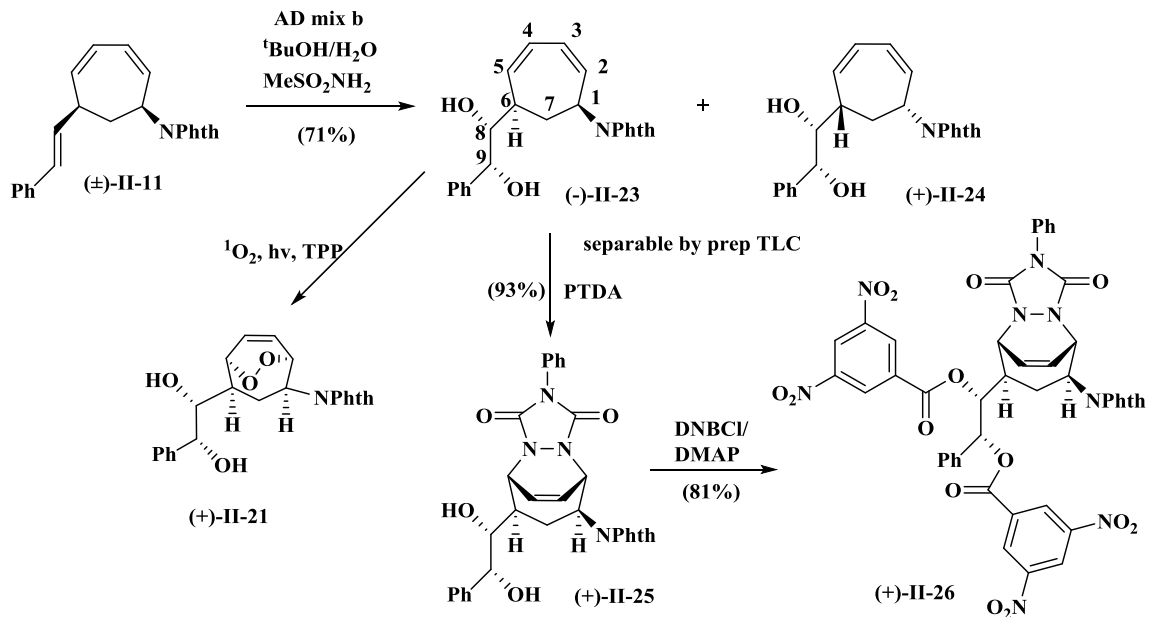


Figure II-1. Kishi's model for osmylation reaction.

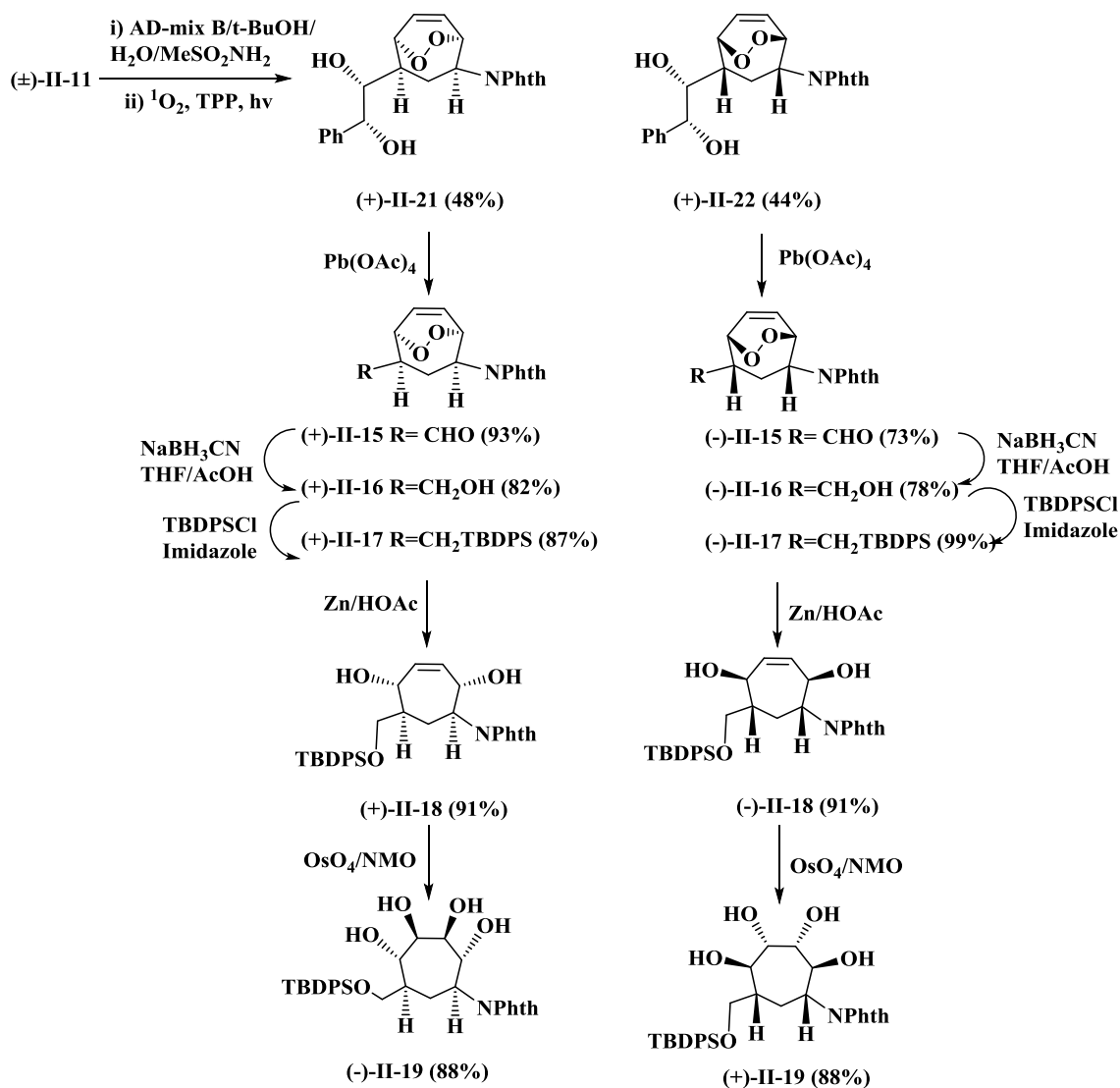
In an attempt to obtain optically active tetraols, successful separation of the diastereomeric mixture of endoperoxide diols (+)-**II-21** and (+)-**II-22** using column chromatography was shown to be feasible on > 1 g scale (Scheme II-9).

The absolute stereochemistry of (+)-**II-21** and (+)-**II-22** was assigned by a former graduate student in our group.¹²⁹ Asymmetric dihydroxylation of (±)-**II-11** gave a mixture of diastereomers which was separable by preparative thin layer chromatography. Diels-Alder reaction of *N*-phenyl-1,3,5-triaza-2,4-dione (PTAD) with the less polar cycloheptadiene diastereomer (-)-**II-23** gave adduct (+)-**II-25** which undergoes protection with 3,5-dinitrobenzoyl chloride to give (+)-**II-26** (Scheme II-9). The relative stereochemistry of all chiral centers of (+)-**II-26** were assigned based on its single crystal X-ray diffraction analysis.¹²⁹ Singlet oxygen cycloaddition of the isolated dienediol (-)-**II-23** gave a compound which was identical with (+)-**II-21**.



Scheme II-9. Assignment of the stereocenters configurations of (-)-II-21 and (+)-II-22.

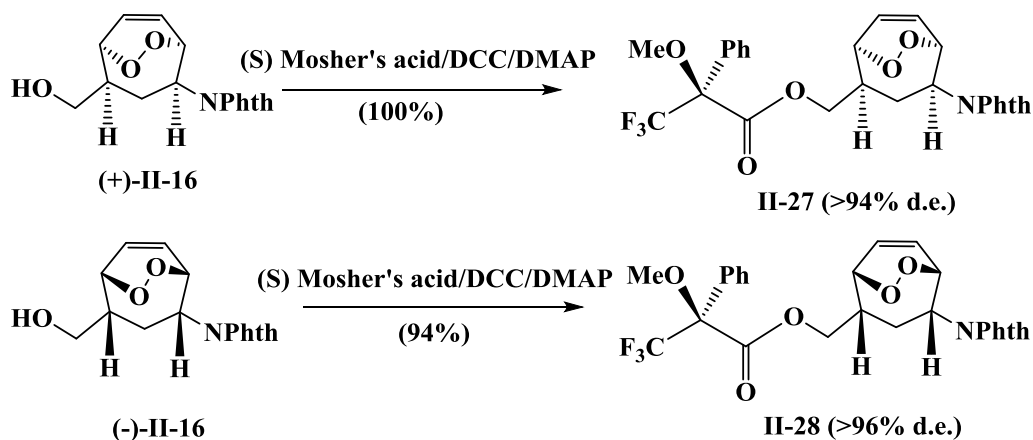
Separate diol cleavage of optically enriched endoperoxide diols (+)-II-21 and (+)-II-22 gave the aldehydes (+)-II-15 and (-)-II-15 respectively (Scheme II-10). Reduction of (+)-II-15 and (-)-II-15 to the corresponding alcohols (+)-II-16 and (-)-II-16 was achieved by activated zinc in glacial acetic acid, followed by protection using *t*-butyldiphenylsilyl chloride to give (+)-II-17 and (-)-II-17. Reduction of the endoperoxide moiety gave optically active diols (+)-II-18 and (-)-II-18. Dihydroxylation of each optically enriched diol afforded the optically enriched tetraols (+)-II-19 and (-)-II-19.



Scheme II-10. Preparation of optically active tetraols (-)-II-19 and (+)-II-19.

While asymmetric dihydroxylation of styrene is known to proceed with high enantioselectivity,¹³⁵ an independent method of assaying the optical purity of the endoperoxide alcohols (+)-II-16 and (-)-II-16 was sought. To this end the (*S*)(-)- α -methoxy- α -trifluoromethylphenylacetyl of both (+)-II-16 and (-)-II-16 were prepared (II-27 and II-28 respectively, Scheme II-11). Portions of the ^1H NMR spectra of II-27 and

II-28 are similar (but not identical) to that obtained for racemic alcohol (\pm)-**II-16**. The main point of differences were found to be the diastereotopic alkoxy methylene signals which appear at δ 3.38-3.47 and 3.60-3.66 ppm for **II-16** and are found downfield for **II-27** (δ 4.27 and 4.39 ppm) as well as for **II-28** (δ 4.27-4.38). Also, one olefinic peak for **II-27** appears at δ 6.22 ppm while for **II-28** it shows at δ 6.31 ppm (Figure II-2). The clean baseline separation of these signals allowed for establishment of a lower limit for the diastereomeric excess by integration. Using this method each was determined to be \geq 94% de and thus the enantiomeric excess of the optically active **II-15** to **II-19** and diastereomers (+)-**II-21** and (-)-**II-22** to be \geq 94% ee.



Scheme II-11. Preparation of Mosher's esters **II-27** and **II-28**.

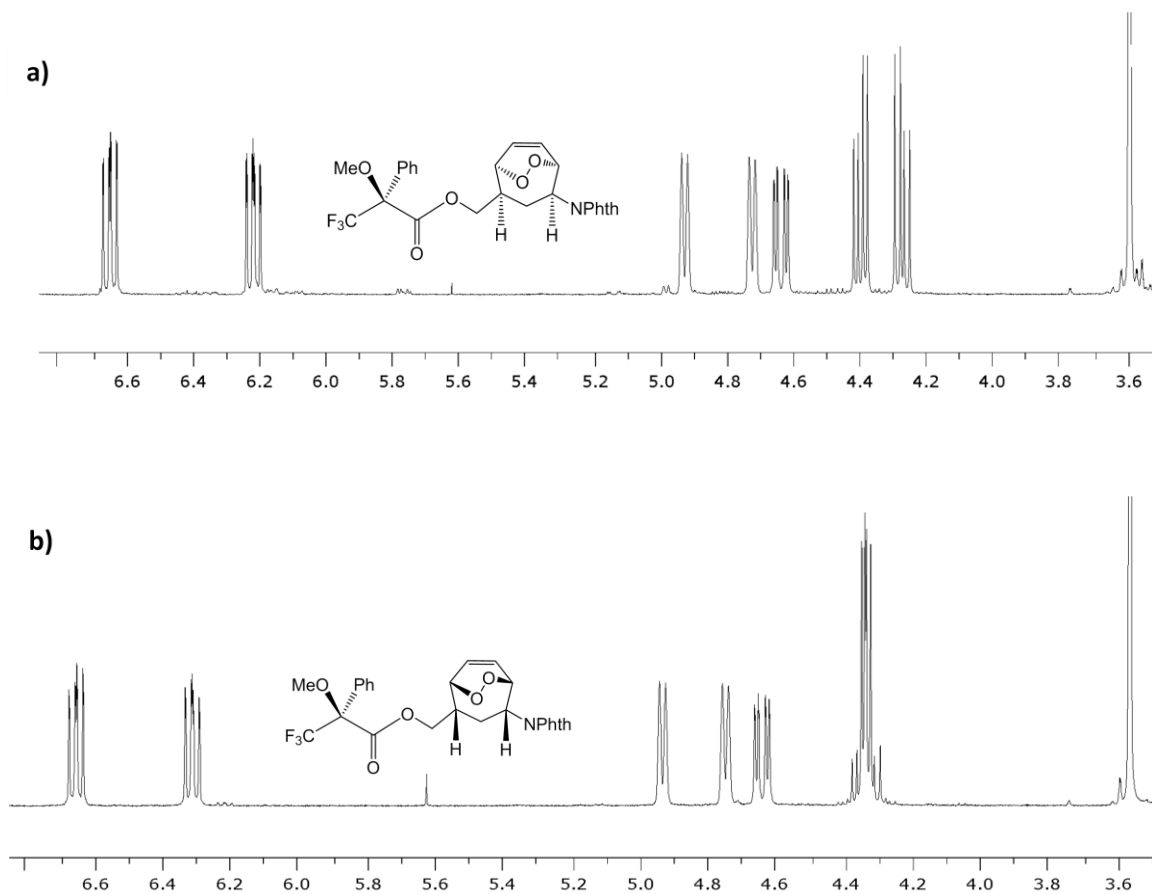
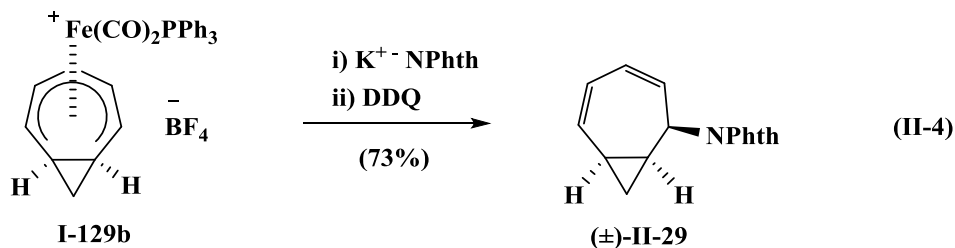


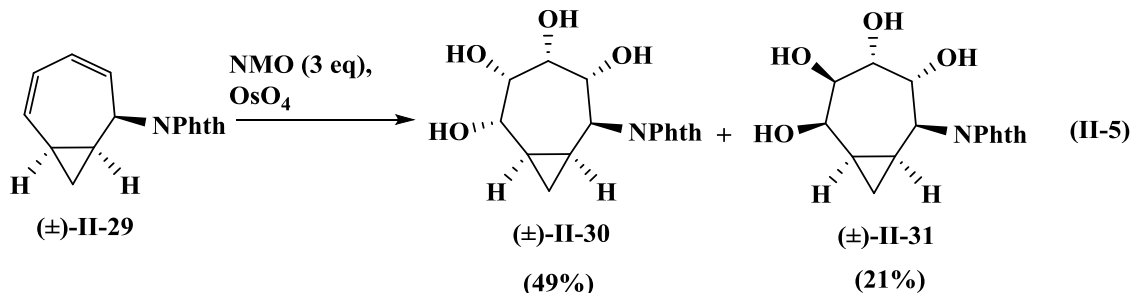
Figure II-2. a) Partial ^1H NMR spectra of **II-27** in $(\text{CD}_3)_2\text{CO}$ (scale in δ ppm). b) Partial ^1H NMR spectra of **II-28** in $(\text{CD}_3)_2\text{CO}$ (scale in δ ppm).

II.3. Preparation of bicyclo[5.1.0]octane derivatives of cyclitols

The preparation of the bicyclooctadienyl phthalimide (\pm)-**II-29** was accomplished by nucleophilic attack of potassium phthalimide on the bicyclic cation **I-129b**. The purification of the resultant complex was found to be challenging due to its relative instability in solutions and/or to exposure to typical chromatographic adsorbents (Al_2O_3 , SiO_2) which promotes the elimination reaction to go back to (\pm)-**I-118**.¹²⁵ For this reason, oxidative decomplexation of the crude complex using 2,3-dichloro-5,6-dicyano-1,4-benzoquinone (instead of CAN which was reported in literature¹²⁵) led to good isolated yield of the corresponding bicyclic phthalimide compound (\pm)-**II-29** (eqn. II-4). The NMR spectral data of (\pm)-**II-29** was consistent with the literature values.¹²⁵



With this bicyclic free ligand (\pm)-**II-29** in our hands, routes to a diverse series of polyols were explored. Exhaustive dihydroxylation using excess of *N*-methylmorpholine-*N*-oxide and catalytic amount of OsO_4 resulted in two separable diastereomers (\pm)-**II-30** and (\pm)-**II-31** respectively (eqn. II-5).



The assignment of the relative stereochemistry for (\pm)-**II-30** was based on its ^1H NMR spectral data; in particular the coupling constant between H^2 and H^3 is large (10.6 Hz) indicating that those two protons exhibit a *trans* diaxial orientation. Protons H^3 and H^4 must be *cis* to each other because dihydroxylation takes place in a *syn* fashion. The coupling constant for H^4 and H^5 is small (2.2 Hz) showing that they possess *cis* orientation and again H^6 and H^5 must be same side. The ^{13}C NMR spectrum of (\pm)-**II-30** showed a separate signal for each of the six aromatic carbons. It is proposed that these carbons are magnetically non-equivalent due to restricted rotation of the phthalimide group as a result of the hydrogen bond formation as shown in (Figure II-3).

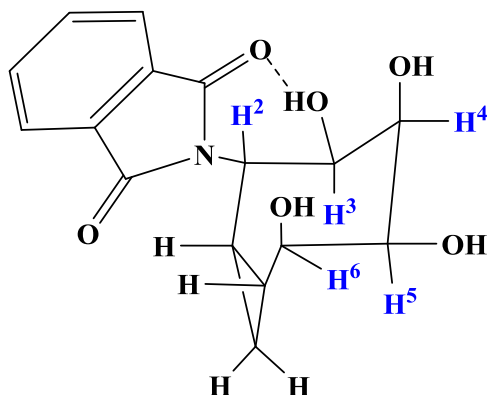


Figure II-3. Structural assignment of (\pm)-**II-30**.

This assignment was consistent with the structure obtained from single crystal X-ray diffraction analysis (Figure II-4) where all OH groups are in same side and *trans* to the phthalimide group.

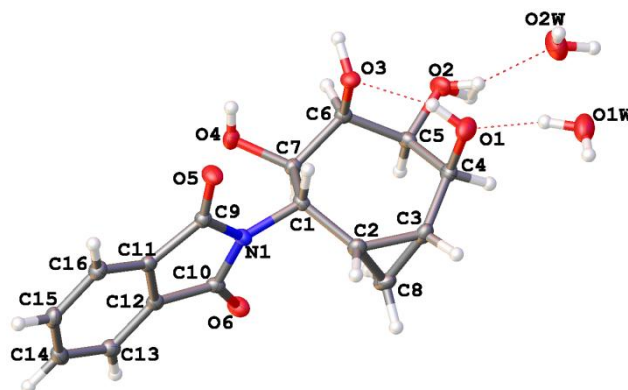


Figure II-4. X-ray crystal structure of (±)-II-30.

In similar fashion, the relative stereochemistry of (±)-II-31 was assigned on the basis of its ^1H NMR spectral data; the large coupling constant between the H^2 and H^3 (11.2 Hz) is consistent with their *trans* diaxial orientation. This was confirmed by single crystal X-ray diffraction analysis (Figure II-5).

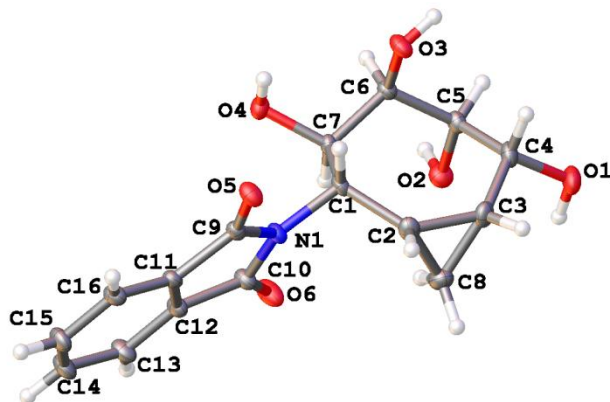
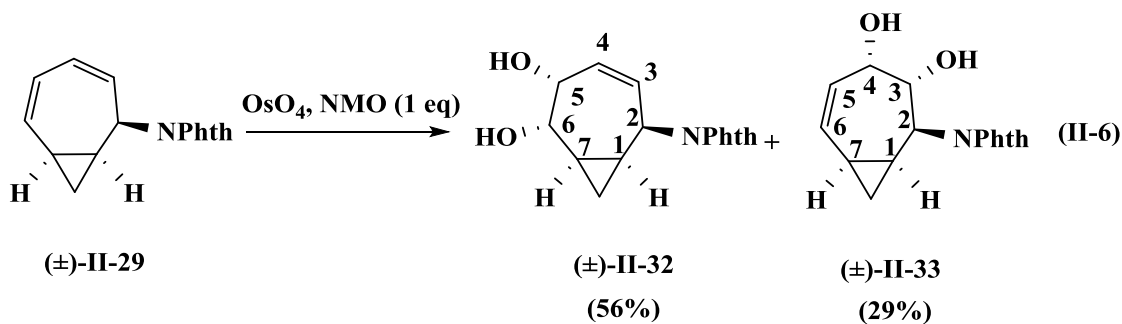


Figure II-5. X-ray crystal structure of (±)-II-31.

When (±)-II-29 was treated with one equivalent of methylmorpholine-*N*-oxide in the presence of a catalytic amount of OsO₄, two regioisomeric diols were obtained, a major product (±)-II-32 and a minor one (±)-II-33 (eqn. II-6).



The structures of the two regioisomers were assigned by comparison of their ¹H NMR spectral data. The major product (±)-II-32 arises due to reaction of the more electron rich double bond remote to the phthalimide group and close to cyclopropane ring. The chemical shift for the H² proton of (±)-II-32 (δ = 5.68 ppm) is shifted more downfield than it is for (±)-II-33 (δ = 5.25 ppm) indicating the proximity of this proton to

the double bond in (\pm)-**II-32**. The relative stereochemistry of (\pm)-**II-33** was assigned due to the large coupling constant (10.6 Hz) between H² and H³ which indicates a *trans*-diaxial orientation for these two protons (Figure II-6).

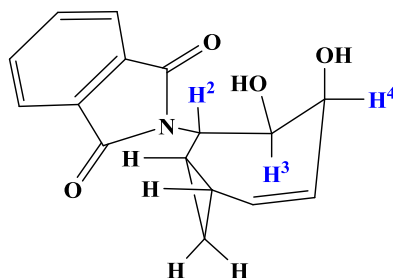
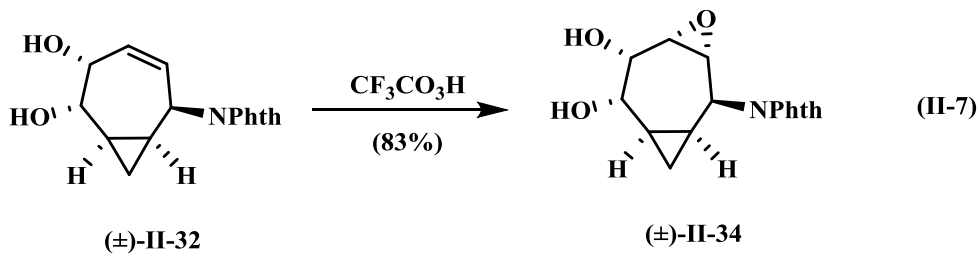
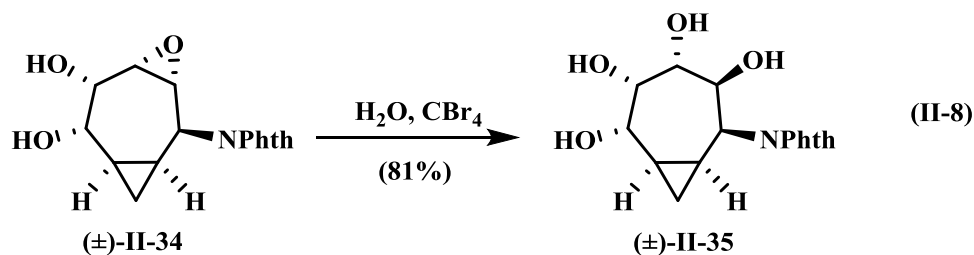


Figure II-6. Structural assignments of (\pm)-**II-33**.

Epoxidation of the major regioisomer (\pm)-**II-32** was carried out using trifluoroperacetic acid to give the corresponding epoxydiol compound (\pm)-**II-34** (eqn. II-7). The ¹H NMR spectrum shows an absence of signals for olefinic protons and new peaks appeared at the range of δ 3-5 ppm. The relative stereochemistry of (\pm)-**II-34** was assigned tentatively based on the precedent⁸⁶ that epoxidation is assisted by hydrogen bonding between the allylic alcohol and the peracid reagent.

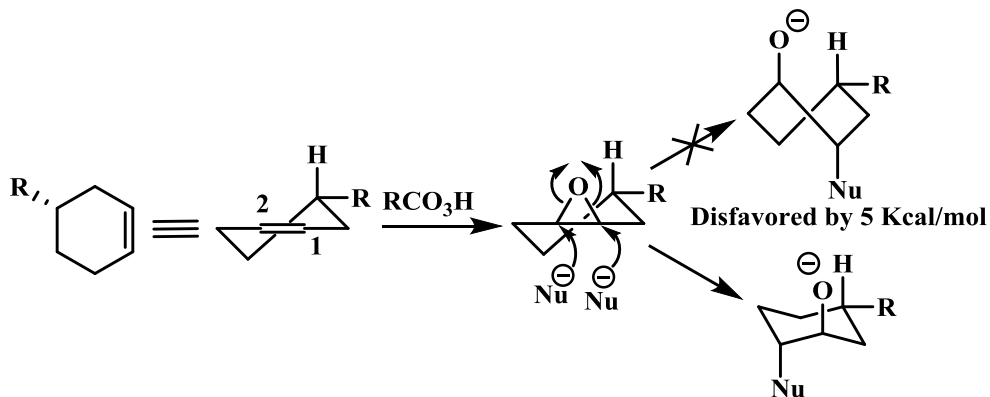


Epoxide hydrolysis was carried out in a mild condition using deionized water in the presence of a catalytic amount of CBr_4 ¹³⁸ to afford tetraol compound (\pm)-**II-35** (eqn. II-8).



The relative stereochemistry of (\pm)-**II-35** was assigned on the basis of its ^1H NMR spectral data; a small coupling constant between H^2 and H^3 (2.2 Hz) indicated a *cis* orientation of these two protons.

The stereochemical outcome of the epoxide hydrolysis is controlled by Fürst-Plattner rule which also known as the *trans*-diaxial effect¹³⁹ in which epoxidation of substituted cyclohexene give the corresponding epoxy product where R substituent locks the conformation of the epoxycyclohexene in the *pseudo*-equatorial position (Scheme II-12). Two potential sites for epoxide ring opening, position 1 where it ends up having twisted boat product and this path is disfavored because it about 5 Kcal/mol higher than opening at position 2 which gives chair form product leading to the formation of *trans*-diaxial products.



Scheme II-12. Mechanism and stereochemistry of epoxycyclohexene hydrolysis.

Since epoxide ring opening takes place in an *anti* fashion,¹³⁹ the two hydroxyl group at C3 and C4 must be *trans* to each other (Figure II-7).

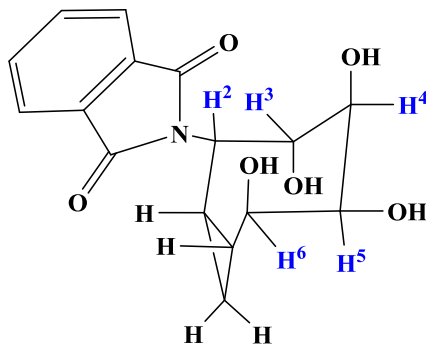
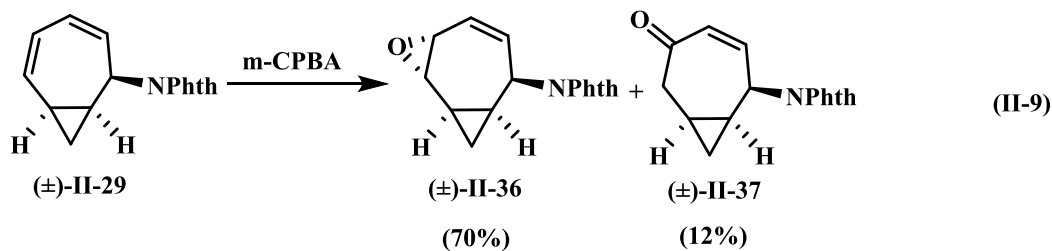


Figure II-7. Epoxide ring opening product (±)-II-35.

The reaction of (±)-II-29 with one equivalent of meta-chloroperoxybenzoic acid led to a separable mixture of mono-epoxide (±)-II-36 and enone (±)-II-37 (eqn. II-9). Evidence of epoxidation of only a single olefin in (±)-II-36 was found in its NMR spectral data; in the ¹H NMR spectrum only two olefinic signals were observed and two

new peaks appeared at $\delta \approx 3$ ppm corresponding to the oxirane hydrogens. In the ^{13}C NMR spectrum of (\pm)-**II-36** there are only two sp^2 olefinic carbons compared to (\pm)-**II-29** and two new sp^3 C-O peaks appear for (\pm)-**II-36** at δ 52.8 and 54.9 ppm. The relative stereochemistry of (\pm)-**II-36** was assigned by single crystal X-ray diffraction analysis (Figure II-8) where the epoxide ring shows to be *trans* to the phthalimide group. On the other hand, the ^1H NMR spectrum of the enone (\pm)-**II-37** showed two new peaks at δ 2.93 and 3.10 ppm corresponding to the α -keto methylene with a large coupling constant ($J = 15.2$ Hz) indicating a geminal relationship. Moreover, there were two fewer olefinic peaks in the ^{13}C NMR spectrum of (\pm)-**II-37** compared to (\pm)-**II-36**. This also was supported by the ^{13}C NMR spectral data of (\pm)-**II-37** where a new signals for a CH_2 signal and a $\text{C}=\text{O}$ were observed at δ 41.5 and 198.9 ppm respectively.



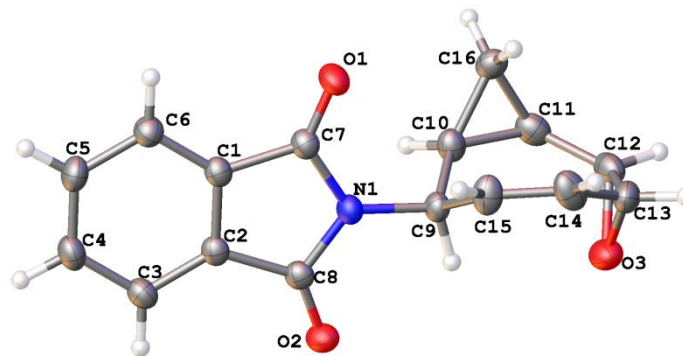
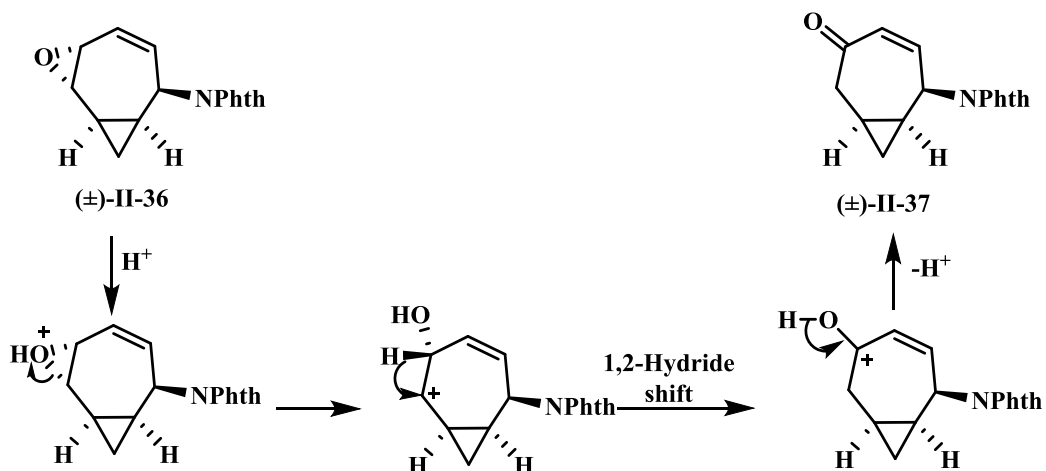


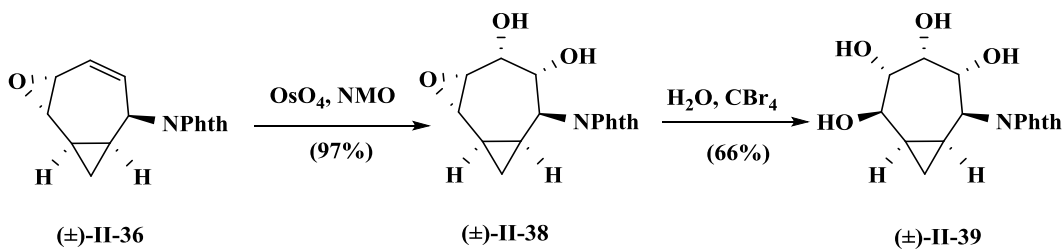
Figure II-8. X-ray crystal structure of (±)-**II-36**.

The proposed mechanism for formation of (±)-**II-37** is shown in (Scheme II-13); under acidic conditions (±)-**II-36** gets protonated. Oxirane ring opening occurs at the bond adjacent to the cyclopropane ring to give a carbocation intermediate followed by 1,2-hydride shift to afford an oxycarbenium cation which deprotonated to provide (±)-**II-37**.



Scheme II-13. Mechanism of enone (±)-**II-37** formation.

Dihydroxylation of (\pm)-**II-36** using a catalytic amount of OsO₄ and *N*-methylmorpholine-*N*-oxide gave (\pm)-**II-38** in a good yield (Scheme II-14). The structure of (\pm)-**II-38** was assigned on the basis of single crystal X-ray diffraction analysis where the newly installed OH groups are on the same side as the peroxide ring and opposite to the phthalimide group (Figure 6). Peroxide ring opening of (\pm)-**II-38** was carried out in water using carbon tetrabromide as a catalyst to afford the corresponding bicyclic tetraol (\pm)-**II-39**. The structure of (\pm)-**II-39** was assigned based on its ¹H NMR spectral data; in particular the large coupling constant between H²-H³ (J = 11.0 Hz) and between H⁵-H⁶ (J = 9.6 Hz) are consistent with a *trans*-diaxial relationship for each pair of protons (Figure II-10).



Scheme II-14. Formation of bicyclic tetraol (\pm)-**II-39**.

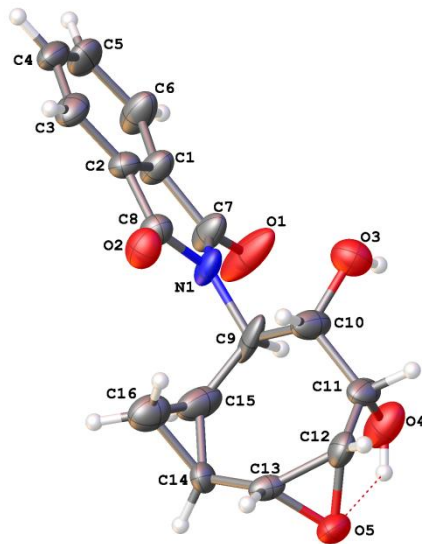


Figure II-9. X-ray crystal structure of (±)-**II-38**.

The stereochemistry observed in tetraol (±)-**II-39** represents epoxide ring opening of (±)-**II-38** by exclusive cleavage of the C13-O5 bond (vs C12-O5 bond; arbitrary X-ray structure numbering). This might be rationalized on the basis of a greater stabilization of the partial positive charge on the protonated carbon adjacent to the cyclopropane ring.

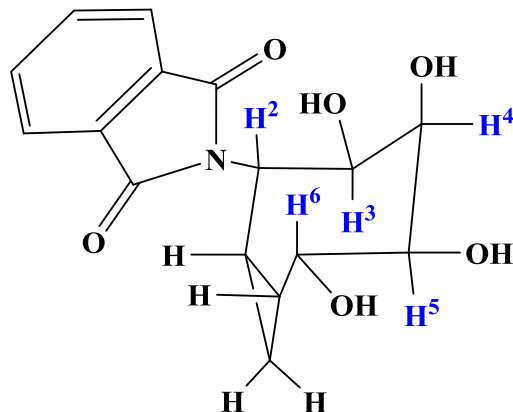
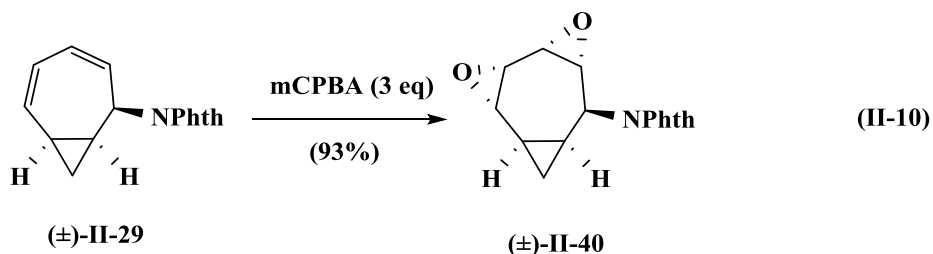


Figure II-10. Structural assignments of (±)-II-39.

Reaction of (±)-II-29 with an excess of meta-chloroperoxybenzoic acid led to the formation of bis-epoxide compound (±)-II-40 (eqn. II-10).



The structure of (±)-II-40 was assigned based on its ^1H NMR spectral data; no olefinic proton signals were observed and instead, four new peaks showed up at $\delta \approx 3$ ppm. This also was observed in the ^{13}C NMR spectrum where four new signals appeared in the range of 50-60 ppm. The relative stereochemistry of (±)-II-40 was assigned based on single crystal X-ray diffraction showing the two epoxide rings are *anti* to the phthalimide group (Figure II-11).

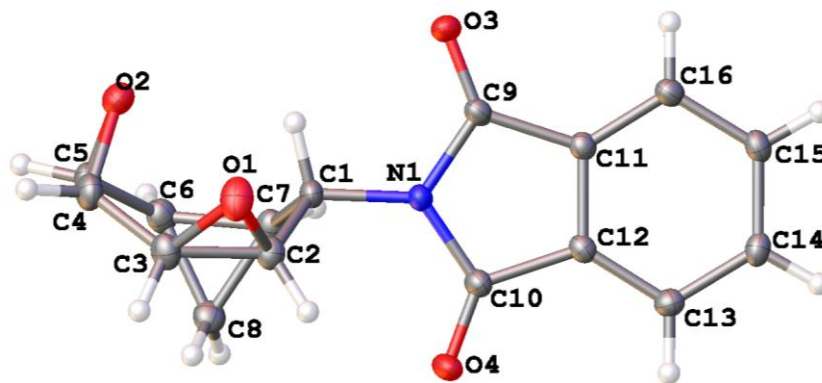
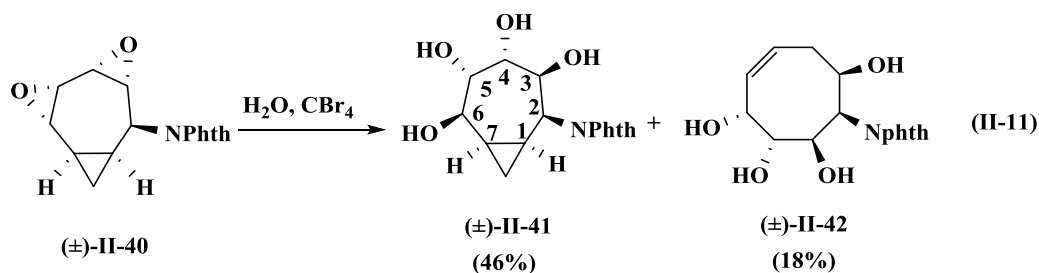


Figure II-11. X-ray crystal structure of (±)-II-40.

This bisepoxide compound (±)-II-40 underwent epoxide ring opening using water and CBr_4 in a catalytic amount to give bicyclic tetraol (±)-II-41 and the 8-membered ring tetraol (±)-II-42 (eqn. II-11).



The assignment of stereochemistry of (±)-II-41 was based on its ^1H NMR spectral data; in particular the coupling constant between H^2 and H^3 is small (2.2 Hz) indicating that they possess a *cis* orientation since the H^2 proton adjacent to the bulky phthalimide is axial, the H^3 proton must be equatorial. In contrast, the relatively large coupling constant for H^5 - H^6 reveals that these two protons must have a *trans*-diaxial relationship. Since epoxide ring openings are known to occur in an *anti* fashion, the H^3 -

H^4 and H^5 - H^6 relative stereochemistry is assigned as indicated (Figure II-12). It is interesting to note that opening of the C4-C5 oxirane occurs by cleavage of the C5-O2 bond, which is adjacent to the cyclopropane ring. As in the case of the epoxide ring opening of (\pm)-**II-38**, this may be due to the stabilizing effect of the adjacent three-membered ring on the partial positive charge in the protonated oxirane.

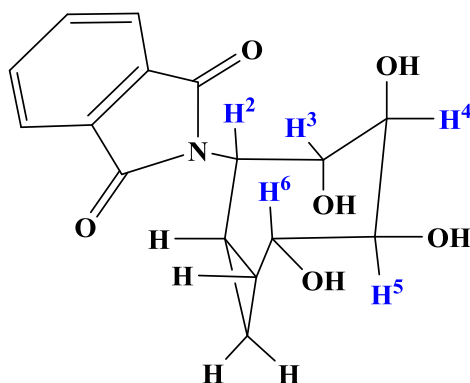


Figure II-12. The assignment of stereochemistry of (\pm)-**II-41**.

Examination of the 1H NMR spectral data for (\pm)-**II-42** revealed an absence of cyclopropane ring protons, the presence of the two olefinic protons and two new geminal aliphatic protons. The structure of (\pm)-**II-42**, including the relative stereochemistry was assigned based on single crystal X-ray diffraction (Figure II-13).

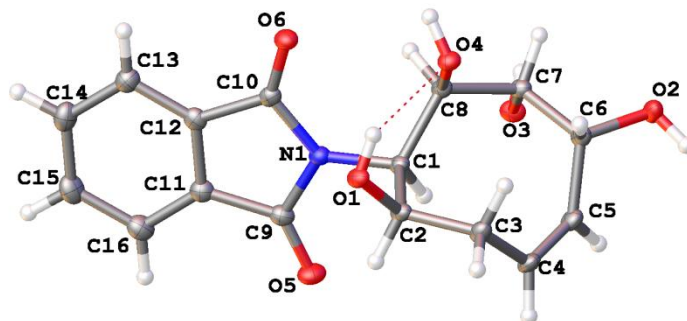
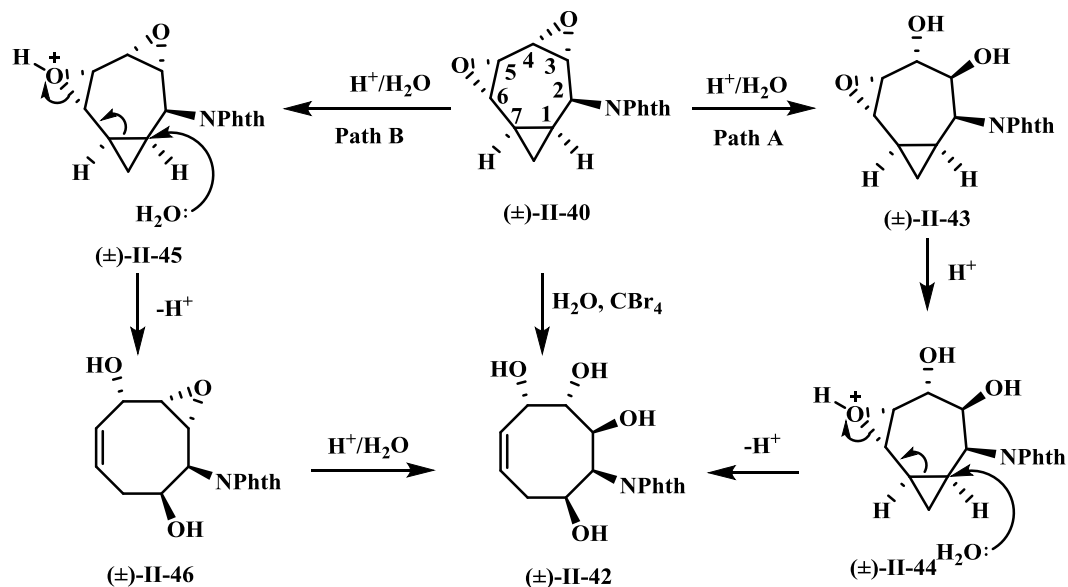


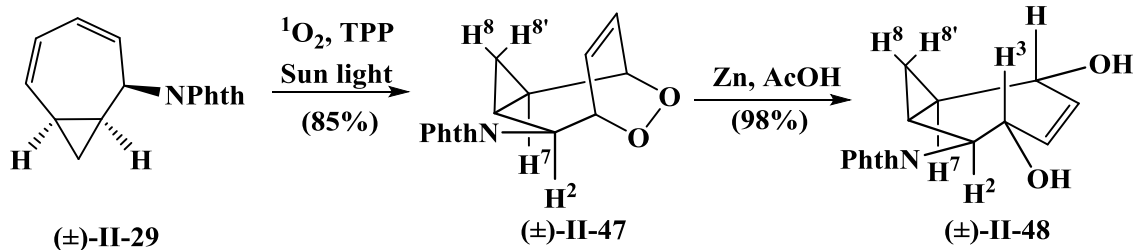
Figure II-13. X-ray crystal structure of (±)-**II-42**.

The proposed mechanism for ring expansion to afford (±)-**II-42** is rationalized through two different pathways (Scheme II-15). In path A, hydrolysis of the epoxide at C3,C4 takes place first to give epoxydiol compound (±)-**II-43** which under protonation of C5,C6 epoxide gave the intermediate (±)-**II-44**. A concerted S_N2' type mechanism with attack of the weak nucleophile water at the cyclopropane ring carbon of (±)-**II-44** opens the cyclopropane ring with inversion and relieves the strain to end up with octene-tetraol compound (±)-**II-42**. While in path B, initial concerted S_N2' attack of a water molecule on the protonated intermediate (±)-**II-45** gives epoxyoctene (±)-**II-46** that undergoes epoxide ring opening to give (±)-**II-42**.



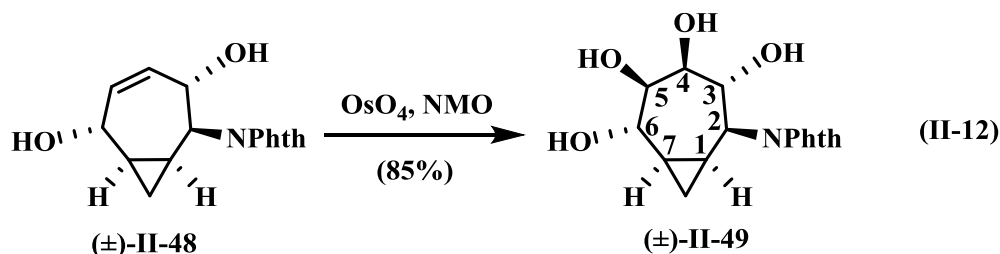
Scheme II-15. Ring expansion mechanism and formation of **(±)-II-42**.

Cycloaddition of **(±)-II-29** with singlet oxygen gave **(±)-II-47** as a single diastereomer (Scheme II-16). The relative stereochemistry of **(±)-II-47** was tentatively assigned on the basis of the stereochemistry observed for the cycloaddition of **(±)-II-29** with nitrosobenzene.¹⁴⁰ This tentative assignment was eventually corroborated by further chemical reaction including X-ray crystal structure of one derivative. Reduction of **(±)-II-47** was carried out using activated zinc and glacial acetic acid to afford the diol derivative **(±)-II-48** in a good yield. The relative stereochemistry of **(±)-II-48** was assigned on the basis of its NMR spectral data; in particular the large coupling constant between H^2 and H^3 (10.8) Hz indicating these two protons are *trans* diaxial with respect to each other. Based on this the endoperoxide ring in **(±)-II-47** must be *trans* to the phthalimide group.



Scheme II-16. Singlet oxygen cycloaddition of $(\pm)\text{-II-29}$ followed by endoperoxide ring opening.

Dihydroxylation of $(\pm)\text{-II-48}$ using a catalytic amount of OsO_4 and *N*-methylmorpholine-*N*-oxide gave $(\pm)\text{-II-49}$ in a good yield (eqn. II-12).



The structural assignment of $(\pm)\text{-II-49}$ was based on its ^1H NMR spectral data; in particular the large coupling constants between H^2 and H^3 (10.2 Hz) and between H^3 - H^4 (10.0 Hz) indicate the *trans*-diaxial orientations of these three protons. Since dihydroxylation takes place in a *syn* fashion then H^4 and H^5 are *cis* with respect to each other (Figure II-14). This was confirmed by having small coupling constant between H^4 and H^5 (2.7 Hz). This assignment is consistent with the Kishi model^{136,137} for osmium dihydroxylation of allylic alcohols.

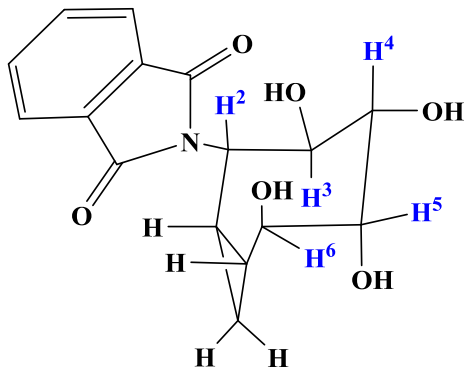
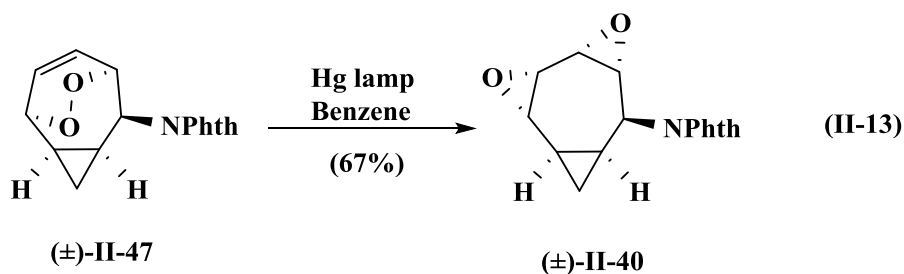


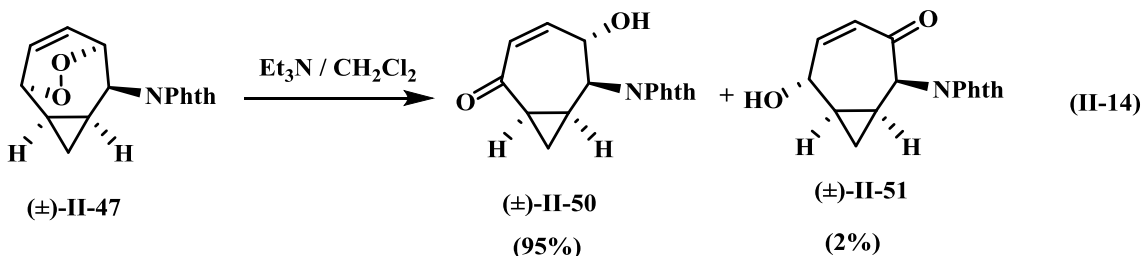
Figure II-14. Structural assignment of (±)-**II-49**.

Photochemical rearrangement of (±)-**II-47** was carried out in benzene as a solvent and using a medium-pressure mercury lamp to give the bisepoxide compound (±)-**II-40** which was identified by comparison to a sample previously made (*vide supra*) (eqn. II-13).

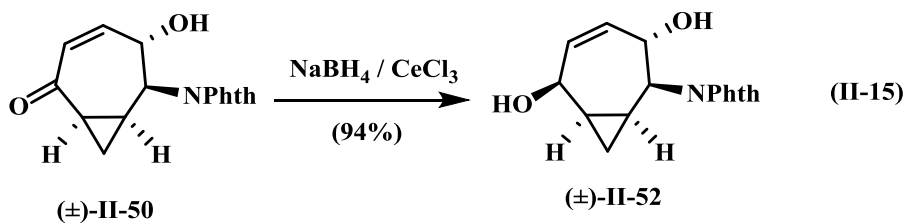


Kornblum–DeLaMare rearrangement⁸⁴ of (±)-**II-47** in the presence of Et₃N as a base afforded primarily one regioisomer; (±)-**II-50** along with a very small amount of (±)-**II-51** (eqn. II-14). The structural assignment of (±)-**II-50** was based on its ¹H NMR spectral data; in particular the signal for the H² proton appears at δ 4.95 has a large

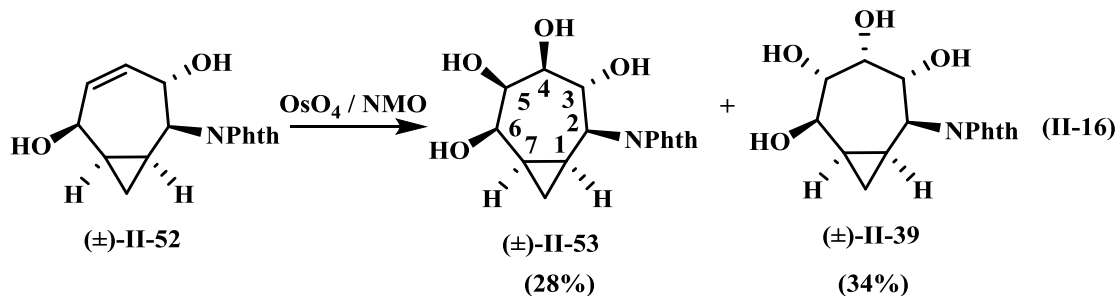
coupling constant ($J = 10.2$ Hz) indicating a *trans*-diaxial orientation with the proton next to it (H^3).



Reduction of α,β -unsaturated ketone $(\pm)\text{-II-50}$ under Luche conditions⁸⁵ provided *trans* enediol $(\pm)\text{-II-52}$ (eqn. II-15). The stereochemistry of the OH group at C6 was assigned in order to be unique compared to $(\pm)\text{-II-48}$.



Dihydroxylation of $(\pm)\text{-II-52}$ using a catalytic amount of OsO_4 and *N*-methylmorpholine-*N*-oxide gave a separable mixture of two diastereomers $(\pm)\text{-II-53}$ and $(\pm)\text{-II-39}$ (eqn. II-16). Product $(\pm)\text{-II-39}$ was assigned by comparison of its NMR spectral data with that previously obtained.



The other tetraol product was tentatively assigned structure $(\pm)\text{-II-53}$ in order to have a unique structure arising from a *syn*-dihydroxylation. This tentative assignment was corroborated by its ^1H NMR spectral data; large couplings constant between H^2 and H^3 (11.0 Hz) and between H^3 and H^4 (9.8 Hz) indicating a *trans*-diaxial orientation of these three protons. The small coupling constant between H^4 and H^5 (1.4 Hz), is consistent with an axial-equatorial stereochemical relationship between these protons (Figure II-15).

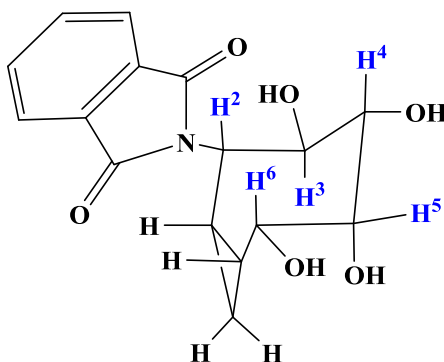
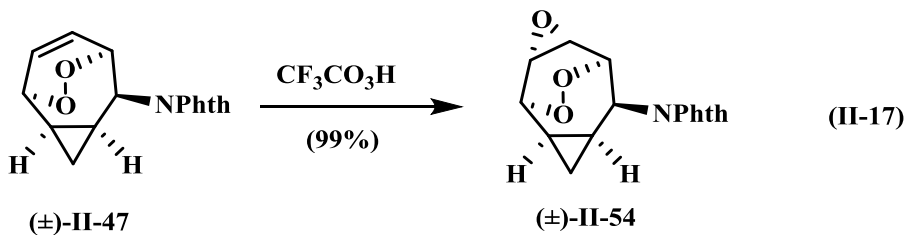


Figure II-15. Structural assignment of $(\pm)\text{-II-53}$.

Epoxidation of $(\pm)\text{-II-47}$ using trifluoroperacetic acid gave a unique epoxyendoperoxide structure $(\pm)\text{-II-54}$ in a very high yield (eqn. II-17).



The relative stereochemistry of (±)-II-54 was assigned based on single crystal X-ray diffraction showing the endoperoxide ring and the epoxy ring are *syn* with respect to each other (Figure II-16).

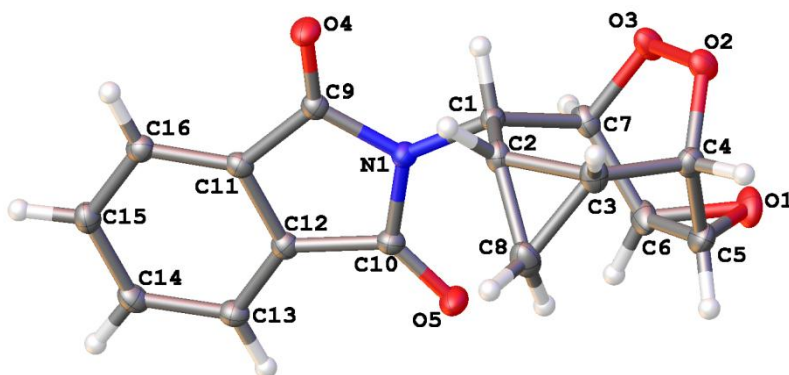
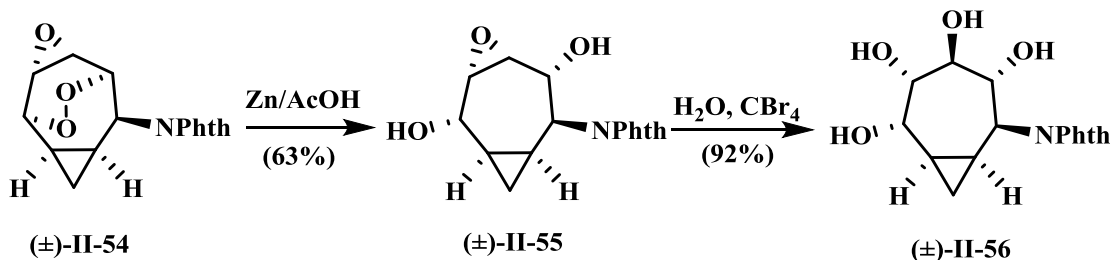


Figure II-16. X-ray crystal structure of (±)-II-54.

Reduction of epoxyendoperoxide compound (±)-II-54 using zinc in glacial acetic acid gave epoxydiol (±)-II-55 (Scheme II-17). Hydrolysis of (±)-II-55 in water and catalytic amount of CBr_4 ¹³⁸ gave the bicyclic tetraol (±)-II-56.



Scheme II-17. Synthesis of $(\pm)\text{-II-56}$.

The structural assignment of $(\pm)\text{-II-56}$ was based on its ^1H NMR spectral data; large coupling constants between H^1 and H^2 (10.8 Hz), H^3 and H^4 (9.0 Hz) and H^4 and H^5 ($J = 8.8$ Hz) indicating a *trans*-diaxial orientation of these four protons (Figure II-17).

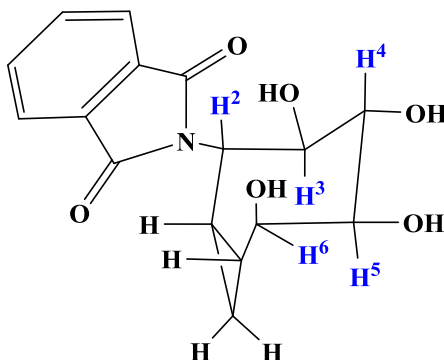


Figure II-17. Structural assignment of $(\pm)\text{-II-56}$.

This structural assignment for $(\pm)\text{-II-56}$ was corroborated by single crystal X-ray diffraction (Figure II-18). This structural assignment also confirmed the structural assignment for the hydroxyl groups of epoxydiol $(\pm)\text{-II-55}$.

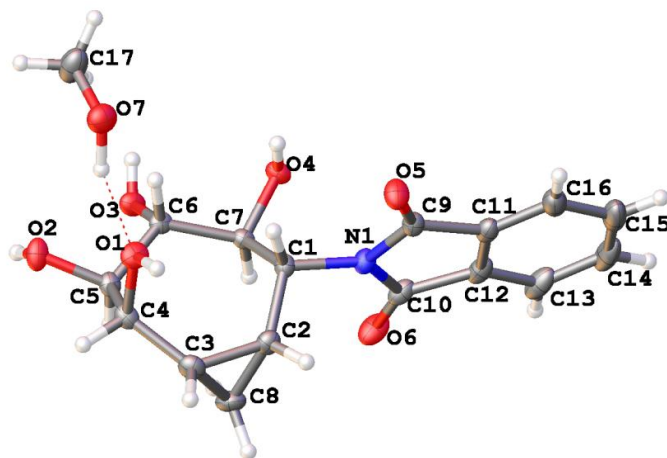
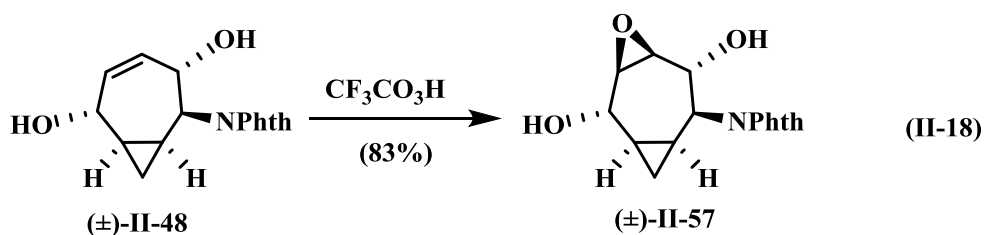


Figure II-18. X-ray crystal structure of (±)-II-56.

Epoxidation of (±)-II-48 using trifluoroacetic acid gave the corresponding epoxydiol (±)-II-57 (eqn. II-18). The relative stereochemistry of (±)-II-57 was assigned in order to be unique compared to (±)-II-55. This tentative stereochemical assignment was eventually corroborated by single crystal X-ray diffraction that shows the epoxide ring is opposite to the installed diol (Figure II-19).



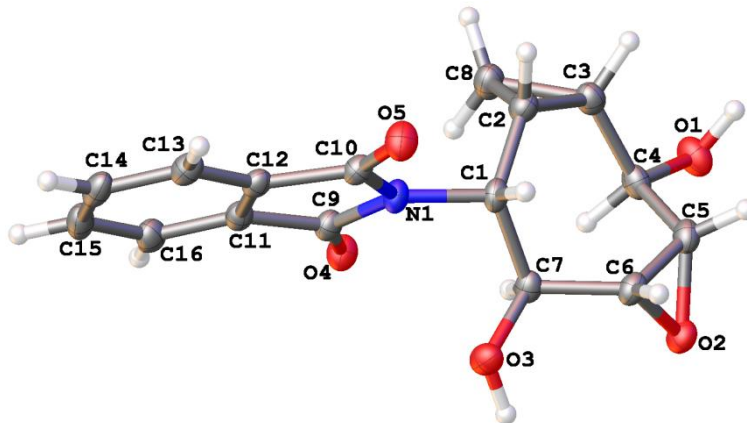
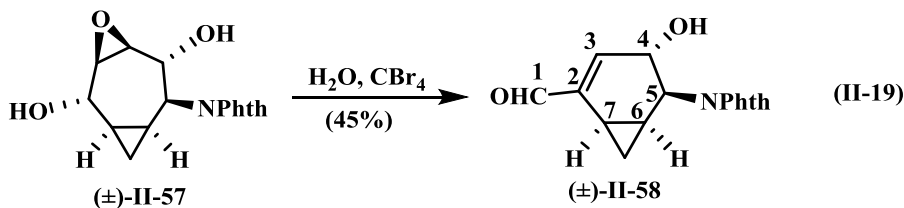


Figure II-19. X-ray crystal structure of (±)-II-57.

Epoxide ring opening under the standard conditions using deionized water and CBr_4 afforded the corresponding unsaturated aldehyde (±)-II-58 (eqn. II-19).



The structural assignment of (±)-II-58 was based on its ^1H NMR spectral data; in particular the peak at δ 9.54 shows one aldehydic proton. The large coupling constant (8.2 Hz) between the H4 and H5 is indicative of their *trans*-diaxial orientation. This assignment was corroborated by single crystal X-ray diffraction analysis that shows ring contraction with exocyclic aldehyde group (Figure II-20).

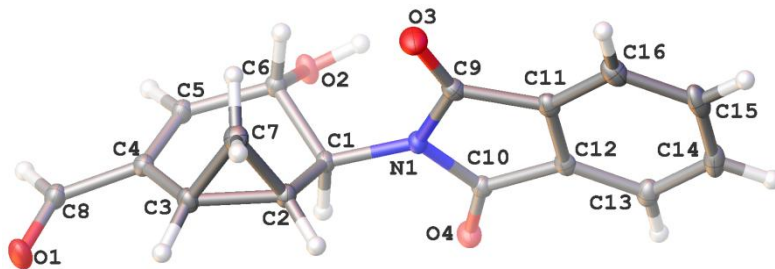
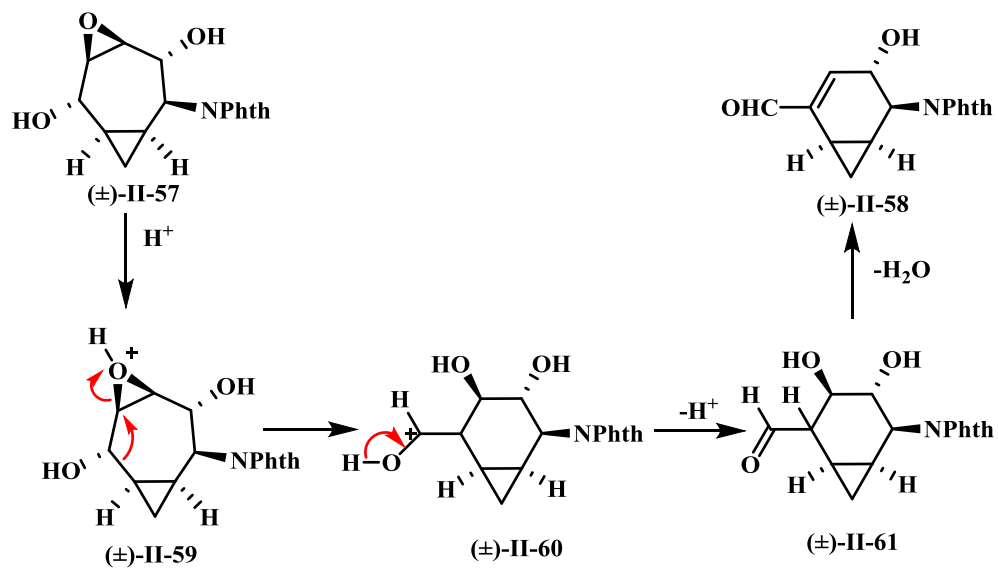


Figure II-20. X-ray crystal structure of (±)-**II-58**.

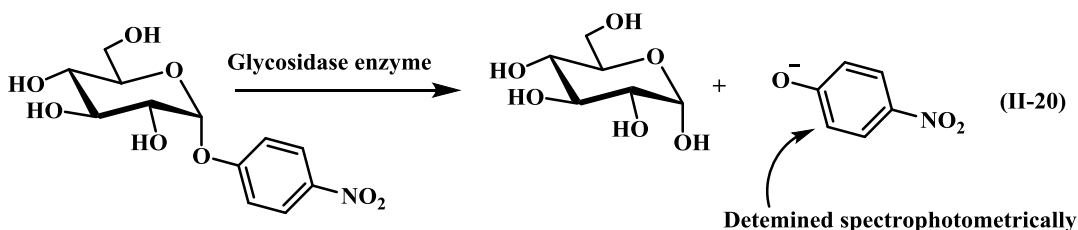
The proposed ring contraction mechanism is initiated by protonating the epoxide oxygen making it a good electron sink to give intermediate (±)-**II-59** (Scheme II-18). The nearly antiperiplanar alignment of (±)-**II-59** between C3-C4 bond and C5-O2 bond (X-ray crystallographic numbering, Figure II-19) triggers $\sigma \rightarrow \sigma^*$ type interaction between the filled bonding orbital between C3-C4 bond and the antibonding orbital of C5-O2 bond (Figure II-19) giving oxocarbenium intermediate (±)-**II-60** which upon deprotonation leads to the aldehyde diol compound (±)-**II-61**. To extend the conjugation and to attain more stability, dehydration takes place to give the corresponding α,β -unsaturated aldehyde (±)-**II-58**. Similar ring contraction reactions have been reported by different research groups where they observed ring contraction from epoxycyclohexanol to 2-hydroxycyclopentenal¹⁴¹⁻¹⁴³.



Scheme II-18. Ring contraction mechanism and formation of (±)-II-58.

II.4. Evaluation of potential β -glycosidase inhibitors

β -Glucosidase is an enzyme which cleaves the β linkage between the β -D-glucoside and an attached substituent, for the purposes of this assay, the substrate is p- β -D-glucoside, since the p-nitrophenolate anion may be quantified spectrophotometrically (Equation II-20). This system was selected for the initial assay as both the enzyme (isolated from almonds) and substrate are commercially available at reasonable cost. Depending on the results from this assay, a determination would be made if further assays against other glucosidases enzyme was warranted on cost and time basis. The enzymatic activity is determined spectrophotometrically by monitoring the release of p-nitrophenol/ p-nitrophenolate anion from the substrate in sodium acetate buffer (pH 4.8, 37 °C) by measuring the absorbance at 405 nm. Assays will be conducted under conditions where the amount of p-nitrophenol released is linear with both time and protein concentrations.



The assay was validated by measuring the initial rate of reaction at a variety of different enzyme concentrations. An increase in the initial reaction rate was observed with each increase in enzyme concentration. The linear region was then selected which shows increase in reaction rate with time for each enzyme concentration (Figure II-21).

The initial rates were plotted against enzyme concentration to produce a validation curve (Figure II-22).

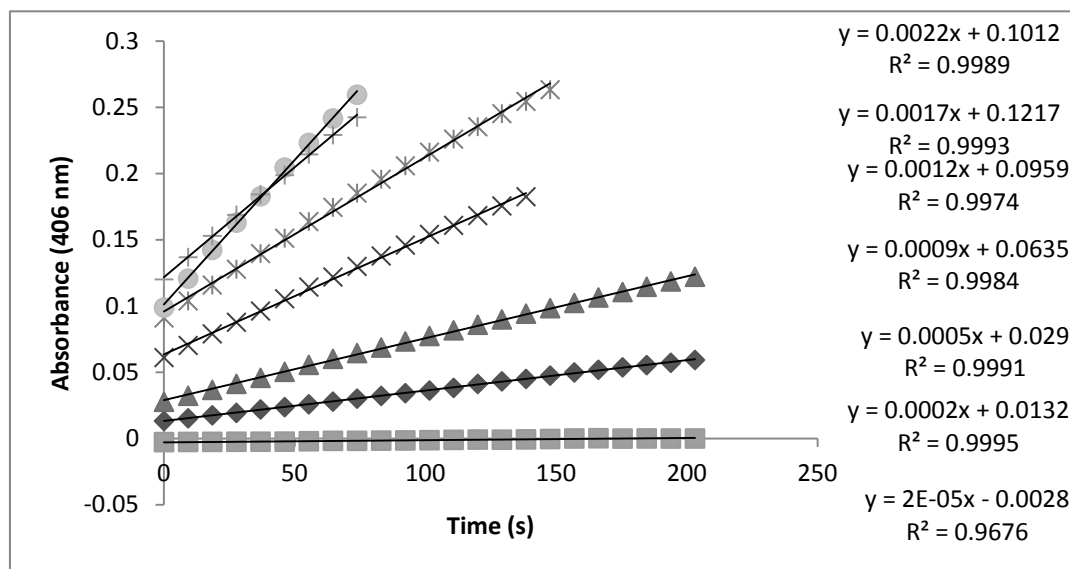


Figure II-21. Linear relationship between initial reaction rate for each enzyme and time.

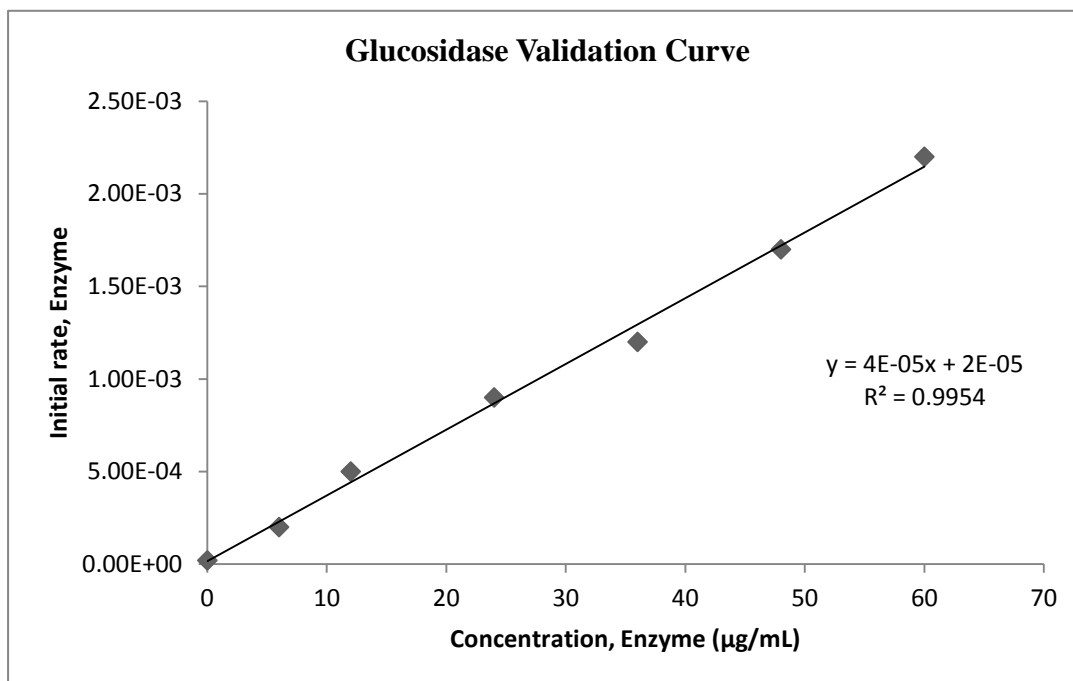


Figure II-22. β -glucosidase validation curve.

Once the linear rate of the hydrolysis versus protein concentration was established, an assay was run using the known β -glucosidase xylitol.¹⁴⁴ The inhibitory effect measured at 100mM xylitol concentration was similar to that reported by Kelemen and Whelan (43% inhibition). With this assay validation complete, the assay was performed by preparing serial dilution of each potential enzyme and the 50% inhibitory concentration for each compound was determined. The results are summarized in Table II-1. The error limitations listed were determined by a non-linear least square fit. For nearly all the phthalimido polyols examined, except **II-49**, the error limitations were on the same order as the IC_{50} values. This indicates that the inhibitory activities of these compounds is negligible. Only for **II-49** was the error ~15%, which demonstrated an

acceptable reliability. The IC_{50} for **II-49** indicates it has limited inhibitory action at approximately 1 mM.

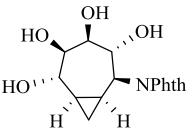
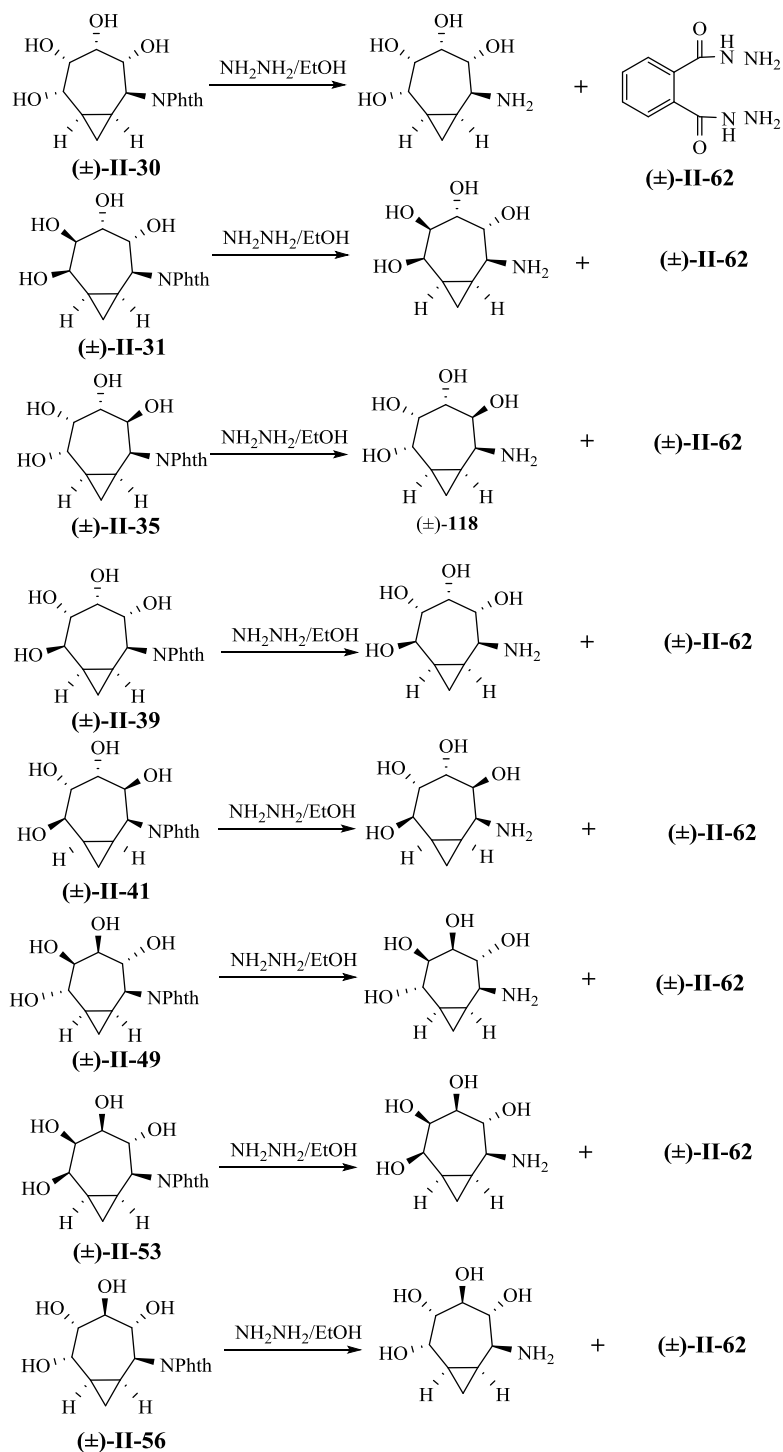
Compound	Inhibition
II-30	$IC_{50} = 1.7 \text{ mM} \pm 1.2 \text{ mM}$
II-31	$IC_{50} = 160 \text{ } \mu\text{M} \pm 60 \text{ } \mu\text{M}$
II-35	$IC_{50} = 42 \text{ } \mu\text{M} \pm 48 \text{ } \mu\text{M}$
II-39	$IC_{50} = 1.9 \text{ mM} \pm 3.2 \text{ mM}$
II-41	$IC_{50} = 43 \text{ } \mu\text{M} \pm 34 \text{ } \mu\text{M}$
 II-49	$IC_{50} = 0.91 \text{ } \mu\text{M} \pm 0.14 \text{ mM}$
II-53	$IC_{50} = 1.9 \text{ mM} \pm 3.2 \text{ mM}$
II-56	$IC_{50} = 75 \text{ } \mu\text{M} \pm 83 \text{ } \mu\text{M}$

Table II-1. The inhibition of the generated phthalimide tetraols.

The most likely reason that none of the phthalimido polyols exhibit significant β -glucosidase inhibitory activity is that at the pH of the assay, these compounds are neutral (i.e. the phthalimido group is not protonated). So it was important to cleave the phthalimide group. Different attempts were made to cleave the phthalimido group to generate aminocyclitols. Attempted acid hydrolysis lead to products which lacked cyclopropane ring in their ^1H NMR spectra. The exact nature of these ring opened

products was not established. Basic hydrolysis also was not ideal way to cleave the phthalimido group as we observed elimination products along with the desired compound. Use of anion exchange resins¹⁴⁵ gave a mixture of compounds also with very low overall yield. Ganem's research group¹⁴⁶ reported the deprotection of phthalimides using partial reduction of phthalimide by NaBH₄ in acidic medium followed by reflux. Unfortunately this did not produce the free amines for these compounds. *n*-Butylamine¹⁴⁷ and methylamine¹⁴⁸ also were used to deprotect the aminocyclitols but these procedures gave a mixture of products in addition to unreacted starting material left over. Finally, the cleavage of the phthalimido tetraols was carried out using hydrazine hydrate in ethanol to give the corresponding aminobicyclooctitols and the 2,3-dihydro-1,4-phthalazinedione **II-62** (Scheme II-19). Attempts to separate these reaction mixtures either by normal or reverse phase chromatography, met with failure. For this reason the crude residue was washed multiple times with diethyl ether and dried under vacuum. In order to determine if further experimentation to produce pure aminopolyols was warranted (on the basis of significant inhibitory activity) the mixture of the aminopolyol and phthalhydroazide were assayed against β -glucosidase using the standard protocol.¹⁴⁴ The assay results for these mixtures (Figure II-23) indicated an *activation* of the enzyme at higher concentration instead of inhibition. Separate assay of the 2,3-dihydro-1,4-phthalazinedione **II-62** against β -glucosidase revealed that this increase in enzyme activity could be attributed to the hydrazinolysis by-product, and not to any specific aminobicyclooctitol. Since the aminobicyclooctitols did not exhibit any significant activity against β -glucosidase, further assay against other commercially available enzymes was abandoned.



Scheme II-19. Deprotection of the phthalimidetetraols.

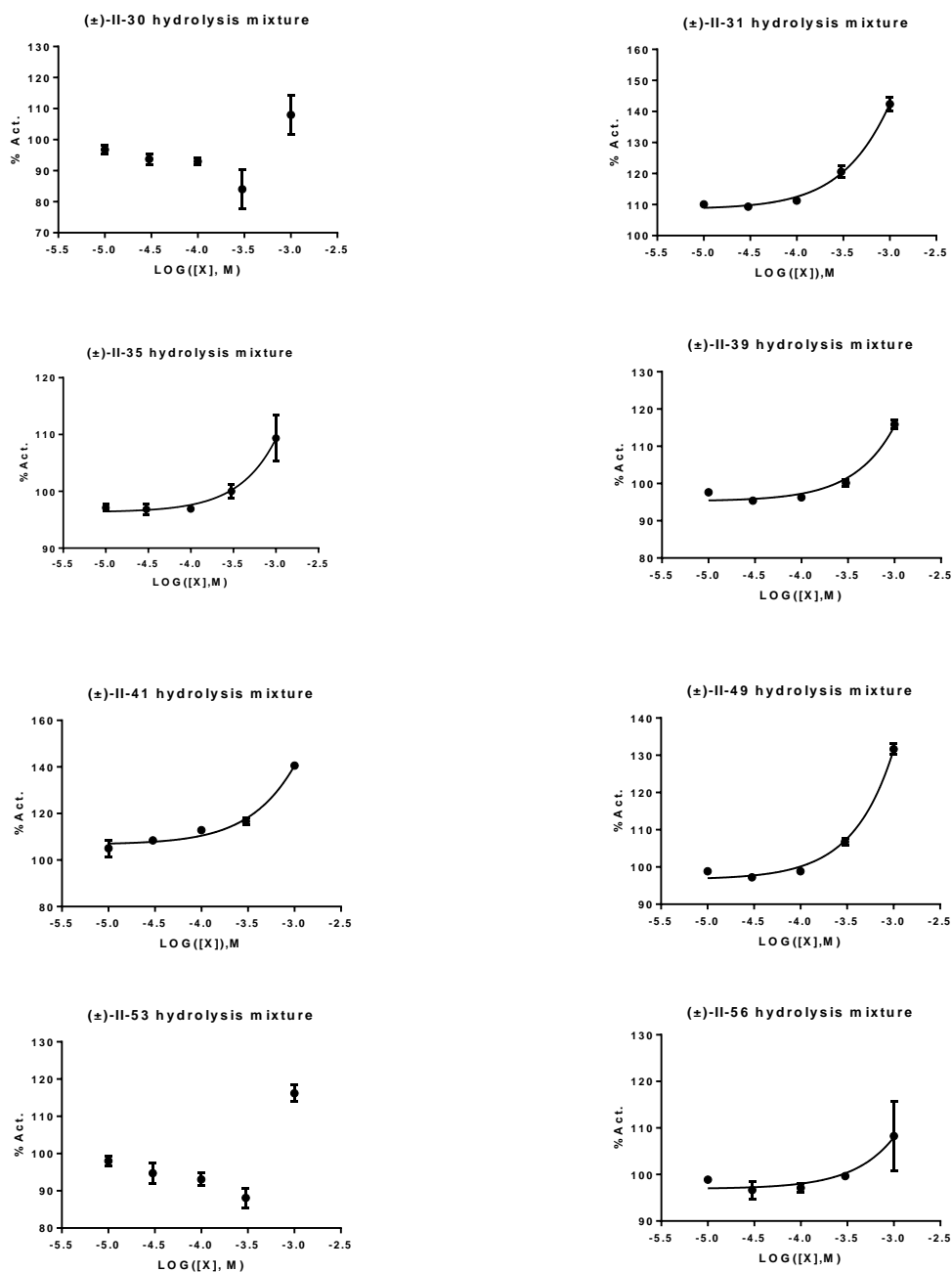
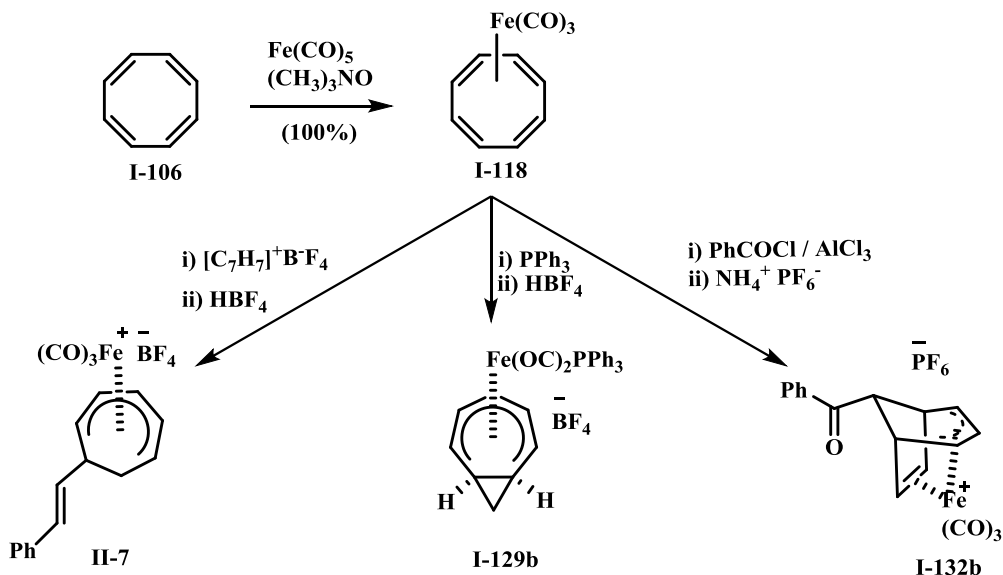


Figure II-23. The activity of the bicyclooctitols/phthalhydrazide mixtures against β -glucosidase from almond.

III- SUMMARY

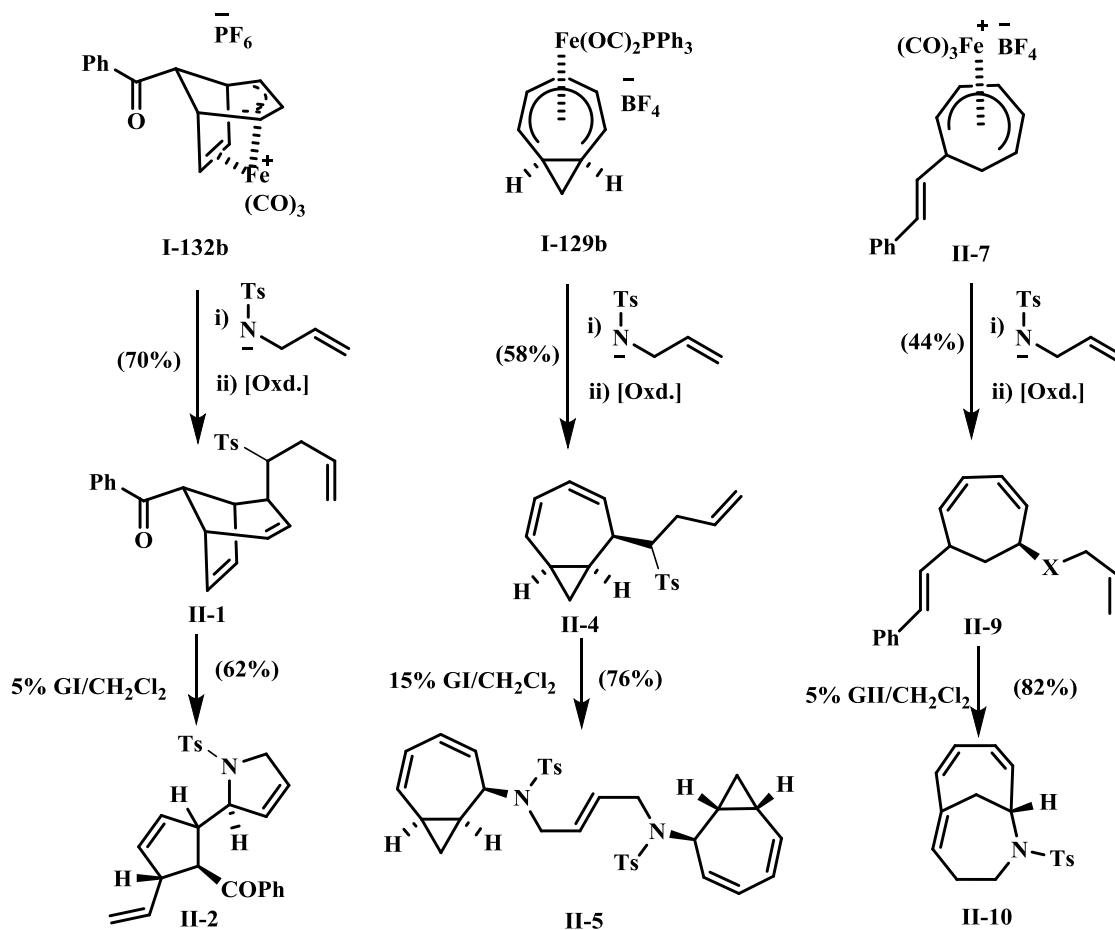
The hydrocarbon cyclooctatetraene **I-106** [COT] is formed by the Ni-catalyzed cyclotetramerization of acetylene. The use of COT **I-106** as a starting material for synthesis has experienced a rebirth in the last 6 years, as exemplified by its use in the synthesis of bis-homocon-duritols, bis-homoinositol, pentacycloanammoxic acid methyl ester, and the polyene segment of roxiticin. Complexation of **I-106** readily generates $(\text{COT})\text{Fe}(\text{CO})_3$ **I-118**, the reaction of which with electrophiles gives rise to a wide variety of cationic iron complexes via skeletal rearrangements **II-7**, **I-129b** and **I-132b** (Scheme III-1).



Scheme III-1. Preparation of different variety of cationic iron complexes.

III.1. Skeletal diversity via ring-rearrangement metathesis

Within the general build/couple/pair or functional group pairing strategy for diversity oriented synthesis (DOS), folding pathways allow for the transformation of different substrates into different scaffolds using a common reagent. Toward this end, reaction of cations **II-7**, **I-129b** and **I-132b** with (allyl)tosylamine nucleophiles, followed by oxidative decomplexation and reaction with Grubbs' 1st or 2nd generation catalyst gave a diverse group of polycyclic products **II-2**, **II-5** and **II-10** either via ring-rearrangement metathesis or RCM (Scheme III-2).

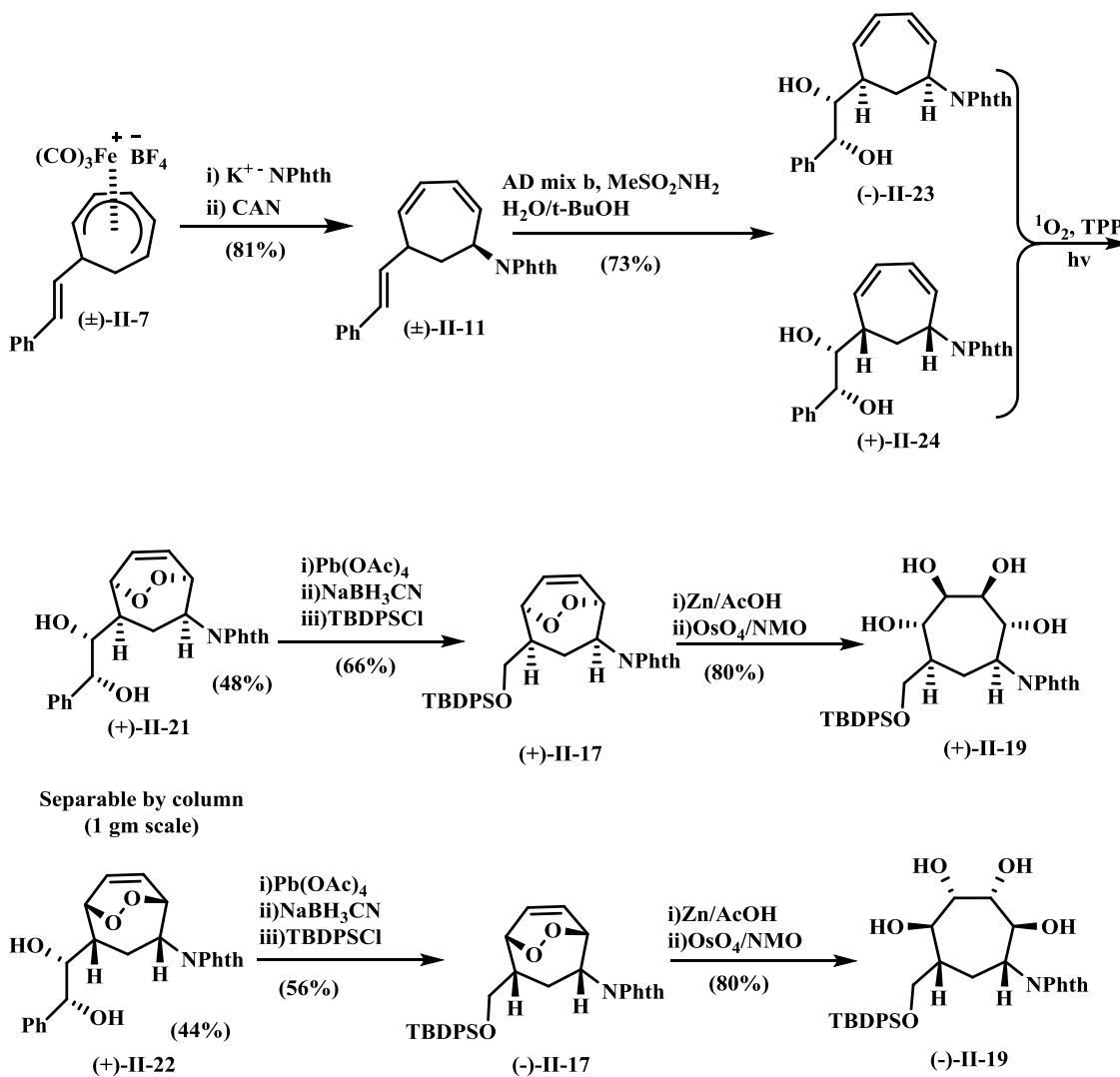


Scheme III-2. Skeletal diversity from COT via ring rearrangement metathesis.

III.2. Preparation of racemic and optically active aminocycloheptitols

Addition of potassium phthalimide to (6-styrylcycloheptadienyl)Fe(CO)₃⁺ cation **II-7** followed by decomplexation gave (6-styryl-2,4-cycloheptadien-1-yl)phthalimide (Scheme III-3). Sharpless asymmetric dihydroxylation gave a mixture of diastereomeric glycols, which were separable only by prep TLC. Cycloaddition of the mixture of diastereomeric diendiols with singlet oxygen gave a mixture of two

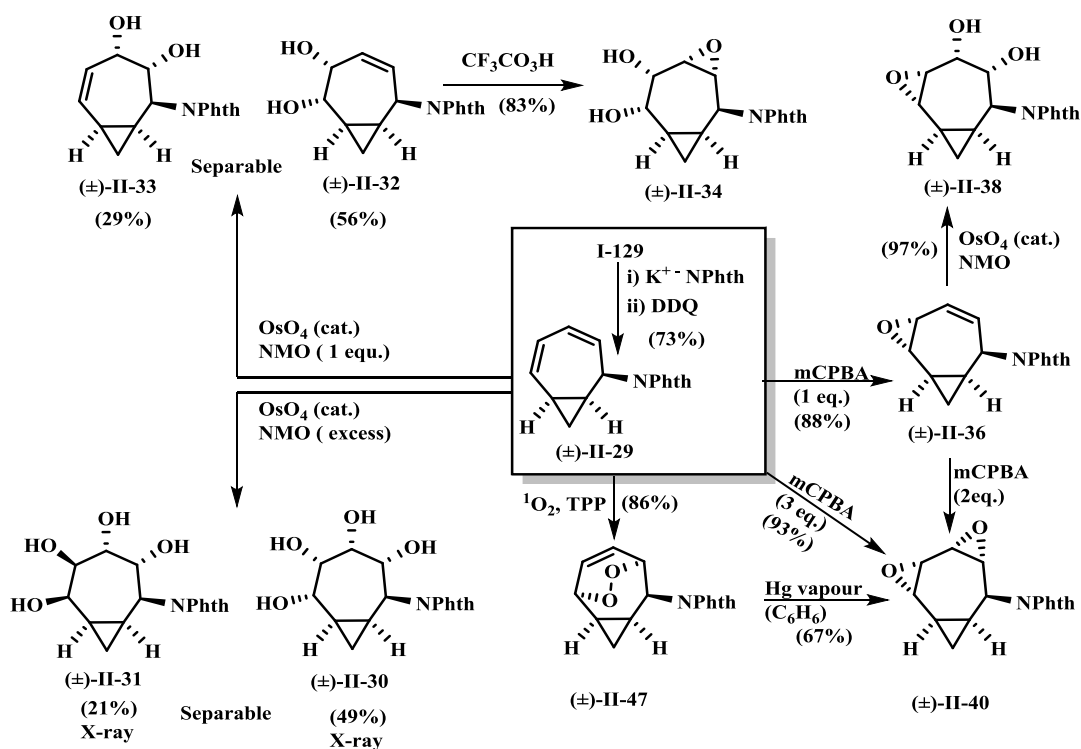
diastereomeric endoperoxides (+)-**II-21** and (+)-**II-22** which were separable by column chromatography on a 1 gram scale. Each of the individual endoperoxides were further transformed into the enantiomeric protected aminocycloheptitols (>94% ee each). The racemic mixture was prepared without separating (+)-**II-21** and (+)-**II-22** and carry the synthesis as shown in scheme III-3.



Scheme III-3. Asymmetric preparation aminocycloheptitols from COT.

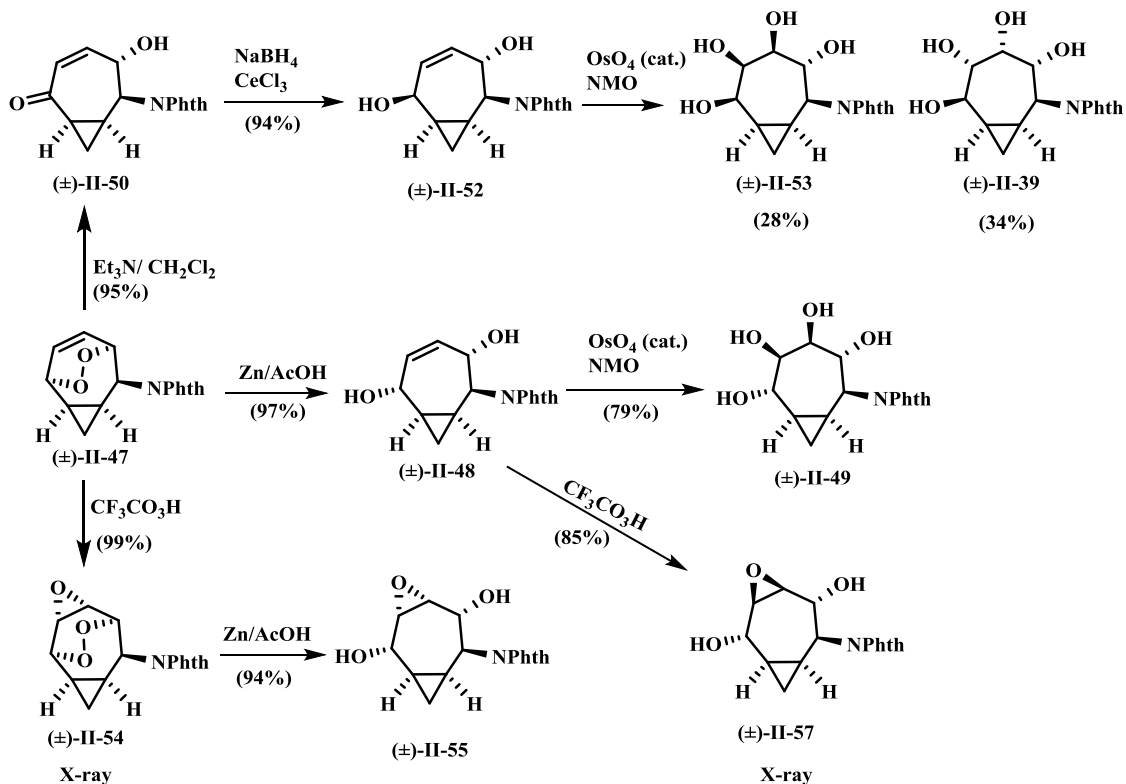
III.3. Novel synthesis of bicyclic aminopolyols

Nucleophilic attack of phthalimide on cation **I-129** gave the phthalimide derivative, which undergoes oxidative decomplexation using DDQ to give the free bicyclic diene (\pm)-**II-29** (Scheme III-4). Dihydroxylation or tetrahydroxylation of (\pm)-**II-29**, using a controlled amount of NMO reoxidant gave a separable mixture of dienediols or tetraols respectively. Reaction of (\pm)-**II-29** with one or two equivalents of mCPBA gave a mono- or bis-epoxide respectively. Singlet oxygen cycloaddition gave single endo peroxide (\pm)-**II-47**, which upon further photolysis gave a bis-epoxide diastereomeric to that obtained from the reaction with mCPBA.



Scheme III-4. Oxidation of bicyclo[5.1.0]octadiene (\pm)-**II-29**.

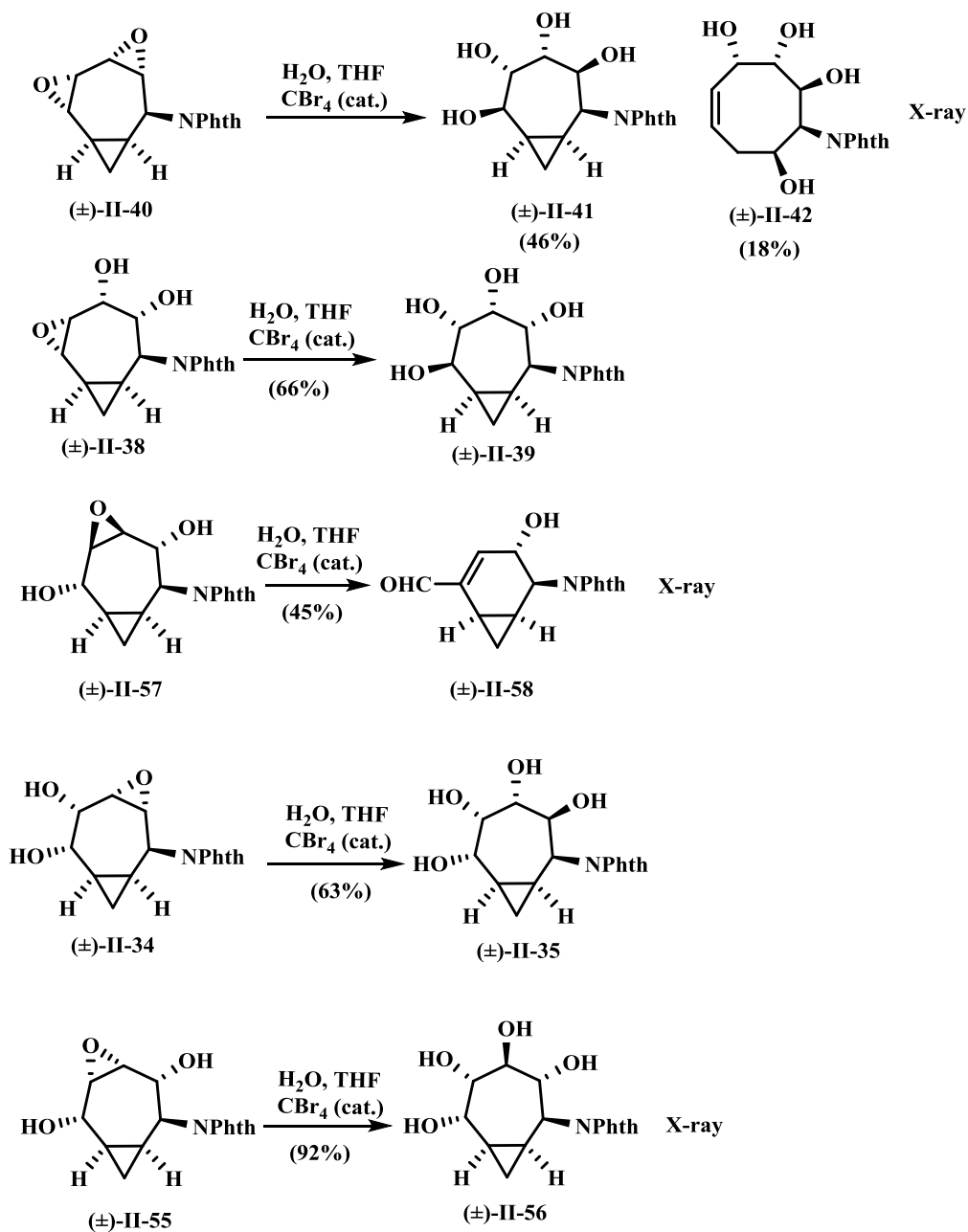
Further elaboration of the tricyclic endoperoxide can be effected by Kornblum-DeLeMare rearrangement, by O-O bond reduction or by epoxidation (Scheme III-5). These products can be further manipulated to generate diastereomeric tetraols, or diastereomeric epoxydiols.



Scheme III-5. Elaboration of tricyclic endoperoxide.

Hydrolysis of the epoxydiols or bis-epoxides generally proceeds via anti addition to give further diastereomeric tetraols (Scheme III-6). One notable exception is hydrolysis of the epoxydiol $(\pm)\text{-II-57}$ which gave the 2-formyl-bicyclo[4.1.0]hept-2-ene

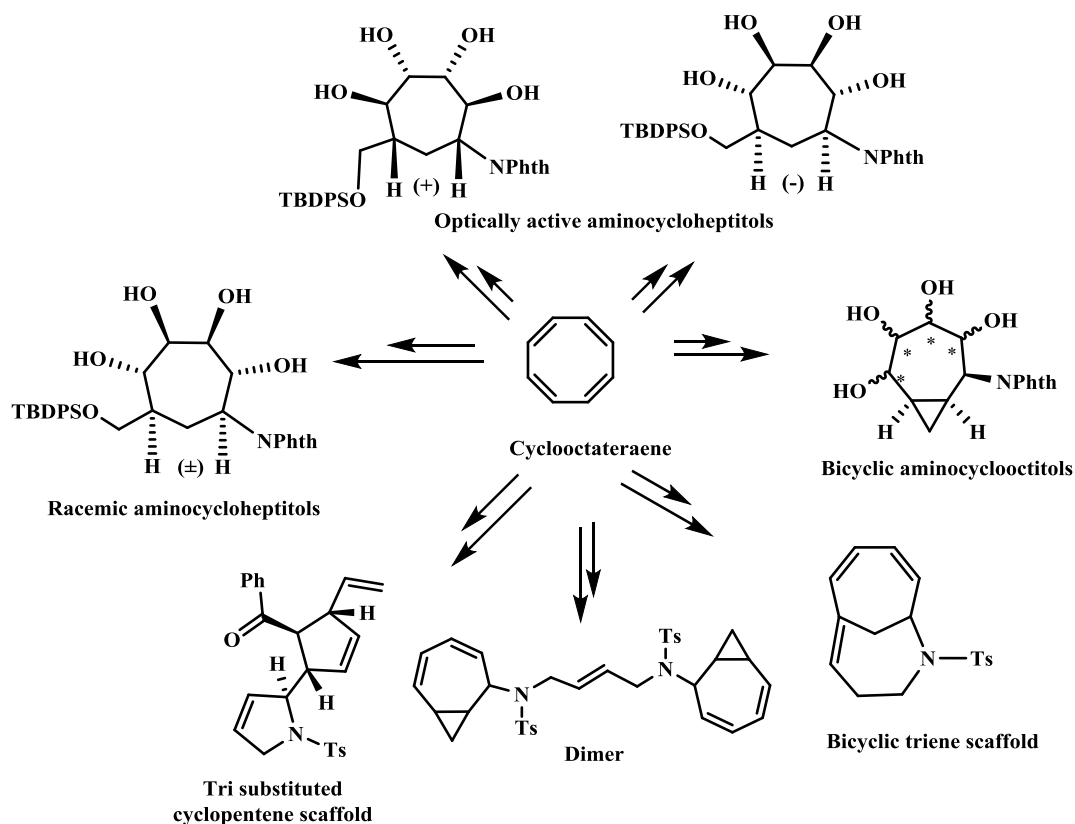
(±)-**II-58**. This outcome was attributed to a stereoelectronic effect due to alignment of the C-C bond in **II-57** nearly antiperiplanar with one of the epoxide C-O bonds.



Scheme III-6. Epoxydiols and bisepoxides hydrolyses.

IV- CONCLUSIONS AND RECOMMENDATIONS

In this work we have developed a new approach of making aminocycloheptitols and bicyclic aminocyclooctitols using organoiron chemistry. The advantages of this method over the other existing methods are using one simple and cheap hydrocarbon starting material to target these molecules and this method give the access to many stereochemical isomers. We have reported also the possibility of obtaining the optically enriched aminocycloheptitols using this approach with high enantiomeric excess (>94%). Ring rearrangement metathesis reaction was employed to generate molecular complexity and to make diverse structure from cyclooctatetraene (Scheme IV-1). This reactivity could be exploited in the future for natural products synthesis.



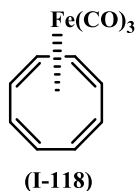
Scheme IV-1. Generation of molecular diversity from cyclooctatetraene.

We produced eight bicyclic aminocyclooctitol isomers out of 16 possible ones. The hydrolysis of epoxide functionality adjacent to cyclopropane functionality in bicycle[5.1.0]octanes proceeded via selective cleavage of the C-O bond in proximity to the three-membered ring. This was attributed to stabilization of the cyclopropane ring on partial positive charges at one adjacent carbon. A quantification of this effect could be explored by computational analysis at the DFT/B3LYP level. We encountered purification problems for the hydrolysis of the phthalimido group. The reaction of alternative nitrogen-based nucleophiles in reaction with I-129b might lead to systems more amenable to clean deprotection / separation. Docking the aminobicyclooctitols in

crystallographically characterized enzyme active sites would be useful tool to see the different types of interactions between the ligand and the amino acid residues in the active site of the enzyme.

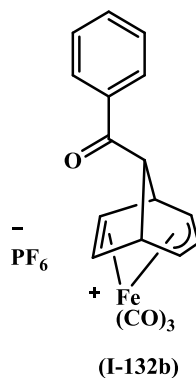
V- EXPERIMENTAL

General methods: All reactions involving moisture- or air-sensitive reagents were carried out under a nitrogen atmosphere in oven-dried glassware with anhydrous solvents. THF and diethyl ether were distilled from sodium/benzophenone. Purifications by chromatography were carried out by using flash silica gel (32–63 μ m). NMR spectra were recorded on either a Varian Mercury+ 300 MHz or a Varian UnityInova 400 MHz instrument. CDCl_3 , CD_3OD , and $[\text{D}_6]$ acetone were purchased from Cambridge Isotope Laboratories. ^1H NMR spectra were calibrated to $\delta=7.27$ ppm for residual CHCl_3 , $\delta=3.31$ ppm for CD_2HOD , or $\delta=2.05$ ppm for $[\text{D}_5]$ acetone. ^{13}C NMR spectra were calibrated from the central peak at $\delta=77.23$ ppm for CDCl_3 , $\delta=49.15$ ppm for CD_3OD , or $\delta=29.92$ ppm for $[\text{D}_6]$ acetone. Coupling constants are reported in Hz.



Tricarbonyl(η^4 -cyclooctatetraene)iron(0) (I-118): To a 500 mL round bottomed flask was added cyclooctatetraene **I-106** (5.0 mL, 48 mmol) dissolved in benzene (200 mL). Iron pentacarbonyl (14 mL, 96 mmol) was added followed by the addition of trimethylamine N-oxide dihydrate (21.33 g, 191.9 mmol). The reaction mixture was heated at reflux for 2 h then filtered and concentrated. The solid residue was washed several times with benzene and the washings were filtered and concentrated. The deep-brownish residue was purified through column chromatography (SiO_2 , hexane-ethyl

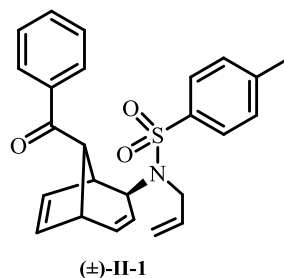
acetate = 20:1) to give **I-118** as deep brown crystals (9.83 g, 100%). mp 82 – 86 °C (lit.³⁹, 92 – 93.5°C); IR (KBr, cm⁻¹) 2043, 1960; ¹H NMR (300 MHz, CDCl₃) δ 5.25 (s, 8H); ¹³C NMR (75 MHz, CDCl₃) δ 100.1, 212.5. The NMR spectral data were consistent with the literature values.¹¹³



(2-4:6-7-η-8-Benzoylbicyclo[3.2.1]octadienylium)tricarbonyliron

hexafluorophosphate: I-132b. Anhydrous AlCl₃, (3.3 g, 25 mmol) was added to dry dichloromethane (60 mL). Freshly distilled acetyl chloride (4.50 mL, 63.5 mmol) was added from a syringe. The resulting deep red solution was added dropwise to a stirred solution of [Fe(C₈H₈)(CO)₃] **I-118** (6.00 g, 25.0 mmol) in dichloromethane (60 mL) at 0 °C over a 20 min period. Stirring was continued for another 10 min at 0 °C, and the reaction mixture then hydrolyzed with ice-cold 5% hydrochloric acid solution (75 mL). Diethyl ether (60 mL) was added and the organic phase separated, then washed with water (3 x 50 mL). The combined aqueous fractions were extracted several times with diethyl ether and the golden yellow aqueous solution cooled to 0 °C. Addition of 15% aqueous ammonium hexafluorophosphate solution (50 mL) gave a pale yellow precipitate which was collected and washed with diethyl ether, then dried in vacuo to give the

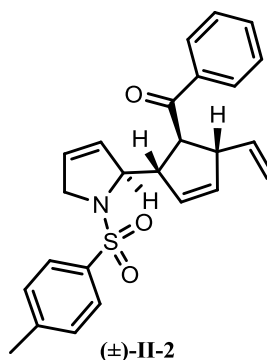
product. Further purification by dissolving in the minimum volume of acetone and reprecipitating with diethyl ether gave a pale yellow precipitate (9.0 g, 74 %). This product was used without further characterization.¹²⁴



***N*-(8-Benzoylbicyclo[3.2.1]octa-3,6-dien-2-yl)-4-methyl-*N*-2-propen-1-yl-**

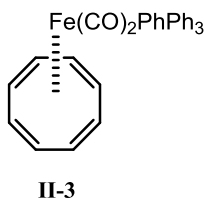
benzenesulfonamide:(±)-II-1. To a solution of **I-132b** (0.20 g, 0.40 mmol) in acetonitrile (15 mL) under N₂, was added the potassium salt of tosyl allylamine (0.250 g, 1.00 mmol). The mixture was stirred at room temperature for 3 h, at which time monitoring by TLC indicated the disappearance of **I-132b**. The reaction mixture was filtered under vacuum and the filter bed washed with acetonitrile. To the combined filtrates was added cerium ammonium nitrate (0.42 g, 0.77 mmol). The mixture was stirred under nitrogen for 2 h, and then filtered through a short column of silica gel, using CH₂Cl₂ to complete the elution. The combined filtrates were concentrated and the residue purified by column chromatography (SiO₂, hexanes–ethyl acetate = 4:1) to give (±)-II-1 (0.117g, 70%) as a colorless solid. mp 137-138 °C; IR (CH₂Cl₂) 1676, 1330, 1157 cm⁻¹; ¹H NMR (400 MHz, CDCl₃) δ 2.43 (s, 3H), 3.11 (br s, 1H), 3.22 (dd, J = 3.0, 6.6 Hz, 1H), 3.88 (s, 1H), 3.98 (dd, J = 6.4, 16.8 Hz, 1H), 4.13 (br dd, J = 5.0, 16.8 Hz, 1H), 4.27-4.30 (m, 1H), 5.04-5.11 (m, 2H), 5.23 (dd, J = 1.2, 17.6 Hz, 1H), 5.86-5.93 (m, 2H), 6.18 (dd, J = 3.2, 5.6 Hz, 1H), 6.39 (ddd, J = 2.5, 6.4, 9.2 Hz, 1H), 7.30 (d, J = 7.6

Hz, 2H), 7.45 (t, $J = 7.8$ Hz, 2H), 7.55 (tt, $J = 1.6, 7.6$ Hz, 1H), 7.74 (d, $J = 8.4$ Hz, 2H), 7.89 (dd, $J = 1.6, 8.4$ Hz, 2H); ^{13}C NMR (100 MHz, CDCl_3) δ 21.7, 42.9, 47.3, 48.9, 55.3, 57.2, 117.5, 124.6, 127.3, 128.5, 128.8, 129.9, 130.0, 133.1, 135.9, 136.2, 137.9, 138.5, 140.4, 143.6, 199.4. Anal. Calcd for $\text{C}_{25}\text{H}_{25}\text{NO}_3\text{S}\cdot\frac{1}{2}\text{H}_2\text{O}$: C, 70.07; H, 6.11. Found: C, 70.29; H, 5.90.



2-(5-Benzoyl-4-ethenyl-2-cyclopenten-1-yl)-2,5-dihydro-1-[(4-methylphenyl)sulfonyl]-1H-pyrrole:(±)-II-2. To a solution of (±)-II-1 (45 mg, 0.11 mmol) in freshly distilled dichloromethane (25 mL), under N_2 , was added Grubbs' 1st generation catalyst (5 mg, 0.006 mmol, 5 mol %). The reaction progress was monitored by ^1H NMR spectroscopy, which revealed that no starting material was left after 90 min. The reaction mixture was concentrated under reduced pressure and the residue was purified by column chromatography (SiO_2 , hexanes–ethyl acetate = 4:1) to give (±)-II-2 (36 mg, 80%) as a colorless oil. IR (CH_2Cl_2) 1678, 1340, 1162 cm^{-1} ; ^1H NMR (400 MHz, CDCl_3) δ 2.37 (s, 3H), 3.39-3.46 (br m, 1H), 3.76 (tdd, $J = 2.4, 4.8, 15.2$ Hz, 1H), 3.80-3.85 (m, 1H), 4.02-4.10 (m, 2H), 4.63-4.68 (m, 1H), 4.93 (d, $J = 16.8$ Hz, 1H), 5.01 (dd, $J = 1.4, 9.4$ Hz, 1H), 5.54 (qd, $J = 2.0, 6.2$ Hz, 1H), 5.59 (td, $J = 2.2, 6.0$ Hz, 1H), 5.65-5.70 (m, 2H), 5.91 (ddd, $J = 8.8, 10.2, 17.0$ Hz, 1H), 7.22 (t, $J = 8.0$ Hz, 2H), 7.46 (t, $J = 7.4$

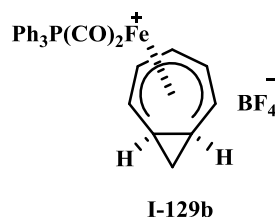
Hz, 2H), 7.56 (br t, $J = 7.6$ Hz, 1H), 7.60 (d, $J = 8.4$ Hz, 2H), 8.00 (dd, $J = 2.0, 7.6$ Hz, 2H); ^{13}C NMR (100 MHz, CDCl_3) δ 21.7, 52.1, 55.0, 56.0, 56.3, 69.5, 115.9, 126.7, 127.7, 128.6, 128.7, 129.2, 129.8, 129.9, 133.1, 133.9, 134.5, 137.4, 140.3, 143.7, 202.3. HRMS (ESI): m/z calcd for $\text{C}_{25}\text{H}_{25}\text{NO}_3\text{S}$: $[\text{M}+\text{Na}^+]$; 442.1453, found 442.1451.



Dicarbonyl(cyclooctatetraene)(triphenylphosphine)-iron: II-3. To a solution of tricarbonyl(cyclooctatetraene)iron **I-118** (2.50 g, 10.0 mmol) and triphenylphosphine (4.00 g, 15.1 mmol) in acetone (90 mL) was added anhydrous trimethylamine N-oxide (1.34 g, 17.5 mmol) in one portion. Effervescence was observed upon the addition. The reaction was stirred at room temperature under a blanket of N_2 and was monitored by TLC. After 60 min, additional triphenylphosphine (1.00 g, 3.77 mmol) and TMANO (0.36 g, 4.7 mmol) were added. After another 30 min, a final portion of TMANO (0.36 g, 4.7 mmol) was added. After being stirred for a total of 2 h and 30 min, the reaction mixture was passed through a short bed of silica and the filter bed was washed with reagent acetone until the washings were colorless. The filtrates were concentrated, and the resulting red solid was adsorbed to silica using acetone. The material was purified by column chromatography (SiO_2 , hexanes-ethyl acetate = 20:1 to 4:1 gradient) to give the product as a red solid (4.46 g, 93%): mp 169-171 $^\circ\text{C}$; IR (KBr) 3053, 1969, 1913, 1481, 1433 cm^{-1} ; ^1H NMR (400 MHz, CDCl_3) δ 4.95 (d, $J_{\text{HP}} = 1.5$ Hz, 8H), 7.37-7.43 (m, 9H),

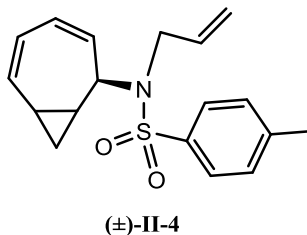
7.47-7.57 (m, 6H); ^{13}C NMR (100 MHz, CDCl_3) δ 99.4, 128.4 (d, $J_{\text{CP}} = 9.5$ Hz), 130.0 (d, $J_{\text{CP}} = 1.7$ Hz), 133.3 (d, $J_{\text{CP}} = 10.4$ Hz), 135.9 (d, $J_{\text{CP}} = 39.2$ Hz), 217.6 (d, $J_{\text{CP}} = 14.1$ Hz).

The NMR spectral data was consistent with the literature values.¹²⁵



Dicarbonyl(bicyclo[5.1.0]octadienyl)(triphenylphosphine)iron(1+)

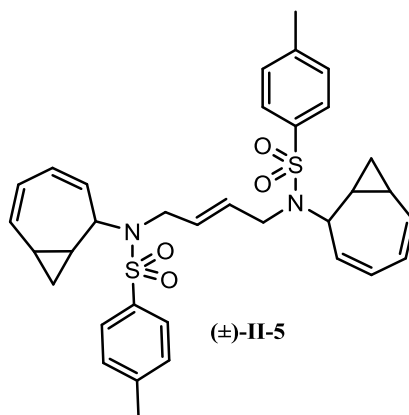
Tetrafluoroborate: I-129b. To an ice-cold solution of iron complex **II-3** (4.00 g, 8.36 mmol) in Ac_2O (37 mL) was carefully added a cold solution of aqueous tetrafluoroboric acid (60 wt %, 7.8 mL) in Ac_2O (19 mL). After several minutes of stirring, the orange solution was added dropwise to a large excess of ether (1300 mL). The resulting precipitate was collected by vacuum filtration, washed with ether, and dried in vacuo to give **I-129b** as an orange powder (4.34 g, 92%): mp >133 °C dec; IR (KBr) 3075, 2025, 1984, 1481, 1437 cm^{-1} ; ^1H NMR (400 MHz, CD_3OD) δ 1.09-1.19 (m, 1H), 1.24-1.34 (m, 1H), 2.20-2.34 (br m, 1H), 2.34-2.48 (br m, 1H), 3.63-3.79 (br m, 1H), 4.91-5.06 (br m, 1H), 5.30-5.43 (br m, 1H), 5.43-5.55 (br m, 1H), 7.45-7.68 (m, 15H), 7.71 (br t, $J = 5.9$ Hz, 1H); The NMR spectral data was consistent with the literature values.¹²⁵



***N*-(Bicyclo[5.1.0]octa-3,5-dien-2-yl)-4-methyl-*N*-2-propen-1-yl-**

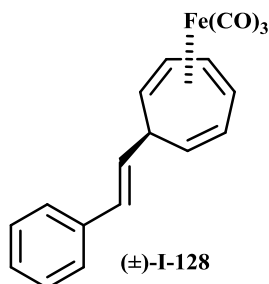
benzenesulfonamide:(±)-II-4. To a stirring suspension of cation **I-129b** (1.00 g, 1.77 mmol) in water-saturated ether (60 mL) was added the potassium salt of *N*-tosyl allylamine (2.76 g, 11.1 mmol). After 30 min the orange ethereal layer was decanted from any solid and additional moist ether (60 mL) was added to the solid and the mixture stirred for 10 min. This was repeated until the mother liquor was colorless. The collected ethereal layers were combined and concentrated to give a yellow solid (1.10 g, 90%): mp 108-109 °C. To a stirring solution of the intermediate complex (0.30 g, 0.44 mmol) in dry acetonitrile (20 mL) was added 2,3-dichloro-5,6-dicyano-1,4-benzoquinone (0.11 g, 0.48 mmol). After 1 h, the starting material had been consumed as indicated by TLC monitoring. The reaction mixture was passed through a short column of silica gel and the column flushed with CH₂Cl₂ until no further product appeared by TLC monitoring. These fractions were combined and concentrated, and the residue was purified by column chromatography (SiO₂, hexanes–ethyl acetate = 4:1) to give (±)-**II-4** (81 mg, 58%) as a pale yellow oil. IR (CH₂Cl₂) 1346, 1162 cm⁻¹; ¹H NMR (400 MHz, CDCl₃) δ 0.77 (dt, *J* = 4.5, 8.4 Hz, 1H), 1.11-1.19 (m, 1H), 1.71 (dt, *J* = 4.8, 5.6 Hz, 1H), 1.79 (q, *J* = 8.4 Hz, 1H), 2.35 (s, 3H), 3.75 (dd, *J* = 6.2, 16.2 Hz, 1H), 3.95 (dd, *J* = 5.8, 16.2 Hz, 1H), 4.96 (br d, *J* = 11.6 Hz, 1H), 5.07 (dd, *J* = 2.0, 10.4 Hz, 1H), 5.08-5.12 (br s, 1H), 5.21 (dd, *J* = 1.6, 18.8 Hz, 1H), 5.44 (dd, *J* = 6.0, 11.6 Hz, 1H), 5.60 (ddd, *J* = 2.8, 6.4, 11.6 Hz, 1H),

5.93 (tdd, $J = 6.2, 10.0, 17.2$ Hz, 1H), 6.10 (dd, $J = 7.2, 12.0$ Hz, 1H), 7.25 and 7.70 (ABq, $J = 8.4$ Hz, 4H total); ^{13}C NMR (100 MHz, CDCl_3) δ 8.4, 14.8, 21.7, 44.1, 48.1, 57.6, 117.1, 122.6, 126.6, 127.5, 127.9, 129.8, 135.3, 136.1, 137.7, 143.3. HRMS (ESI): m/z calcd for $\text{C}_{18}\text{H}_{21}\text{NO}_2\text{SNa}$: $[\text{M}+\text{Na}^+]$; 338.1191, found 338.1180.



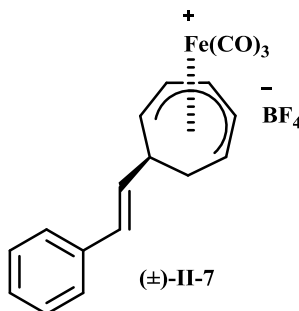
Self metathesis dimer:(±)-II-5. To a solution of (±)-II-4 (248 mg, 0.786 mmol) in freshly distilled CH_2Cl_2 (100 mL) under N_2 was added Grubbs' 1st generation catalyst (39 mg, 0.047 mmol, 6 mol%). The mixture was heated at reflux and the reaction progress was monitored by NMR spectroscopy. After 6 h additional Grubbs' I (39 mg, 0.047 mmol, 6 mol %) was added and heating continued for 12 h. A final portion of Grubbs' catalyst (20 mg, 0.024 mmol, 3 mol %) was added and heating continued for 12 h. The reaction mixture was concentrated and purified by column chromatography (SiO_2 , hexanes–ethyl acetate = 7:3) to afford a mixture of diastereomeric dimers (±)-II-5 (180 mg, 76%) as a colorless solid. mp 162-163 °C; IR (CH_2Cl_2) 1336, 1161 cm^{-1} ; ^1H NMR (400 MHz, CDCl_3) δ 0.81-0.87 (m, 2H), 1.12-1.22 (m, 2H), 1.73-1.85 (m, 4H), 2.42 (s, 6H), 3.73 (dd, $J = 2.4, 16.0$ Hz, 2H), 3.92 (br d, $J = 14.8$ Hz, 2H), 4.94 (dt, $J = 2.8, 12.0$

Hz, 2H), 5.05-5.10 (br s, 2H), 5.46 (dd, $J = 6.2, 11.4$ Hz, 2H), 5.61 (dtd, $J = 2.8, 6.0, 12.0$ Hz, 2H), 5.83 (q, $J = 3.2$ Hz, 2H), 6.14 (dd, $J = 7.4, 11.4$ Hz, 2H), 7.29 and 7.72 (ABq, $J = 8.0$ Hz, 8H total); ^{13}C NMR (100 MHz, CDCl_3) δ 8.2, 14.7, 21.7, 44.1, 46.9, 57.6, 122.6, 126.7, 127.5, 127.7, 129.9, 130.5, 135.3, 137.5, 143.4. Anal. Calcd for $\text{C}_{34}\text{H}_{38}\text{N}_2\text{O}_4\text{S}_2$: C, 67.75; H, 6.35. Found: C, 67.29; H, 5.92.



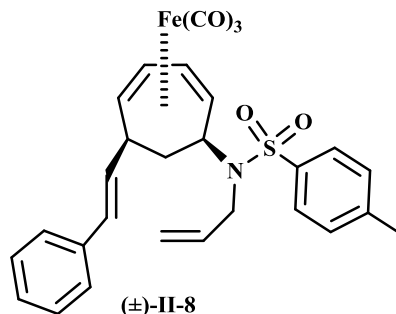
Tricarbonyl(η^4 -7-styrylcyclohepta-1,3,5-triene)iron:(\pm)-I-128. To a 1 L round-bottomed flask, (cyclooctatetraene) $\text{Fe}(\text{CO})_3$ **I-118** (10.0 g, 40.9 mmol) was dissolved in dry acetone (50 mL) at -23 $^\circ\text{C}$ under N_2 . Dry pyridine (3 mL, 40.9 mmol)¹²⁹ was added and mixture stirred for 5 min. A solution/suspension of tropylium tetrafluoroborate (8.73 g, 49.1 mmol) in dry acetone (400 mL) was added and the reaction mixture was stirred for 8 h maintaining the temperature at -23 $^\circ\text{C}$. The reaction mixture was warmed to room temperature and stirred overnight. The clear reddish solution was concentrated under reduced pressure and dried. To the solid residue was added ether (200 mL) and the slurry stirred for 2 h and filtered. The above process was repeated three times with the solid residue. The combined filtrate was concentrated and applied to a column of silica. Elution (100% hexane) gave a bright yellow solid (\pm)-**I-128** (10.42 g, 75%). mp $43 - 47$ $^\circ\text{C}$; ^1H NMR (300 MHz, CDCl_3) δ 3.10-3.03 (m, 1H), 3.34-3.21 (m, 2H), 5.18-5.10 (m, 1H),

5.43-5.33 (m, 2H), 5.92-5.82 (m, 2H), 6.46 (d, $J = 16.0$ Hz, 1H), 7.37-7.19 (m, 5H); ^{13}C NMR (75 MHz, CDCl_3) δ 46.9, 55.8, 64.9, 87.6, 95.3, 126.4, 127.6, 128.1, 128.9, 129.1, 130.4, 134.2, 137.6 211.3. The NMR spectral data was consistent with the literature values.¹¹³



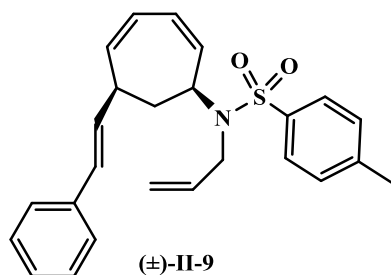
Tricarbonyl(η^5 -7-styrylcyclohepta-2,4-dien-1-yl)iron(+1) tetrafluoroborate:(\pm)-II-7.

To a 250 mL round bottomed flask, (7-styrenyl-1,3,5-cycloheptatriene) $\text{Fe}(\text{CO})_3$ (\pm)-**I-87** (8.0 g, 24 mmol) was dissolved in acetic anhydride (150 mL) at 0 °C with stirring. An ice-cold solution of fluoroboric acid (60 wt%, 23.40 mL, 240.0 mmol) in acetic anhydride (25 mL) was added dropwise to the stirring mixture. After 20 min of stirring a yellow-gray precipitate began to form. The reaction mixture was added dropwise into a large excess of ether (3.5 L). The solid yellow cation was isolated by filtration and dried under high vacuum (8.88 g, 88%). IR (KBr) 2112, 2067, 760, 697 cm^{-1} ; ^1H NMR (300 MHz, d_6 -acetone) δ 1.41 (m, 1H), 2.68 (m, 1H), 4.25 (m, $J = 8.0$ Hz, 1H), 5.16 (m, 2H), 5.93 (dd, $J = 16.0, 8.3$ Hz, 1H), 6.29 (m, 1H), 6.62 (m, $J = 16.0$ Hz, 1H), 7.33 (m, 5H), 7.47 (tq, $J = 6.1, 1.2$ Hz, 1H). The NMR spectral data was consistent with the literature values.¹¹³



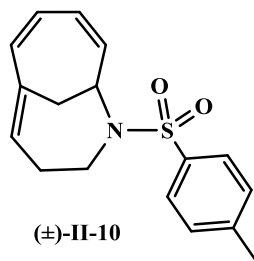
***N*-(6-styryl-2,4-cycloheptadien-1-yl)-4-methyl-*N*-2-propen-1-yl-**

benzenesulfonamide:(±)-II-8. To a solution of (±)-II-7 (0.10 g, 0.24 mmol) in acetonitrile (10 mL), under N₂, was added the potassium salt of tosyl allylamine (0.140 g, 0.562 mmol). The mixture was stirred for 2 h, at which time TLC indicated the disappearance of (±)-II-7. The reaction mixture was dried under reduced pressure and the solid residue was purified by column chromatography (SiO₂, hexanes–ethyl acetate = 4:1) to give the product (0.113 g, 86%) as a yellow foam. mp 47-48 °C; IR (CH₂Cl₂) 2047, 1965, 1338, 1157 cm⁻¹; ¹H NMR (400 MHz, CDCl₃) δ 1.14 (q, J = 12.4 Hz, 1H), 1.55 (br d, J = 13.2 Hz, 1H), 1.91 (d, J = 7.2 Hz, 1H), 2.40 (s, 3H), 2.82-2.92 (m, 2H), 3.68 (dd, J = 6.0, 16.8 Hz, 1H), 3.93 (dd, J = 5.2, 16.8 Hz, 1H), 4.38 (dd, J = 3.6, 12.0 Hz, 1H), 5.14 (d, J = 10.4 Hz, 1H), 5.22-5.33 (m, 3H), 5.80-5.94 (m, 2H), 6.33 (d, J=15.2 Hz, 1H), 7.20-7.38 (m, 7H), 7.77 (d, J = 8.0 Hz, 2H); ¹³C NMR (100 MHz, CDCl₃) δ 21.6, 36.4, 44.0, 46.2, 57.1, 58.6, 61.5, 88.3, 88.6, 117.0, 126.3, 127.3, 127.6, 128.8, 129.1, 130.1, 135.2, 136.5, 137.1, 137.9, 143.8.

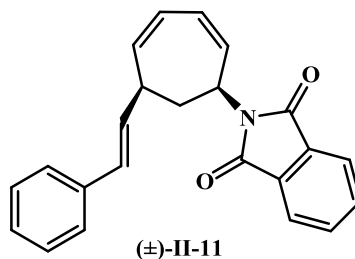


N-(6-styryl-2,4-cycloheptadien-1-yl)-4-methyl-N-2-propen-1-yl-

benzenesulfonamide:(±)-II-9. To the prior complex (±)-II-8 (0.277 g, 0.509 mmol) in acetonitrile (15 mL), under N₂, was added cerium ammonium nitrate (0.470 g, 0.858 mmol). The mixture was stirred at room temperature for 1 h, at which time TLC indicated complete disappearance of the starting material. The reaction mixture was filtered through a short column of silica gel, which was washed with CH₂Cl₂ until the entire product was eluted. These fractions were combined, concentrated, and the residue was purified by column chromatography (SiO₂, hexanes–ethyl acetate = 17:3) to give (±)-II-9 (0.106 g, 51%) as a faint yellow oil. IR (CH₂Cl₂) 1336, 1162 cm⁻¹; ¹H NMR (300 MHz, CDCl₃) δ 1.96 (br d, J = 12.6 Hz, 1H), 2.08 (td, J = 10.9, 12.6 Hz, 1H), 2.42 (s, 3H), 3.30-3.42 (m, 1H), 3.73 (dd, J = 6.0, 16.5 Hz, 1H), 3.85 (dd, J = 6.0, 16.5 Hz, 1H), 4.85-4.94 (m, 1H), 5.13 (dd, J = 0.9, 8.7 Hz, 1H), 5.23 (dd, J = 1.5, 16.8 Hz, 1H), 5.39 (br d, J = 11.1 Hz, 1H), 5.64-5.75 (m, 3H), 5.91 (tdd, J = 6.0, 10.5, 17.1 Hz, 1H), 6.11 (dd, J = 8.4, 15.9 Hz, 1H), 6.39 (d, J = 15.9 Hz, 1H), 7.20-7.38 (m, 7H), 7.77 (d, J = 8.0 Hz, 2H); ¹³C NMR (75 MHz, CDCl₃) δ 21.7, 39.0, 43.2, 47.9, 59.1, 117.6, 123.9, 125.1, 126.3, 127.4, 127.5, 128.8, 129.8, 129.9, 132.6, 134.4, 136.1, 137.3, 137.6, 137.9, 143.5. HRMS (ESI): m/z calcd for C₂₅H₂₇NO₂SNa: [M+Na⁺]; 428.1660, found 428.1657.

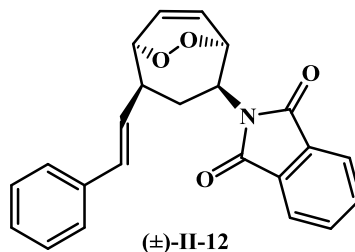


***N*-Toluenesulfonyl-2-azabicyclo[4.4.1]undeca-5,7,9-triene: (±)-II-10.** To a solution of (±)-II-9 (60 mg, 0.15 mmol) in freshly distilled dichloromethane (20 mL), was added Grubbs' 2nd generation catalyst (7 mg, 0.008 mmol, 5 mol %). The reaction mixture was stirred under N₂ and the reaction progress was monitored by ¹H NMR spectroscopy. After 4 h all signals for the starting material disappeared. The reaction mixture was concentrated under a flow of N₂, and the residue purified by column chromatography (SiO₂, hexanes–ethyl acetate = 4:1) to afford (±)-II-10 as a colorless oil (37 mg, 82%). ¹H NMR (400 MHz, CDCl₃) δ 2.43 (s, 3H), 2.81 (ddd, J = 1.2, 8.8, 14.4 Hz, 1H), 2.97-2.99 (narrow m, 2H), 3.06 (ddd, J = 1.2, 3.6, 14.4 Hz, 1H), 4.06-4.09 (narrow m, 2H), 4.59 (td, J = 4.0, 8.4 Hz, 1H), 5.56-5.60 (narrow m, 2H), 6.20-6.24 (m, 1H), 6.30 (qd, J = 1.2, 5.4 Hz, 1H), 6.43 (qd, J = 2.0, 5.4 Hz, 1H), 7.31 and 7.73 (ABq, J_{AB} = 8.2 Hz, 4H total); ¹³C NMR (100 MHz, CDCl₃) δ 21.7, 38.0, 44.6, 55.9, 67.6, 125.0, 127.6, 129.5, 130.0, 130.1, 131.9, 132.6, 134.8, 143.7, 144.5. This compound decomposed upon standing and thus a satisfactory HRMS was not obtained.

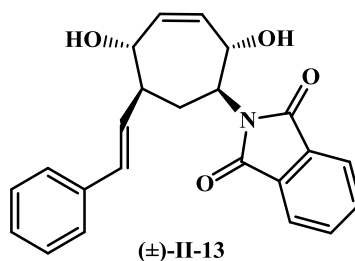


(6-Styrenyl-2,4-cyclohepta-1-yl)phthalimide: (±)-II-11. In 250 mL round bottom flask cation (±)-II-7 (1.000 g, 2.375 mmol) was added freshly distilled CH_2Cl_2 (100 mL). To this suspension was added potassium phthalimide (0.659 g, 3.356 mmol). The whole mixture was stirred at room temperature under N_2 for 3 h and then quenched by adding water (50 mL). The mixture was extracted several times with CH_2Cl_2 , the combined extracts were dried (Na_2SO_4) and concentrated to give a pale yellow crude solid (1.257 g). This crude material was dissolved in methanol (50 mL) and stirred under N_2 at room temperature for 10 min, then solid cerium ammonium nitrate (IV) (3.42 g, 6.24 mmol) was added and the mixture was stirred for 2 h. The solvent was evaporated and water (50 mL) was added to the solid residue. The product was extracted several times with CH_2Cl_2 ; the combined extracts were dried (Na_2SO_4) and concentrated. The residue was purified by column chromatography (SiO_2 , hexane-ethyl acetate = 3:1) to afford a light white solid (±)-II-11 (648 mg, 81%). mp 107-108 $^\circ\text{C}$; ^1H NMR (300 MHz, CDCl_3) δ 2.05 (br d, $J = 13.2$ Hz, 1H), 2.86 (td, $J = 11.1, 13.2$ Hz, 1H), 3.56-3.58 (m, 1H), 5.29 (d, $J = 10.5$ Hz, 1H), 5.78-5.89 (m, 4H), 6.18 (dd, $J = 8.4, 15.9$ Hz, 1H), 6.48 (d, $J = 15.9$ Hz, 1H), 7.21-7.35 (m, 5H), 7.72 (dd, $J = 3.1, 5.4$ Hz, 2H), 7.87 (dd, $J = 3.1, 5.4$ Hz, 2H); ^{13}C NMR (100 MHz, CDCl_3) δ 38.2, 44.0, 50.5, 123.3, 123.9, 124.0, 126.2, 127.3, 128.6,

129.8, 132.0, 132.2, 133.6, 134.1, 136.9, 137.2, 167.7. elemental analysis calcd (%) for $C_{23}H_{19}NO_2$: C 80.92, H 5.61; found: C 80.61, H 5.67.

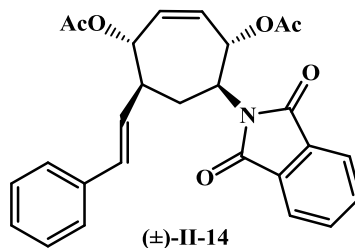


2-Phthalimido-4-(2'-styrenyl)-6,7-dioxabicyclo[3.2.2]non-8-ene: (±)-II-12. To a 50 mL two-necked round bottom flask equipped with a condenser, was charged with (±)-II-11 (1.00 g, 2.93 mmol) in dry chloroform (40 mL) and tetraphenylporphine (TPP) (36 mg, 3 mol %). The resulting deep purple solution was irradiated with a 100-W halogen lamp, while ultra pure O_2 was bubbled through the solution and stirred at 0 °C for 8 h. The mixture was concentrated and the residue was purified by column chromatography (SiO_2 , hexane: ethyl acetate= 1:1) to give the endoperoxide (±)-II-12 (923 mg, 91%) as a colorless solid, mp 180-181 °C. 1H NMR (400 MHz, $CDCl_3$) δ 1.77 (br d, $J = 9.6$ Hz, 1H), 2.11 (q, $J = 10.1$ Hz, 1H), 3.01 (q, $J = 3.3$ Hz, 1H), 4.79 (m, 2H), 4.84 (dd, $J = 3.1$, 9.9 Hz, 1H), 5.98 (dd, $J = 6.3$, 11.1 Hz, 1H), 6.43-6.51 (m, 2H), 6.89 (dd, $J = 6.3$, 6.1 Hz, 1H), 7.21-7.33 (m, 5H), 7.75 (dd, $J = 3.6$, 5.6 Hz, 2H), 7.86 (dd, $J = 3.5$, 5.6 Hz, 2H); ^{13}C NMR (100 MHz, $CDCl_3$) δ 29.8, 45.8, 52.0, 80.4, 81.1, 123.6, 123.8, 126.4, 127.9, 128.7, 128.8, 130.8, 131.8, 131.9, 134.5, 136.8, 167.8. Anal. Calcd for $C_{23}H_{19}NO_4$: C, 73.98; H 5.13. Found: C, 73.87; H, 5.27.



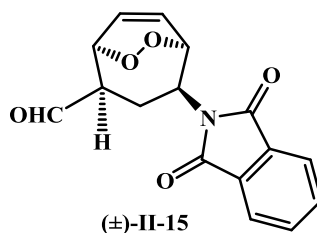
4-Phthalimido-6-(2'-styryl)-3,7-dihydroxycycloheptene: (±)-II-13. To a solution of (±)-II-12 (50 mg, 0.15 mmol) in CH₂Cl₂ (1 mL) was added activated zinc dust (50 mg). To the resulting suspension was added a solution of glacial acetic acid (0.02 mL, 0.34 mmol) in CH₂Cl₂ (2 mL) in 3 portions over 30 min. The reaction mixture was stirred at room temperature for 15 min, after which the mixture was loaded onto a column chromatography (SiO₂, hexanes-ethyl acetate = 2:3) to give (±)-II-13 (47 mg, 92%) as a colorless solid; mp 225-227 °C; ¹H NMR (400 MHz, CD₃OD) δ 1.95 (td, J = 2.8, 14.0 Hz, 1H), 2.47 (dq, J = 2.8, 10.1 Hz, 1H), 2.70 (td, J = 11.8, 14.0 Hz, 1H), 4.25-4.10 (m, 2H), 4.99-4.93 (m, 1H), 5.70 (td, J = 2.8, 12.6 Hz, 1H), 5.80 (td, J = 2.8, 12.6 Hz, 1H), 6.19 (dd, J = 9.0, 16.4 Hz, 1H), 6.46 (d, J = 16.4 Hz, 1H), 7.16 (t, J = 7.4, 1H), 7.25 (t, J = 7.6 Hz, 2H), 7.37 (d, J = 7.6 Hz, 2H), 7.88-7.75 (m, 4H); ¹H NMR (400 MHz, d₆-acetone) δ 2.01 (td, J = 2.8, 14.0 Hz, 1H), 2.53-2.42 (m, 1H), 2.73 (td, J = 11.8, 14.4 Hz, 1H), 3.99 (d, J = 4.8 Hz, 1H), 4.16 (ddd, J = 3.2, 10.4, 12.4 Hz, 1H), 4.31-4.25 (m, 1H), 4.53 (d, J = 5.6 Hz, 1H), 4.99-4.93 (m, 1H), 5.73 (td, J = 2.8, 12.4 Hz, 1H), 5.82 (td, J = 2.7, 12.8 Hz, 1H), 6.28 (dd, J = 8.8, 16.0 Hz, 1H), 6.50 (d, J = 16.0 Hz, 1H), 7.18 (tt, J = 1.6, 7.4 Hz, 1H), 7.28 (t, J = 7.2 Hz, 2H), 7.39 (d, J = 8.0 Hz, 2H), 7.82 (s, 4H); ¹³C NMR (75 MHz, d₆-acetone) δ 37.7, 50.5, 55.5, 70.2, 73.5, 123.7, 127.1, 127.9, 129.2, 131.9,

133.3, 134.4, 134.5, 134.8, 137.4, 138.6, 168.9. HRMS (ESI): m/z calcd for $C_{23}H_{21}NO_4$: $[M+Na^+]$; 398.1363, found 398.1358.



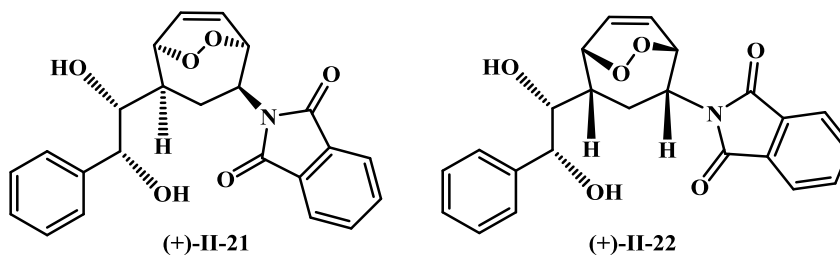
(1S*,2S*,5S*,6S*) N-(2,5-Diacetoxy-6-styryl-3-cyclohepten-1(S*)-yl)phthalimide:

(±)-II-14. To a mixture of diol (±)-II-13 (400 mg, 1.11 mmol) and p-toluenesulfonyl chloride (21 mg, 0.1 mmol) was added acetic anhydride (5 mL). The resulting suspension was heated at reflux under N_2 for 1 h. The reaction mixture was concentrated and the residue was purified by column chromatography (SiO_2 , hexanes–ethyl acetate = 3:2) to afford (±)-II-14 (406 mg, 82%) as a colorless solid: mp 65–66 °C; 1H NMR (400 MHz, $CDCl_3$) δ 1.75 (s, 3H), 1.87 (s, 3H), 2.01 (br d, $J = 14.4$ Hz, 1H), 2.63 (br q, $J = 9.6$ Hz, 1H), 2.85 (q, $J = 12.8$ Hz, 1H), 4.42 (t, $J = 10.8$ Hz, 1H), 5.57–5.49 (br m, 2H), 5.70 (br d, $J = 13.2$ Hz, 1H), 5.86 (dd, $J = 9.4, 15.6$ Hz, 1H), 6.02 (br d, $J = 10.4$ Hz, 1H), 6.34 (d, $J = 15.6$ Hz, 1H), 7.25–7.10 (m, 5H), 7.80–7.63 (m, 4H); ^{13}C NMR (100 MHz, $CDCl_3$) δ 20.9, 21.2, 36.2, 47.6, 51.4, 72.1, 74.1, 123.6, 126.4, 127.7, 128.8, 130.2, 130.3, 131.6, 131.9, 132.7, 134.4, 137.0, 167.9, 169.6, 170.3. Anal. Calcd for $C_{27}H_{25}NO_6$: C, 70.58; H 5.48. Found: C, 70.28; H, 5.45.



rac-2-Formyl-4-phthalimido-6,7-dioxabicyclo[3.2.2]non-8-ene: (±)-II-15. To a mixture of (±)-II-11 (1.00 g, 2.93 mmol) in a mixture of t-BuOH (20 mL), ethyl acetate (5 mL) and water (25 mL), was added at room temperature methanesulfonamide (60 mg, 0.59 mmol). The mixture was cooled to 0 °C with an ice bath and then solid AD-mix β (4.325 g) was added. The reaction mixture was stirred for 34 h at 0 °C, after which monitoring by TLC indicated the disappearance of starting material. The reaction was quenched with water (20 mL). The mixture was transferred to separatory funnel, and the top, organic layer was decanted. The aqueous layer was extracted several times with ethyl acetate and the combined organic layers were dried (Na₂SO₄), concentrated and the residue purified by column chromatography (SiO₂, hexanes:ethyl acetate = 2:3) to afford a 1:1 mixture of diastereomeric diols (1.050 g, 96%) as a colorless foam. This material was used in the next step without further characterization. To a solution of diastereomeric diols (1.00 g, 2.67 mmol) in CHCl₃ (30 mL) was added tetraphenylporphine (15 mg). The deep purple solution was irradiated for a 5 h period with a commercially 100-W halogen lamp, while ultra pure O₂ was bubbled through the solution. The organic solvent was removed to afford a mixture of diastereomeric endoperoxide diols, (+)-II-21 and (+)-II-22 which were used in the next step without further purification (1.005 g). To a solution of (+)-II-21 / (+)-II-22 (500 mg, 1.29 mmol) in dry CH₂Cl₂ (25 mL) at -78 °C was added solid Pb(OAc)₄ (544 mg, 1.23 mmol). The

mixture was stirred for 30 min, and then quenched with water. The mixture was extracted several times with CH_2Cl_2 , and the combined extracts were dried (Na_2SO_4) and concentrated. Purification of the residue by column chromatography (SiO_2 , hexanes:ethyl acetate = 3:2) gave **(±)-II-15** (244 mg, 63%) as a colorless solid: mp 179-180 °C; ^1H NMR (400 MHz, CDCl_3) δ 2.05-1.97 (m, 1H), 2.11 (q, $J = 13.0$ Hz, 1H), 3.16 (dd, $J = 5.0, 13.0$ Hz, 1H), 4.86-4.80 (m, 2H), 5.26 (d, $J = 7.2$ Hz, 1H), 6.43 (dd, $J = 7.2, 9.3$ Hz, 1H), 6.77 (dd, $J = 7.2, 9.3$ Hz, 1H), 7.88-7.78 (m, 4H), 9.65 (s, 1H); ^{13}C NMR (100 MHz, CDCl_3) δ 23.9, 52.1, 54.3, 75.4, 80.0, 123.7, 124.6, 129.8, 131.7, 134.6, 167.7, 199.0 ppm; HRMS (ESI): m/z calcd for $\text{C}_{16}\text{H}_{13}\text{NO}_5 + \text{Na}^+$: 322.0686 [$\text{M} + \text{Na}^+$]; found: 322.0685.



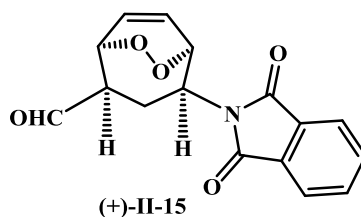
Singlet oxygen cycloaddition of diastereomeric diol mixture: To a stirred solution of the diastereomeric mixture of diols (1.300 g, 3.467 mmol) in 35 ml CHCl_3 was added tetraphenylporphine (TPP) (25 mg, 0.041 mmol). The deep purple solution was irradiated with a 100-W halogen lamp, while ultra pure O_2 was bubbled through the solution and stirred at room temperature for 6 h. The mixture was concentrated and the residue was purified by column chromatography (SiO_2 , hexanes:ethyl acetate 3:2) to give **(+)-II-21** as a white foam (671 mg, 48 %) followed by **(+)-II-22** as a white foam (626 mg, 44%).

(Less polar) 4-(1'R,2'R-Dihydroxy-2'-phenylethyl)-2-phthalimido-6S,7R-

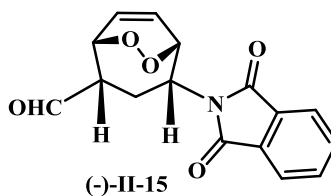
dioxabicyclo[3.2.2]non-8-ene: (+)-II-21. mp 97-98 °C; $[\alpha]_D^{20} = +41.17$ (c=0.0011, CH₂Cl₂); ¹H NMR (300 MHz, CDCl₃) δ 1.60 (br d, J = 12.6 Hz, 1H), 2.10-2.03 (m, 1H), 2.29 (dd, J = 5.7, 12.6 Hz, 1H), 2.48 (d, J = 4.8 Hz, 1H), 2.68 (d, J = 3.9 Hz, 1H), 3.43-3.39 (narrow m, 1H), 4.73-4.68 (m, 3H), 5.18 (d, J = 7.2 Hz, 1H), 6.41 (dd, J = 7.5, 8.4 Hz, 1H), 6.71 (dd, J = 7.2, 9.1 Hz, 1H), 7.39-7.26 (m, 5H), 7.85-7.71 (m, 4H); ¹³C NMR δ (75 MHz, CDCl₃) 27.6, 43.8, 52.2, 74.0, 76.9, 78.1, 79.8, 123.6, 125.8, 126.5, 128.4, 128.8, 128.9, 131.8, 134.5, 141.0, 167.8; HRMS (ESI): m/z calcd for C₂₃H₂₁NO₆+Na⁺: 430.1261 [M+Na⁺]; found: 430.1254.

(More polar) 4-(1'R,2'R-Dihydroxy-2'-phenylethyl)-2-phthalimido-6R,7S-

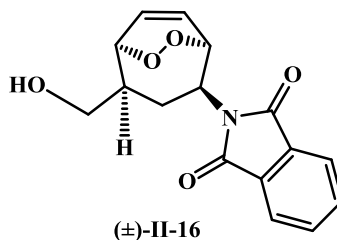
dioxabicyclo[3.2.2]non-8-ene: (+)-II-22. mp 90-92°C. $[\alpha]_D^{20} = +33$ (c=0.0011, CH₂Cl₂); ¹H NMR (300 MHz, CDCl₃) δ 1.65 (td, J = 4.0, 12.8 Hz, 1H), 2.07-1.98 (m, 1H), 2.23 (q, J = 12.6 Hz, 1H), 3.25-3.10 (br s, 2H), 3.80-3.75 (narrow m, 1H), 4.49 (dd, J = 2.4, 6.9 Hz, 1H), 4.58 (dd, J = 4.4, 12.8 Hz, 1H), 4.70 (d, J = 7.2 Hz, 2H), 6.47 (dd, J = 8.0, 8.8 Hz, 1H), 6.65 (dd, J = 7.6, 8.8 Hz, 1H), 7.40-7.25 (m, 5H), 7.90-7.70 (m, 4H); ¹³C NMR δ (75 MHz, CDCl₃) 23.4, 44.0, 52.4, 75.1, 77.0, 79.7, 81.4, 123.5, 126.5, 126.6, 127.3, 128.7, 129.0, 131.8, 134.4, 140.7, 167.0. HRMS (ESI): m/z calcd for C₂₃H₂₁NO₆+Na⁺ [M+Na⁺]; found: 430.1252.



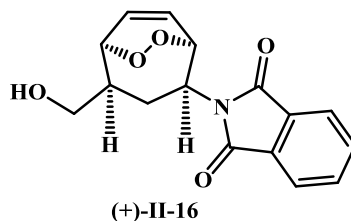
2R-Formyl-4S-phthalimido-6,7-dioxabicyclo[3.2.2]non-8-ene: (+)-II-15. To a solution of the less polar endoperoxide diol (+)-II-21 (650 mg, 1.60 mmol) dissolved in dry CH₂Cl₂ (30 mL) was added solid Pb(OAc)₄ (1.061 g, 2.396 mmol). The reaction mixture was stirred for 15 min, and then quenched with water, and the mixture was extracted several times with CH₂Cl₂. The combined extracts were dried (Na₂SO₄) and concentrated, and the residue was purified by column chromatography (SiO₂, hexanes-ethyl acetate = 3:2) to afford (+)-II-15 (439 mg, 93%) as a colorless solid. m.p. 55-57 °C; $[\alpha]_D^{20} = +88$ (c 0.0011, CH₂Cl₂); the NMR spectral data for (+)-II-15 was identical to that for the racemic material (±)-II-15.



2S-Formyl-4R-phthalimido-6,7-dioxabicyclo[3.2.2]non-8-ene: (-)-II-15. The diol cleavage of (+)-II-22 (0.668, 1.641 mmol) was carried out in a fashion similar to the cleavage of (+)-II-21 to afford the optically active aldehyde (-)-II-15 (371 mg, 75%). mp 95-97 °C; $[\alpha]_D^{20} = -102$ (c 0.00102, CH₂Cl₂). The NMR spectral data for (-)-II-15 was identical with that for the racemic compound (±)-II-15.

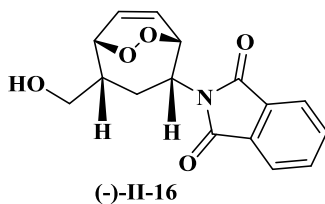


4-Hydroxymethyl-2-phthalimido-8,9-dioxabicyclo[3.2.2]non-6-ene: (±)-II-16. To a mixture of THF (10 mL) and glacial acetic acid (2 mL) was added (±)-II-15 (50.0 mg, 0.167 mmol) and the mixture was stirred for 5 min. Solid NaBH₃CN (16 mg, 0.254 mmol) was added, and monitoring of the reaction by TLC indicated complete disappearance of starting material after 1 h. The solvent was evaporated and the residue was purified by column chromatography (SiO₂, hexanes:ethyl acetate = 2:3) to afford (±)-II-16 (51 mg, quant.) as a colorless solid: mp = 139-141°C; ¹H NMR (400 MHz, CDCl₃) δ 1.53 (br s, 1H), 1.61 (td, J = 4.4, 12.8 Hz, 1H), 1.84 (q, J = 12.8 Hz, 1H), 2.40-2.31 (m, 1H), 3.47-3.38 (m, 1H), 3.66-3.60 (m, 1H), 4.81-4.73 (m, 2H), 4.98 (d, J = 7.2 Hz, 1H), 6.45 (dd, J = 6.8, 9.8 Hz, 1H), 6.77 (dd, J = 7.2, 9.8 Hz, 1H), 7.90-7.72 (m, 4H); ¹³C NMR (100 MHz, d₆-acetone) δ 26.6, 44.7, 52.3, 64.2, 78.3, 80.0, 123.6, 124.9, 129.7, 131.9, 134.5, 167.8. HRMS (ESI): m/z calcd for C₁₆H₁₅NO₅: [M+Na⁺]; 324.0842, found 324.0839.



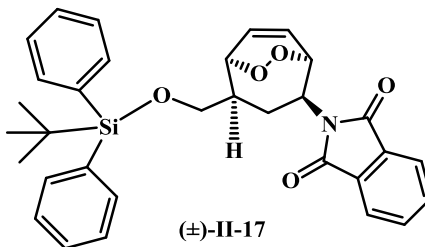
4(S)-Hydroxymethyl-2(S)-phthalimido-8,9-dioxabicyclo[3.2.2]non-6-ene: (+)-II-16.

The reduction of (+)-II-15 (400 mg, 1.34 mmol) was carried out in a fashion similar to the reduction of (±)-102, to afford the optically active primary alcohol (+)-II-16 (329 mg, 82%). mp 163-166 °C; $[\alpha]_D^{20} = +119$ (c 0.00176, CH₂Cl₂). The NMR spectral data for (+)-II-16 was identical with that for the racemic compound (±)-II-16.



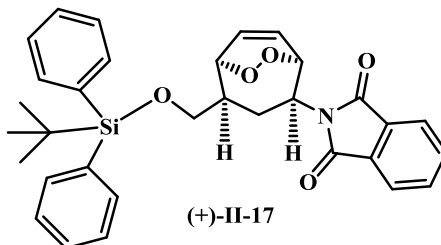
4(R)-Hydroxymethyl-2(R)-phthalimido-8,9-dioxabicyclo[3.2.2]non-6-ene: (-)-II-16.

The reduction of (-)-II-15 (360 mg, 1.204 mmol) was carried out in a fashion similar to the reduction of (±)-II-15, to afford the optically active primary alcohol (-)-II-16 (281 mg, 78%). mp 167-169 °C; $[\alpha]_D^{20} = -95$ (c 0.00082, CH₂Cl₂). The NMR spectral data for (-)-II-16 was identical with that for the racemic compound (±)-II-16.

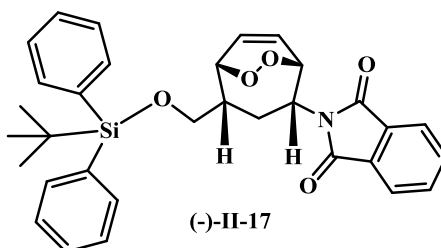


4-(t-Butyldiphenylsilyloxy)methyl-2-phthalimido-8,9-dioxabicyclo[3.2.2]non-6-ene:

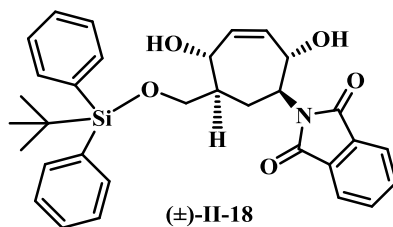
(±)-II-17. To a solution of (±)-II-16 (40.0 mg, 0.133 mmol) in freshly distilled CH₂Cl₂ (5 mL) cooled to 0 °C, was added imidazole (18 mg, 0.3 mmol), followed by dropwise addition of t-butylchlorodiphenylsilane (44 mg, 0.2 mmol) over a period of 15 min at 0 °C. After stirring at room temperature for 3 h, monitoring of the reaction mixture by TLC indicated complete disappearance of starting material. The mixture was quenched with water and extracted several times with CH₂Cl₂. The combined extracts were concentrated and the residue was purified by column chromatography (SiO₂, hexanes:ethyl acetate = 4:1) to give (±)-II-17 (65 mg, 91%) as a colorless foam; mp 44-46 °C; ¹H NMR (400 MHz, CDCl₃) δ 1.06 (s, 9H), 1.47 (td, J = 4.8, 12.8 Hz, 1H), 1.78 (q, J = 12.7 Hz, 1H), 2.50-2.38 (m, 1H), 3.36 (dd, J = 8.6, 10.6, 1H), 3.60 (dd, J = 5.0, 10.4 Hz, 1H), 4.72 (d, J = 6.8 Hz, 1H), 4.75 (dd, J = 4.8, 12.8 Hz, 1H), 5.01 (d, J = 7.2 Hz, 1H), 6.25 (ddd, J = 0.8, 7.2, 9.2 Hz, 1H), 6.71 (ddd, J = 1.2, 7.2, 9.6 Hz, 1H), 7.48-7.37 (m, 6H), 7.65-7.60 (m, 4H), 7.87-7.70 (m, 4H); ¹³C NMR (100 MHz, CDCl₃) δ 19.4, 26.3, 27.0, 44.5, 52.4, 65.0, 78.6, 80.0, 123.5, 125.0, 128.0, 129.4, 130.0, 131.9, 133.3, 134.4, 135.7, 167.7. HRMS (ESI): m/z calcd for C₃₂H₃₃NO₅Si: [M+Na⁺]; 562.2020, found 562.2009.



4S-(t-Butyldiphenylsilyloxy)methyl-2S-phthalimido-8,9-dioxabicyclo[3.2.2]non-6-ene: (+)-II-17. Protection of (+)-II-17 (200 mg, 0.664 mmol) with t-butyldiphenylsilyl chloride was carried out in a fashion similar to the reaction of (±)-II-16, to afford (+)-104 (311 mg, 87%). mp 44-47 °C; $[\alpha]_D^{20} = +48.5$ (c 0.00132, CH₂Cl₂). The NMR spectral data for (+)-II-17 was identical with that for the racemic compound (±)-II-17.

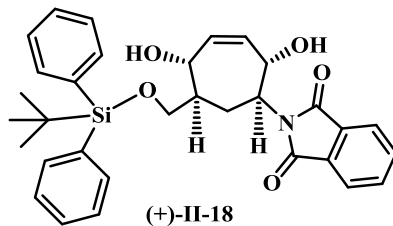


4R-(t-Butyldiphenylsilyloxy)methyl-2R-phthalimido-8,9-dioxabicyclo[3.2.2]non-6-ene: (-)-II-17. Protection of (-)-II-16 (200 mg, 0.664 mmol) with t-butyldiphenylsilyl chloride was carried out in a fashion similar to the reaction of (±)-II-16, except for 15 hrs to afford (-)-II-17 (358 mg, 99%). mp 45-47 °C; $[\alpha]_D^{20} = -47.5$ (c 0.00122, CH₂Cl₂). The NMR spectral data for (-)-II-17 was identical with that for the racemic compound (±)-II-17.



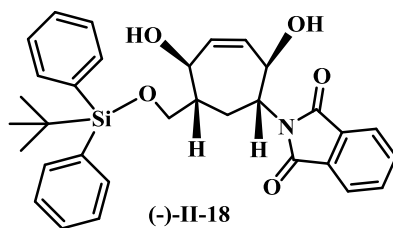
6-(t-Butyldiphenylsilyloxy)methyl-3,7-dihydroxy-4-phthalimido-cycloheptene (±)-II-

18. To a solution of (±)-II-17 (55.0 mg, 0.102 mmol) in CH₂Cl₂ (5 mL) was added activated zinc dust (55 mg). To this suspension was added acetic acid (61 mg, 1.020 mmol) dissolved in CH₂Cl₂ (3 mL) dropwise over a 10 min period. The reaction mixture was stirred for 15 min at room temperature, the solvent was evaporated, and the residue was purified by column chromatography (SiO₂, hexanes:ethyl acetate = 2:3) to afford (±)-II-18 (52 mg, 94%) as a colorless foam: mp = 51-53°C; ¹H NMR (400 MHz, CDCl₃) δ 1.07 (s, 9H), 1.56 (td, J = 2.4, 14.4 Hz, 1H), 1.87 (d, J = 6.8 Hz, 1H), 2.00-1.90 (br m, 1H), 2.38 (td, J = 12.0, 14.8 Hz, 1H), 3.69 (dd, J = 7.2, 10.2 Hz, 1H), 3.75 (dd, J = 4.0, 10.2 Hz, 1H), 4.07 (d, J = 2.4 Hz, 1H), 4.14 (ddd, J = 2.4, 10.0, 12.4 Hz, 1H), 4.45 (br d, J = 9.6 Hz, 1H), 4.93-4.87 (m, 1H), 5.68 (td, J = 2.6, 12.8 Hz, 1H), 5.80 (td, J = 2.8, 12.8 Hz, 1H), 7.45-7.34 (m, 6H), 7.85-7.63 (m, 8H); ¹³C NMR (100 MHz, CDCl₃) δ 19.3, 27.0, 33.1, 44.8, 55.0, 68.7, 70.2, 74.1, 123.4, 128.06, 128.11, 130.17, 130.23, 132.02, 132.07, 132.7, 134.2, 135.7, 135.8, 136.3, 168.7. Anal. Calcd for C₃₂H₃₅NO₆Si: C, 70.95; H 6.51. Found: C, 70.66; H, 6.60.



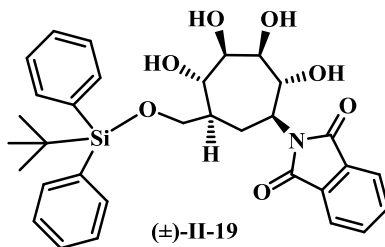
6S-(t-Butyldiphenylsilyloxy)methyl-3S,7R-dihydroxy-4S-phthalimido-cycloheptene:

(+)-II-18. The reduction of endoperoxide **(+)-II-17** (80 mg, 0.15 mmol) with Zn and acetic acid was carried out in a fashion similar to reduction of the racemic endoperoxide **(±)-II-17**, to afford **(+)-II-18** (73 mg, 91%). mp 53-55 °C; $[\alpha]_D^{20} = +17$ (c 0.0011, CH₂Cl₂). The NMR spectral data for **(+)-II-18** was identical with that for the racemic compound **(±)-II-18**.



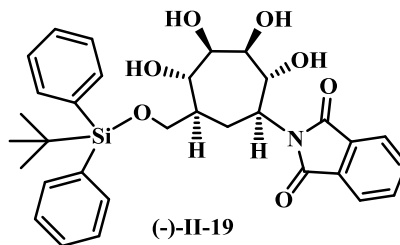
6R-(t-Butyldiphenylsilyloxy)methyl-3R,7S-dihydroxy-4S-phthalimido-cycloheptene:

(-)-II-18. The reduction of endoperoxide **(-)-II-17** (80 mg, 0.15 mmol) with Zn and acetic acid was carried out in a fashion similar to reduction of the racemic endoperoxide **(±)-II-17**, to afford **(-)-II-18** (80 mg, 91%). mp 57-59 °C; $[\alpha]_D^{20} = -11$ (c 0.00062, CH₂Cl₂). The NMR spectral data for **(-)-II-18** was identical with that for the racemic compound **(±)-II-18**.

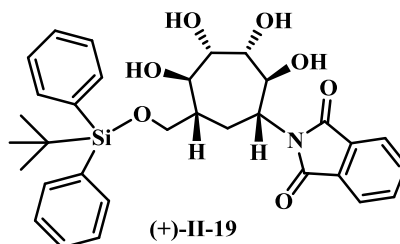


6-(t-Butyldiphenylsilyloxy)methyl-2,3,4,5-tetrahydroxy-1-phthalimido-

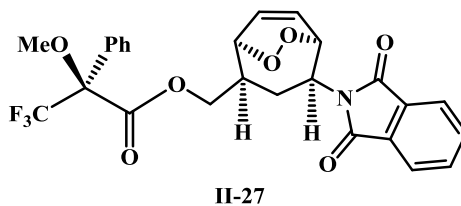
cycloheptane: (±)-II-19. To a solution of (±)-II-18 (44 mg, 0.081 mmol) in acetone (5 mL) was added a solution of N-methylmorpholine N-oxide (14 mg, 0.122 mmol) in water (1 mL), followed by a solution of OsO₄ (0.05 mL, 0.2 M in toluene, 0.01 mmol). The reaction mixture was stirred for 2 h at room temperature under N₂. The solvent was evaporated and the residue was purified by column chromatography (SiO₂, hexanes:ethyl acetate = 1:4) to afford (±)-II-19 (41 mg, 88%) as a colorless foam; mp 86-87 °C; ¹H NMR (400 MHz, CD₃OD) δ 1.00 (s, 9H), 1.56 (d, J = 14.0 Hz, 1H), 1.76-1.67 (m, 1H), 2.61 (td, J = 12.0, 14.4 Hz, 1H), 3.68-3.58 (m, 2H), 3.83 (d, J = 6.8 Hz, 1H), 3.89 (dd, J=4.2, 9.8 Hz, 1H), 3.97 (d, J = 4.8 Hz, 1H), 4.11 (dt, J = 1.6, 11.0 Hz, 1H), 4.5 (dd, J = 7.0, 10.2 Hz, 1H), 7.35-7.22 (m, 6H), 7.65-7.55 (m, 4H), 7.90-7.78 (m, 4H); ¹³C NMR (100 MHz, CD₃OD) δ 20.2, 27.5, 29.4, 58.5, 67.9, 72.1, 73.6, 75.8, 78.5, 124.2, 128.84, 128.88, 130.88, 130.93, 133.5, 135.4, 136.8, 136.9, 169.8. HRMS (ESI): m/z calcd for C₃₂H₃₇NO₇Si: [M+Na⁺]; 598.2232, found 598.2219.



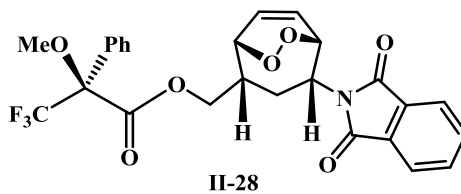
6S-(t-Butyldiphenylsilyloxy)methyl-2R,3S,4R,5S-tetrahydroxy-1S-phthalimido-cycloheptane: (-)-II-19. The dihydroxylation of (+)-II-18 (65 mg, 0.12 mmol) with catalytic OsO₄ was carried out in a fashion to the dihydroxylation of (±)-II-18, to afford (-)-II-19 (61 mg, 88%). mp 86-88 °C; [α]_D²⁰ = -17 (c 0.0010, MeOH). The NMR spectral data for (-)-II-19 was identical with that for the racemic compound (±)-II-19.



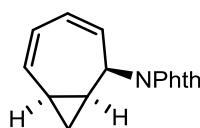
6R-(t-Butyldiphenylsilyloxy)methyl-2S,3R,4S,5R-tetrahydroxy-1S-phthalimido-cycloheptane: (+)-II-19. The dihydroxylation of (+)-II-18 (75 mg, 0.138 mmol) with catalytic OsO₄ was carried out in the same fashion as the dihydroxylation of (±)-II-18, to afford (+)-II-19 (70 mg, 88%). mp 74-76 °C; [α]_D²⁰ = +14 (c 0.00090, MeOH). The NMR spectral data for (+)-II-19 was identical with that for the racemic compound (±)-II-19.



(S)(-)- α -methoxy- α -trifluoromethylphenylacetic ester: II-27. To a solution of optically enriched endoperoxide alcohol (+)-**II-16** (20 mg, 0.066 mmol) in dry THF (3 mL) was added (S)(-)- α -methoxy- α -trifluoromethylphenylacetic acid (50 mg, 0.21 mmol) followed by *N,N'*-dicyclohexylcarbodiimide (44 mg, 0.21 mmol) and 4-dimethylaminopyridine (5 mg, 0.004 mmol). The reaction mixture was stirred for 2 h, then concentrated and water (5 mL) was added. The mixture was extracted several times with ether, and the combined extracts were washed with 10% HCl, and concentrated. The residue was purified by column chromatography (SiO₂, hexanes:ethyl acetate = 7:3) to give a colorless oil (34 mg, 100 %); ¹H NMR (400 MHz, d₆-acetone) δ 1.64 (td, J = 4.4, 12.8 Hz, 1H), 2.03 (q, J = 12.7 Hz, 1H), 2.44-2.55 (m, 1H), 3.58 (q, J = 1.2 Hz, 3H), 4.27 (dd, J = 7.0 and 11.2 Hz, 1H), 4.39 (dd, J = 5.4, 11.2 Hz, 1H), 4.63 (ddd, J = 0.9, 4.5, 12.7 Hz, 1H), 4.72 (br d, J = 7.2 Hz, 1H), 4.92 (br d, J = 7.2 Hz, 1H), 6.22 (ddd, J = 1.2, 7.2, 9.2 Hz, 1H), 6.65 (ddd, J = 0.9, 7.2, 9.2 Hz, 1H), 7.37-7.47 (m, 3H), 7.51-7.56 (m, 2H), 7.85 (s, 4H); ¹³C NMR (100 MHz, CDCl₃) δ 26.2, 41.1, 51.7, 55.7, 66.6, 77.8, 79.8, 121.8, 123.5, 123.7, 124.6, 127.1, 128.6, 129.8, 130.1, 131.6, 132.0, 134.4, 166.5, 167.5.

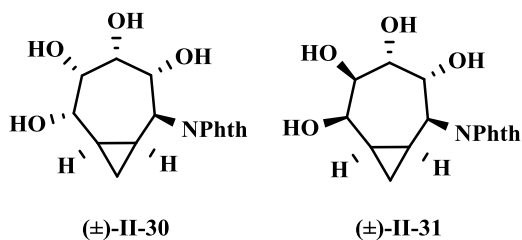


(S)(-)- α -methoxy- α -trifluoromethylphenylacetic ester: II-28. The esterification of optically enriched endoperoxide alcohol (-)-**II-16** (20 mg, 0.066 mmol) with (S)(-)- α -methoxy- α -trifluoromethylphenylacetic acid was carried out in a fashion to the esterification of (+)-**II-16**, to afford **II-28** (32 mg, 94%). mp 43-45 °C; ^1H NMR (400 MHz, d_6 -acetone) δ 1.67 (td, $J = 4.6, 12.8$ Hz, 1H), 1.99 (q, $J = 12.8$ Hz, 1H), 2.45-2.54 (m, 1H), 3.55 (s, 3H), 4.38-4.27 (m, 2H), 4.64 (dd, $J = 5.0, 13.2$ Hz, 1H), 4.74 (br d, $J = 7.2$ Hz, 1H), 4.93 (br d, $J = 7.2$ Hz, 1H), 6.31 (ddd, $J = 0.8, 7.1, 9.1$ Hz, 1H), 6.66 (ddd, $J = 0.9, 7.3, 9.1$ Hz, 1H), 7.45-7.51 (m, 3H), 7.53-7.58 (m, 2H), 7.85 (br s, 4H); ^{13}C NMR (100 MHz, CDCl_3) δ 26.2, 41.1, 51.5, 55.4, 66.5, 77.6, 79.8, 121.7, 123.4, 123.6, 124.6, 127.2, 128.6, 129.8, 130.2, 131.6, 131.8, 134.3, 166.5, 167.4.



N-(Bicyclo[5.1.0]octa-3,5-dien-2-yl)phthalimide: (±)-II-29. To a stirred suspension of cation **I-88b** (8.00 g, 14.2 mmol) in solution of water saturated-ether (water: ether = 1:5) was added potassium phthalimide (20.22 g, 109.3 mmol). This suspension was stirred for 150 min, the ether layer was decanted and to the residual solid was added ether (100 mL)

and the mixture was stirred for 1 h. This step was repeated 3 times. The combined ethereal fractions were concentrated at low temperature under vacuum to give a yellow foam (10.21 g, >100%) which was used in the next step without purification. To a solution of the unpurified complex (9.00 g) dissolved in acetonitrile (100 mL) was added 2,3-dichloro-5,6-dicyano-1,4-benzoquinone (DDQ) (5.10 g, 22.5 mmol). After 2 h, monitoring by TLC showed complete disappearance of the complex. The mixture was passed through a short column of silica gel and washed with dichloromethane. The combined fractions were concentrated and the residue purified by column chromatography (SiO₂, hexanes-ethyl acetate = 4:1) to give a (±)-**II-29** as colorless solid (2.66 g, 73%): mp 162-163 °C; IR (KBr) 3023, 1765, 1711, 1607, 1381 cm⁻¹; ¹H NMR (300 MHz, CDCl₃) δ 0.99 (dddd, J = 0.9, 4.7, 8.5, 8.8 Hz, 1H), 1.22- 1.34 (m, 1H), 1.85- 1.95 (m, 1H), 2.25 (ddd, J = 5.6, 5.6, 5.6 Hz, 1H), 5.43-5.62 (m, 3H), 5.83 (ddd, J = 2.8, 6.0, 11.5 Hz, 1H), 6.23 (dd, J = 7.5, 11.5 Hz, 1H), 7.69-7.76 (m, 2H), 7.82-7.89 (m, 2H); ¹³C NMR (75 MHz, CDCl₃) δ 9.0, 15.2, 43.8, 49.8, 122.6, 123.4, 126.2, 126.9, 132.1, 134.1, 135.2, 167.9. The NMR spectral data was consistent with the literature values.¹²⁵



N-(3R*,4R*,5S*,6S*-tetrahydroxybicyclo[5.1.0]oct-2S*-yl)phthalimide (±)-**II-30** and

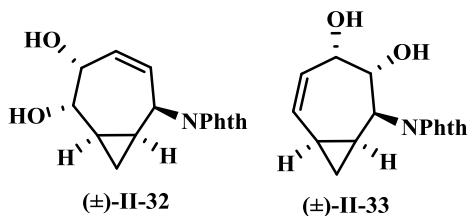
N-(3R*,4R*,5R*,6R*-tetrahydroxybicyclo[5.1.0]oct-2S*-yl)phthalimide (±)-**II-31**:

To a stirring solution of the diene (±)-**II-29** (300 mg, 1.20 mmol) in acetone (5 ml) was

added a solution of *N*-methylmorpholine-*N*-oxide (419 mg, 3.59 mmol) in water (1 mL), followed by addition of a solution of OsO₄ (0.1 mL, 0.2 M in toluene). The mixture was stirred for 24 h at room temperature. Solid Na₂S₂O₄ (440 mg) was added to the mixture and stirred for 30 min, the mixture was concentrated and the residue was dry loaded onto column chromatography for purification (SiO₂, CH₂Cl₂:MeOH = 10:1) to give (±)-**II-30** (187 mg, 49%) followed by (±)-**II-31** (79 mg, 21%) both as a colorless solids.

(±)-**II-30**: mp 229–230 °C; ¹H NMR (400 MHz, CD₃OD) δ 0.74–0.89 (m, 2H), 1.19 (ddt, J = 2.6, 6.6, 9.2 Hz, 1H), 1.39 (ddt, J = 4.8, 7.0, 9.2 Hz, 1H), 3.54 (t, J = 2.2 Hz, 1H), 4.10–4.14 (m, 1H), 4.27 (dd, J = 1.8, 11.0 Hz, 1H), 4.44–4.50 (m, 1H), 5.16 (dd, J = 2.6, 10.6 Hz, 1H), 7.76–7.89 (m, 4H); ¹³C NMR (100 MHz, CD₃OD, “doublets” due to slowed rotation of the phthalimide substituent shown in parentheses) δ 6.7, 18.6, 20.7, 50.7, 68.7, 69.6, 76.0, 80.9, 123.7 (124.1), 133.2 (133.6), 135.1 (135.2), 169.8 (170.2).
Anal. Calcd for C₁₆H₁₇NO₆·0.2H₂O: C, 59.51; H, 5.43; N, 4.34. Found: C, 59.56; H, 5.49; N, 4.35.

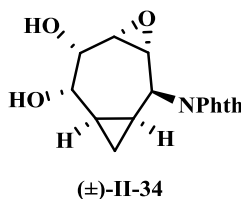
(±)-**II-31** : mp 241–244 °C; ¹H NMR (400 MHz, CD₃OD) δ 0.63 (dt, J = 5.3, 9.0 Hz, 1H), 1.02–1.23 (m, 2H), 1.53–1.63 (m, 1H), 4.00 (s, 2H), 4.34 (d, J = 3.5 Hz, 1H), 4.59 (d, J = 10.6 Hz, 1H), 5.05 (dd, J = 2.9, 11.2 Hz, 1H), 7.75–7.87 (m, 4H); ¹³C NMR (100 MHz; CD₃OD) δ 7.2, 18.0, 19.7, 51.6, 66.2, 68.6, 75.8, 76.3, 123.9 (br), 133.2 (br), 135.1 (br), 170.1 (br). Anal. Calcd for C₁₆H₁₇NO₆: C, 60.18; H, 5.37. Found: C, 60.18; H, 5.32.



N-(5R*,6S*-dihydroxybicyclo[5.1.0]oct-3-en-2S*-yl)phthalimide (**(±)-II-32**) and *N*-(3R*,4S*-dihydroxybicyclo[5.1.0]oct-5-en-2S*-yl)phthalimide (**(±)-II-33**). To a solution of bicyclic diene (**(±)-II-29**) (300 mg, 1.20 mmol) in acetone (10 mL) was added a solution of *N*-methylmorpholine-*N*-oxide (0.32 mL, 1.2 mmol, 50% wt in water), followed by a solution of OsO₄ (0.2 mL, 0.2 M in toluene). The mixture was stirred for 1 h at room temperature. The reaction was quenched with NaHSO₃ (100 mg) and stirred for 30 min then adsorbed onto silica gel for purification (SiO₂, hexanes:ethyl acetate gradient = 3:1 to 3:7) to give the starting material (**(±)-II-29**) (81 mg) followed by (**(±)-II-32**) (138 mg, 56% based on recovered starting material) and (**(±)-II-33**) (72 mg, 29% based on recovered starting material) both as colorless solids.

(±)-II-32: mp 218-221 °C; ¹H NMR (400 MHz, CDCl₃) δ 0.84 (dq, J = 2.0, 7.2 Hz, 1H), 1.09 (q, J = 5.6 Hz, 1H), 1.15-1.23 (m, 1H), 1.49 (pentet, J = 7.6 Hz, 1H), 2.20-2.43 (br s, 2H), 4.11-4.18 (m, 1H), 4.64 (d, J = 6.0 Hz, 1H), 5.44 (qd, J = 2.3, 12.9 Hz, 1H), 5.56, (qd, J = 2.3, 12.9 Hz, 1H), 5.68 (quin, J = 2.7 Hz, 1H), 7.69-7.77 (m, 2H), 7.82-7.90 (m, 2H); ¹³C NMR (100 MHz, CDCl₃) δ 6.9, 16.3, 17.6, 48.4, 71.7, 72.7, 123.3, 127.1, 128.4, 131.9, 134.0, 167.8. HRMS (FAB): *m/z* calcd for C₁₆H₁₅NO₄: [M+Na⁺]; 308.0893, found 308.0894.

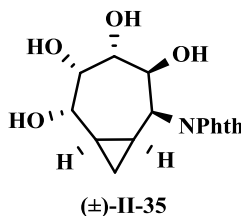
(±)-**II-33**: mp 219-220 °C; ¹H NMR (400 MHz, CDCl₃) δ 0.90 (q, J = 5.9 Hz, 1H), 1.05 (dt, J = 4.9, 9.1 Hz, 1H), 1.41 (dq, J = 4.3, 7.0 Hz, 1H), 1.45-1.54 (m, 1H), 1.98 (d, J = 5.5 Hz, 1H), 2.43 (d, J = 9.0 Hz, 1H), 4.33-4.42 (m, 2H), 5.25 (dd, J = 3.9, 10.6 Hz, 1H), 5.65 (dd, J = 7.4, 12.1 Hz, 1H), 6.16 (dd, J = 5.9, 12.1 Hz, 1H), 7.67-7.76 (m, 2H), 7.79 - 7.88 (m, 2H); ¹³C NMR (100 MHz, CDCl₃) δ 13.2, 15.7, 19.4, 49.9, 68.5, 70.9, 123.0, 123.2, 132.0, 133.9, 134.4, 169.0. HRMS (FAB): m/z calcd for C₁₆H₁₅NO₄: [M+Na⁺]; 308.0893, found 308.0894.



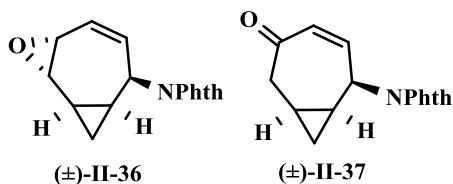
N-(5S*,6S*-dihydroxy-3R*,4R*-epoxybicyclo[5.1.0]oct-2S*-yl)phthalimide (±)-II-

34: Preparation of trifluorooperacetic acid: To an ice cold solution of trifluoroacetic anhydride (0.70 mL, 4.8 mmol) in CH₂Cl₂ (5 mL) was added H₂O₂ (0.33 mL, 4.8 mmol, 50% wt solution). The mixture was stirred for 5 min in the ice cold bath then at room temperature for 1 h. To ice-cold solution of enediol (±)-**II-32** (138 mg, 0.484 mmol) in CH₂Cl₂ (5 mL) cooled in an ice bath was added the previously prepared solution (CF₃CO₃H) drop by drop at 0 °C. After 10 min the mixture was warmed to room temperature and stirred for 1 h and then concentrated. The residue was purified by column chromatography (SiO₂, hexanes:ethyl acetate = 3:7) to give (±)-**II-34** as a colorless solid (121 mg, 83%): mp > 250 °C; ¹H NMR (400 MHz, DMSO-d₆) δ 0.84 (dt, J = 6.7, 8.6 Hz, 1H), 1.04 (tt, J = 5.9, 8.6 Hz, 1H), 1.20 (q, J = 5.9 Hz, 1 H), 1.61 (dq, J =

5.1, 8.6 Hz, 1H), 3.73 (d, J = 5.9 Hz, 1H), 3.98 (t, J = 5.5 Hz, 1H), 4.36 (t, J = 5.9 Hz, 1H), 4.49 (d, J = 8.2 Hz, 1H), 4.59 (d, J = 5.1 Hz, 1H), 4.82 (t, J = 6.5 Hz, 1H), 4.94 (d, J = 5.9 Hz, 1H), 7.81-7.93 (m, 4H); ^{13}C NMR (100 MHz, DMSO- d_6) δ 7.6, 14.1, 15.4, 50.7, 70.2, 72.8, 80.6, 81.9, 123.1, 131.2, 134.6, 168.4. HRMS (FAB): m/z calcd for $\text{C}_{16}\text{H}_{15}\text{NO}_5$: [M+Na $^+$]; 324.0842, found 324.0846.



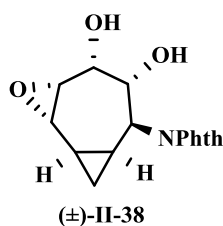
***N*-(3*S**,4*R*8,5*S**,6*S**-tetrahydroxybicyclo[5.1.0]oct-2*S**-yl)phthalimide (±)-II-35:** A mixture of the epoxy compound (±)-II-34 (120 mg, 0.399 mmol) in THF (5 mL) and deionized water (10 mL) was heated until all the solid had dissolved. Carbon tetrabromide (26 mg, 0.079 mmol) was added and the mixture was heated at reflux with stirring for 7 h. The solvent was evaporated and the residue was purified by column chromatography (SiO_2 , CH_2Cl_2 :MeOH = 19:1 to 9:1 gradient) to give the starting material (±)-II-34 (26 mg) followed by (±)-II-35 as a colorless solid (81 mg, 81% based on recovered starting material) : mp 202-204 °C; ^1H NMR (400 MHz, CD_3OD) δ 0.81 (td, J = 5.5, 9.4 Hz, 1H), 1.11 (q, J = 7.8, 16.0 Hz, 1H), 1.28-1.41 (m, 1H), 1.51 (q, J = 5.9 Hz, 1H), 3.83 (br s, 1H), 4.04 (td, J = 1.6, 5.9 Hz, 1H), 4.07 (dt, J = 1.6, 6.3 Hz, 1H), 4.63 (d, J = 4.7 Hz, 1H), 5.33 (t, J = 2.2 Hz, 1H), 7.81-7.86 (m, 2H), 7.86-7.92 (m, 2H); ^{13}C (100 MHz; CD_3OD) δ 9.0, 18.3, 20.1, 50.2, 68.4, 76.4, 77.9, 78.1, 124.3, 133.2, 135.5, 170.8. HRMS (FAB): m/z calcd for $\text{C}_{16}\text{H}_{17}\text{NO}_6$: [M+Na $^+$]; 342.0948, found 342.0950.



***N*-(5R*,6S*-epoxybicyclo[5.1.0]oct-3-en-2S*-yl)phthalimide (±)-II-36 and *N*-(5-oxobicyclo[5.1.0]oct-3-en-2S*-yl)phthalimide (±)-II-37:** A solution of diene (±)-II-29 (200 mg, 0.794 mmol) in freshly distilled CH₂Cl₂ (6 mL) was stirred for 5 min. A solution of meta-chloroperoxybenzoic acid (mCPBA) (196 mg, ~ 70% wt, ~ 0.794 mmol) in freshly distilled CH₂Cl₂ (2 mL) was added dropwise. The solution was stirred under N₂ for 5 h, at which time monitoring by TLC showed complete disappearance of starting material. The solvent was evaporated and the residue was treated with saturated bicarbonate solution (5 mL) with stirring for 30 min. The mixture was extracted several times with CH₂Cl₂, concentrated and purified by column chromatography (SiO₂, hexanes:ethyl acetate = 7:3) to give (±)-II-37 as a colorless solid (28 mg, 12%) followed by (±)-II-36 as a colorless solid (158 mg, 70%).

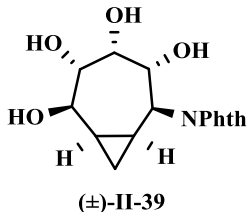
7-Phthalimido-2-oxatricyclo[6.1.0^{1,3}.0^{4,6}]non-8-ene (±)-II-36; mp 196-198 °C; ¹H NMR (400 MHz, CDCl₃) δ 0.93 (dq, J = 3.9, 8.2 Hz, 1H), 1.07 (br q, J = 8.2 Hz, 1H), 1.53-1.65 (m, 2H), 3.19 (t, J = 4.8 Hz, 1H), 3.57 (t, J = 4.8 Hz, 1H), 5.63 (br d, J = 12.0 Hz, 1H), 5.78 (ddd, J = 2.9, 5.5, 12.0 Hz, 1H), 5.91 (d, J = 2.4 Hz, 1H), 7.70-7.93 (m, 4H); ¹³C NMR (100 MHz, CDCl₃) δ 8.3, 13.8, 18.8, 47.6, 52.8, 54.9, 123.4, 123.5, 132.2, 132.8, 134.2, 167.9. HRMS (FAB): m/z calcd for C₁₆H₁₃NO₃: [M+Na⁺]; 290.0788, found 290.0789.

7-Phthalimido-8-oxatricyclo[6.1.0^{1,3}.0^{4,6}]non-2-ene (±)-II-37: mp 122-123 °C; ¹H NMR (400 MHz, CDCl₃) δ 0.74 (dt, J = 6.4, 9.0 Hz, 1H), 1.03 (q, J = 5.7 Hz, 1H), 1.21-1.28 (m, 2H), 2.95 (d, J = 15.2 Hz, 1H), 3.11 (d, J = 15.2 Hz, 1H), 5.61-5.64 (br s, 1H), 6.11 (ddd, J = 1.8, 3.1, 12.6 Hz, 1H), 6.23 (dd, J = 2.4, 12.6 Hz, 1H), 7.75-7.91 (m, 4H); ¹³C NMR (100 MHz, CDCl₃) δ 4.6, 8.3, 17.8, 41.5, 49.3, 123.7, 132.0, 132.5, 141.8, 167.7, 198.9.

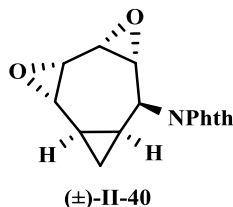


N-(5S*,6S*-Epoxy-3R*,4R*-dihydroxybicyclo[5.1.0]oct-2S*-yl)phthalimide (±)-II-38: To a solution of the epoxy compound (±)-II-36 (100 mg, 0.373 mmol) in acetone (5 mL), was added a solution of *N*-methylmorpholine-*N*-oxide (100 mg, 0.857 mmol) in water (1 mL), followed by addition of a solution of OsO₄ (0.14 mL, 0.2 M in toluene). The mixture was stirred for 4 h at room temperature. Solid Na₂S₂O₄ (60 mg) was added to the mixture and stirred for 30 min, the mixture was concentrated and the residue purified by column chromatography (SiO₂, hexanes:ethyl acetate gradient = 1:1 to 1:4) to give (±)-II-38 as a colorless solid (109 mg, 97 %): mp >220 °C; ¹H NMR (400 MHz, acetone-d₆) δ 0.85 (dt, J = 4.7, 9.3 Hz, 1H), 0.97 (dt, J = 4.7, 6.9 Hz, 1H), 1.19-1.27 (m, 1H), 1.56 (br q, J = 8.2 Hz, 1H), 3.19 (d, J = 4.8 Hz, 1H), 3.35 (ddd, J = 0.8, 4.2, 6.6 Hz, 1H), 3.58 (br d, J = 4.8 Hz, 1H), 4.17 (d, J = 6.6 Hz, 1H), 4.35-4.42 (m, 2H), 5.19 (dd, J = 5.8, 10.8, 1H), 7.84 (s, 4H); ¹³C NMR (100 MHz, acetone-d₆) δ 5.8, 15.5, 19.5, 51.6,

55.1, 57.0, 66.6, 69.3, 122.8, 132.2, 134.0, 168.3. HRMS (FAB): m/z calcd for $C_{16}H_{15}NO_5$: $[M+Na^+]$; 324.0842, found 324.0843.

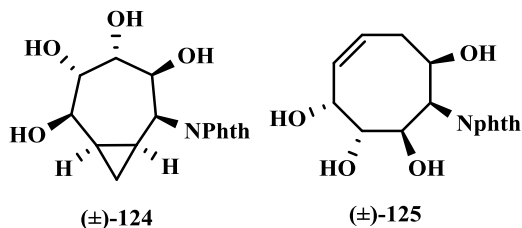


***N*-(3*R**,4*R**,5*S**,6*R**-tetrahydroxybicyclo[5.1.0]oct-4-en-2*S**-yl)phthalimide(±)-II-39.** The hydrolysis of epoxy compound (±)-II-38 (87 mg, 0.29 mmol) in water (3 mL) with carbon tetrabromide (20 mg, 0.058 mmol) as catalyst was carried out in a fashion similar to the preparation of (±)-II-34. Recrystallization of the residue from methanol gave (±)-II-39 (61 mg, 66 %) as colorless crystals: mp > 230 °C; 1H NMR (400 MHz, CD_3OD) δ 0.67 (dt, $J = 6.0, 9.0$ Hz, 1H), 0.90 (q, $J = 6.4$ Hz, 1H), 1.16 (ddt, $J = 3.0, 6.6, 9.6$ Hz, 1H), 1.31 (ddt, $J = 3.6, 6.8, 9.6$ Hz, 1H), 4.06 (s, 1H), 4.26 (dd, $J = 3.6, 9.6$ Hz, 1H), 4.30 (d, $J = 10.4$ Hz, 1H), 5.50 (dd, $J = 3.0, 11.0$ Hz, 1H), 7.76-7.90 (m, 4H), one proton hidden underneath CD_3OD peak at 3.31; ^{13}C NMR (100 MHz, CD_3OD) δ 4.9, 18.1, 20.0, 50.9, 68.6, 69.3, 74.1, 78.1, 123.9, 124.2, 133.4, 133.8, 135.3, 135.4, 170.2, 170.5. Anal. Calcd for $C_{16}H_{17}NO_6$: C, 60.18; H, 5.37. Found: C, 59.65; H, 5.38.



N-(**3R***,**4R***,**5S***,**6S***-diepoxybicyclo[5.1.0]oct-**2S***-yl)phthalimide (**±**)-**123**: To a solution of bicyclic diene (**±**)-**II-29** (130 mg, 0.516 mmol) in freshly distilled CH₂Cl₂ (5 mL) was added mCPBA (319 mg, ~70% wt, ~1.29 mmol). The reaction mixture was stirred under N₂ for 12 h, after which monitoring by TLC indicated the disappearance of starting material. The mixture was concentrated and the solid residue was treated with saturated aqueous bicarbonate (5 mL) with stirring for 30 min. The mixture was extracted several times with ethyl acetate then dried over anhydrous Na₂SO₄. The combined organic layers were concentrated and the crude was recrystallized from benzene to give colorless crystals of the bisepoxide (**±**)-**II-40** (137 mg, 93%): mp >250°C; ¹H NMR (400 MHz, CDCl₃) δ 1.03-1.13 (m, 2H), 1.29 (td, J = 4.3, 5.9 Hz, 1H), 1.46 (tt, J = 5.9, 9.2 Hz, 1H), 3.31 (dd, J = 2.5, 4.5 Hz, 1H), 3.48 (dd, J = 2.5, 4.1 Hz, 1H), 3.51 (dd, J = 4.5, 5.9 Hz, 1H), 3.70 (dd, J = 4.3, 5.5 Hz, 1H), 5.16 (d, J = 5.9 Hz, 1H), 7.72-7.80 (m, 2H), 7.84-7.93 (m, 2H); ¹³C NMR (100 MHz, CDCl₃) δ 10.9, 11.1, 19.7, 47.3, 50.9, 52.0, 53.5, 58.3, 123.4, 131.9, 134.1, 167.9. Anal. Calcd for C₁₆H₁₃NO₄: C, 67.84; H 4.62. Found: C, 67.44; H, 4.68.

This compound also was prepared as follows: In Schlenk flask was added endoperoxide (**±**)-**II-47** (100 mg, 0.352 mmol) in benzene (5 mL) and irradiated with Hg lamp for 6 h, the solvent was evaporated and the residue was washed with diethyl ether, solid precipitate was obtained (67 mg, 67%).

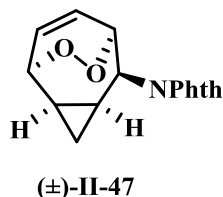


N-(3*R**,4*S**,5*R**,6*R**-tetrahydrobicyclo[5.1.0]oct-2*S**-yl)phthalimide (\pm)-124 and *N*-(1*R**,3*R**,4*R**,5*S**-tetrahydroxy-6-cycloocten-2*R**-yl)phthalimide (\pm)-II-42: To a solution of bisepoxide (\pm)-II-40 (90 mg, 0.32 mmol) in THF (5 mL) and deionized water (7 mL) was added a catalytic amount of CBr₄ (42 mg, 0.13 mmol). The reaction mixture was heated at reflux for 8 h. The mixture was concentrated and the residue was purified by column chromatography (SiO₂, CH₂Cl₂:MeOH = 19:1) to give bicyclic tetraol (\pm)-II-41 (46 mg, 46%) followed by 8-membered ring tetraol (\pm)-II-42 (17 mg, 18%) both as colorless solids.

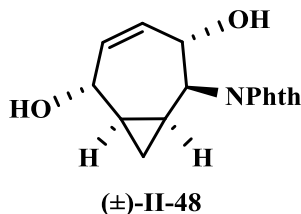
(\pm)-II-41 : mp 218-220°C; ¹H NMR (400 MHz, CD₃OD) δ 0.70 (dt, *J* = 5.5, 9.0 Hz, 1 H), 1.03 (q, *J* = 8.2 Hz, 1H), 1.32 (ddt, *J* = 3.1, 6.7, 9.8 Hz, 1H), 1.56 (q, *J* = 5.9 Hz, 1H), 3.64 (dd, *J* = 1.6, 9.4 Hz, 1H), 3.99 (dd, *J* = 2.0, 6.3 Hz, 1H), 4.03 (td, *J* = 1.6, 6.3 Hz, 1H), 4.28 (dd, *J* = 3.5, 9.8 Hz, 1H), 5.16 (t, *J* = 2.0 Hz, 1H), 7.78-7.95 (m, 4H); ¹³C NMR (100 MHz, CD₃OD) δ 6.3, 15.4, 18.3, 49.0, 68.7, 70.8, 73.2, 74.6, 123.1, 132.1, 134.4, 169.7. Anal. Calcd for C₁₆H₁₇NO₆: C, 60.18; H 5.37. Found: C, 59.84; H, 5.29.

(\pm)-II-42: mp 236-238°C; ¹H NMR (400 MHz; CD₃OD) δ 2.3 (td, *J* = 6.2, 12.5 Hz, 1H), 2.89 (dt, *J* = 9.8, 12.5 Hz, 1H), 3.86-3.93 (m, 1H), 4.08 (dd, *J* = 1.0, 6.1 Hz, 1H), 4.30 (d, *J* = 6.3 Hz, 1H), 4.88 (d, *J* = 4.0 Hz, 1H), 4.93 (d, *J* = 6.3 Hz, 1H), 5.74 (ddt, *J* = 1.6, 6.7, 10.6 Hz, 1H), 5.82 (dd, *J* = 6.3, 11.0 Hz, 1H), 7.77-7.83 (m, 2H), 7.84-7.89 (m, 2H); ¹³C

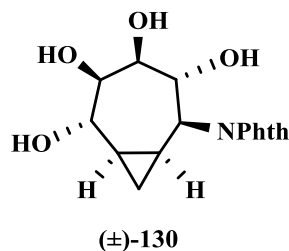
NMR (100 MHz; CD₃OD) δ 33.2, 50.9, 67.4, 74.7, 75.5, 76.1, 122.7, 124.5, 131.9, 133.9, 136.8, 169.0. HRMS (FAB): m/z calcd for C₁₆H₁₇NO₆: [M+Na⁺]; 342.094808, found 342.094911.



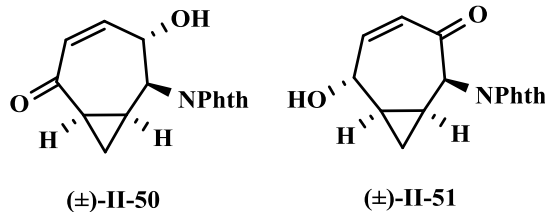
Phthalimido-7,8-dioxatricyclo[4.2.2.0^{2,4}]dec-9-ene (±)-II-47 To a stirred solution of the diene (±)-II-29 (350 mg, 1.40 mmol) in a test tube dissolved in CCl₄ (15 mL) was added tetraphenylporphine (TPP) (9 mg, 0.1 mmol). The deep purple solution was irradiated with a 100-W halogen lamp, while ultra pure O₂ was bubbled through the solution and stirred in water bath at room temperature for 7 h. The reaction mixture was concentrated and the residue was purified by column chromatography (SiO₂, hexanes:ethyl acetate = 2:3) to give (±)-II-47 as a colorless solid (340 mg, 85 %): mp 159-162 °C; ¹H NMR (400 MHz, CDCl₃) δ 0.64-0.74 (m, 1H), 1.44 (pent, J = 8.4 Hz, 1H), 1.62-1.71 (m, 2H), 4.45-4.48 (br s, 1H), 5.26-5.33 (m, 2H), 6.26 (dd, J = 8.2, 9.0 Hz, 1H), 6.55 (dd, J = 8.2, 8.6 Hz, 1H), 7.70-7.90 (m, 4H); ¹³C (100 MHz, CDCl₃) δ 11.1, 15.4, 17.5, 52.2, 77.4, 77.9, 123.6, 127.4, 128.7, 132.0, 134.4, 168.4. Anal. Calcd for C₁₆H₁₃NO₄: C, 67.84; H, 4.63. Found: C, 67.81; H, 4.64.



***N*-(3*S**,6*S**-Dihydroxybicyclo[5.1.0]oct-4-en-2*S**-yl)phthalimide: (±)-II-48** To a solution of endoperoxide (±)-II-47 (250 mg, 0.880 mmol) in CH₂Cl₂ (20 mL) was added activated zinc dust (250 mg), followed by dropwise addition of a solution of acetic acid (537 mg, 8.80 mmol) in CH₂Cl₂ (2 mL) over a 10 min period. The reaction mixture was stirred for 2 h at 0 °C, and then filtered through a celite column. The column was washed with methanol, and the fractions collected were allowed to slowly evaporate under atmospheric pressure and the residue was purified by column chromatography (SiO₂, hexanes:ethyl acetate = 1:4) to give (±)-II-48 (249 mg, 98 %) as colorless crystals: mp 217-219 °C; ¹H NMR (600 MHz, CD₃OD) δ 0.81 (dt, *J* = 5.4, 9.0 Hz, 1H), 0.95 (q, *J* = 5.8, 1H), 1.21 (ddt, *J* = 4.5, 6.3, 9.0 Hz, 1H), 1.35 (tt, *J* = 5.7, 9.0 Hz, 1H), 4.47 (dt, *J* = 1.5, 5.8 Hz, 1H), 4.66 (dd, *J* = 4.2, 10.8 Hz, 1H), 4.78 (td, *J* = 3.0, 10.8 Hz, 1H), 5.62 (ddd, *J* = 1.2, 3.6, 12.0 Hz, 1H), 5.82 (ddd, *J* = 2.1, 6.3, 12.0 Hz, 1H), 7.79-7.90 (m, 4H); ¹³C NMR (100 MHz, CD₃OD) δ 9.2, 17.1, 23.2, 53.5, 67.2, 70.6, 124.1, 133.3, 133.5, 134.4, 135.4, 170.3. HRMS (FAB): *m/z* calcd for C₁₆H₁₅NO₄: [M+Na⁺]; 308.0893, found 308.0895.



***N*-(3R*,4S*,5R*,6S*-tetrahydroxybicyclo[5.1.0]oct-2S*-yl)phthalimide (±)-II-49:** To a solution of bicyclic enediol (±)-II-48 (140 mg, 0.489 mmol) in acetone (10 mL) was added a solution of *N*-methylmorpholine-*N*-oxide (85 mg, 0.73 mmol) in water (2 mL), followed by a solution of OsO₄ (0.1 mL, 0.2 M in toluene). The mixture was stirred for 1 h at room temperature under nitrogen. The reaction was quenched with Na₂S₂O₄ (140 mg) and stirred for 30 min. The mixture was passed through a short column of silica gel while was then washed with ethyl acetate. The combined fractions were concentrated and the residue purified by column chromatography (SiO₂, hexanes:ethyl acetate = 1:4) to give (±)-II-49 (133 mg, 85%) as a colorless solid: mp 254-255 °C; ¹H NMR (400 MHz, CD₃OD) δ 0.71 (dt, *J* = 5.5, 9.4 Hz, 1H), 1.11 (ddt, 3.9, 7.0, 9.4 Hz, 1H), 1.17-1.26 (m, 1H), 1.50 (q, *J* = 5.9 Hz, 1H), 3.64 (dd, *J* = 2.7, 9.3 Hz, 1H), 4.05 (dd, *J* = 2.7, 5.9 Hz, 1H), 4.31 (t, *J* = 5.4 Hz, 1H), 4.37 (t, *J* = 10.0 Hz, 1H), 4.71 (dd, *J* = 3.8, 10.2 Hz, 1H), 7.71-7.93 (m, 4H); ¹³C NMR (100 MHz, CD₃OD) δ 6.1, 16.2, 18.9, 53.8, 64.8, 70.3, 72.0, 74.7, 122.8, 131.8, 133.9, 168.6. Anal. Calcd for C₁₆H₁₇NO₆: C, 60.18; H 5.36. Found: C, 60.01; H, 5.36.

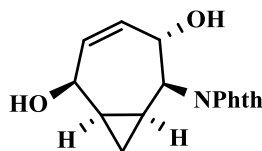


***N*-(3*S**-hydroxy-6-oxobicyclo[5.1.0]oct-4-en-2*S**-yl)phthalimide (±)-II-50 and *N*-(6*S**-hydroxy-3-oxobicyclo[5.1.0]oct-4-en-2*S**-yl)phthalimide (±)-II-51:** To a solution of endoperoxide (±)-II-47 (250mg, 0.880 mmol) in freshly distilled CH₂Cl₂ (15 mL) at 0°C was added a solution of Et₃N (0.25 mL, 1.8 mmol) in CH₂Cl₂ (5 mL). The reaction mixture was stirred for 2 h, the solvent was evaporated and the residue was purified by column chromatography (SiO₂, CH₂Cl₂) to give two regioisomers; (±)-II-50 (238 mg, 95%) followed by (±)-II-51 (5 mg, 2 %) both as colorless solids.

(±)-II-50: mp 227-228 °C; ¹H NMR (400 MHz, CD₃OD) δ 1.44 (td, J = 5.7, 8.7 Hz, 1 H), 1.65 (td, J = 5.7, 7.4 Hz, 1H), 1.84 (q, J = 8.6 Hz, 1H), 2.08 (ddt, J = 1.6, 5.5, 8.7 Hz, 1H), 4.68 (d, J = 10.2 MHz, 1H), 4.95 (dt, J = 2.5, 10.2 Hz, 1H), 5.85 (ddd, J = 2.0, 2.0, 13.7 Hz, 1H), 6.40 (dd, J = 2.0, 13.7 Hz, 1H), 7.78-7.86 (m, 2H), 7.86-7.92 (m, 2H); ¹³C NMR (100 MHz, CD₃OD) δ 12.6, 20.2, 27.2, 52.4, 67.0, 122.9, 126.1, 132.2, 134.1, 144.0, 167.7, 198.0. Anal. Calcd for C₁₆H₁₃NO₄: C, 67.84; H 4.62. Found: C, 67.92; H, 4.65.

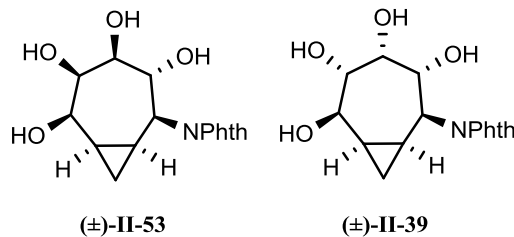
(±)-II-51: mp 182-183 °C; ¹H NMR (400 MHz, CD₃OD) δ 1.01 (q, J = 5.1 Hz, 1H), 1.25 (dt, J = 5.1, 7.8 Hz, 1H), 1.61-1.69 (m, 1H), 2.08 (ddt, J = 4.9, 7.5, 10.4 Hz, 1H), 4.48 (td, J = 2.9, 9.1 Hz, 1H), 4.52 (d, J = 11.0 Hz, 1H), 6.09 (dd, J = 2.7, 12.2 Hz, 1H), 7.01 (dd,

$J = 3.1, 12.2$ Hz, 1H), 7.77-7.93 (m, 4H); ^{13}C NMR (100 MHz; CD_3OD) δ 13.6, 18.2, 27.5, 64.3, 74.1, 124.5, 129.5, 135.8, 158.2, 194.7.



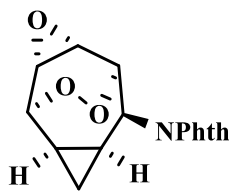
(±)-II-52

***N*-(3*S**,6*R**-dihydroxybicyclo[5.1.0]oct-4-en-2*S**-yl)Phthalimide (±)-II-52:** To a solution of (±)-II-50 (230 mg, 0.810 mmol) in THF (4 mL) and methanol (7 mL) was added $\text{CeCl}_3 \cdot 7\text{H}_2\text{O}$ (604 mg, 1.62 mmol) and the mixture stirred for 30 min at room temperature until it turned to clear solution. The solution was cooled to -78°C and NaBH_4 (62 mg, 1.6 mmol) was added portionwise. The mixture was stirred at -78°C for 5 h. The solvent was evaporated and the residue was partitioned between water and ethyl acetate. After the solvent was evaporated, examination by NMR spectroscopy showed only a single product (±)-II-52 (220 mg, 94%): mp $225\text{-}227^\circ\text{C}$; ^1H NMR (400 MHz, CD_3OD) δ 0.70 (dt, $J = 5.9, 8.6$ Hz, 1H), 0.96 (q, $J = 5.9$ Hz, 1H), 1.21 (dt, $J = 6.3, 9.4$ Hz, 1H), 1.34-1.42 (m, 1H), 4.49 (d, $J = 10.2$ Hz, 1H), 4.60 (qd, $J = 2.4, 10.2$ Hz, 1H), 4.81-4.84 (m, 1H), 5.47 (qd, $J = 2.0, 13.3$ Hz, 1H), 5.55 (td, $J = 2.3, 13.3$ Hz, 1H), 7.78-7.90 (m, 4H); ^{13}C NMR (100 MHz; CD_3OD) δ 2.5, 14.7, 18.3, 52.0, 66.8, 67.5, 122.6, 128.8, 130.5, 132.0, 133.8, 168.4. HRMS (FAB): m/z calcd for $\text{C}_{16}\text{H}_{15}\text{NO}_4$: $[\text{M}+\text{Na}^+]$; 308.0893, found 308.0895.



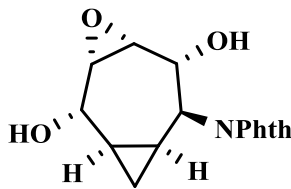
***N*-(3R*,4S*,5R*,6R*-tetrahydroxybicyclo[5.1.0]oct-2S*-yl)phthalimide (±)-II-53 and *N*-(3R*,4R*,5S*,6R*-tetrahydroxybicyclo[5.1.0]oct-4-en-2S*-yl)phthalimide(±)-II-39:** To a solution of (±)-II-52 (300 mg, 1.05 mmol) in acetone (8 mL) was added a solution of *N*-methylmorpholine-*N*-oxide (184 mg, 1.57 mmol) in water (1 mL), followed by a solution of OsO₄ (0.5 mL, 0.2 M in toluene). The mixture was stirred for 12 h at room temperature. The reaction was quenched with NaHSO₃ (250 mg) and stirred for 30 min, the solvent was removed and the residue was purified by column chromatography (SiO₂, CH₂Cl₂:MeOH = 2:3) to give (±)-II-53 (93 mg, 28%) followed by (±)-II-39 (117 mg, 34%) both as colorless solids. Compound (±)-II-39 was identified by comparison of its NMR spectral data with that previously obtained.

(±)-II-53: mp 201-203 °C; ¹H NMR (400 MHz, CD₃OD) δ 0.69 (td, J = 5.5, 9.0 Hz, 1H), 1.09 (ddt, J = 2.7, 6.3, 9.4 Hz, 1H), 1.14-1.24 (m, 1H), 1.70 (q, J = 6.3 Hz, 1H), 3.27 (dd, J = 1.6, 9.4 Hz, 1H), 4.10-4.17 (m, 2H), 4.45 (t, J = 10.2, 1H), 4.56 (dd, J = 2.7, 11.0 Hz, 1H), 7.72-7.91 (m, 4H), CD₃OD peak at 3.31; ¹³C NMR (100 MHz, CD₃OD) δ 8.4, 17.8, 20.2, 55.5, 66.4, 70.1, 76.0, 77.0, 124.0, 124.2, 133.3, 133.8, 135.2, 135.5, 170.0, 170.1. Anal. Calcd for C₁₆H₁₇NO₆: C, 60.18; H 5.36. Found: C, 59.93; H, 5.29. Anal. Calcd for C₁₆H₁₇NO₆: C, 60.18; H, 5.37. Found: C, 59.93; H, 5.29.



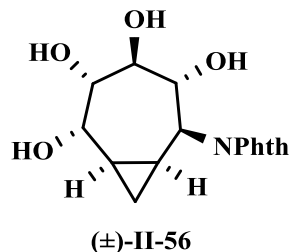
(±)-II-54

Epoxidation of endoperoxide (±)-II-54 : To an ice cold solution of trifluoroacetic anhydride (0.50 mL, 3.5 mmol) in CH_2Cl_2 (5 mL) was added H_2O_2 (0.25 mL, 3.5 mmol, 50% wt solution). After stirring for 5 min in the ice cold bath it was then warmed to room temperature for 1 h. To a solution of endoperoxide (±)-II-47 (130 mg, 0.458 mmol) in CH_2Cl_2 : THF (1:1, 5 mL) cooled in an ice bath was added dropwise the previously prepared solution ($\text{CF}_3\text{CO}_3\text{H}$). After 10 min the mixture warmed to room temperature and stirred for 4 h. The solvent was evaporated using nitrogen gas to give (±)-II-54 as a colorless solid (136 mg, 99%): mp 205-206 °C; ^1H NMR (400 MHz, CDCl_3) δ 0.96 (td, $J = 6.3, 8.8$ Hz, 1H), 1.49 (pent, $J = 7.9$ Hz, 1H), 1.77 (ddt, $J = 2.0, 6.8, 8.7$ Hz, 1H), 1.91 (q, $J = 6.1$ Hz, 1H), 3.40 (t, $J = 4.5$ Hz, 1H), 3.85 (t, $J = 4.1$ Hz, 1H), 4.49 (q, $J = 3.5$ Hz, 1H), 5.08 (dt, $J = 3.6, 6.8$ Hz, 1H), 5.59 (dd, $J = 3.5, 7.0$ Hz, 1H), 7.73-7.82 (m, 2H), 7.85-7.93 (m, 2H); ^{13}C NMR (100 MHz, CDCl_3) δ 9.5, 15.6, 16.3, 46.8, 47.7, 52.1, 74.5, 78.8, 123.6, 131.6, 134.5, 168.2. HRMS (FAB): m/z calcd for $\text{C}_{16}\text{H}_{13}\text{NO}_5$: $[\text{M}+\text{Na}^+]$; 322.0686, found 322.0688.

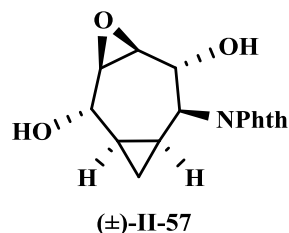


(±)-II-55

***N*-(4R*, 5S*-Epoxy-3R*, 6S*-dihydroxybicyclo[5.1.0]oct-2S*-yl)phthalimide (±)-II-55** : To a solution of (±)-II-54 (110 mg, 0.367 mmol) in CH₂Cl₂ (5 mL) was added activated zinc dust (110 mg), followed by dropwise addition of a solution of acetic acid (100 mg, 1.54 mmol) in CH₂Cl₂ (2 mL) over a 10 min period. The reaction mixture was stirred for 3 h at 0 °C, and then filtered through a celite column. The column was washed with methanol, and the fractions collected were allowed to slowly evaporate under atmospheric pressure and the residue was purified by column chromatography (SiO₂, CH₂Cl₂:MeOH = 19:1) to give (±)-II-55 (63 mg, 63%) as colorless solid: mp 194-195 °C; ¹H NMR (400 MHz, CD₃OD) δ 0.68 (q, J = 6.3 Hz, 1H), 0.78 (td, J = 5.5, 9.2 Hz, 1H), 1.07 (dddt, J = 0.8, 4.0, 6.7, 9.3 Hz, 1H), 1.15 (ddt, J = 3.5, 6.7, 9.3 Hz, 1H), 3.20-3.25 (m, 1H), 3.29 (d, J = 1.2 Hz, 1H), 4.43 (t, J = 3.5 Hz, 1H), 4.54 (dd, J = 0.8, 11 Hz, 1H), 4.80 (dd, J = 3.5, 11.0 Hz, 1H), 7.73-7.91 (m, 4H); ¹³C NMR (100 MHz, CD₃OD) δ 5.6, 16.9, 18.2, 50.1, 56.4, 59.4, 64.0, 68.5, 122.6, 131.9, 133.9, 168.6. HRMS (FAB): m/z calcd for C₁₆H₁₅NO₅: [M+Na⁺]; 324.0842, found 324.0846.

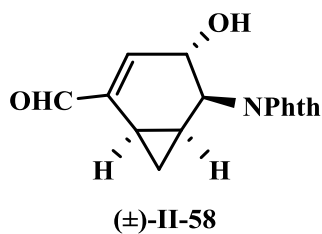


***N*-(3R*,4S*,5S*,6S*-tetrahydroxybicyclo[5.1.0]oct-2S*-yl)phthalimide (±)-II-56:** To a solution of (±)-II-55 (40 mg, 0.13 mmol) in THF (1 mL) and deionized water (5 mL) was added a catalytic amount of CBr₄ (9 mg, 0.03 mmol). The reaction mixture was heated at reflux for 2 h. The mixture was concentrated and the residue was purified by column chromatography (SiO₂, CH₂Cl₂:MeOH = 9:1) to give (±)-II-56 (39 mg, 92%) as a colorless solid; mp 126-128°C; ¹H NMR (400 MHz, CD₃OD) δ 0.80 (td, J = 6.1, 9.1 Hz, 1H), 0.90 (q, J = 6.3 Hz, 1H), 1.17 (ddt, J = 3.1, 6.3, 9.2 Hz, 1H), 1.33 (tt, J = 6.2, 9.3 Hz, 1H), 3.45 (d, J = 8.8 Hz, 1H), 3.53 (t, J = 8.8 Hz, 1H), 4.00 (dd, J = 9.0, 10.2 Hz, 1H), 4.30-4.44 (br m, 1H), 4.79 (dd, J = 2.8, 10.8, Hz, 1H), 7.67-7.91 (m, 4H); ¹³C NMR (100 MHz, CD₃OD) δ 6.3, 16.7, 17.7, 51.9, 65.7, 68.1, 71.5, 73.2, 122.6, 132.0, 133.8, 168.5. Anal. Calcd for C₁₆H₁₇NO₆: C, 60.18; H 5.36. Found: C, 59.97; H, 5.36.



***N*-(4S*,5R*-Epoxy-3R*,6S*-dihydroxybicyclo[5.1.0]oct-2S*-yl)phthalimide (±)-II-57:** To an ice cold solution of trifluoroacetic anhydride (0.35 mL, 2.44 mmol) in CH₂Cl₂

(5 mL) was added H₂O₂ (0.17 mL, 2.4 mmol, 50% wt solution). The mixture was stirred and warmed to room temperature for 1 h. To a solution of enediol (\pm)-**II-48** (70 mg, 0.25 mmol) in CH₂Cl₂ (2.5 mL) and THF (2.5 mL) cooled in an ice bath was added dropwise the previously prepared solution (CF₃CO₃H). After 10 min the mixture was warmed to room temperature and stirred for 3 h. The solvent was concentrated and the residue was purified by column chromatography (SiO₂, hexanes:ethyl acetate gradient = 2:3 to 3:7) to give the starting material (\pm)-**II-48** (9 mg) followed by (\pm)-**II-57** as a colorless solid (53 mg, 83% based on recovered starting material); mp 205-206 °C; ¹H NMR (400 MHz, acetone-d₆) δ 0.86 (td, J = 4.7, 8.8 Hz, 1H), 0.992-1.01 (m, 1H), 1.20-1.29 (m, 1H), 1.34 (tt, J = 7.2, 9.2 Hz, 1H), 3.03 (dd, J = 4.7, 6.8 Hz, 1H) 3.19-3.32 (m, 2 H), 4.01 (ddd, J = 4.9, 6.9, 11.7 Hz, 1H), 4.68-4.86 (m, 3H), 7.85 (br s, 4 H); ¹³C NMR (100 MHz, CD₃OD) δ 12.9, 17.3, 23.6, 53.1, 58.0, 59.7, 68.2, 76.3, 123.7, 123.9, 131.8, 135.1, 135.2, 168.9. HRMS (FAB): m/z calcd for C₁₆H₁₅NO₅: [M+Na⁺]; 324.0842, found 324.0844.



(\pm)-II-58: To a solution of epoxydiol (\pm)-**II-57** (150 mg, 0.497 mmol) in THF (2 mL) and deionized water (10 mL) was added a catalytic amount of CBr₄ (33 mg, 0.099 mmol). The reaction mixture was heated to reflux for 5 h. The mixture was concentrated and the residue was purified by column chromatography (SiO₂, hexanes:ethyl acetate gradient = 11:9 to 3:7) to give (\pm)-**II-58** as a colorless solid (53 mg, 52% based on recovered

starting material) followed by the starting material (\pm)-**II-57** (41 mg); mp 215-216 °C; ^1H NMR (400 MHz, CD_3OD) δ 1.03 (q, $J = 5.1$ Hz, 1H), 1.13 (dt, $J = 5.1, 8.4$ Hz, 1H), 1.52 (ddt, $J = 3.9, 6.3, 8.4$ Hz, 1H), 2.09 (dt, $J = 4.7, 8.2$ Hz, 1H), 4.49 (dd, $J = 3.9, 9.8$ Hz, 1H), 5.09 (d, $J = 9.8$ Hz, 1H), 6.52 (d, $J = 1.2$ Hz, 1H), 7.76-7.96 (m, 4H), 9.54 (s, 1H); ^{13}C (100 MHz, CD_3OD) δ 10.0, 14.4, 14.9, 54.7, 64.9, 124.2, 133.5, 135.5, 144.6, 148.0, 170.3, 194.0. HRMS (FAB): m/z calcd for $\text{C}_{16}\text{H}_{13}\text{NO}_4$: $[\text{M}+\text{Na}^+]$; 306.0737, found 306.0739.

Materials and Methods: Beta-glucosidase Spectrophotometric Kinetics Assay

Chemicals:

p-Nitrophenyl β -D-glucoside, xylitol. p-nitrophenyl β -D-glucoside and β -glucosidase were purchased from SigmaAldrich

Enzyme Assay:

To determine the potency of each potential inhibitor, a spectrophotometric kinetic assay was utilized. The assay was modified from one developed by Kelemen and Whelan at Royal Free Hospital School of Medicine, London, England (Kelemen and Whelan 1966).¹⁴⁴

A 100 mM sodium acetate buffer stock was prepared in double deionized water and the pH adjusted to 4.8. A 600 $\mu\text{g}/\text{mL}$ stock was prepared of the enzyme, β -glucosidase (from almonds), in double deionized water. A 33 mM stock was prepared of the substrate, p-nitrophenyl β -D-glucoside (F.W. 301.2494 g/mol) in NaOAc buffer, and a 1M stock was made in double deionized water of xylitol, a known inhibitor of the enzyme. The final concentrations of each reagent in the assay were 70 mM NaOAc, 24

$\mu\text{g/mL}$ β -glucosidase and 6.6 mM (2.0 mg/mL) 4-nitrophenyl β -D-glucoside. When xylitol was utilized as a positive control for inhibition, the final concentration utilized was 100 mM.

The assay was monitored directly at 405 nm, the wavelength of light at which p-nitrophenolate, the cleavage product of the substrate p-nitrophenyl β -D-glucoside, absorbs light. With an increase in concentration of product formed, an increase in absorbance at 405 nm was observed, therefore enabling the calculation of rate and percent inhibition, relative to full enzyme activity, attributable to each inhibitor at a given concentration.

Initially, the assay was validated in a 1 mL quartz cuvette. An aliquot of buffer stock was added first, followed by the addition of substrate. The cuvette volume was subsequently adjusted with double deionized water, to produce the appropriate concentrations of each reagent. The reaction was initiated with enzyme. Directly after the addition of enzyme, the cuvette was capped and inverted, to ensure even incorporation of reagents throughout the solution.

Prior to measuring rates, however, a reading was taken where the cuvette contained only buffer and substrate, to ensure the absence of background rate due to uncatalyzed substrate dissociation. The results demonstrated a lack of background rate. Six readings were then taken, measuring the initial rate of reaction. The concentration of enzyme utilized increased linearly with each subsequent reading. The concentrations tested were 6, 12, 24, 36, 48 and 60 μmL . The volume of water added to the cuvette was adjusted, to accommodate varying enzyme aliquot volumes.

The linear region was consequently selected from each cuvette reading. An appropriate and proportional increase in rate was observed with each increase in enzyme concentration, and initial rates were therefore plotted against concentration to produce a validation curve. From the six readings taken, 24 $\mu\text{g/mL}$ was the concentration of enzyme selected to utilize in the 96-well plate assay format. As Keleman and Whelan identified xylitol as a known inhibitor of β -glucosidase, this compound was purchased and utilized as a positive control for inhibition. According to Keleman and Whelan, xylitol has a 43% inhibitory capacity at a concentration of 100 mM.¹⁴⁴ When a rate was measured in the presence of 100 mM xylitol and compared against full activity of enzyme at the utilized concentration, a similar inhibitory affect was observed, therefore reproducing previously observed effects and further validating the assay.

Prior to performing the assay in 96-well plate format, a series of stocks were prepared by serial dilution for each potential inhibitor, a 25 mM stock, 5 mM stock, and 0.5 mM stock. Incomplete solubility in water was experienced at higher stock concentrations. Therefore, each stock was made in 50% DMSO, 50% water, which permitted complete solubility. However, as each stock contained DMSO, the enzyme was tested for DMSO sensitivity prior to running the IC_{50} assay. This was accomplished by measuring rate in a series of eight wells in the absence of DMSO in the same plate as a series of 8 wells containing 10% DMSO. The average rate between the two sets of wells was compared, and no notable difference was observed, therefore demonstrating a lack of DMSO sensitivity. The assay was subsequently run in 96-well plate format. A 5-point IC_{50} was performed for each potential inhibitor, testing compound concentrations ranging from 10 μM -1 mM, equally spaced on a logarithmic scale.

The first column of each plate served as the plate blank, containing solely buffer and substrate. Column two served as a negative control for inhibition, containing buffer, enzyme and substrate, and reflecting full activity of the enzyme. Column three served as a positive control for inhibition, containing buffer, enzyme, substrate, and 100 mM xylitol. The following columns contained increasing concentrations of inhibitor in quadruplicate.

First, buffer was added to each well utilizing a multi-channel pipette. Substrate was then added, also using a multi-channel pipette. Each well volume was adjusted with double deionized water, taking into account the volume of inhibitor added to each set of wells. Again, this was performed utilizing a multi-channel pipette. The plate was allowed to equilibrate in the spectrophotometer at 25 °C for 30 min prior to initiation. After incubation, the reaction was initiated with enzyme, using a single channel pipette and reverse pipetting technique. Enzyme aliquots were hung on the side of each well, directly above the meniscus of solution. This was done to ensure uniform initiation of the reaction.

To initiate the reaction, the plate was tapped gently on the bench top. Prior to inserting the plate into the spectrophotometer, the bottom was quickly cleaned with laboratory tissue to ensure the removal of dust or particles that could interfere with experimental readings. The plate was then placed in the spectrophotometer, shaken for 5 seconds to promote adequate incorporation of reagents into solution, and a ten-minute kinetic read immediately taken.

For each plate assayed, the reduced slope values for all negative control wells were averaged and the obtained value considered representative of full enzymatic activity. Fractional activity was then calculated by dividing the slope of each well by this value and multiplying by 100%. Fractional activity values were used to determine the amount of activity observed at each concentration of inhibitor. These values were then copied to Graph Pad and plotted as percent activity versus the log of the concentration of inhibitor. Data was fit as a nonlinear regression curve, according to the formula $y = \text{Bottom} + \frac{(\text{Top} - \text{Bottom})}{(1 + 10^{x - \log \text{IC}_{50}})}$. The fit of the curve permitted the determination of the 50% inhibitory concentration of each compound.

VI- REFERENCES

- (1) Schreiber, S. L. *Bioorg. Med. Chem.* **1998**, *6*, 1127–1152.
- (2) Schreiber, S. L. *Chem. Eng. News Arch.* **2003**, *81*, 51–60.
- (3) Duester, G. *Cell (Cambridge, MA, United States)* **2008**, *134*, 921–931.
- (4) Schreiber, S. L. *Nat. Chem. Biol.* **2005**, *1*, 64–66.
- (5) Frearson, J. A.; Collie, I. T. *Drug Discov. Today* **2009**, *14*, 1150–1158.
- (6) O'Connor, C. J.; Laraia, L.; Spring, D. R. *Chem. Soc. Rev.* **2011**, *40*, 4332–4345.
- (7) Feher, M.; Schmidt, J. M. *J. Chem. Inf. Comput. Sci.* **2003**, *43*, 218–227.
- (8) Haggarty, S. J. *Curr. Opin. Chem. Biol.* **2005**, *9*, 296–303.
- (9) Maclean, D.; Baldwin, J. J.; Ivanov, V. T.; Kato, Y.; Shaw, A.; Schenider, P.; Gordon, E. M. *J. Comb. Chem.* **2000**, *2*, 562–578.
- (10) Tan, D. S.; Foley, M. A.; Stockwell, B. R.; Shair, M. D.; Schreiber, S. L. *J. Am. Chem. Soc.* **1999**, *121*, 9073–9087.
- (11) Nicolaou, K. C.; Pfefferkorn, J. A.; Barluenga, S.; Mitchell, H. J.; Roecker, A. J.; Cao, G.-Q. *J. Am. Chem. Soc.* **2000**, *122*, 9968–9976.
- (12) Stavenger, R. A.; Schreiber, S. L. *Angew. Chemie, Int. Ed.* **2001**, *40*, 3417–3421.
- (13) Micalizio, G. C.; Schreiber, S. L. *Angew. Chemie, Int. Ed.* **2002**, *41*, 152–154.
- (14) Tietze, L. F.; Lieb, M. E. *Curr. Opin. Chem. Biol.* **1998**, *2*, 363–371.
- (15) Denmark, S. E.; Thorarensen, A. *Chem. Rev. (Washington, D. C.)* **1996**, *96*, 137–165.
- (16) Lee, D.; Sello, J. K.; Schreiber, S. L. *Org. Lett.* **2000**, *2*, 709–712.
- (17) Domling, A.; Ugi, I. *Angew. Chemie, Int. Ed.* **2000**, *39*, 3168–3210.
- (18) Armstrong, R. W.; Combs, A. P.; Tempest, P. A.; Brown, S. D.; Keating, T. A. *Acc. Chem. Res.* **1996**, *29*, 123–131.
- (19) Paulvannan, K. *Tetrahedron Lett.* **1999**, *40*, 1851–1854.

- (20) Dandapani, S.; Comer, E.; Duvall, J. R.; Munoz, B. *Future Med. Chem.* **2012**, *4*, 2279–94.
- (21) O' Connor, C. J.; Beckmann, H. S. G.; Spring, D. R. *Chem. Soc. Rev.* **2012**, *41*, 4444–56.
- (22) Sunderhaus, J. D.; Dockendorff, C.; Martin, S. F. *Tetrahedron* **2009**, *65*, 6454–6469.
- (23) Jacobson, A. E.; Mokotoff, M. *J. Med. Chem.* **1970**, *13*, 7–9.
- (24) Weber, E.; Keana, J.; Barmettler, P. PCP receptor ligands and their use in treatment of neuronal loss, Alzheimer's disease and other diseases., November 01, 1990.
- (25) Plouffe, D.; Brinker, A.; McNamara, C.; Henson, K.; Kato, N.; Kuhlen, K.; Nagle, A.; Adrián, F.; Matzen, J. T.; Anderson, P.; Nam, T.-G.; Gray, N. S.; Chatterjee, A.; Janes, J.; Yan, S. F.; Trager, R.; Caldwell, J. S.; Schultz, P. G.; Zhou, Y.; Winzeler, E. A. *Proc. Natl. Acad. Sci. U. S. A.* **2008**, *105*, 9059–64.
- (26) Smilkstein, M.; Sriwilaijaroen, N.; Kelly, J. X.; Wilairat, P.; Riscoe, M. *Antimicrob. Agents Chemother.* **2004**, *48*, 1803–1806.
- (27) Bennett, T. N.; Paguio, M.; Gligorijevic, B.; Seudieu, C.; Kosar, A. D.; Davidson, E.; Roepe, P. D. *Antimicrob. Agents Chemother.* **2004**, *48*, 1807–1810.
- (28) Grigoryan, N. P.; Pogosyan, S. A.; Paronikyan, R. G. *Hayastani Kim. H.* **2005**, *58*, 100–104.
- (29) Ang, S. H.; Krastel, P.; Leong, S. Y.; Tan, L. J.; Wong, W. L. J.; Yeung, B. K.; Zou, B. Spiro-indole derivatives for the treatment of parasitic diseases and their preparation and compositions., November 05, 2009.
- (30) Yeung, B. K. S.; Zou, B.; Rottmann, M.; Lakshminarayana, S. B.; Ang, S. H.; Leong, S. Y.; Tan, J.; Wong, J.; Keller-Maerki, S.; Fischli, C.; Goh, A.; Schmitt, E. K.; Krastel, P.; Francotte, E.; Kuhlen, K.; Plouffe, D.; Henson, K.; Wagner, T.; Winzeler, E. a; Petersen, F.; Brun, R.; Dartois, V.; Diagona, T. T.; Keller, T. H. *J. Med. Chem.* **2010**, *53*, 5155–64.
- (31) Vilsmeier, A.; Haack, A. *Berichte der Dtsch. Chem. Gesellschaft (A B Ser.)* **1927**, *60*, 119–122.
- (32) Wang, Q.; Graham, R. W.; Trimbur, D.; Warren, R. A. J.; Withers, S. G. *J. Am. Chem. Soc.* **1994**, *116*, 11594–11595.
- (33) McCarter, J. D.; Stephen Withers, G. *Curr. Opin. Struct. Biol.* **1994**, *4*, 885–892.

- (34) Zechel, D. L.; Withers, S. G. *Acc. Chem. Res.* **2000**, *33*, 11–18.
- (35) Lillelund, V. H.; Jensen, H. H.; Liang, X.; Bols, M. *Chem. Rev.* **2002**, *102*, 515–554.
- (36) Tanaka, K. S. E.; Winters, G. C.; Batchelor, R. J.; Einstein, F. W. B.; Bennet, A. J. *J. Am. Chem. Soc.* **2001**, *123*, 998–999.
- (37) Thomas, J. A.; Koshland Jr., D. E. *J. Biol. Chem.* **1960**, *235*, 2511–2517.
- (38) Wacharasindhu, S.; Worawalai, W.; Rungprom, W.; Phuwapraisirisan, P. *Tetrahedron Lett.* **2009**, *50*, 2189–2192.
- (39) Ogawa, S.; Asada, M.; Ooki, Y.; Mori, M.; Itoh, M.; Korenaga, T. *Bioorg. Med. Chem.* **2005**, *13*, 4306–4314.
- (40) Yu, J.; Spencer, J. B. *Tetrahedron Lett.* **2001**, *42*, 4219–4221.
- (41) Pelyvas, I. F.; Madi-Puskas, M.; Toth, Z. G.; Varga, Z.; Batta, G.; Sztaricskai, F. *Carbohydr. Res.* **1995**, *272*, C5–C9.
- (42) Bauder, C. *Org. Biomol. Chem.* **2008**, *6*, 2952–2960.
- (43) Marco-Contelles, J.; Pozuelo, C.; Jimeno, M. L.; Martinez, L.; Martinez-Grau, A. *J. Org. Chem.* **1992**, *57*, 2625–2631.
- (44) Doddi, V. R.; Kumar, A.; Vankar, Y. D. *Tetrahedron* **2008**, *64*, 9117–9122.
- (45) Alegret, C.; Benet-Buchholz, J.; Riera, A. *Org. Lett.* **2006**, *8*, 3069–3072.
- (46) Diaz, L.; Delgado, A. *Curr. Med. Chem.* **2010**, *17*, 2393–2418.
- (47) Arya, D. P.; Editor. *Aminoglycoside Antibiotics: From Chemical Biology to Drug Discovery*; John Wiley & Sons, Inc., 2007; p. 319 pp.
- (48) Park, S. R.; Park, J. W.; Ban, Y. H.; Sohng, J. K.; Yoon, Y. J. *Nat. Prod. Rep.* **2013**, *30*, 11–20.
- (49) Waksman, S. A.; Lechevalier, H. A. *Science* **1949**, *109*, 305–307.
- (50) Umezawa, H.; Ueda, M.; Maeda, K.; Yagishita, K.; Kondo, S.; Okami, Y.; Utahara, R.; Osato, Y.; Nitta, K.; Takeuchi, T. *J. Antibiot. Ser. A* **1957**, *10*, 181–188.

- (51) Weinstein, M. J.; Luedemann, G. M.; Oden, E. M.; Wagman, G. H.; Rosselet, J. P.; Marquez, J. A.; Coniglio, C. T.; Charney, W.; Herzog, H. L.; Black, J. *J. Med. Chem.* **1963**, *6*, 463–464.
- (52) Higgens, C. E.; Kastner, R. E. *Antimicrob. Agents Chemother.* **1968**, 324–331.
- (53) Weinstein, M. J.; Marquez, J. A.; Testa, R. T.; Wagman, G. H.; Oden, E. M.; Waitz, J. A. *J. Antibiot. (Tokyo)*. **1970**, *23*, 551–554.
- (54) Weinstein, M. J.; Wagman, G. H.; Marquez, J. A.; Testa, R. T.; Waitz, J. A. *Antimicrob. Agents Chemother.* **1975**, *7*, 246–249.
- (55) Shomura, T.; Ezaki, N.; Tsuruoka, T.; Niwa, T.; Akita, E. *J. Antibiot. (Tokyo)*. **1970**, *23*, 155–161.
- (56) Kim, C. U.; Lew, W.; Williams, M. A.; Zhang, L.; Liu, H.; Swaminathan, S.; Bischofberger, N.; Chen, M. S.; Tai, C. Y.; Mendel, D. B.; Laver, W. G.; Stevens, R. C. *J. Am. Chem. Soc.* **1997**, *119*, 681–690.
- (57) Trapero, A.; Llebaria, A. *ACS Med. Chem. Lett.* **2011**, *2*, 614–619.
- (58) Kameda, Y.; Horii, S. *J. Chem. Soc. Chem. Commun.* **1972**, 746–747.
- (59) Kameda, Y.; Horii, S.; Yamano, T. *J. Antibiot. (Tokyo)*. **1975**, *28*, 298–306.
- (60) Chen, X.; Fan, Y.; Zheng, Y.; Shen, Y. *Chem. Rev. (Washington, DC, United States)* **2003**, *103*, 1955–1977.
- (61) Kameda, Y.; Asano, N.; Yoshikawa, M.; Takeuchi, M.; Yamaguchi, T.; Matsui, K.; Horii, S.; Fukase, H. *J. Antibiot. (Tokyo)*. **1984**, *37*, 1301–1307.
- (62) Horii, S.; Iwasa, T.; Kameda, Y. *J. Antibiot. (Tokyo)*. **1971**, *24*, 57–58.
- (63) Iwasa, T.; Yamamoto, H.; Shibata, M. *J. Antibiot. (Tokyo)*. **1970**, *23*, 595–602.
- (64) Ogawa, S.; Nose, T.; Ogawa, T.; Toyokuni, T.; Iwasawa, Y.; Suami, T. *J. Chem. Soc. Perkin Trans. 1 Org. Bio-Organic Chem.* **1985**, 2369–2374.
- (65) Frommer, W.; Junge, B.; Mueller, L.; Schmidt, D.; Truscheit, E. *Planta Med.* **1979**, *35*, 195–217.
- (66) Wehmeier, U. F.; Piepersberg, W. *Appl. Microbiol. Biotechnol.* **2004**, *63*, 613–625.
- (67) Ogawa, S.; Shibata, Y. *Carbohydr. Res.* **1988**, *176*, 309–315.

- (68) Ogawa, S.; Nishi, K.; Shibata, Y. *Carbohydr. Res.* **1990**, *206*, 352–360.
- (69) Ogawa, S.; Sato, K.; Miyamoto, Y. *J. Chem. Soc. Perkin Trans. 1 Org. Bio-Organic Chem.* **1993**, 691–696.
- (70) Ogawa, S.; Aso, D. *Carbohydr. Res.* **1993**, *250*, 177–184.
- (71) Horii, S.; Fukase, H.; Matsuo, T.; Kameda, Y.; Asano, N.; Matsui, K. *J. Med. Chem.* **1986**, *29*, 1038–1046.
- (72) Gravier-Pelletier, C.; Maton, W.; Dintinger, T.; Tellier, C.; Le Merrer, Y. *Tetrahedron* **2003**, *59*, 8705–8720.
- (73) Tsunoda, H.; Inokuchi, J.; Yamagishi, K.; Ogawa, S. *Liebigs Ann.* **1995**, 279–284.
- (74) Ogawa, S.; Ashiura, M.; Uchida, C.; Watanabe, S.; Yamazaki, C.; Yamagishi, K.; Inokuchi, J. *Bioorg. Med. Chem. Lett.* **1996**, *6*, 929–932.
- (75) Ringe, D.; Petsko, G. A. *J. Biol.* **2009**, *8*, 80.
- (76) Matsuda, J.; Suzuki, O.; Oshima, A.; Yamamoto, Y.; Noguchi, A.; Takimoto, K.; Itoh, M.; Matsuzaki, Y.; Yasuda, Y.; Ogawa, S.; Sakata, Y.; Nanba, E.; Higaki, K.; Ogawa, Y.; Tominaga, L.; Ohno, K.; Iwasaki, H.; Watanabe, H.; Brady, R. O.; Suzuki, Y. *Proc. Natl. Acad. Sci. U. S. A.* **2003**, *100*, 15912–15917.
- (77) Sar, A.; Lindeman, S.; Donaldson, W. A. *Org. Biomol. Chem.* **2010**, *8*, 3908–3917.
- (78) Fischer, E. O.; Fischer, R. D. *Angew. Chemie* **1960**, *72*, 919–919.
- (79) Jones, D.; Pratt, L.; Wilkinson, G. *J. Chem. Soc.* **1962**, 4458–4463.
- (80) Tao, C. No Title. *Encyclopedia of Reagents in Organic Synthesis*, ed. Paquette, L. A., 1995, 5043–5044.
- (81) Herz, W.; Ligon, R. C.; Turner, J. A.; Blount, J. F. *J. Org. Chem.* **1977**, *42*, 1885–1895.
- (82) Sutbeyaz, Y.; Secen, H.; Balci, M. *J. Org. Chem.* **1988**, *53*, 2312–2317.
- (83) Suzuki, M.; Ohtake, H.; Kameya, Y.; Hamanaka, N.; Noyori, R. *J. Org. Chem.* **1989**, *54*, 5292–5302.
- (84) Kornblum, N.; DeLaMare, H. E. *J. Am. Chem. Soc.* **1951**, *73*, 880–881.
- (85) Luche, J. L. *J. Am. Chem. Soc.* **1978**, *100*, 2226–2227.

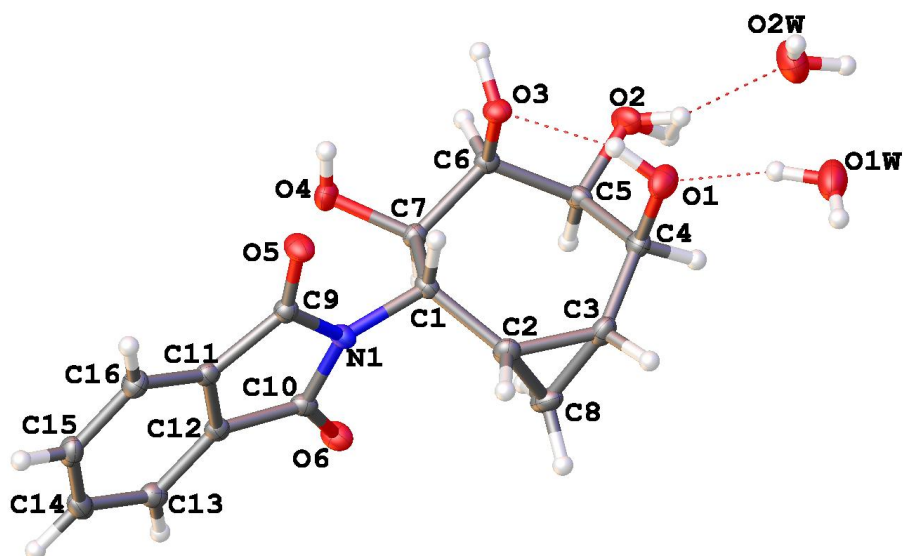
- (86) Henbest, H. B.; Wilson, R. A. L. *J. Chem. Soc.* **1957**, 1958.
- (87) Curti, C.; Zanardi, F.; Battistini, L.; Sartori, A.; Rassu, G.; Auzzas, L.; Roggio, A.; Pinna, L.; Casiraghi, G. *J. Org. Chem.* **2006**, *71*, 225–230.
- (88) Girard, E.; Desvergnès, V.; Tarnus, C.; Landais, Y. *Org. Biomol. Chem.* **2010**, *8*, 5628–5634.
- (89) Johnson, C. R.; Bis, S. J. **1995**, 615–623.
- (90) Reingold, I. D.; DiNardo, L. J. *J. Org. Chem.* **1982**, *47*, 3544–3545.
- (91) Baeckvall, J. E.; Bystroem, S. E.; Nordberg, R. E. *J. Org. Chem.* **1984**, *49*, 4619–4631.
- (92) Lindlar, H. *Helv. Chim. Acta* **1952**, *35*, 446–450.
- (93) H. Lindlar and R. Dubuis. *Org. Synth.* **1966**, *46*, 89.
- (94) Rassu, G.; Auzzas, L.; Pinna, L.; Zambrano, V.; Zanardi, F.; Battistini, L.; Gaetani, E.; Curti, C.; Casiraghi, G. *J. Org. Chem.* **2003**, *68*, 5881–5885.
- (95) Mukaiyama, T.; Kobayashi, S. *Org. React. (Hoboken, NJ, United States)* **1994**, *46*, No pp. given.
- (96) Baylis, A. B.; Hillman, M. E. D. *Acrylic compounds.*, May 10, 1972.
- (97) Fleming, I.; Henning, R.; Plaut, H. *J. Chem. Soc. Chem. Commun.* **1984**, 29–31.
- (98) Andriuzzi, O.; Gravier-Pelletier, C.; Le Merrer, Y. *Tetrahedron Lett.* **2004**, *45*, 8043–8046.
- (99) Le Merrer, Y.; Dureault, A.; Greck, C.; Micas-Languin, D.; Gravier, C.; Depezay, J. C. *Heterocycles* **1987**, *25*, 541–548.
- (100) Saniere, M.; Le Merrer, Y.; Barbe, B.; Koscielniak, T.; Dumas, J.; Micas-Languin, D.; Depezay, J. C. *Angew. Chemie* **1989**, *101*, 645–647.
- (101) Jones, T. H.; Blum, M. S. *Tetrahedron Lett.* **1981**, *22*, 4373–4376.
- (102) Andriuzzi, O.; Gravier-Pelletier, C.; Bertho, G.; Prange, T.; Le Merrer, Y. *Beilstein J. Org. Chem.* **2005**, *1*, 12, No pp. given.
- (103) Kelebekli, L.; Kara, Y.; Balci, M. *Carbohydr. Res.* **2005**, *340*, 1940–1948.
- (104) Wang, Y.; Bennet, A. J. *Org. Biomol. Chem.* **2007**, *5*, 1731–1738.

- (105) Hostettmann, K.; Hostettmann-Kaldas, M.; Sticher, O. *J. Chromatogr.* **1980**, *202*, 154–156.
- (106) Furukawa, J.; Kawabata, N.; Nishimura, J. *Tetrahedron* **1968**, *24*, 53–58.
- (107) Reppe, W.; Schlichting, O.; Klager, K.; Toepel, T. *Justus Liebigs Ann. Chem.* **1948**, *560*, 1–92.
- (108) Barnes, C. E. Method of preparing cyclooctatetraene, 1951.
- (109) Canale, A. J.; Kincaid, J. F. Preparation of cyclooctatetraene, 1952.
- (110) Kelebekli, L.; Celik, M.; Sahin, E.; Kara, Y.; Balci, M. *Tetrahedron Lett.* **2006**, *47*, 7031–7035.
- (111) Kara, Y.; Balci, M. *Tetrahedron* **2003**, *59*, 2063–2066.
- (112) Mehta, G.; Pallavi, K. *Chem. Commun. (Camb)*. **2002**, 2828–2829.
- (113) Shvo, Y.; Hazum, E. *J. Chem. Soc. Chem. Commun.* **1975**, 829–830.
- (114) Heil, V.; Johnson, B. F. G.; Lewis, J.; Thompson, D. J. *J. Chem. Soc. Chem. Commun.* **1974**, 270–271.
- (115) Paquette, L. A.; Ley, S. V.; Broadhurst, M. J.; Truesdell, D.; Fayos, J.; Clardy, J. *Tetrahedron Lett.* **1973**, 2943–2946.
- (116) Paquette, L. A.; Ley, S. V.; Farnham, W. B. *J. Am. Chem. Soc.* **1974**, *96*, 312–313.
- (117) Paquette, L. A.; Ley, S. V.; Maiorana, S.; Schneider, D. F.; Broadhurst, M. J.; Boggs, R. A. *J. Am. Chem. Soc.* **1975**, *97*, 4658–4667.
- (118) Johnson, B. F. G.; Lewis, J.; Parkins, A. W.; Randall, G. L. P. *J. Chem. Soc. D Chem. Commun.* **1969**, 595.
- (119) Broadley, K.; Connelly, N. G.; Graham, P. G.; Howard, J. A. K.; Risse, W.; Whiteley, M. W. *J. Chem. Soc. Dalton Trans. Inorg. Chem.* **1985**, 777–781.
- (120) Davison, A.; McFarlane, W.; Pratt, L.; Wilkinson, G. *J. Chem. Soc.* **1962**, 4821.
- (121) Johnson, B. F. G.; Lewis, J.; Randall, G. L. P. *J. Chem. Soc. A Inorganic, Phys. Theor.* **1971**, 422.
- (122) Brookhart, M.; Davis, E. R.; Harris, D. L. *J. Am. Chem. Soc.* **1972**, *94*, 7853–7858.

- (123) Connelly, N. G.; Lucy, A. R.; Whiteley, M. W. *J. Chem. Soc. Dalt. Trans. Inorg. Chem.* **1983**, 111–115.
- (124) Charles, A. D.; Diversi, P.; Johnson, B. F. G.; Karlin, K. D.; Lewis, J.; Rivera, A. V.; Sheldrick, G. M. *J. Organomet. Chem.* **1977**, 128, C31–C34.
- (125) Wallock, N. J.; Donaldson, W. A. *J. Org. Chem.* **2004**, 69, 2997–3007.
- (126) Chaudhury, S.; Lindeman, S.; Donaldson, W. A. *Tetrahedron Lett.* **2007**, 48, 7849–7852.
- (127) Chaudhury, S. *Unpubl. Results* Marquette University.
- (128) Wallock, N. *Ph.D. Diss.* **2004**, Marquette University.
- (129) Sar, A. *Ph.D. Diss.* **2011**, Marquette University.
- (130) Bondzić, B. P.; Eilbracht, P. *Org. Lett.* **2008**, 10, 3433–6.
- (131) Schmidt, B.; Krehl, S.; Jablowski, E. *Org. Biomol. Chem.* **2012**, 10, 5119–30.
- (132) Ingold, C. K.; Sako, S.; Thorpe, J. F. *J. Chem. Soc. Trans.* **1922**, 121, 1177–1198.
- (133) Hoye, T. R.; Jeon, J.; Tennakoon, M. A. *Angew. Chem. Int. Ed. Engl.* **2011**, 50, 2141–3.
- (134) Broadley, K.; Connelly, N. G.; Mills, R. M.; Whiteley, M. W.; Woodward, P. *J. Chem. Soc. Dalt. Trans.* **1984**, 683.
- (135) Kolb, H. C.; VanNieuwenhze, M. S.; Sharpless, K. B. *Chem. Rev.* **1994**, 94, 2483–2547.
- (136) Christ, W. J.; Cha, J. K.; Kishi, Y. *Tetrahedron Lett.* **1983**, 24, 3947–3950.
- (137) Cha, J. K.; Christ, W. J.; Kishi, Y. *Tetrahedron* **1984**, 40, 2247–2255.
- (138) Yadav, J. S.; Reddy, B. V. S.; Harikishan, K.; Madan, C.; Narsaiah, A. V. *Synthesis (Stuttg.)* **2005**, 2897–2900.
- (139) Furst, A.; Plattner, P. A. *Helv. Chim. Acta* **1949**, 32, 275–283.
- (140) Templin, S. S.; Wallock, N. J.; Bennett, D. W.; Siddiquee, T.; Haworth, D. T.; Donaldson, W. A. *J. Heterocycl. Chem.* **2007**, 44, 719–723.
- (141) Zhao, X. Z.; Jia, Y. X.; Tu, Y. Q. *J. Chem. Res. Synopses* **2003**, 54–55, 210–217.

- (142) Angeles, A. R.; Dorn, D. C.; Kou, C. A.; Moore, M. A. S.; Danishefsky, S. J. *Angew. Chemie, Int. Ed.* **2007**, *46*, 1451–1454.
- (143) Wang, C.; Zhang, H.; Liu, J.; Ji, Y.; Shao, Z.; Li, L. *Synlett* **2006**, 1051–1054.
- (144) Kelemen, M. V.; Whelan, W. J. *Arch. Biochem. Biophys.* **1966**, *117*, 423–428.
- (145) Kuriyama, N.; Inoue, Y.; Kitagawa, K. *Synthesis (Stuttg)*. **1990**, *1990*, 735–738.
- (146) Osby, J. O.; Martin, M. G.; Ganem, B. *Tetrahedron Lett.* **1984**, *25*, 2093–2096.
- (147) Durette, P. L.; Meitzner, E. P.; Shen, T. Y. *Tetrahedron Lett.* **1979**, *20*, 4013–4016.
- (148) Motawia, M. S.; Wengel, J.; Abdel-Megid, A. E.-S.; Pedersen, E. B. *Synthesis (Stuttg)*. **1989**, *1989*, 384–387.

VII- APPENDIX

**Table 1 Crystal data and structure refinement for (±)-II-30.**

Identification code	don1v
Empirical formula	C ₁₆ H ₁₉ NO ₇
Formula weight	337.32
Temperature/K	99.95(10)
Crystal system	triclinic
Space group	P-1
a/Å	8.1821(3)
b/Å	8.3349(4)
c/Å	11.7398(5)
α/°	78.776(4)
β/°	89.260(3)
γ/°	69.061(4)
Volume/Å ³	732.04(5)
Z	2
ρ _{calc} /mg/mm ³	1.530
m/mm ⁻¹	0.121
F(000)	356.0
Crystal size/mm ³	0.35 × 0.18 × 0.12
2θ range for data collection	5.78 to 58.04°
Index ranges	-11 ≤ h ≤ 10, -11 ≤ k ≤ 11, -14 ≤ l ≤ 15
Reflections collected	14805

Independent reflections 3552[R(int) = 0.0288]
 Data/restraints/parameters 3552/0/252
 Goodness-of-fit on F^2 1.092
 Final R indexes [$I \geq 2\sigma(I)$] $R_1 = 0.0447$, $wR_2 = 0.1058$
 Final R indexes [all data] $R_1 = 0.0541$, $wR_2 = 0.1123$
 Largest diff. peak/hole / $e \text{ \AA}^{-3}$ 0.46/-0.32

Table 2 Fractional Atomic Coordinates ($\times 10^4$) and Equivalent Isotropic Displacement Parameters ($\text{\AA}^2 \times 10^3$) for don1v. U_{eq} is defined as 1/3 of the trace of the orthogonalised U_{ij} tensor.

Atom	<i>x</i>	<i>y</i>	<i>z</i>	$U(eq)$
O1	3552.5 (17)	3001.3 (17)	6828.5 (12)	25.8 (3)
O2	2479.5 (17)	3397.7 (16)	4471.9 (11)	23.9 (3)
O3	146.2 (15)	3610.1 (15)	6400 (1)	17.6 (2)
O4	-1694.1 (15)	1142.3 (17)	6170.9 (11)	20.8 (3)
O5	-1792.7 (15)	888.4 (15)	9276.2 (10)	21.5 (3)
O6	962.0 (15)	-3316.7 (15)	7182.8 (10)	19.9 (3)
N1	-65.3 (17)	-1019.5 (16)	8167.5 (11)	14.3 (3)
C1	806 (2)	144.1 (19)	7566.7 (13)	14.4 (3)
C2	2773 (2)	-749 (2)	7820.7 (14)	18.1 (3)
C3	4150 (2)	-114 (2)	7227.6 (14)	19.3 (3)
C4	3848 (2)	1511 (2)	6299.0 (14)	17.7 (3)
C5	2463 (2)	1908 (2)	5320.6 (13)	16.5 (3)
C6	573 (2)	2340.5 (19)	5671.8 (13)	14.8 (3)
C7	152.8 (19)	747 (2)	6278.1 (13)	14.6 (3)
C8	3985 (2)	-1784 (2)	7023.5 (15)	22.7 (4)
C9	-1316.8 (19)	-511 (2)	8972.5 (13)	15.1 (3)
C10	51 (2)	-2625.7 (19)	7900.6 (13)	14.9 (3)
C11	-1932.7 (19)	-2001 (2)	9344.3 (13)	14.6 (3)
C12	-1146.8 (19)	-3248.0 (19)	8676.9 (13)	14.5 (3)
C13	-1478 (2)	-4787 (2)	8811.6 (14)	17.5 (3)
C14	-2616 (2)	-5050 (2)	9665.5 (14)	20.1 (3)
C15	-3384 (2)	-3813 (2)	10345.7 (15)	20.3 (3)
C16	-3062 (2)	-2247 (2)	10189.9 (14)	18.7 (3)
O1W	6252 (4)	3831 (4)	7168 (3)	36.7 (7)
O2W	4524 (4)	5280 (5)	4551 (3)	43.7 (8)

Table 3 Anisotropic Displacement Parameters ($\text{\AA}^2 \times 10^3$) for don1v. The Anisotropic displacement factor exponent takes the form: $-2\pi^2[h^2a^*^2U_{11}+\dots+2hka \times b \times U_{12}]$

Atom	U_{11}	U_{22}	U_{33}	U_{23}	U_{13}	U_{12}
O1	20.2 (6)	26.8 (7)	34.1 (7)	-14.0 (6)	-0.1 (5)	-8.7 (5)
O2	24.5 (6)	20.2 (6)	22.6 (6)	3.0 (5)	7.3 (5)	-6.8 (5)
O3	18.3 (6)	14.2 (5)	19.7 (6)	-5.5 (4)	3.0 (4)	-4.2 (4)
O4	15.1 (6)	22.0 (6)	25.9 (7)	-2.7 (5)	-1.7 (5)	-8.3 (5)
O5	24.1 (6)	16.5 (6)	26.1 (6)	-9.4 (5)	8.3 (5)	-7.4 (5)
O6	26.2 (6)	18.5 (6)	16.8 (6)	-7.0 (4)	5.6 (5)	-8.6 (5)
N1	18.2 (6)	13.1 (6)	12.6 (6)	-3.3 (5)	3.1 (5)	-6.5 (5)
C1	17.6 (7)	13.1 (7)	13.6 (7)	-2.1 (5)	2.2 (6)	-7.3 (6)
C2	18.5 (8)	19.4 (8)	14.4 (7)	0.7 (6)	-0.8 (6)	-6.6 (6)
C3	13.4 (7)	24.3 (8)	17.1 (8)	-0.5 (6)	-1.0 (6)	-5.2 (6)
C4	14.5 (7)	18.0 (7)	20.3 (8)	-4.1 (6)	3.4 (6)	-5.4 (6)
C5	18.6 (7)	14.3 (7)	15.4 (7)	-0.8 (6)	3.8 (6)	-5.8 (6)
C6	15.3 (7)	14.1 (7)	13.7 (7)	-1.8 (6)	0.1 (5)	-4.5 (6)
C7	13.9 (7)	15.0 (7)	14.4 (7)	-3.0 (6)	-0.2 (5)	-4.7 (6)
C8	18.9 (8)	17.9 (8)	24.1 (9)	0.3 (6)	2.5 (6)	-0.4 (6)
C9	14.4 (7)	15.5 (7)	14.6 (7)	-2.3 (6)	0.3 (6)	-4.9 (6)
C10	17.9 (7)	12.6 (7)	13.0 (7)	-1.3 (5)	-1.2 (6)	-4.7 (6)
C11	13.9 (7)	14.4 (7)	14.0 (7)	-1.0 (6)	-1.8 (5)	-4.0 (6)
C12	14.7 (7)	14.8 (7)	13.0 (7)	-1.2 (6)	-1.2 (5)	-4.7 (6)
C13	19.0 (7)	15.6 (7)	17.6 (8)	-3.1 (6)	-1.8 (6)	-5.9 (6)
C14	20.6 (8)	18.4 (8)	21.8 (8)	0.3 (6)	-3.1 (6)	-10.1 (6)
C15	15.8 (7)	24.6 (8)	19.9 (8)	-0.3 (6)	1.8 (6)	-8.9 (6)
C16	16.3 (7)	20.4 (8)	19.0 (8)	-5.1 (6)	2.6 (6)	-5.8 (6)
O1W	26.0 (14)	36.1 (16)	55.6 (19)	-17.7 (14)	9.0 (13)	-16.3 (13)
O2W	38.2 (18)	39.8 (18)	60 (2)	-6.4 (16)	9.5 (14)	-24.6 (15)

Table 4 Bond Lengths for don1v.

Atom	Atom	Length/ \AA	Atom	Atom	Length/ \AA
O1	C4	1.439 (2)	C3	C4	1.509 (2)
O2	C5	1.4372 (18)	C3	C8	1.509 (2)
O3	C6	1.4328 (18)	C4	C5	1.527 (2)
O4	C7	1.4285 (18)	C5	C6	1.527 (2)
O5	C9	1.2133 (19)	C6	C7	1.530 (2)
O6	C10	1.2098 (19)	C9	C11	1.489 (2)
N1	C1	1.4703 (18)	C10	C12	1.489 (2)
N1	C9	1.3936 (19)	C11	C12	1.391 (2)
N1	C10	1.4041 (19)	C11	C16	1.383 (2)

C1	C2	1.517 (2)	C12	C13	1.383 (2)
C1	C7	1.536 (2)	C13	C14	1.399 (2)
C2	C3	1.516 (2)	C14	C15	1.393 (2)
C2	C8	1.511 (2)	C15	C16	1.399 (2)

Table 5 Bond Angles for don1v.

Atom	Atom	Atom	Angle/°	Atom	Atom	Atom	Angle/°
C9	N1	C1	122.27 (12)	O4	C7	C1	110.01 (12)
C9	N1	C10	111.71 (12)	O4	C7	C6	109.62 (12)
C10	N1	C1	125.44 (12)	C6	C7	C1	112.65 (12)
N1	C1	C2	109.09 (12)	C3	C8	C2	60.24 (11)
N1	C1	C7	109.44 (12)	O5	C9	N1	125.38 (14)
C2	C1	C7	116.49 (13)	O5	C9	C11	128.52 (14)
C3	C2	C1	125.56 (14)	N1	C9	C11	106.09 (12)
C8	C2	C1	123.62 (14)	O6	C10	N1	125.24 (14)
C8	C2	C3	59.82 (11)	O6	C10	C12	129.04 (14)
C4	C3	C2	127.32 (14)	N1	C10	C12	105.72 (12)
C4	C3	C8	124.76 (14)	C12	C11	C9	107.91 (13)
C8	C3	C2	59.94 (11)	C16	C11	C9	130.28 (14)
O1	C4	C3	109.92 (13)	C16	C11	C12	121.81 (14)
O1	C4	C5	111.48 (13)	C11	C12	C10	108.24 (13)
C3	C4	C5	117.10 (13)	C13	C12	C10	130.09 (14)
O2	C5	C4	108.91 (13)	C13	C12	C11	121.64 (14)
O2	C5	C6	106.36 (12)	C12	C13	C14	117.01 (15)
C4	C5	C6	116.25 (13)	C15	C14	C13	121.38 (15)
O3	C6	C5	110.63 (12)	C14	C15	C16	121.16 (15)
O3	C6	C7	109.24 (12)	C11	C16	C15	117.00 (15)
C5	C6	C7	114.33 (12)				

Table 6 Hydrogen Bonds for don1v.

D	H	A	d(D-H)/Å	d(H-A)/Å	d(D-A)/Å	D-H-A/°
O1	H1	O3	0.88 (3)	1.89 (3)	2.6841 (17)	150 (3)
O2	H2A	O2W	0.88 (4)	1.87 (4)	2.684 (3)	153 (4)
O3	H3	O2 ¹	0.91 (3)	1.76 (3)	2.6677 (17)	171 (3)
O4	H4	O1W ²	0.80 (3)	1.98 (3)	2.738 (3)	158 (3)
O1WH1WA	O5 ³		0.85	2.30	3.104 (4)	156.8
O1WH1WB	O1		0.85	1.77	2.595 (3)	163.3
O2WH2WB	O1 ⁴		0.85	2.06	2.792 (3)	143.3

¹-X,1-Y,1-Z; ²-1+X,+Y,+Z; ³1+X,+Y,+Z; ⁴1-X,1-Y,1-Z

Table 7 Torsion Angles for don1v.

A	B	C	D	Angle/°	A	B	C	D	Angle/°
O1C4	C5	O2		57.54 (16)	C3	C4	C5	C6	65.25 (18)
O1C4	C5	C6		-62.53 (17)	C4	C3	C8	C2	116.81 (17)
O2C5	C6	O3		-73.73 (15)	C4	C5	C6	O3	47.70 (17)
O2C5	C6	C7		162.45 (13)	C4	C5	C6	C7	-76.12 (17)
O3C6	C7	O4		77.43 (15)	C5	C6	C7	O4	158.01 (13)
O3C6	C7	C1		-45.41 (16)	C5	C6	C7	C1	79.15 (16)
O5C9	C11C12			173.90 (16)	C7	C1	C2	C3	45.9 (2)
O5C9	C11C16			-6.6 (3)	C7	C1	C2	C8	-28.7 (2)
O6C10C12C11				179.29 (16)	C8	C2	C3	C4	112.77 (19)
O6C10C12C13				2.7 (3)	C8	C3	C4	O1	161.45 (14)
N1C1	C2	C3		170.33 (14)	C8	C3	C4	C5	32.9 (2)
N1C1	C2	C8		95.81 (17)	C9	N1	C1	C2	121.89 (15)
N1C1	C7	O4		41.01 (16)	C9	N1	C1	C7	109.59 (15)
N1C1	C7	C6		163.63 (12)	C9	N1	C10O6		175.80 (15)
N1C9	C11C12			-5.16 (16)	C9	N1	C10C12		-4.50 (16)
N1C9	C11C16			174.37 (16)	C9	C11C12C10			2.51 (16)
N1C10C12C11				1.03 (16)	C9	C11C12C13			179.30 (14)
N1C10C12C13				176.96 (15)	C9	C11C16C15			179.56 (15)
C1N1	C9	O5		-1.4 (2)	C10N1	C1	C2		-67.55 (18)
C1N1	C9	C11		177.73 (13)	C10N1	C1	C7		60.97 (18)
C1N1	C10O6			4.4 (2)	C10N1	C9	O5		173.10 (15)
C1N1	C10C12			175.91 (13)	C10N1	C9	C11		6.00 (16)
C1C2	C3	C4		1.0 (3)	C10C12C13C14				176.61 (15)
C1C2	C3	C8		111.82 (18)	C11C12C13C14				-1.1 (2)
C1C2	C8	C3		114.91 (17)	C12C11C16C15				-0.1 (2)
C2C1	C7	O4		165.30 (13)	C12C13C14C15				0.2 (2)
C2C1	C7	C6		-72.08 (17)	C13C14C15C16				0.8 (2)
C2C3	C4	O1		85.19 (19)	C14C15C16C11				-0.9 (2)

C2C3 C4 C5	-43.3(2)	C16C11C12C10	177.07(14)
C3C4 C5 O2	174.68(13)	C16C11C12C13	1.1(2)

Table 8 Hydrogen Atom Coordinates ($\text{\AA} \times 10^4$) and Isotropic Displacement Parameters ($\text{\AA}^2 \times 10^3$) for don1v.

Atom	x	y	z	U(eq)
H1	2410(40)	3490(40)	6830(30)	63(9)
H2A	3280(50)	3760(50)	4700(30)	14(9)
H2B	3350(70)	3120(70)	3970(50)	54(15)
H3	-740(40)	4600(40)	6030(30)	64(8)
H4	-2190(30)	2080(40)	6330(20)	46(8)
H1A	426	1213	7917	17
H2	3101	-1297	8662	22
H3A	5176	-358	7775	23
H4A	4983	1321	5917	21
H5	2783	873	4938	20
H6	-209	2883	4944	18
H7	746	-242	5874	17
H8A	4914	-2910	7384	27
H8B	3485	-1763	6255	27
H13	-956	-5627	8345	21
H14	-2871	-6095	9784	24
H15	-4139	-4037	10926	24
H16	-3594	-1392	10644	22
H1WA	6718	3283	7842	55
H1WB	5253	3753	7091	55
H2WA	4354	5797	5122	66
H2WB	5447	5334	4232	66

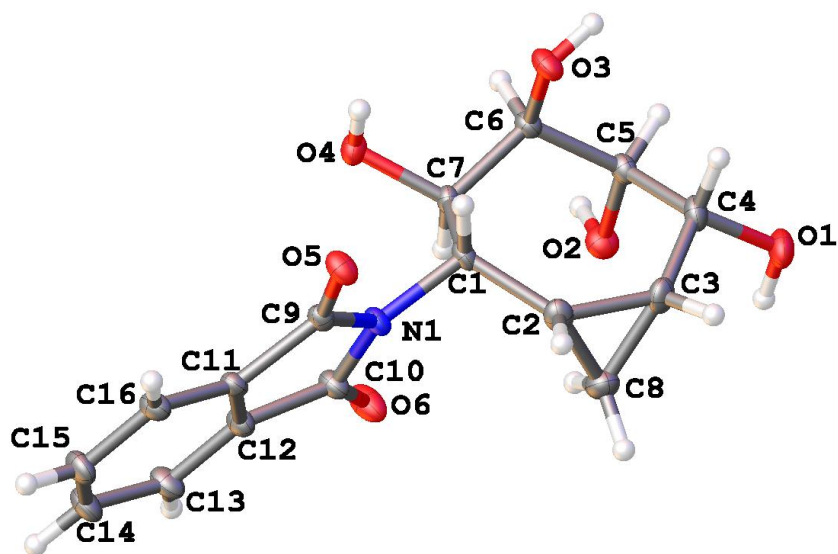


Table 1 Crystal data and structure refinement for (±)-II-31.

Identification code	don1w
Empirical formula	C ₁₆ H ₁₇ NO ₆
Formula weight	319.31
Temperature/K	99.95(10)
Crystal system	monoclinic
Space group	P2 ₁ /c
a/Å	10.91018(19)
b/Å	7.79863(13)
c/Å	17.1421(3)
α/°	90.00
β/°	99.5114(16)
γ/°	90.00
Volume/Å ³	1438.47(4)
Z	4
ρ _{calc} /mg/mm ³	1.474
m/mm ⁻¹	0.114
F(000)	672.0
Crystal size/mm ³	0.33 × 0.14 × 0.09
2θ range for data collection	5.76 to 57.9°
Index ranges	-13 ≤ h ≤ 14, -9 ≤ k ≤ 10, -23 ≤ l ≤ 23
Reflections collected	16375
Independent reflections	3507[R(int) = 0.0298]
Data/restraints/parameters	3507/0/224
Goodness-of-fit on F ²	1.085
Final R indexes [I ≥ 2σ (I)]	R ₁ = 0.0510, wR ₂ = 0.1337

Final R indexes [all data] $R_1 = 0.0585$, $wR_2 = 0.1394$
 Largest diff. peak/hole / e \AA^{-3} 0.83/-0.26

Table 2 Fractional Atomic Coordinates ($\times 10^4$) and Equivalent Isotropic Displacement Parameters ($\text{\AA}^2 \times 10^3$) for don1w. U_{eq} is defined as 1/3 of the trace of the orthogonalised U_{IJ} tensor.

Atom	x	y	z	U(eq)
O1	4476.4 (13)	5722.2 (19)	2891.4 (8)	24.7 (3)
O2	4381.7 (12)	7438.3 (17)	4264.2 (8)	21.0 (3)
O3	6776.4 (12)	10059.9 (18)	3549.5 (7)	19.9 (3)
O4	7339.6 (12)	10398.3 (17)	5267.3 (7)	17.5 (3)
O5	10502.6 (11)	8019.7 (18)	5241.0 (7)	19.6 (3)
O6	6981.4 (12)	6542 (2)	6221.4 (8)	25.9 (3)
N1	8567.8 (13)	7329.0 (19)	5532.3 (8)	15.3 (3)
C1	7850.4 (15)	7692 (2)	4736.5 (9)	14.8 (3)
C2	7576.2 (16)	6022 (2)	4295.8 (10)	19.2 (4)
C3	6534.0 (17)	5634 (2)	3619.7 (11)	20.7 (4)
C4	5505.2 (16)	6787 (2)	3220.5 (10)	19.2 (4)
C5	5008.7 (15)	8206 (2)	3695.7 (10)	16.5 (3)
C6	5979.4 (15)	9505 (2)	4078.5 (10)	15.1 (3)
C7	6789.6 (15)	8919 (2)	4840.8 (9)	14.2 (3)
C8	6544.0 (18)	4824 (2)	4420.3 (11)	23.8 (4)
C9	9844.6 (15)	7602 (2)	5716.9 (10)	14.9 (3)
C10	8061.8 (16)	6882 (2)	6207.5 (10)	17.9 (4)
C11	10190.0 (16)	7304 (2)	6584.1 (10)	15.2 (3)
C12	9114.1 (16)	6914 (2)	6880.8 (10)	17.1 (4)
C13	9123.8 (17)	6663 (3)	7680.8 (10)	21.7 (4)
C14	10273.3 (18)	6799 (3)	8177.6 (11)	23.5 (4)
C15	11354.1 (18)	7165 (3)	7877.8 (11)	22.8 (4)
C16	11331.4 (16)	7427 (2)	7066.8 (10)	18.5 (4)

Table 3 Anisotropic Displacement Parameters ($\text{\AA}^2 \times 10^3$) for don1w. The Anisotropic displacement factor exponent takes the form: $-2\pi^2[h^2a^{*2}U_{11} + \dots + 2hka \times b \times U_{12}]$

Atom	U_{11}	U_{22}	U_{33}	U_{23}	U_{13}	U_{12}
O1	25.0 (7)	30.4 (8)	17.5 (6)	-4.8 (6)	-0.3 (5)	-8.8 (6)
O2	19.9 (6)	24.2 (7)	19.8 (6)	1.1 (5)	6.0 (5)	-0.9 (5)
O3	17.2 (6)	28.3 (7)	13.8 (6)	5.2 (5)	1.6 (5)	-2.3 (5)
O4	17.4 (6)	19.3 (6)	15.9 (6)	-3.6 (5)	2.9 (5)	-3.0 (5)
O5	14.7 (6)	29.7 (7)	14.8 (6)	3.3 (5)	3.7 (5)	0.1 (5)
O6	15.9 (6)	40.3 (8)	20.9 (6)	9.2 (6)	1.6 (5)	-5.1 (6)

N1	13.3 (7)	20.3 (7)	11.6 (6)	2.6 (5)	0.1 (5)	0.2 (5)
C1	13.2 (7)	20.7 (8)	9.9 (7)	1.3 (6)	0.5 (6)	1.5 (6)
C2	17.9 (8)	20.4 (9)	18.9 (8)	-2.1 (7)	1.6 (7)	5.0 (7)
C3	22.4 (9)	20.2 (9)	19.2 (8)	-7.6 (7)	2.1 (7)	1.8 (7)
C4	18.4 (8)	25.4 (9)	12.9 (7)	-3.5 (7)	0.3 (6)	-2.9 (7)
C5	13.7 (8)	20.8 (9)	14.3 (7)	0.0 (6)	-0.1 (6)	-0.8 (6)
C6	14.5 (8)	17.1 (8)	13.5 (7)	1.5 (6)	1.7 (6)	0.5 (6)
C7	14.0 (7)	16.2 (8)	11.8 (7)	-1.8 (6)	0.1 (6)	-1.0 (6)
C8	27 (1)	17.6 (9)	25.6 (9)	1.9 (7)	0.9 (7)	-0.3 (7)
C9	13.9 (8)	15.9 (8)	14.1 (7)	0.9 (6)	0.5 (6)	2.9 (6)
C10	16.1 (8)	22.5 (9)	14.9 (8)	4.6 (7)	1.2 (6)	-0.9 (7)
C11	16.8 (8)	15.5 (8)	12.7 (7)	2.7 (6)	0.9 (6)	1.8 (6)
C12	15.6 (8)	20.0 (8)	14.9 (8)	2.7 (6)	0.0 (6)	-1.4 (7)
C13	19.7 (9)	29.4 (10)	16.1 (8)	6.9 (7)	3.2 (7)	-0.8 (7)
C14	24.6 (9)	31.9 (10)	13.2 (8)	5.0 (7)	0.3 (7)	-0.3 (8)
C15	20.2 (9)	29.7 (10)	16.1 (8)	4.1 (7)	-3.8 (7)	-2.1 (7)
C16	16.3 (8)	20.8 (9)	17.9 (8)	4.3 (7)	1.4 (6)	-0.7 (7)

Table 4 Bond Lengths for don1w.

Atom	Atom	Length/Å	Atom	Atom	Length/Å
O1	C4	1.435 (2)	C3	C4	1.511 (3)
O2	C5	1.413 (2)	C3	C8	1.509 (3)
O3	C6	1.423 (2)	C4	C5	1.525 (3)
O4	C7	1.442 (2)	C5	C6	1.533 (2)
O5	C9	1.217 (2)	C6	C7	1.522 (2)
O6	C10	1.212 (2)	C9	C11	1.490 (2)
N1	C1	1.484 (2)	C10	C12	1.488 (2)
N1	C9	1.393 (2)	C11	C12	1.388 (2)
N1	C10	1.406 (2)	C11	C16	1.380 (2)
C1	C2	1.511 (2)	C12	C13	1.384 (2)
C1	C7	1.535 (2)	C13	C14	1.399 (3)
C2	C3	1.514 (2)	C14	C15	1.392 (3)
C2	C8	1.505 (3)	C15	C16	1.401 (2)

Table 5 Bond Angles for don1w.

Atom	Atom	Atom	Angle/°	Atom	Atom	Atom	Angle/°
C9	N1	C1	122.38 (14)	O4	C7	C1	107.40 (13)
C9	N1	C10	111.40 (13)	O4	C7	C6	109.21 (14)

C10	N1	C1	125.80 (14)	C6	C7	C1	115.43 (13)
N1	C1	C2	109.01 (14)	C2	C8	C3	60.30 (12)
N1	C1	C7	107.78 (13)	O5	C9	N1	124.56 (15)
C2	C1	C7	120.33 (14)	O5	C9	C11	129.10 (16)
C1	C2	C3	128.05 (15)	N1	C9	C11	106.33 (14)
C8	C2	C1	123.72 (16)	O6	C10	N1	125.85 (16)
C8	C2	C3	59.99 (12)	O6	C10	C12	128.08 (16)
C4	C3	C2	129.48 (16)	N1	C10	C12	106.07 (14)
C8	C3	C2	59.71 (12)	C12	C11	C9	108.06 (15)
C8	C3	C4	123.65 (16)	C16	C11	C9	129.92 (16)
O1	C4	C3	107.95 (15)	C16	C11	C12	121.98 (16)
O1	C4	C5	107.82 (14)	C11	C12	C10	108.09 (15)
C3	C4	C5	119.51 (14)	C13	C12	C10	130.17 (16)
O2	C5	C4	108.43 (15)	C13	C12	C11	121.73 (16)
O2	C5	C6	111.34 (13)	C12	C13	C14	116.86 (17)
C4	C5	C6	115.27 (14)	C15	C14	C13	121.33 (17)
O3	C6	C5	112.33 (14)	C14	C15	C16	121.27 (17)
O3	C6	C7	107.99 (13)	C11	C16	C15	116.81 (17)
C7	C6	C5	115.54 (14)				

Table 6 Hydrogen Bonds for don1w.

D H A	d(D-H)/Å	d(H-A)/Å	d(D-A)/Å	D-H-A/°
O1H1O6 ¹	0.94 (3)	2.08 (3)	2.960 (2)	156 (3)
O2H2O4 ²	1.03 (4)	1.71 (4)	2.7417 (18)	175 (3)
O3H3O1 ³	0.85 (3)	1.84 (3)	2.6684 (18)	166 (3)
O4H4O5 ⁴	0.84 (3)	2.13 (3)	2.9158 (18)	155 (2)

¹1-X,1-Y,1-Z; ²1-X,2-Y,1-Z; ³1-X,1/2+Y,1/2-Z; ⁴2-X,2-Y,1-Z

Table 7 Torsion Angles for don1w.

A B C D	Angle/°	A B C D	Angle/°
O1C4 C5 O2	55.84 (17)	C3 C4 C5 C6	57.8 (2)
O1C4 C5 C6	178.61 (14)	C4 C3 C8 C2	119.72 (19)
O2C5 C6 O3	169.17 (14)	C4 C5 C6 O3	45.1 (2)
O2C5 C6 C7	44.7 (2)	C4 C5 C6 C7	-79.37 (19)
O3C6 C7 O4	72.60 (16)	C5 C6 C7 O4	160.68 (14)
O3C6 C7 C1	-48.49 (19)	C5 C6 C7 C1	78.24 (19)

O5C9 C11C12	177.71 (18)	C7 C1 C2 C3	30.9 (3)
O5C9 C11C16	0.2 (3)	C7 C1 C2 C8	-45.1 (2)
O6C10C12C11	177.6 (2)	C8 C2 C3 C4	110.5 (2)
O6C10C12C13	-3.8 (3)	C8 C3 C4 O1	-77.8 (2)
N1C1 C2 C3	156.06 (17)	C8 C3 C4 C5	45.8 (3)
N1C1 C2 C8	80.0 (2)	C9 N1 C1 C2	102.95 (18)
N1C1 C7 O4	55.34 (17)	C9 N1 C1 C7	-
N1C1 C7 C6	177.40 (14)	C9 N1 C10O6	124.88 (16)
N1C9 C11C12	-1.51 (19)	C9 N1 C10O6	-
N1C9 C11C16	-	C9 N1 C10C12	178.59 (19)
N1C10C12C11	-2.3 (2)	C9 N1 C10C12	1.3 (2)
N1C10C12C13	176.30 (19)	C9 C11C12C10	2.3 (2)
C1N1 C9 O5	-6.2 (3)	C9 C11C12C13	-
C1N1 C9 C11	173.03 (15)	C9 C11C12C13	176.40 (17)
C1N1 C10O6	8.7 (3)	C9 C11C16C15	176.26 (18)
C1N1 C10C12	-	C10N1 C1 C2	-85.1 (2)
C1C2 C3 C4	-0.7 (3)	C10N1 C1 C7	47.0 (2)
C1C2 C3 C8	-111.2 (2)	C10N1 C9 O5	-
C1C2 C8 C3	118.05 (19)	C10N1 C9 O5	179.21 (17)
C2C1 C7 O4	-	C10N1 C9 C11	0.06 (19)
C2C1 C7 C6	-56.9 (2)	C10C12C13C14	-
C2C3 C4 O1	154.09 (18)	C10C12C13C14	179.10 (19)
C2C3 C4 C5	-30.5 (3)	C11C12C13C14	-0.7 (3)
C3C4 C5 O2	-67.8 (2)	C12C11C16C15	-1.0 (3)
		C12C13C14C15	-0.2 (3)
		C13C14C15C16	0.6 (3)
		C14C15C16C11	0.0 (3)
		C16C11C12C10	-
		C16C11C12C10	179.92 (16)
		C16C11C12C13	1.4 (3)

Table 8 Hydrogen Atom Coordinates ($\text{\AA}\times 10^4$) and Isotropic Displacement Parameters ($\text{\AA}^2\times 10^3$) for don1w.

Atom	x	y	z	U(eq)
H1	4110 (30)	5220 (40)	3290 (18)	55 (9)
H2	3740 (40)	8300 (50)	4410 (20)	86 (12)
H3	6300 (30)	10370 (40)	3130 (17)	39 (7)
H4	7820 (20)	10830 (30)	4985 (14)	25 (6)
H1A	8419	8350	4445	18

H2A	8354	5386	4242	23
H3A	6804	4803	3237	25
H4A	5816	7351	2767	23
H5	4375	8856	3322	20
H6	5513	10538	4213	18
H7	6245	8333	5174	17
H8A	5931	5242	4742	29
H8B	6738	3586	4476	29
H13	8385	6409	7883	26
H14	10317	6639	8731	28
H15	12122	7239	8230	27
H16	12067	7676	6859	22

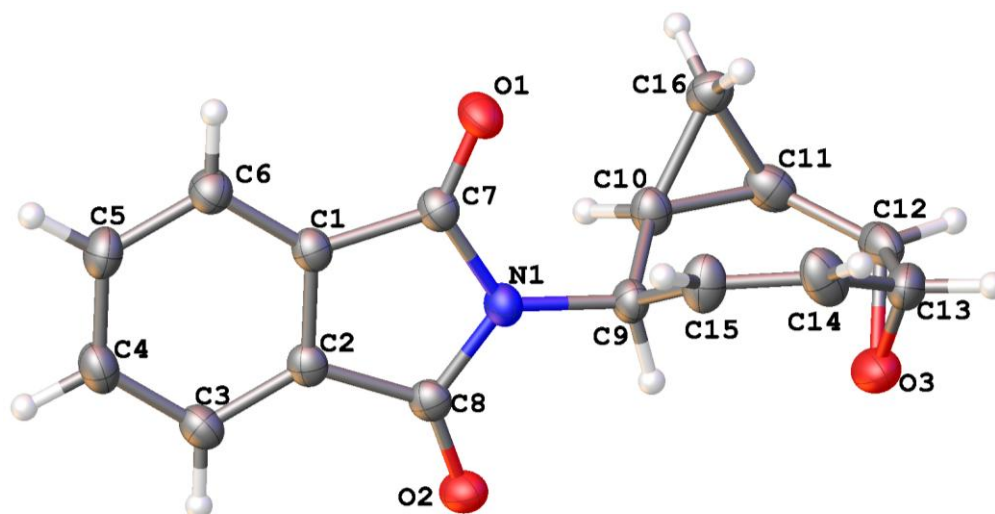


Table 1 Crystal data and structure refinement for (±)-II-36.

Identification code	don1q
Empirical formula	C ₁₆ H ₁₃ NO ₃
Formula weight	267.27
Temperature/K	100.00(10)
Crystal system	monoclinic
Space group	P2 ₁ /n
a/Å	10.8711(3)
b/Å	10.1720(3)
c/Å	11.3216(4)
α/°	90.00
β/°	94.004(3)
γ/°	90.00
Volume/Å ³	1248.90(7)
Z	4
ρ _{calc} /mg/mm ³	1.421
m/mm ⁻¹	0.811
F(000)	560
Crystal size/mm ³	0.32 × 0.14 × 0.08
2θ range for data collection	10.9 to 147.58°
Index ranges	-13 ≤ h ≤ 13, -12 ≤ k ≤ 12, -13 ≤ l ≤ 14
Reflections collected	10144
Independent reflections	2495[R(int) = 0.0288]
Data/restraints/parameters	2495/0/191
Goodness-of-fit on F ²	1.056
Final R indexes [I ≥ 2σ (I)]	R ₁ = 0.0418, wR ₂ = 0.1074

Final R indexes [all data] $R_1 = 0.0480$, $wR_2 = 0.1126$
 Largest diff. peak/hole / $e \text{ \AA}^{-3}$ 0.338/-0.316

Table 2 Fractional Atomic Coordinates ($\times 10^4$) and Equivalent Isotropic Displacement Parameters ($\text{\AA}^2 \times 10^3$) for don1q. U_{eq} is defined as 1/3 of the trace of the orthogonalised U_{ij} tensor.

Atom	x	y	z	U(eq)
O1	5310 (1)	2871.5 (12)	-887 (1)	31.4 (3)
O2	1719.6 (10)	841.2 (11)	-31.1 (10)	31.8 (3)
O3	2460.7 (12)	-516.7 (13)	-4027.4 (11)	40.9 (3)
N1	3523.2 (11)	1663.6 (12)	-716 (1)	23.9 (3)
C1	4137.6 (13)	2984.4 (14)	874.9 (13)	23.5 (3)
C2	3056.0 (13)	2349.4 (14)	1139.4 (13)	23.0 (3)
C3	2519.8 (14)	2557.8 (16)	2196.8 (13)	27.8 (3)
C4	3115.1 (16)	3444.1 (16)	2986.9 (14)	31.6 (4)
C5	4195.9 (15)	4078.2 (16)	2726.0 (14)	31.2 (4)
C6	4730.7 (14)	3861.5 (16)	1655.1 (14)	28.3 (3)
C7	4446.0 (13)	2554.6 (15)	-329.1 (13)	24.4 (3)
C8	2636.7 (13)	1515.4 (14)	109.2 (13)	23.8 (3)
C9	3385.3 (14)	1079.6 (14)	-1906.4 (12)	24.3 (3)
C12	2994.3 (15)	564.4 (18)	-4641.6 (14)	33.2 (4)
C13	3770.5 (17)	-522.4 (17)	-4185.1 (15)	34.7 (4)
C10	3123.0 (14)	2152.0 (15)	-2823.0 (13)	27.4 (3)
C11	2914.2 (16)	1880.6 (17)	-4107.9 (14)	32.9 (4)
C14	4631.5 (17)	-482.6 (18)	-3107.3 (15)	37.7 (4)
C15	4475.6 (16)	208.2 (17)	-2105.0 (14)	33.3 (4)
C16	3992.7 (19)	2649.0 (19)	-3679.8 (17)	29.5 (5)
C10A	4475.6 (16)	208.2 (17)	-2105.0 (14)	33.3 (4)
C11A	4631.5 (17)	-482.6 (18)	-3107.3 (15)	37.7 (4)
C14A	2914.2 (16)	1880.6 (17)	-4107.9 (14)	32.9 (4)
C15A	3123.0 (14)	2152.0 (15)	-2823.0 (13)	27.4 (3)
C16A	5402 (7)	306 (8)	-2721 (7)	29 (2)

Table 3 Anisotropic Displacement Parameters ($\text{\AA}^2 \times 10^3$) for don1q. The Anisotropic displacement factor exponent takes the form: $-2\pi^2[h^2a^*^2U_{11}+\dots+2hka \times b \times U_{12}]$

Atom	U_{11}	U_{22}	U_{33}	U_{23}	U_{13}	U_{12}
O1	25.9 (6)	42.2 (7)	26.8 (6)	-3.4 (5)	5.5 (4)	-5.0 (5)
O2	31.1 (6)	35.7 (6)	28.5 (6)	0.2 (5)	1.4 (4)	-9.5 (5)
O3	44.6 (7)	44.1 (7)	34.4 (7)	-5.2 (5)	6.1 (5)	-17.7 (6)
N1	25.6 (6)	27.4 (6)	18.5 (6)	-0.9 (5)	0.2 (5)	-0.8 (5)
C1	24.2 (7)	25.5 (7)	20.8 (7)	0.9 (6)	0.7 (5)	2.9 (6)
C2	25.4 (7)	23.5 (7)	19.8 (7)	2.5 (5)	-0.5 (5)	2.9 (5)
C3	28.4 (8)	32.1 (8)	23.2 (7)	2.7 (6)	3.6 (6)	0.7 (6)
C4	38.3 (9)	34.8 (8)	22.1 (7)	-1.9 (6)	5.1 (6)	3.2 (7)
C5	36.1 (8)	31.7 (8)	25.3 (8)	-6.8 (6)	-1.2 (6)	0.1 (7)
C6	27.2 (7)	30.9 (8)	26.8 (8)	-2.0 (6)	1.4 (6)	-1.4 (6)
C7	24.3 (7)	27.1 (7)	21.4 (7)	1.2 (6)	-0.4 (6)	1.6 (6)
C8	25.8 (7)	24.4 (7)	20.9 (7)	3.7 (5)	-0.4 (5)	1.0 (6)
C9	28.2 (7)	26.3 (7)	18.1 (7)	-2.2 (6)	-0.1 (5)	-0.7 (6)
C12	34.3 (8)	44.8 (9)	20.4 (7)	-0.2 (7)	1.1 (6)	-9.4 (7)
C13	43.6 (9)	31.7 (8)	29.7 (8)	-8.5 (7)	9.1 (7)	-6.9 (7)
C10	32.0 (8)	27.0 (7)	23.0 (7)	0.1 (6)	0.8 (6)	4.5 (6)
C11	34.4 (8)	35.4 (9)	29.1 (8)	8.2 (7)	3.9 (6)	3.3 (7)
C14	44.9 (10)	35.8 (9)	33.0 (9)	3.0 (7)	8.0 (7)	15.1 (8)
C15	39.4 (9)	32.6 (8)	26.8 (8)	-1.1 (6)	-5.7 (7)	10.3 (7)
C16	34.7 (11)	25.6 (10)	27.6 (10)	2.5 (7)	-2.3 (8)	-3.6 (8)
C10A	39.4 (9)	32.6 (8)	26.8 (8)	-1.1 (6)	-5.7 (7)	10.3 (7)
C11A	44.9 (10)	35.8 (9)	33.0 (9)	3.0 (7)	8.0 (7)	15.1 (8)
C14A	34.4 (8)	35.4 (9)	29.1 (8)	8.2 (7)	3.9 (6)	3.3 (7)
C15A	32.0 (8)	27.0 (7)	23.0 (7)	0.1 (6)	0.8 (6)	4.5 (6)
C16A	22 (4)	34 (4)	30 (4)	-7 (3)	5 (3)	-3 (3)

Table 4 Bond Lengths for don1q.

Atom	Atom	Length/ \AA	Atom	Atom	Length/ \AA
O1	C7	1.2115 (18)	C3	C4	1.397 (2)
O2	C8	1.2114 (18)	C4	C5	1.390 (2)
O3	C12	1.444 (2)	C5	C6	1.398 (2)
O3	C13	1.447 (2)	C9	C10	1.519 (2)
N1	C7	1.3994 (19)	C9	C15	1.509 (2)
N1	C8	1.3965 (18)	C12	C13	1.463 (3)

N1	C9	1.4709 (18)	C12	C11	1.474 (2)
C1	C2	1.392 (2)	C13	C14	1.486 (3)
C1	C6	1.383 (2)	C10	C11	1.483 (2)
C1	C7	1.492 (2)	C10	C16	1.489 (2)
C2	C3	1.384 (2)	C11	C16	1.463 (3)
C2	C8	1.488 (2)	C14	C15	1.355 (2)

Table 5 Bond Angles for don1q.

Atom	Atom	Atom	Angle/°	Atom	Atom	Atom	Angle/°
C12	O3	C13	60.79 (11)	N1	C8	C2	105.96 (12)
C7	N1	C9	124.98 (12)	N1	C9	C10	109.77 (12)
C8	N1	C7	111.95 (12)	N1	C9	C15	110.05 (12)
C8	N1	C9	122.57 (12)	C15	C9	C10	115.59 (13)
C2	C1	C7	107.92 (13)	O3	C12	C13	59.71 (11)
C6	C1	C2	121.66 (14)	O3	C12	C11	117.20 (13)
C6	C1	C7	130.41 (14)	C13	C12	C11	126.20 (14)
C1	C2	C8	108.24 (12)	O3	C13	C12	59.50 (11)
C3	C2	C1	121.87 (14)	O3	C13	C14	117.87 (14)
C3	C2	C8	129.86 (14)	C12	C13	C14	125.75 (15)
C2	C3	C4	116.65 (15)	C11	C10	C9	123.05 (13)
C5	C4	C3	121.61 (15)	C11	C10	C16	58.99 (11)
C4	C5	C6	121.32 (15)	C16	C10	C9	126.25 (14)
C1	C6	C5	116.88 (14)	C12	C11	C10	124.19 (14)
O1	C7	N1	125.03 (14)	C16	C11	C12	123.51 (15)
O1	C7	C1	129.07 (14)	C16	C11	C10	60.74 (12)
N1	C7	C1	105.89 (12)	C15	C14	C13	126.40 (16)
O2	C8	N1	125.00 (14)	C14	C15	C9	125.07 (15)
O2	C8	C2	129.04 (14)	C11	C16	C10	60.27 (11)

Table 6 Torsion Angles for don1q.

A	B	C	D	Angle/°
O3	C12	C13	C14	-104.14 (18)
O3	C12	C11	C10	41.8 (2)
O3	C12	C11	C16	116.80 (18)
O3	C13	C14	C15	-37.5 (3)

N1	C9	C10	C11	-178.85	(13)
N1	C9	C10	C16	107.71	(17)
N1	C9	C15	C14	179.60	(17)
C1	C2	C3	C4	0.3	(2)
C1	C2	C8	O2	-177.47	(15)
C1	C2	C8	N1	1.88	(16)
C2	C1	C6	C5	0.2	(2)
C2	C1	C7	O1	-179.87	(15)
C2	C1	C7	N1	-0.58	(16)
C2	C3	C4	C5	-0.4	(2)
C3	C2	C8	O2	0.7	(3)
C3	C2	C8	N1	-179.91	(15)
C3	C4	C5	C6	0.4	(3)
C4	C5	C6	C1	-0.3	(2)
C6	C1	C2	C3	-0.2	(2)
C6	C1	C2	C8	178.16	(13)
C6	C1	C7	O1	1.3	(3)
C6	C1	C7	N1	-179.41	(15)
C7	N1	C8	O2	177.06	(14)
C7	N1	C8	C2	-2.32	(16)
C7	N1	C9	C10	-63.09	(18)
C7	N1	C9	C15	65.20	(18)
C7	C1	C2	C3	-179.18	(14)
C7	C1	C2	C8	-0.80	(16)
C7	C1	C6	C5	178.92	(15)
C8	N1	C7	O1	-178.82	(14)
C8	N1	C7	C1	1.85	(16)
C8	N1	C9	C10	108.16	(15)
C8	N1	C9	C15	-123.55	(15)
C8	C2	C3	C4	-177.71	(15)
C9	N1	C7	O1	-6.8	(2)
C9	N1	C7	C1	173.90	(12)
C9	N1	C8	O2	4.8	(2)
C9	N1	C8	C2	-174.60	(12)
C9	C10	C11	C12	-3.0	(2)
C9	C10	C11	C16	-115.60	(17)
C9	C10	C16	C11	110.38	(18)
C12	O3	C13	C14	117.10	(17)

C12 C13 C14 C15	33.4 (3)
C12 C11 C16 C10	-113.68 (17)
C13 O3 C12 C11	-117.96 (17)
C13 C12 C11 C10	-29.1 (3)
C13 C12 C11 C16	45.9 (2)
C13 C14 C15 C9	-0.4 (3)
C10 C9 C15 C14	-55.4 (2)
C11 C12 C13 O3	103.21 (17)
C11 C12 C13 C14	-0.9 (3)
C15 C9 C10 C11	56.0 (2)
C15 C9 C10 C16	-17.5 (2)
C16 C10 C11 C12	112.61 (19)

Table 7 Hydrogen Atom Coordinates ($\text{\AA} \times 10^4$) and Isotropic Displacement Parameters ($\text{\AA}^2 \times 10^3$) for don1q.

Atom	<i>x</i>	<i>y</i>	<i>z</i>	U(eq)
H3	1784	2120	2376	33
H4	2773	3618	3721	38
H5	4579	4671	3287	37
H6	5467	4296	1472	34
H9	2641	500	-1929	29
H12	2812	549	-5520	40
H13	4022	-1145	-4808	42
H10	2568	2854	-2545	33
H11	2244	2433	-4502	39
H14	5363	-991	-3122	45
H15	5101	138	-1479	40
H16A	3988	3603	-3851	35
H16B	4812	2224	-3682	35
H10A	4682	-351	-1392	40
H11A	4912	-1394	-2896	45
H14A	2716	2601	-4620	39
H15A	3091	3038	-2561	33
H16C	5484	1130	-3175	34
H16D	6194	-53	-2376	34

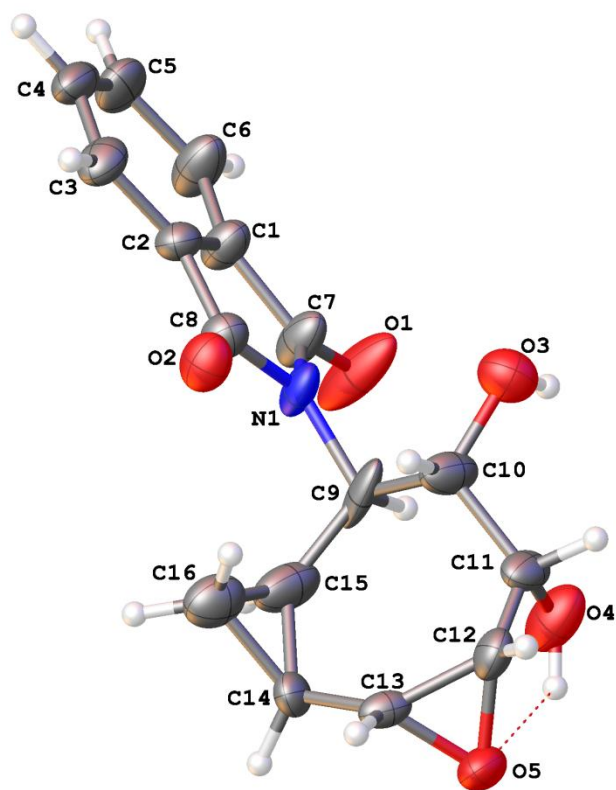


Table 1 Crystal data and structure refinement for (±)-II-38.

Identification code	don1r5
Empirical formula	$C_{16.04948}H_{14.82598}NO_5$
Formula weight	301.71
Temperature/K	99.9(3)
Crystal system	monoclinic
Space group	$P2_1/m$
$a/\text{\AA}$	8.4819(5)
$b/\text{\AA}$	7.2208(4)
$c/\text{\AA}$	11.3135(7)
$\alpha/^\circ$	90.00
$\beta/^\circ$	106.409(6)
$\gamma/^\circ$	90.00
Volume/ \AA^3	664.68(7)
Z	2
$\rho_{\text{calc}}/\text{mg}/\text{mm}^3$	1.507
m/mm^{-1}	0.946

F(000)	316.0
Crystal size/mm ³	0.22 × 0.12 × 0.03
2 Θ range for data collection	8.14 to 148.08°
Index ranges	-10 ≤ h ≤ 10, -8 ≤ k ≤ 8, -14 ≤ l ≤ 14
Reflections collected	4117
Independent reflections	4117[R(int) = 0.0000]
Data/restraints/parameters	4117/80/204
Goodness-of-fit on F ²	1.115
Final R indexes [$I \geq 2\sigma(I)$]	R ₁ = 0.0937, wR ₂ = 0.2778
Final R indexes [all data]	R ₁ = 0.1028, wR ₂ = 0.2891
Largest diff. peak/hole / e Å ⁻³	1.03/-0.40

Table 2 Fractional Atomic Coordinates ($\times 10^4$) and Equivalent Isotropic Displacement Parameters ($\text{\AA}^2 \times 10^3$) for don1r5. U_{eq} is defined as 1/3 of of the trace of the orthogonalised U_{ij} tensor.

Atom	x	y	z	U(eq)
O1	4232 (4)	2932 (13)	-309 (3)	87 (3)
O2	2273 (3)	2194 (11)	3016 (2)	46.0 (19)
O3	5120 (4)	5891 (4)	2486 (3)	53.0 (8)
O4	8548 (4)	4110 (6)	3036 (3)	62.6 (9)
O5	9517 (3)	2238 (15)	5082 (3)	47 (2)
N1	3666 (3)	2630 (17)	1550 (2)	40.6 (13)
C1	1453 (4)	2586 (10)	-173 (3)	42.7 (9)
C2	844 (4)	2350 (7)	832 (3)	35.6 (7)
C3	-814 (4)	2155 (7)	712 (4)	44.5 (17)
C4	-1856 (4)	2211 (13)	-489 (4)	49 (2)
C5	-1276 (4)	2430 (20)	-1486 (3)	53.2 (11)
C6	407 (5)	2660 (20)	-1361 (3)	58 (2)
C7	3239 (4)	2747 (17)	288 (3)	49 (2)
C8	2267 (4)	2350 (20)	1965 (3)	38.4 (14)
C9	5407 (4)	2609 (13)	2310 (3)	51.9 (13)
C10	5752 (14)	4291 (13)	3168 (8)	49 (2)
C11	7557 (6)	4494 (8)	3805 (5)	42.3 (12)
C12	8168 (17)	3570 (20)	4949 (15)	42 (2)
C13	7924 (15)	1580 (20)	5101 (12)	33.0 (18)
C14	7105 (6)	146 (7)	4074 (5)	37.1 (10)
C15	5882 (14)	777 (16)	2823 (9)	60 (2)
C16	5279 (5)	18 (7)	3821 (4)	54.4 (10)

Table 3 Anisotropic Displacement Parameters ($\text{\AA}^2 \times 10^3$) for don1r5. The Anisotropic displacement factor exponent takes the form: $-2\pi^2[h^2a^{*2}U_{11} + \dots + 2hka \times b \times U_{12}]$

Atom	U_{11}	U_{22}	U_{33}	U_{23}	U_{13}	U_{12}
O1	35.9(12)	181(10)	43.8(13)	32(3)	10.1(10)	-29(3)
O2	45.7(11)	55(6)	39.2(11)	1.1(13)	15.2(9)	-8.4(16)
O3	55.4(17)	50.1(18)	51.5(16)	6.9(12)	11.8(13)	6.1(13)
O4	42.7(16)	91(3)	54.4(17)	5.2(15)	13.8(13)	-17.0(16)
O5	27.7(10)	41(6)	66.0(13)	-1.1(15)	1.3(9)	0.1(14)
N1	26.1(10)	54(3)	38.5(11)	11(3)	3.7(9)	-18(3)
C1	29.1(13)	55(2)	39.6(13)	7(5)	2.9(11)	-7(5)
C2	25.9(11)	33.4(19)	43.8(13)	3(3)	3.6(10)	4(3)
C3	28.7(14)	43(5)	62.5(19)	-8.8(18)	14.6(13)	0.9(15)
C4	26.0(13)	36(7)	76(2)	-6(2)	-3.1(13)	0.3(16)
C5	37.0(16)	55(3)	54.0(16)	-2(7)	-8.7(13)	-12(7)
C6	42.6(16)	80(5)	44.0(15)	16(4)	-1.8(13)	-20(4)
C7	31.7(14)	71(7)	41.3(14)	18(3)	4.7(12)	-15(3)
C8	33.4(12)	40(4)	39.3(13)	4(3)	5.8(10)	-1(3)
C9	34.6(16)	84(3)	32.9(12)	9(3)	2.4(11)	-40(3)
C10	38(3)	40(3)	55(4)	-15(3)	-8(3)	10(2)
C11	31(2)	27(2)	62(3)	-10.8(18)	2.4(19)	6.9(17)
C12	29(4)	43(3)	52(5)	2(3)	10(2)	-12(3)
C13	25(4)	39(3)	31(3)	-7.1(19)	2(2)	8(3)
C14	34(2)	21(2)	51(2)	-1.4(16)	3.9(18)	-4.1(17)
C15	36(3)	64(4)	68(5)	-26(3)	-6(3)	8(3)
C16	45(2)	59(3)	52(2)	-12(2)	1.0(18)	2.7(19)

Table 4 Bond Lengths for don1r5.

Atom	Atom	Length/ \AA	Atom	Atom	Length/ \AA
O1	C7	1.226(5)	C2	C8	1.492(4)
O2	C8	1.194(4)	C3	C4	1.397(6)
O3	C10	1.408(11)	C4	C5	1.361(6)
O4	C11	1.397(7)	C5	C6	1.404(5)
O5	C12	1.470(13)	C9	C10	1.531(10)
O5	C13	1.437(11)	C9	C15	1.455(12)
N1	C7	1.374(4)	C10	C11	1.503(12)

N1	C8	1.407 (5)	C11	C12	1.417 (15)
N1	C9	1.484 (4)	C12	C13	1.467 (7)
C1	C2	1.386 (5)	C13	C14	1.566 (12)
C1	C6	1.387 (5)	C14	C15	1.568 (12)
C1	C7	1.461 (5)	C14	C16	1.497 (7)
C2	C3	1.381 (4)	C15	C16	1.471 (10)

Table 5 Bond Angles for don1r5.

Atom	Atom	Atom	Angle/°	Atom	Atom	Atom	Angle/°
C13	O5	C12	60.6 (3)	C15	C9	N1	111.0 (8)
C7	N1	C8	110.9 (3)	C15	C9	C10	119.1 (4)
C7	N1	C9	122.0 (3)	O3	C10	C9	109.1 (6)
C8	N1	C9	126.9 (3)	O3	C10	C11	111.2 (8)
C2	C1	C6	121.0 (3)	C11	C10	C9	111.6 (6)
C2	C1	C7	107.9 (3)	O4	C11	C10	113.1 (5)
C6	C1	C7	131.1 (3)	O4	C11	C12	110.2 (6)
C1	C2	C8	107.8 (3)	C12	C11	C10	116.9 (9)
C3	C2	C1	122.5 (3)	C11	C12	O5	118.3 (10)
C3	C2	C8	129.7 (3)	C11	C12	C13	122.7 (18)
C2	C3	C4	116.1 (4)	C13	C12	O5	58.6 (7)
C5	C4	C3	122.1 (3)	O5	C13	C12	60.8 (8)
C4	C5	C6	121.7 (3)	O5	C13	C14	115.4 (8)
C1	C6	C5	116.6 (4)	C12	C13	C14	127.5 (17)
O1	C7	N1	124.0 (3)	C13	C14	C15	121.2 (9)
O1	C7	C1	128.1 (3)	C16	C14	C13	113.7 (6)
N1	C7	C1	107.9 (3)	C16	C14	C15	57.3 (5)
O2	C8	N1	125.4 (3)	C9	C15	C14	131.5 (9)
O2	C8	C2	129.1 (3)	C9	C15	C16	121.8 (8)
N1	C8	C2	105.5 (3)	C16	C15	C14	58.9 (4)
N1	C9	C10	109.9 (8)	C15	C16	C14	63.8 (5)

Table 6 Hydrogen Bonds for don1r5.

D	H	A	d(D-H)/Å	d(H-A)/Å	d(D-A)/Å	D-H-A/°
O3	H3	O1 ¹	0.84	2.05	2.803 (5)	149.2
O4	H4	O5	0.84	2.05	2.604 (7)	122.7

¹I-X,I-Y,-Z**Table 7 Torsion Angles for don1r5.**

A	B	C	D	Angle/°
O3	C10	C11	O4	-82.1 (6)
O3	C10	C11	C12	148.3 (9)
O4	C11	C12	O5	-7.9 (16)
O4	C11	C12	C13	-77.0 (14)
O5	C12	C13	C14	-100.9 (13)
O5	C13	C14	C15	-94.0 (13)
O5	C13	C14	C16	-158.9 (9)
N1	C9	C10	O3	-47.6 (8)
N1	C9	C10	C11	-170.8 (7)
N1	C9	C15	C14	-146.7 (9)
N1	C9	C15	C16	-71.9 (10)
C1	C2	C3	C4	-0.1 (4)
C1	C2	C8	O2	179.7 (12)
C1	C2	C8	N1	1.0 (9)
C2	C1	C6	C5	-1.8 (12)
C2	C1	C7	O1	178.4 (10)
C2	C1	C7	N1	-0.7 (9)
C2	C3	C4	C5	0.3 (11)
C3	C2	C8	O2	-0.4 (17)
C3	C2	C8	N1	-179.1 (5)
C3	C4	C5	C6	-1.4 (17)
C4	C5	C6	C1	2.1 (17)
C6	C1	C2	C3	0.9 (6)
C6	C1	C2	C8	-179.3 (8)
C6	C1	C7	O1	-2.6 (15)
C6	C1	C7	N1	178.2 (8)
C7	N1	C8	O2	179.7 (12)
C7	N1	C8	C2	-1.5 (12)
C7	N1	C9	C10	118.3 (10)
C7	N1	C9	C15	-107.9 (10)
C7	C1	C2	C3	179.9 (5)
C7	C1	C2	C8	-0.2 (7)
C7	C1	C6	C5	179.4 (9)

C8	N1	C7	O1	-177.8(11)
C8	N1	C7	C1	1.5(12)
C8	N1	C9	C10	-68.6(13)
C8	N1	C9	C15	65.3(13)
C8	C2	C3	C4	-179.9(8)
C9	N1	C7	O1	-3.6(17)
C9	N1	C7	C1	175.6(9)
C9	N1	C8	O2	6(2)
C9	N1	C8	C2	-175.3(10)
C9	C10	C11	O4	39.9(9)
C9	C10	C11	C12	-89.7(11)
C9	C15	C16	C14	-122.4(10)
C10	C9	C15	C14	-17.6(10)
C10	C9	C15	C16	57.2(9)
C10	C11	C12	O5	123.1(11)
C10	C11	C12	C13	54.0(14)
C11	C12	C13	O5	105.6(11)
C11	C12	C13	C14	5(2)
C12	O5	C13	C14	120.5(19)
C12	C13	C14	C15	-22.4(17)
C12	C13	C14	C16	-87.3(14)
C13	O5	C12	C11	-113(2)
C13	C14	C15	C9	7.1(14)
C13	C14	C15	C16	-99.7(7)
C13	C14	C16	C15	113.1(9)
C15	C9	C10	O3	-177.2(8)
C15	C9	C10	C11	59.6(9)
C16	C14	C15	C9	106.8(11)

Table 8 Hydrogen Atom Coordinates ($\text{\AA}\times 10^4$) and Isotropic Displacement Parameters ($\text{\AA}^2\times 10^3$) for don1r5.

Atom	x	y	z	U(eq)
H3	5676	6132	1997	80
H4	9372	3498	3428	94
H3A	-1221	1993	1406	53
H4A	-3007	2089	-614	59
H5	-2030	2436	-2286	64

H6	808	2857	-2054	70
H9	6066	2821	1715	62
H10	5164	4112	3811	59
H11	7722	5843	4003	51
H12	8232	4346	5693	50
H13	7854	1236	5940	40
H14	7711	-1040	4067	44
H15	5814	-160	2159	72
H16A	4782	-1234	3699	65
H16B	4745	889	4264	65

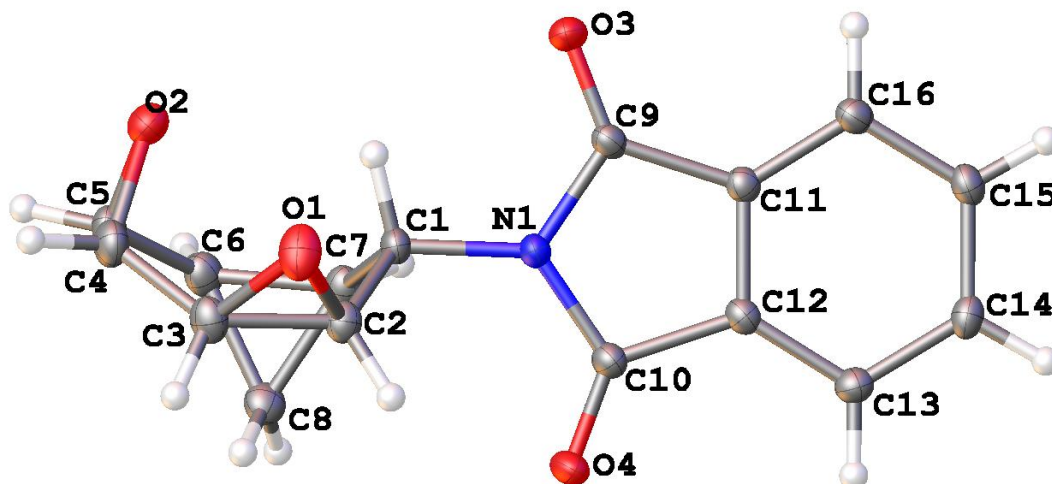


Table 1 Crystal data and structure refinement for (±)-II-40.

Identification code	don1u
Empirical formula	C ₁₆ H ₁₃ NO ₄
Formula weight	283.27
Temperature/K	99.8(3)
Crystal system	monoclinic
Space group	C2/c
a/Å	22.7463(8)
b/Å	7.8917(3)
c/Å	14.3099(6)
α/°	90.00
β/°	100.110(4)
γ/°	90.00
Volume/Å ³	2528.85(17)
Z	8
ρ _{calc} /mg/mm ³	1.488
m/mm ⁻¹	0.897
F(000)	1184.0
Crystal size/mm ³	0.1 × 0.02 × 0.02
2θ range for data collection	7.9 to 147.68°
Index ranges	-27 ≤ h ≤ 28, -8 ≤ k ≤ 9, -17 ≤ l ≤ 17
Reflections collected	8848
Independent reflections	2514[R(int) = 0.0286]
Data/restraints/parameters	2514/0/226
Goodness-of-fit on F ²	1.058

Final R indexes [$I \geq 2\sigma(I)$] $R_1 = 0.0351$, $wR_2 = 0.0875$

Final R indexes [all data] $R_1 = 0.0414$, $wR_2 = 0.0930$

Largest diff. peak/hole / $e \text{ \AA}^{-3}$ 0.20/-0.21

Table 2 Fractional Atomic Coordinates ($\times 10^4$) and Equivalent Isotropic Displacement Parameters ($\text{\AA}^2 \times 10^3$) for don1u. U_{eq} is defined as 1/3 of the trace of the orthogonalised U_{ij} tensor.

Atom	x	y	z	U(eq)
O1	3378.6 (5)	999.6 (14)	2929.5 (7)	26.8 (3)
O2	2302.9 (4)	1143.0 (13)	1413.7 (7)	24.9 (2)
O3	3575.7 (4)	5558.5 (12)	1370.7 (7)	22.0 (2)
O4	4812.1 (4)	1007.5 (12)	1252.3 (8)	24.3 (2)
N1	4071.0 (5)	3005.1 (14)	1323.7 (8)	16.8 (2)
C1	3545.8 (5)	1911.4 (16)	1307.3 (9)	16.5 (3)
C2	3654.6 (6)	651.7 (17)	2111.1 (9)	18.1 (3)
C3	3179.3 (6)	-441.5 (18)	2328.9 (10)	21.5 (3)
C4	2550.6 (6)	-432.9 (19)	1810.3 (11)	23.7 (3)
C5	2390.3 (6)	-244.4 (18)	772.6 (10)	22.2 (3)
C6	2803.5 (6)	61.4 (18)	93.3 (10)	21.0 (3)
C7	3372.3 (6)	1078.9 (17)	338.9 (9)	18.4 (3)
C8	3406.0 (6)	-798.2 (18)	185.3 (10)	21.4 (3)
C9	4029.7 (6)	4773.1 (16)	1332.2 (9)	16.3 (3)
C10	4651.7 (6)	2466.2 (16)	1276.7 (9)	17.2 (3)
C11	4638.5 (6)	5423.0 (16)	1288.9 (9)	15.5 (3)
C12	5012.5 (6)	4037.8 (16)	1269.9 (9)	16.0 (3)
C13	5614.5 (6)	4226.7 (17)	1250.0 (9)	18.2 (3)
C14	5830.9 (6)	5885.0 (17)	1238.1 (9)	18.8 (3)
C15	5452.9 (6)	7276.3 (17)	1232.9 (9)	18.8 (3)
C16	4845.6 (6)	7066.6 (17)	1264.8 (9)	18.2 (3)

Table 3 Anisotropic Displacement Parameters ($\text{\AA}^2 \times 10^3$) for don1u. The Anisotropic displacement factor exponent takes the form: $-2\pi^2[h^2a^{*2}U_{11} + \dots + 2hka \times b \times U_{12}]$

Atom	U_{11}	U_{22}	U_{33}	U_{23}	U_{13}	U_{12}
O1	28.4 (5)	34.2 (6)	19.0 (5)	-4.6 (4)	7.6 (4)	-8.8 (4)
O2	18.5 (5)	24.2 (5)	32.5 (6)	-0.5 (4)	6.1 (4)	0.3 (4)
O3	15.6 (4)	16.6 (5)	33.5 (5)	0.3 (4)	3.2 (4)	2.1 (4)

O4	22.0 (5)	13.2 (5)	39.5 (6)	0.8 (4)	10.5 (4)	1.4 (4)
N1	14.1 (5)	12.6 (5)	23.8 (5)	0.3 (4)	3.8 (4)	-1.1 (4)
C1	14.7 (5)	13.7 (6)	21.5 (6)	0.4 (5)	4.1 (5)	-2.5 (5)
C2	17.7 (6)	20.3 (6)	16.3 (6)	-0.5 (5)	2.8 (5)	-2.5 (5)
C3	24.0 (7)	21.3 (7)	19.3 (6)	3.1 (5)	3.6 (5)	-4.3 (5)
C4	20.9 (7)	22.8 (7)	28.4 (7)	2.7 (6)	7.1 (6)	-5.7 (5)
C5	17.1 (6)	19.5 (7)	29.1 (7)	0.8 (5)	1.2 (5)	-4.1 (5)
C6	20.2 (6)	20.9 (7)	20.3 (6)	0.2 (5)	-1.0 (5)	-3.0 (5)
C7	18.0 (6)	18.9 (7)	18.0 (6)	2.8 (5)	2.5 (5)	-2.3 (5)
C8	22.7 (7)	20.3 (7)	21.3 (7)	-4.2 (5)	4.1 (5)	-1.7 (5)
C9	17.1 (6)	12.9 (6)	18.0 (6)	0.6 (5)	0.9 (5)	0.1 (5)
C10	17.5 (6)	14.2 (6)	20.4 (6)	1.1 (5)	4.8 (5)	-0.2 (5)
C11	15.8 (6)	14.7 (6)	15.6 (6)	-0.5 (5)	1.6 (4)	-0.9 (5)
C12	18.1 (6)	13.6 (6)	16.3 (6)	0.5 (4)	2.9 (5)	-0.8 (5)
C13	17.1 (6)	17.7 (6)	20.3 (6)	0.0 (5)	4.3 (5)	1.6 (5)
C14	15.7 (6)	21.8 (7)	19.1 (6)	-1.2 (5)	3.5 (5)	-4.7 (5)
C15	20.1 (6)	15.5 (6)	20.6 (6)	-0.1 (5)	2.8 (5)	-4.0 (5)
C16	18.1 (6)	14.7 (6)	21.1 (6)	-0.6 (5)	1.4 (5)	0.4 (5)

Table 4 Bond Lengths for don1u.

Atom	Atom	Length/Å	Atom	Atom	Length/Å
O1	C2	1.4488 (16)	C4	C5	1.473 (2)
O1	C3	1.4494 (17)	C5	C6	1.485 (2)
O2	C4	1.4400 (18)	C6	C7	1.5109 (18)
O2	C5	1.4642 (18)	C6	C8	1.5141 (19)
O3	C9	1.2139 (16)	C7	C8	1.5015 (19)
O4	C10	1.2099 (16)	C9	C11	1.4883 (17)
N1	C1	1.4705 (15)	C10	C12	1.4882 (17)
N1	C9	1.3986 (17)	C11	C12	1.3884 (18)
N1	C10	1.4005 (16)	C11	C16	1.3825 (18)
C1	C2	1.5075 (18)	C12	C13	1.3826 (18)
C1	C7	1.5217 (18)	C13	C14	1.3994 (18)
C2	C3	1.4590 (18)	C14	C15	1.3938 (19)
C3	C4	1.4911 (19)	C15	C16	1.4001 (18)

Table 5 Bond Angles for don1u.

Atom	Atom	Atom	Angle/°	Atom	Atom	Atom	Angle/°
C2	O1	C3	60.45 (8)	C7	C6	C8	59.52 (9)
C4	O2	C5	60.95 (9)	C6	C7	C1	121.06 (11)
C9	N1	C1	122.01 (10)	C8	C7	C1	123.20 (11)
C9	N1	C10	111.63 (10)	C8	C7	C6	60.35 (9)
C10	N1	C1	126.25 (11)	C7	C8	C6	60.14 (9)
N1	C1	C2	110.54 (10)	O3	C9	N1	124.66 (12)
N1	C1	C7	110.37 (10)	O3	C9	C11	129.13 (12)
C2	C1	C7	113.06 (11)	N1	C9	C11	106.21 (11)
O1	C2	C1	117.10 (11)	O4	C10	N1	125.60 (12)
O1	C2	C3	59.80 (9)	O4	C10	C12	128.55 (12)
C3	C2	C1	121.63 (11)	N1	C10	C12	105.85 (11)
O1	C3	C2	59.75 (8)	C12	C11	C9	107.89 (11)
O1	C3	C4	117.67 (12)	C16	C11	C9	130.39 (12)
C2	C3	C4	124.95 (12)	C16	C11	C12	121.72 (12)
O2	C4	C3	118.34 (12)	C11	C12	C10	108.40 (11)
O2	C4	C5	60.34 (9)	C13	C12	C10	129.74 (12)
C5	C4	C3	123.24 (12)	C13	C12	C11	121.86 (12)
O2	C5	C4	58.71 (9)	C12	C13	C14	116.93 (12)
O2	C5	C6	117.36 (11)	C15	C14	C13	121.25 (12)
C4	C5	C6	127.08 (12)	C14	C15	C16	121.20 (12)
C5	C6	C7	123.26 (12)	C11	C16	C15	117.01 (12)
C5	C6	C8	122.50 (12)				

Table 6 Torsion Angles for don1u.

A	B	C	D	Angle/°
O1	C2	C3	C4	104.38 (16)
O1	C3	C4	O2	39.15 (18)
O1	C3	C4	C5	110.56 (15)
O2	C4	C5	C6	102.41 (15)
O2	C5	C6	C7	37.37 (19)
O2	C5	C6	C8	109.82 (15)
O3	C9	C11	C12	179.01 (13)
O3	C9	C11	C16	-1.2 (2)
O4	C10	C12	C11	178.90 (14)

O4	C10	C12	C13	-1.2(2)
N1	C1	C2	O1	102.61(12)
N1	C1	C2	C3	172.21(12)
N1	C1	C7	C6	-172.46(11)
N1	C1	C7	C8	114.77(13)
N1	C9	C11	C12	-0.79(14)
N1	C9	C11	C16	178.95(13)
N1	C10	C12	C11	-1.42(14)
N1	C10	C12	C13	178.49(13)
C1	N1	C9	O3	3.5(2)
C1	N1	C9	C11	-176.66(10)
C1	N1	C10	O4	-3.0(2)
C1	N1	C10	C12	177.28(11)
C1	C2	C3	O1	-105.09(14)
C1	C2	C3	C4	-0.7(2)
C1	C7	C8	C6	109.69(14)
C2	O1	C3	C4	-116.29(14)
C2	C1	C7	C6	63.15(16)
C2	C1	C7	C8	-9.62(17)
C2	C3	C4	O2	-31.7(2)
C2	C3	C4	C5	39.7(2)
C3	O1	C2	C1	112.57(13)
C3	C4	C5	O2	-106.26(15)
C3	C4	C5	C6	-3.9(2)
C4	O2	C5	C6	-118.69(14)
C4	C5	C6	C7	-32.6(2)
C4	C5	C6	C8	39.8(2)
C5	O2	C4	C3	114.18(14)
C5	C6	C7	C1	-2.0(2)
C5	C6	C7	C8	111.07(15)
C5	C6	C8	C7	-112.31(15)
C7	C1	C2	O1	-133.09(11)
C7	C1	C2	C3	-63.49(16)
C8	C6	C7	C1	-113.11(14)
C9	N1	C1	C2	-126.07(12)
C9	N1	C1	C7	108.11(13)
C9	N1	C10	O4	-179.38(13)
C9	N1	C10	C12	0.92(14)

C9	C11	C12	C10	1.35 (14)
C9	C11	C12	C13	-178.57 (12)
C9	C11	C16	C15	179.46 (12)
C10	N1	C1	C2	57.93 (16)
C10	N1	C1	C7	-67.89 (15)
C10	N1	C9	O3	-179.94 (12)
C10	N1	C9	C11	-0.13 (14)
C10	C12	C13	C14	179.33 (12)
C11	C12	C13	C14	-0.77 (19)
C12	C11	C16	C15	-0.82 (19)
C12	C13	C14	C15	-0.88 (19)
C13	C14	C15	C16	1.7 (2)
C14	C15	C16	C11	-0.82 (19)
C16	C11	C12	C10	-178.42 (11)
C16	C11	C12	C13	1.7 (2)

Table 7 Hydrogen Atom Coordinates ($\text{\AA}\times 10^4$) and Isotropic Displacement Parameters ($\text{\AA}^2\times 10^3$) for don1u.

Atom	x	y	z	U(eq)
H1	3216 (7)	2690 (20)	1402 (11)	16 (4)
H2	4057 (8)	250 (20)	2258 (11)	17 (4)
H3	3300 (8)	-1530 (20)	2612 (13)	28 (4)
H4	2281 (8)	-1070 (20)	2153 (12)	24 (4)
H5	1997 (7)	-740 (20)	496 (11)	17 (4)
H6	2587 (8)	210 (20)	-555 (13)	27 (4)
H7	3462 (8)	1800 (20)	-188 (12)	25 (4)
H8A	3530 (8)	-1170 (20)	-403 (13)	24 (4)
H8B	3523 (8)	-1510 (20)	747 (13)	27 (4)
H13	5869	3275	1245	22
H14	6243	6066	1233	23
H15	5610	8387	1207	23
H16	4587	8011	1270	22

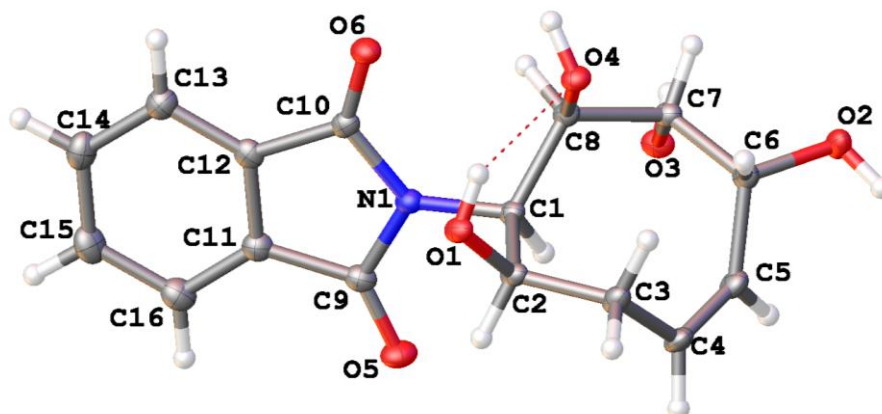


Table 1 Crystal data and structure refinement for (±)-II-42.

Identification code	don1x
Empirical formula	$C_{16.75}H_{20}NO_{6.75}$
Formula weight	343.34
Temperature/K	100.00(10)
Crystal system	triclinic
Space group	P-1
$a/\text{\AA}$	10.4024(3)
$b/\text{\AA}$	12.8740(4)
$c/\text{\AA}$	14.1877(4)
$\alpha/^\circ$	95.258(2)
$\beta/^\circ$	108.218(3)
$\gamma/^\circ$	111.130(3)
Volume/ \AA^3	1638.06(8)
Z	4
$\rho_{\text{calc}}/\text{mg/mm}^3$	1.392
m/mm^{-1}	0.108
F(000)	726.0
Crystal size/ mm^3	$0.32 \times 0.1 \times 0.03$
2θ range for data collection	5.9 to 58.14°
Index ranges	$-14 \leq h \leq 14$, $-17 \leq k \leq 16$, $-18 \leq l \leq 19$
Reflections collected	28946
Independent reflections	7852[R(int) = 0.0284]
Data/restraints/parameters	7852/0/493
Goodness-of-fit on F^2	1.135
Final R indexes [$I \geq 2\sigma(I)$]	$R_1 = 0.0434$, $wR_2 = 0.1146$

Final R indexes [all data] $R_1 = 0.0530$, $wR_2 = 0.1199$

Largest diff. peak/hole / $e \text{ \AA}^{-3}$ 0.40/-0.25

Table 2 Fractional Atomic Coordinates ($\times 10^4$) and Equivalent Isotropic Displacement Parameters ($\text{\AA}^2 \times 10^3$) for don1x. U_{eq} is defined as 1/3 of the trace of the orthogonalised U_{ij} tensor.

Atom	x	y	z	U(eq)
O1	10200.2 (12)	3048.6 (10)	4490.2 (8)	15.9 (2)
O2	6479.7 (13)	1980.6 (11)	11.1 (9)	19.8 (3)
O3	5097.0 (12)	2008.3 (10)	1509.1 (9)	17.9 (2)
O4	8973.4 (12)	3997.7 (10)	2941.1 (9)	15.8 (2)
O5	6199.3 (13)	737.1 (10)	4483.2 (10)	22.1 (3)
O6	8386.4 (12)	4610.5 (9)	4838.9 (9)	18.3 (2)
N1	7278.9 (14)	2620.4 (11)	4396 (1)	14.4 (3)
C1	7535.4 (16)	2336.4 (13)	3460.9 (11)	13.9 (3)
C2	8939.7 (17)	2088.1 (13)	3774.1 (12)	14.8 (3)
C3	9298.2 (17)	1687.7 (14)	2876.3 (12)	17.6 (3)
C4	7956.6 (18)	734.6 (14)	2073.4 (12)	18.8 (3)
C5	7012.7 (18)	913.0 (14)	1293.9 (12)	18.1 (3)
C6	7213.8 (17)	2077.1 (14)	1085.3 (12)	16.2 (3)
C7	6598.5 (16)	2720.4 (13)	1651.4 (12)	14.8 (3)
C8	7504.1 (16)	3226.5 (13)	2804.4 (11)	14.0 (3)
C9	6637.2 (17)	1744.6 (14)	4843.5 (12)	16.6 (3)
C10	7750.0 (16)	3705.0 (13)	5010.6 (12)	14.9 (3)
C11	6653.9 (17)	2322.7 (14)	5808.7 (12)	17.2 (3)
C12	7299.3 (16)	3497.3 (14)	5898.5 (12)	16.1 (3)
C13	7459.9 (17)	4271.4 (15)	6713.6 (13)	19.0 (3)
C14	6965.2 (18)	3824.3 (16)	7458.2 (13)	22.4 (4)
C15	6335.1 (18)	2647.4 (16)	7374.5 (14)	23.6 (4)
C16	6162.1 (18)	1869.5 (15)	6543.5 (13)	21.5 (3)
O1A	9078.5 (12)	6121.5 (10)	3500.6 (9)	16.2 (2)
O2A	6356.9 (13)	6635.7 (10)	-791.6 (9)	19.4 (2)
O3A	6180.1 (14)	7898.8 (10)	971.0 (9)	22.3 (3)
O4A	6212.7 (12)	5311.1 (9)	1788.4 (9)	17.5 (2)
O5A	6189.5 (12)	5645.8 (10)	3749.6 (9)	19.5 (2)
O6A	8615.9 (14)	9489.8 (10)	4034.0 (9)	23.4 (3)
N1A	7544.9 (14)	7513.5 (11)	3696.5 (10)	15.4 (3)
C1A	7828.5 (16)	7323.6 (13)	2756.7 (11)	13.7 (3)

C2A	9216.1 (16)	7051.2 (13)	3012.2 (12)	14.7 (3)
C3A	9578.8 (17)	6750.0 (14)	2089.7 (12)	17.4 (3)
C4A	9697.8 (18)	7631.5 (15)	1461.8 (13)	20.1 (3)
C5A	8573.0 (18)	7577.4 (15)	659.0 (13)	20.2 (3)
C6A	7044.0 (17)	6623.8 (14)	260.9 (12)	16.6 (3)
C7A	6072.8 (17)	6758.8 (13)	839.7 (12)	15.9 (3)
C8A	6372.4 (16)	6474.7 (13)	1894.4 (12)	14.4 (3)
C9A	6770.4 (17)	6673.1 (14)	4113.2 (12)	16.7 (3)
C10A	7972.8 (17)	8623.6 (14)	4257.4 (12)	17.6 (3)
C11A	6760.9 (17)	7298.0 (15)	5044.9 (12)	19.2 (3)
C12A	7453.7 (18)	8462.7 (15)	5121.5 (12)	19.6 (3)
C13A	7573 (2)	9265.9 (17)	5902.9 (13)	25.7 (4)
C14A	6982 (2)	8850.3 (19)	6614.2 (14)	30.6 (4)
C15A	6309 (2)	7682.2 (19)	6548.5 (14)	30.1 (4)
C16A	6176.5 (18)	6875.2 (17)	5751.7 (13)	24.4 (4)
O1S	3172.7 (14)	-285.3 (11)	1086 (1)	23.7 (3)
C1S	1898 (2)	-99.3 (17)	518.5 (15)	27.3 (4)
O2S	7838 (3)	4284 (2)	-108 (2)	29.8 (6)
C2S	9368 (5)	4666 (4)	107 (4)	48.3 (12)

Table 3 Anisotropic Displacement Parameters ($\text{\AA}^2 \times 10^3$) for don1x. The Anisotropic displacement factor exponent takes the form: $-2\pi^2[h^2a^{*2}U_{11} + \dots + 2hka \times b \times U_{12}]$

Atom	U_{11}	U_{22}	U_{33}	U_{23}	U_{13}	U_{12}
O1	14.8 (5)	12.5 (5)	13.9 (5)	0.5 (4)	-0.4 (4)	4.2 (4)
O2	25.3 (6)	21.5 (6)	12.3 (5)	2.0 (5)	2.3 (5)	13.8 (5)
O3	12.7 (5)	16.7 (6)	19.6 (6)	4.0 (5)	1.3 (4)	5.0 (4)
O4	14.0 (5)	11.6 (5)	17.5 (6)	1.5 (4)	3.3 (4)	3.3 (4)
O5	22.2 (6)	13.3 (6)	28.2 (7)	4.1 (5)	9.4 (5)	4.5 (5)
O6	19.5 (6)	13.1 (5)	17.9 (6)	2.8 (4)	4.4 (4)	4.3 (4)
N1	13.4 (6)	11.7 (6)	14.7 (6)	2.0 (5)	2.7 (5)	4.0 (5)
C1	13.8 (7)	11.3 (7)	12.9 (7)	1.2 (6)	1.5 (5)	4.6 (6)
C2	14.8 (7)	11.5 (7)	13.3 (7)	0.7 (6)	0.1 (6)	5.2 (6)
C3	18.0 (7)	18.3 (8)	15.3 (7)	0.8 (6)	1.7 (6)	10.6 (6)
C4	23.8 (8)	14.0 (8)	16.5 (8)	-0.4 (6)	3.1 (6)	9.9 (6)
C5	19.0 (7)	14.1 (8)	16.0 (8)	-1.8 (6)	2.4 (6)	5.8 (6)
C6	16.4 (7)	16.2 (8)	12.4 (7)	1.6 (6)	0.7 (6)	7.2 (6)
C7	13.0 (7)	12.9 (7)	14.4 (7)	1.8 (6)	1.1 (6)	4.6 (6)

C8	12.3 (7)	12.6 (7)	13.8 (7)	1.2 (6)	1.8 (5)	4.4 (6)
C9	12.3 (7)	16.2 (8)	19.7 (8)	5.4 (6)	4.2 (6)	5.2 (6)
C10	11.8 (7)	15.3 (7)	15.4 (7)	2.2 (6)	1.4 (6)	6.7 (6)
C11	12.8 (7)	17.9 (8)	18.8 (8)	4.0 (6)	3.9 (6)	5.9 (6)
C12	10.7 (7)	19.3 (8)	16.5 (7)	4.8 (6)	2.4 (6)	6.4 (6)
C13	14.7 (7)	20.3 (8)	19.8 (8)	2.6 (6)	4.1 (6)	7.2 (6)
C14	17.5 (8)	30.3 (10)	19.4 (8)	2.0 (7)	6.0 (6)	11.4 (7)
C15	18.2 (8)	32.3 (10)	23.4 (9)	9.2 (7)	10.8 (7)	10.5 (7)
C16	16.3 (7)	23.3 (9)	25.4 (9)	8.6 (7)	8.5 (7)	7.4 (7)
O1A	20.7 (6)	15.9 (6)	13.6 (5)	4.9 (4)	5.1 (4)	10.0 (5)
O2A	17.5 (6)	18.9 (6)	15.2 (6)	3.8 (5)	0.7 (4)	4.8 (5)
O3A	20.8 (6)	15.5 (6)	24.1 (6)	1.9 (5)	-1.6 (5)	9.6 (5)
O4A	18.9 (5)	12.6 (5)	16.1 (6)	2.3 (4)	2.6 (4)	4.6 (4)
O5A	17.4 (5)	17.4 (6)	21.3 (6)	4.5 (5)	6.1 (5)	5.6 (5)
O6A	29.1 (6)	15.2 (6)	20.7 (6)	2.4 (5)	4.2 (5)	8.3 (5)
N1A	16.1 (6)	13.5 (6)	15.1 (6)	1.8 (5)	3.2 (5)	6.9 (5)
C1A	14.5 (7)	12.6 (7)	12.7 (7)	2.3 (6)	3.1 (6)	5.8 (6)
C2A	12.9 (7)	13.3 (7)	14.9 (7)	3.2 (6)	2.3 (6)	4.6 (6)
C3A	13.9 (7)	22.4 (8)	16.3 (8)	5.1 (6)	4.3 (6)	8.8 (6)
C4A	14.4 (7)	22.3 (8)	20.6 (8)	6.8 (7)	5.7 (6)	4.5 (6)
C5A	17.3 (7)	18.9 (8)	21.1 (8)	7.4 (7)	5.8 (6)	4.4 (6)
C6A	14.8 (7)	16.6 (8)	15.0 (7)	4.7 (6)	1.1 (6)	6.3 (6)
C7A	12.5 (7)	12.8 (7)	16.9 (7)	1.3 (6)	0.1 (6)	4.3 (6)
C8A	11.7 (7)	12.8 (7)	16.5 (7)	1.9 (6)	2.9 (6)	5.0 (6)
C9A	14.2 (7)	19.9 (8)	16.6 (7)	4.9 (6)	3.5 (6)	9.5 (6)
C10A	17.4 (7)	18.4 (8)	14.9 (7)	1.5 (6)	-0.3 (6)	11.0 (6)
C11A	15.3 (7)	27.2 (9)	15.5 (7)	3.1 (7)	2.7 (6)	12.2 (7)
C12A	17.8 (7)	25.6 (9)	15.4 (7)	2.2 (6)	1.3 (6)	13.7 (7)
C13A	28.0 (9)	29.4 (10)	19.5 (8)	-0.5 (7)	2.1 (7)	18.9 (8)
C14A	30.2 (9)	48.4 (12)	16.9 (8)	-1.2 (8)	4.2 (7)	26.2 (9)
C15A	23.2 (9)	52.5 (13)	18.1 (8)	5.9 (8)	8.1 (7)	19.6 (9)
C16A	16.7 (8)	36.1 (10)	19.8 (8)	5.5 (7)	5.6 (6)	11.6 (7)
O1S	22.5 (6)	19.0 (6)	25.4 (6)	2.1 (5)	5.9 (5)	7.1 (5)
C1S	24.7 (9)	30.1 (10)	28.4 (9)	6.9 (8)	10.6 (7)	11.9 (8)
O2S	34.4 (14)	27.8 (15)	31.3 (14)	9.0 (12)	15.4 (12)	14.0 (12)
C2S	36 (2)	49 (3)	54 (3)	-5 (2)	19 (2)	13 (2)

Table 4 Bond Lengths for don1x.

Atom	Atom	Length/Å	Atom	Atom	Length/Å
O1	C2	1.4312 (18)	O2A	C6A	1.4441 (18)
O2	C6	1.4459 (18)	O3A	C7A	1.4212 (19)
O3	C7	1.4343 (18)	O4A	C8A	1.4346 (19)
O4	C8	1.4299 (18)	O5A	C9A	1.218 (2)
O5	C9	1.208 (2)	O6A	C10A	1.205 (2)
O6	C10	1.2054 (19)	N1A	C1A	1.471 (2)
N1	C1	1.472 (2)	N1A	C9A	1.398 (2)
N1	C9	1.405 (2)	N1A	C10A	1.409 (2)
N1	C10	1.402 (2)	C1A	C2A	1.549 (2)
C1	C2	1.546 (2)	C1A	C8A	1.545 (2)
C1	C8	1.544 (2)	C2A	C3A	1.526 (2)
C2	C3	1.530 (2)	C3A	C4A	1.500 (2)
C3	C4	1.505 (2)	C4A	C5A	1.328 (2)
C4	C5	1.331 (2)	C5A	C6A	1.503 (2)
C5	C6	1.507 (2)	C6A	C7A	1.531 (2)
C6	C7	1.524 (2)	C7A	C8A	1.536 (2)
C7	C8	1.545 (2)	C9A	C11A	1.488 (2)
C9	C11	1.489 (2)	C10A	C12A	1.489 (2)
C10	C12	1.490 (2)	C11A	C12A	1.386 (2)
C11	C12	1.390 (2)	C11A	C16A	1.383 (2)
C11	C16	1.385 (2)	C12A	C13A	1.387 (2)
C12	C13	1.381 (2)	C13A	C14A	1.390 (3)
C13	C14	1.396 (2)	C14A	C15A	1.391 (3)
C14	C15	1.394 (3)	C15A	C16A	1.400 (3)
C15	C16	1.395 (3)	O1S	C1S	1.436 (2)
O1A	C2A	1.4226 (19)	O2S	C2S	1.405 (5)

Table 5 Bond Angles for don1x.

Atom	Atom	Atom	Angle/°	Atom	Atom	Atom	Angle/°
C9	N1	C1	119.97 (13)	C9A	N1A	C1A	126.61 (13)
C10	N1	C1	128.20 (13)	C9A	N1A	C10A	111.62 (13)
C10	N1	C9	111.41 (13)	C10A	N1A	C1A	121.65 (13)
N1	C1	C2	107.52 (12)	N1A	C1A	C2A	108.60 (12)

N1	C1	C8	112.38 (12)	N1A	C1A	C8A	109.40 (12)
C8	C1	C2	116.86 (13)	C8A	C1A	C2A	118.68 (13)
O1	C2	C1	111.33 (12)	O1A	C2A	C1A	112.26 (12)
O1	C2	C3	110.56 (13)	O1A	C2A	C3A	106.41 (12)
C3	C2	C1	114.24 (12)	C3A	C2A	C1A	114.35 (12)
C4	C3	C2	111.62 (13)	C4A	C3A	C2A	113.05 (14)
C5	C4	C3	123.21 (15)	C5A	C4A	C3A	123.63 (15)
C4	C5	C6	123.92 (15)	C4A	C5A	C6A	124.38 (15)
O2	C6	C5	110.47 (13)	O2A	C6A	C5A	106.54 (13)
O2	C6	C7	106.54 (12)	O2A	C6A	C7A	108.91 (12)
C5	C6	C7	114.53 (13)	C5A	C6A	C7A	113.39 (13)
O3	C7	C6	110.56 (12)	O3A	C7A	C6A	109.87 (13)
O3	C7	C8	108.77 (12)	O3A	C7A	C8A	107.01 (13)
C6	C7	C8	116.17 (12)	C6A	C7A	C8A	117.71 (13)
O4	C8	C1	111.21 (12)	O4A	C8A	C1A	113.14 (12)
O4	C8	C7	108.71 (12)	O4A	C8A	C7A	108.80 (12)
C1	C8	C7	115.16 (12)	C7A	C8A	C1A	116.07 (13)
O5	C9	N1	124.10 (15)	O5A	C9A	N1A	125.75 (15)
O5	C9	C11	129.65 (15)	O5A	C9A	C11A	128.28 (15)
N1	C9	C11	106.25 (13)	N1A	C9A	C11A	105.93 (14)
O6	C10	N1	126.07 (15)	O6A	C10A	N1A	124.18 (16)
O6	C10	C12	127.99 (15)	O6A	C10A	C12A	130.08 (16)
N1	C10	C12	105.94 (13)	N1A	C10A	C12A	105.73 (14)
C12	C11	C9	107.87 (14)	C12A	C11A	C9A	108.43 (15)
C16	C11	C9	130.53 (15)	C16A	C11A	C9A	129.68 (16)
C16	C11	C12	121.59 (16)	C16A	C11A	C12A	121.89 (16)
C11	C12	C10	108.45 (14)	C11A	C12A	C10A	108.21 (14)
C13	C12	C10	129.69 (15)	C11A	C12A	C13A	121.61 (17)
C13	C12	C11	121.86 (15)	C13A	C12A	C10A	130.17 (17)
C12	C13	C14	117.06 (16)	C12A	C13A	C14A	116.98 (18)
C15	C14	C13	121.08 (16)	C13A	C14A	C15A	121.50 (17)
C14	C15	C16	121.56 (16)	C14A	C15A	C16A	121.27 (18)
C11	C16	C15	116.84 (16)	C11A	C16A	C15A	116.75 (18)

Table 6 Hydrogen Bonds for don1x.

D	H	A	d(D-H)/Å	d(H-A)/Å	d(D-A)/Å	D-H-A/°
O1	H1	O4	0.81 (2)	2.16 (2)	2.7955 (16)	135 (2)
O1	H1	O6 ¹	0.81 (2)	2.21 (2)	2.7486 (16)	124 (2)
O2	H2	O1S ²	0.85 (3)	1.90 (3)	2.7595 (18)	178 (3)
O3	H3	O2A ³	0.86 (2)	1.91 (2)	2.7636 (17)	169 (2)
O4	H4	O1A	0.85 (3)	1.88 (3)	2.7294 (17)	176 (2)
O1A	H1A	O1 ¹	0.86 (3)	1.86 (3)	2.7124 (16)	176 (2)
O2A	H2A	O4A ³	0.89 (3)	1.87 (3)	2.7537 (16)	168 (2)
O3A	H3A	O2 ³	0.90 (3)	1.86 (3)	2.7496 (17)	171 (2)
O4A	H4A	O5A	0.86 (3)	2.02 (3)	2.7854 (17)	147 (2)
O1S	H1S	O3	0.89 (3)	1.92 (3)	2.7837 (17)	163 (2)
O2S	H2S	O2	1.00 (7)	1.84 (7)	2.835 (3)	172 (6)

¹2-X,1-Y,1-Z; ²1-X,-Y,-Z; ³1-X,1-Y,-Z

Table 7 Torsion Angles for don1x.

A	B	C	D	Angle/°	A	B	C	D	Angle/°
O1	C2	C3	C4	175.73 (13)	O1A	C2A	C3A	C4A	177.58 (12)
O2	C6	C7	O3	71.96 (15)	O2A	C6A	C7A	O3A	-72.06 (15)
O2	C6	C7	C8	163.48 (12)	O2A	C6A	C7A	C8A	165.18 (13)
O3	C7	C8	O4	176.05 (12)	O3A	C7A	C8A	O4A	177.60 (11)
O3	C7	C8	C1	58.42 (16)	O3A	C7A	C8A	C1A	-53.45 (17)
O5	C9	C11	C12	178.72 (16)	O5A	C9A	C11A	C12A	174.97 (16)
O5	C9	C11	C16	-0.8 (3)	O5A	C9A	C11A	C16A	4.2 (3)
O6	C10	C12	C11	177.37 (15)	O6A	C10A	C12A	C11A	179.58 (16)
O6	C10	C12	C13	1.8 (3)	O6A	C10A	C12A	C13A	-0.2 (3)
N1	C1	C2	O1	-58.30 (16)	N1A	C1A	C2A	O1A	54.50 (16)
N1	C1	C2	C3	175.60 (12)	N1A	C1A	C2A	C3A	175.86 (12)
N1	C1	C8	O4	101.06 (14)	N1A	C1A	C8A	O4A	-94.55 (15)
N1	C1	C8	C7	134.71 (13)	N1A	C1A	C8A	C7A	138.63 (13)
N1	C9	C11	C12	-0.30 (16)	N1A	C9A	C11A	C12A	2.69 (17)
N1	C9	C11	C16	-	N1A	C9A	C11A	C16A	-

C11 C12 C13 C14	1.0 (2)	C11A C12A C13A C14A	0.7 (2)
C12 C11 C16 C15	0.5 (2)	C12A C11A C16A C15A	0.4 (2)
C12 C13 C14 C15	-0.2 (2)	C12A C13A C14A C15A	0.4 (3)
C13 C14 C15 C16	-0.5 (3)	C13A C14A C15A C16A	-1.1 (3)
C14 C15 C16 C11	0.3 (2)	C14A C15A C16A C11A	0.7 (3)
C16 C11 C12 C10	178.12 (14)	C16A C11A C12A C10A	179.06 (14)
C16 C11 C12 C13	-1.2 (2)	C16A C11A C12A C13A	-1.2 (2)

Table 8 Hydrogen Atom Coordinates ($\text{\AA} \times 10^4$) and Isotropic Displacement Parameters ($\text{\AA}^2 \times 10^3$) for don1x.

Atom	<i>x</i>	<i>y</i>	<i>z</i>	U(eq)
H1	10300 (20)	3610 (20)	4253 (17)	28 (6)
H2	6570 (30)	1450 (20)	-340 (20)	45 (7)
H3	4550 (30)	2350 (20)	1242 (18)	34 (6)
H4	9050 (30)	4670 (20)	3128 (19)	42 (7)
H1B	6685	1598	3044	17
H2B	8744	1449	4134	18
H3B	9665	2341	2570	21
H3C	10097	1420	3127	21
H4B	7775	-32	2126	23
H5	6161	268	842	22
H6	8300	2551	1284	19
H7	6571	3377	1331	18
H8	7035	3691	3054	17
H13	7888	5073	6766	23
H14	7060	4331	8031	27
H15	6016	2368	7896	28
H16	5728	1067	6484	26
H1A	9270 (30)	6350 (20)	4140 (20)	40 (7)
H2A	5600 (30)	5950 (20)	-1083 (19)	43 (7)
H3A	5300 (30)	7890 (20)	595 (19)	40 (7)
H4A	6350 (30)	5210 (20)	2400 (20)	48 (7)
H1AA	8102	8072	2551	16
H2AA	10087	7744	3492	18
H3AA	10530	6666	2327	21
H3AB	8795	6004	1655	21
H4AA	10629	8264	1649	24

H5A	8747	8182	313	24
H6A	7127	5877	295	20
H7A	5020	6245	402	19
H8A	5548	6500	2103	17
H13A	8038	10064	5950	31
H14A	7039	9376	7158	37
H15A	5931	7427	7054	36
H16A	5708	6076	5699	29
H1S	3930 (30)	400 (20)	1275 (19)	42 (7)
H1SA	2134	364	35	41
H1SB	1621	303	989	41
H1SC	1067	-838	144	41
H2S	7430 (70)	3460 (60)	-80 (50)	73 (19)
H2SA	9529	4234	-419	72
H2SB	9855	4548	775	72
H2SC	9789	5483	113	72

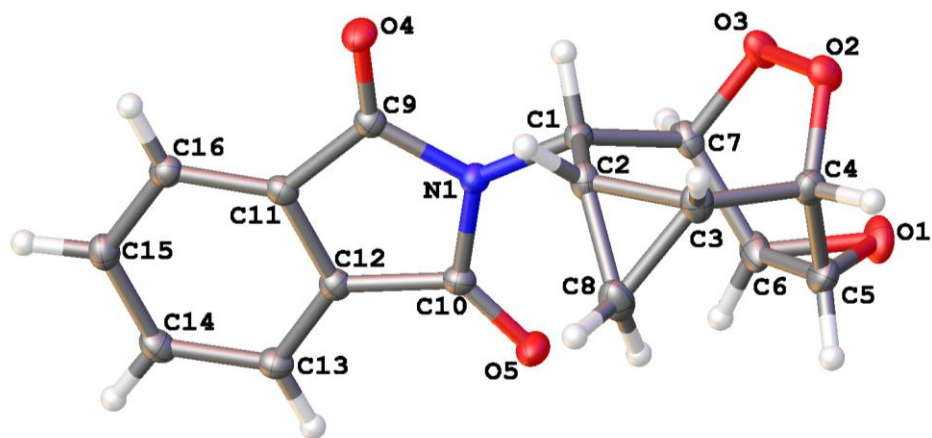


Table 1 Crystal data and structure refinement for (±)-II-54.

Identification code	don2a
Empirical formula	C ₁₆ H ₁₃ NO ₅
Formula weight	299.27
Temperature/K	100.00(10)
Crystal system	orthorhombic
Space group	Pbca
a/Å	15.3092(4)
b/Å	7.2876(2)
c/Å	23.3953(6)
α/°	90.00
β/°	90.00
γ/°	90.00
Volume/Å ³	2610.17(12)
Z	8
ρ _{calc} /mm ³	1.523
m/mm ⁻¹	0.962
F(000)	1248.0
Crystal size/mm ³	0.2135 × 0.0449 × 0.0185
2θ range for data collection	7.56 to 141.94°
Index ranges	-18 ≤ h ≤ 18, -8 ≤ k ≤ 8, -28 ≤ l ≤ 22
Reflections collected	11665
Independent reflections	2444[R(int) = 0.0364]
Data/restraints/parameters	2444/0/199
Goodness-of-fit on F ²	1.028
Final R indexes [I ≥ 2σ (I)]	R ₁ = 0.0361, wR ₂ = 0.0898
Final R indexes [all data]	R ₁ = 0.0438, wR ₂ = 0.0942

Largest diff. peak/hole / e Å⁻³ 0.23/-0.26

Table 2 Fractional Atomic Coordinates ($\times 10^4$) and Equivalent Isotropic Displacement Parameters ($\text{\AA}^2 \times 10^3$) for don2a. U_{eq} is defined as 1/3 of the trace of the orthogonalised U_{IJ} tensor.

Atom	x	y	z	U(eq)
O1	6456.8 (7)	5304.9 (17)	7284.1 (5)	26.0 (3)
O2	4759.3 (7)	4653.6 (14)	7006.5 (5)	18.3 (2)
O3	5167.6 (7)	5725.8 (14)	6528.9 (5)	19.7 (2)
O4	5034.2 (6)	2702.5 (15)	4739.9 (5)	19.8 (2)
O5	7569.8 (7)	2834.3 (16)	5779.3 (5)	23.3 (3)
N1	6181.7 (8)	3009.7 (16)	5378.5 (5)	14.4 (3)
C1	5607.2 (9)	3385.2 (19)	5870.1 (6)	14.3 (3)
C2	5281.5 (9)	1611.9 (19)	6132.7 (6)	17.0 (3)
C3	5069.2 (10)	1445 (2)	6761.4 (7)	19.8 (3)
C4	5229.6 (10)	3035 (2)	7167.1 (6)	18.5 (3)
C5	6197.4 (10)	3414 (2)	7227.6 (7)	23.0 (3)
C6	6575.9 (10)	4376 (2)	6741.1 (7)	22.3 (3)
C7	5928.4 (9)	4909.8 (19)	6278.3 (6)	17.0 (3)
C8	5817.1 (11)	362 (2)	6501.5 (7)	23.7 (3)
C9	5808.9 (9)	2628.1 (18)	4843.2 (6)	15.0 (3)
C10	7084.7 (9)	2703.7 (18)	5373.3 (6)	15.7 (3)
C11	6542.0 (9)	2139.6 (18)	4457.6 (6)	14.9 (3)
C12	7308.2 (9)	2206.5 (18)	4772.6 (6)	15.3 (3)
C13	8114.1 (9)	1867.2 (19)	4527.7 (6)	17.2 (3)
C14	8120.1 (9)	1401 (2)	3946.8 (7)	18.4 (3)

C15	7348.3 (1 0)	1310.1 (19)	3632.5 (18.1 (6) 3)
C16	6540.7 (9)	1706.5 (19)	3882.2 (16.5 (6) 3)

Table 3 Anisotropic Displacement Parameters ($\text{\AA}^2 \times 10^3$) for don2a. The Anisotropic displacement factor exponent takes the form: $-2\pi^2[h^2a^{*2}U_{11}+\dots+2hka \times b \times U_{12}]$

Atom	U_{11}	U_{22}	U_{33}	U_{23}	U_{13}	U_{12}
O1	23.4 (5)	32.7 (6)	21.9 (6)	-12.6 (5)	-0.8 (4)	-5.1 (4)
O2	18.8 (5)	18.8 (5)	17.3 (5)	1.5 (4)	5.5 (4)	0.3 (4)
O3	24.8 (5)	16.7 (5)	17.7 (5)	2.9 (4)	7.5 (4)	3.0 (4)
O4	12.6 (5)	28.4 (5)	18.4 (5)	-1.5 (4)	-1.4 (4)	0.4 (4)
O5	16.6 (5)	35.7 (6)	17.6 (6)	-4.7 (4)	-3.0 (4)	5.2 (4)
N1	12.1 (5)	18.0 (5)	13.2 (6)	-0.3 (4)	0.6 (5)	0.2 (4)
C1	13.4 (6)	16.4 (6)	13.1 (7)	-0.9 (5)	0.5 (5)	0.8 (5)
C2	20.4 (7)	15.8 (6)	14.7 (7)	-2.4 (5)	2.2 (5)	-2.5 (5)
C3	26.1 (7)	16.8 (7)	16.6 (7)	0.9 (5)	3.2 (6)	-2.3 (5)
C4	22.3 (7)	18.2 (7)	15.0 (7)	1.3 (5)	0.6 (6)	1.2 (6)
C5	24.2 (8)	26.2 (8)	18.6 (7)	-5.6 (6)	-5.8 (6)	3.9 (6)
C6	17.2 (7)	27.7 (7)	22.0 (8)	-11.7 (6)	-1.7 (6)	-1.9 (6)
C7	18.2 (7)	15.0 (6)	17.8 (7)	-2.8 (5)	5.5 (5)	-2.1 (5)
C8	33.3 (8)	16.3 (7)	21.4 (8)	0.0 (6)	3.2 (7)	3.1 (6)
C9	15.6 (6)	13.3 (6)	16.1 (7)	0.9 (5)	0.6 (5)	0.2 (5)
C10	14.0 (6)	16.0 (6)	17.1 (7)	0.2 (5)	-0.1 (6)	1.3 (5)
C11	14.1 (7)	12.7 (6)	17.9 (7)	0.3 (5)	1.0 (5)	0.5 (5)
C12	16.2 (7)	13.4 (5)	16.2 (7)	0.3 (5)	0.1 (5)	-0.2 (5)
C13	14.1 (7)	17.5 (6)	20.0 (7)	0.3 (5)	0.1 (5)	0.8 (5)
C14	16.5 (7)	17.5 (6)	21.2 (7)	0.8 (6)	4.6 (6)	1.4 (5)
C15	21.2 (7)	17.4 (6)	15.9 (7)	-0.8 (5)	1.9 (6)	0.5 (5)
C16	16.5 (7)	15.7 (6)	17.2 (7)	-0.4 (5)	-1.3 (5)	-0.2 (5)

Table 4 Bond Lengths for don2a.

Atom	Atom	Length/ \AA	Atom	Atom	Length/ \AA
O1	C5	1.440 (2)	C3	C4	1.518 (2)
O1	C6	1.4512 (18)	C3	C8	1.518 (2)
O2	O3	1.4999 (14)	C4	C5	1.514 (2)
O2	C4	1.4319 (18)	C5	C6	1.457 (2)
O3	C7	1.4331 (17)	C6	C7	1.518 (2)

O4	C9	1.2116 (18)	C9	C11	1.4833 (19)
O5	C10	1.2095 (19)	C10	C12	1.491 (2)
N1	C1	1.4736 (18)	C11	C12	1.386 (2)
N1	C9	1.4040 (18)	C11	C16	1.383 (2)
N1	C10	1.4004 (18)	C12	C13	1.383 (2)
C1	C2	1.5152 (19)	C13	C14	1.401 (2)
C1	C7	1.5454 (19)	C14	C15	1.393 (2)
C2	C3	1.511 (2)	C15	C16	1.398 (2)
C2	C8	1.499 (2)			

Table 5 Bond Angles for don2a.

Atom	Atom	Atom	Angle/°	Atom	Atom	Atom	Angle/°
C5	O1	C6	60.52 (10)	O1	C6	C7	115.00 (13)
C4	O2	O3	114.52 (10)	C5	C6	C7	114.88 (13)
C7	O3	O2	115.29 (10)	O3	C7	C1	107.01 (11)
C9	N1	C1	119.37 (11)	O3	C7	C6	110.19 (12)
C10	N1	C1	128.72 (12)	C6	C7	C1	117.65 (12)
C10	N1	C9	111.22 (12)	C2	C8	C3	60.13 (10)
N1	C1	C2	110.76 (11)	O4	C9	N1	124.53 (13)
N1	C1	C7	115.21 (11)	O4	C9	C11	129.06 (14)
C2	C1	C7	117.87 (12)	N1	C9	C11	106.41 (12)
C3	C2	C1	122.27 (12)	O5	C10	N1	125.93 (14)
C8	C2	C1	124.86 (13)	O5	C10	C12	128.20 (13)
C8	C2	C3	60.55 (10)	N1	C10	C12	105.87 (12)
C2	C3	C4	120.80 (13)	C12	C11	C9	107.96 (13)
C2	C3	C8	59.32 (10)	C16	C11	C9	130.23 (13)
C8	C3	C4	121.69 (14)	C16	C11	C12	121.80 (13)
O2	C4	C3	112.55 (12)	C11	C12	C10	108.39 (12)
O2	C4	C5	111.51 (12)	C13	C12	C10	129.70 (13)
C5	C4	C3	110.86 (13)	C13	C12	C11	121.91 (14)
O1	C5	C4	116.93 (13)	C12	C13	C14	116.82 (13)
O1	C5	C6	60.11 (10)	C15	C14	C13	121.20 (13)
C6	C5	C4	113.81 (13)	C14	C15	C16	121.31 (14)
O1	C6	C5	59.36 (10)	C11	C16	C15	116.93 (13)

Table 6 Torsion Angles for don2a.

A	B	C	D	Angle/°	A	B	C	D	Angle/°
O1	C5	C6	C7	105.48 (14)	C3	C4	C5	C6	76.44 (16)
O1	C6	C7	O3	-19.91 (17)	C4	O2	O3	C7	4.25 (16)
O1	C6	C7	C1	142.90 (13)	C4	C3	C8	C2	109.48 (16)
O2	O3	C7	C1	78.54 (14)	C4	C5	C6	O1	108.50 (14)
O2	O3	C7	C6	-50.48 (15)	C4	C5	C6	C7	3.02 (19)
O2	C4	C5	O1	17.44 (19)	C5	O1	C6	C7	105.26 (15)
O2	C4	C5	C6	-49.81 (18)	C5	C6	C7	O3	46.29 (17)
O3	O2	C4	C3	-79.05 (14)	C5	C6	C7	C1	-76.70 (17)
O3	O2	C4	C5	46.26 (16)	C6	O1	C5	C4	103.32 (15)
O4	C9	C11	C12	178.67 (14)	C7	C1	C2	C3	14.18 (19)
O4	C9	C11	C16	2.4 (2)	C7	C1	C2	C8	-60.23 (18)
O5	C10	C12	C11	177.19 (14)	C8	C2	C3	C4	110.94 (16)
O5	C10	C12	C13	-3.6 (2)	C8	C3	C4	O2	129.60 (14)
N1	C1	C2	C3	149.88 (13)	C8	C3	C4	C5	3.9 (2)
N1	C1	C2	C8	75.47 (17)	C9	N1	C1	C2	81.89 (15)
N1	C1	C7	O3	151.02 (11)	C9	N1	C1	C7	141.15 (13)
N1	C1	C7	C6	-84.39 (16)	C9	N1	C10	O5	176.30 (14)
N1	C9	C11	C12	1.25 (14)	C9	N1	C10	C12	4.01 (15)
N1	C9	C11	C16	177.63 (14)	C9	C11	C12	C10	1.15 (14)
N1	C10	C12	C11	-3.13 (14)	C9	C11	C12	C13	178.16 (12)
N1	C10	C12	C13	176.11 (14)	C9	C11	C16	C15	179.68 (13)
C1	N1	C9	O4	5.3 (2)	C10	N1	C1	C2	-87.71 (16)
C1	N1	C9	C11	174.66 (11)	C10	N1	C1	C7	49.26 (19)
C1	N1	C10	O5	-6.0 (2)	C10	N1	C9	O4	176.57 (13)
C1	N1	C10	C12	174.29 (12)	C10	N1	C9	C11	-3.35 (15)
C1	C2	C3	C4	-3.9 (2)	C10	C12	C13	C14	179.17 (13)
C1	C2	C3	C8	114.81 (16)	C11	C12	C13	C14	-1.7 (2)
C1	C2	C8	C3	110.74 (16)	C12	C11	C16	C15	0.9 (2)
C2	C1	C7	O3	-75.19 (15)	C12	C13	C14	C15	0.8 (2)

C2 C1 C7 C6	49.40 (18)	C13 C14 C15 C16	1.0 (2)
C2 C3 C4 O2	58.88 (18)	C14 C15 C16 C11	-1.8 (2)
C2 C3 C4 C5	-66.79 (18)	C16 C11 C12 C10	179.86 (12)
C3 C4 C5 O1	143.69 (13)	C16 C11 C12 C13	0.8 (2)

Table 7 Hydrogen Atom Coordinates ($\text{\AA} \times 10^4$) and Isotropic Displacement Parameters ($\text{\AA}^2 \times 10^3$) for don2a.

Atom	x	y	z	U(eq)
H1	5072	3925	5692	17
H2	4860	939	5882	20
H3	4536	704	6848	24
H4	5010	2654	7552	22
H5	6564	2465	7422	28
H6	7184	4047	6623	27
H7	6214	5872	6038	20
H8A	6420	749	6596	28
H8B	5738	-977	6453	28
H13	8639	1946	4743	21
H14	8660	1142	3764	22
H15	7371	972	3241	22
H16	6015	1680	3667	20

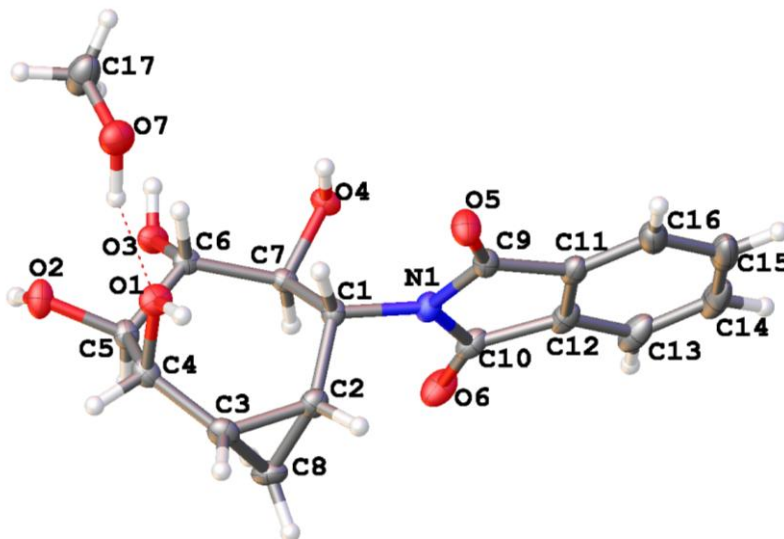


Table 1 Crystal data and structure refinement for (±)-II-56.

Identification code	don2b4
Empirical formula	C ₁₇ H ₂₁ NO ₇
Formula weight	351.35
Temperature/K	100.00(10)
Crystal system	monoclinic
Space group	P2 ₁ /c
a/Å	14.4945(17)
b/Å	10.6522(10)
c/Å	11.1524(14)
α/°	90.00
β/°	108.353(13)
γ/°	90.00
Volume/Å ³	1634.3(3)
Z	4
ρ _{calc} /mm ³	1.428
m/mm ⁻¹	0.941
F(000)	744.0
Crystal size/mm ³	0.32 × 0.06 × 0.05
2θ range for data collection	10.5 to 141.98°
Index ranges	-13 ≤ h ≤ 17, -12 ≤ k ≤ 10, -13 ≤ l ≤ 13
Reflections collected	6895
Independent reflections	3035[R(int) = 0.0290]
Data/restraints/parameters	3035/0/247
Goodness-of-fit on F ²	1.029

Final R indexes [$I \geq 2\sigma(I)$] $R_1 = 0.0377$, $wR_2 = 0.0966$

Final R indexes [all data] $R_1 = 0.0453$, $wR_2 = 0.1012$

Largest diff. peak/hole / $e \text{ \AA}^{-3}$ 0.32/-0.19

Table 2 Fractional Atomic Coordinates ($\times 10^4$) and Equivalent Isotropic Displacement Parameters ($\text{\AA}^2 \times 10^3$) for don2b4. U_{eq} is defined as 1/3 of the trace of the orthogonalised U_{ij} tensor.

Atom	x	y	z	U(eq)
O1	4424.5 (8)	711.1 (11)	5815.9 (10)	21.9 (3)
O2	5162.9 (9)	-352.6 (11)	8203.9 (11)	23.0 (3)
O3	4726.1 (8)	1564.2 (11)	9544.4 (10)	19.7 (2)
O4	3804.8 (8)	3721.3 (10)	8311.1 (10)	17.9 (2)
O5	2744.4 (9)	4729.8 (11)	4688.6 (11)	24.8 (3)
O6	1397.4 (8)	3195.9 (13)	7587.4 (11)	29.0 (3)
N1	2255.9 (9)	3707.7 (13)	6218.7 (12)	17.8 (3)
C1	2921.7 (11)	2620.9 (14)	6409.4 (14)	16.2 (3)
C2	2336.6 (11)	1506.3 (16)	5736.7 (14)	20.1 (3)
C3	2779.0 (12)	231.9 (16)	5731.1 (15)	21.6 (3)
C4	3840.6 (12)	-15.6 (15)	6383.1 (14)	19.2 (3)
C5	4227.1 (11)	238.4 (15)	7791.9 (14)	17.2 (3)
C6	4365.9 (11)	1615.7 (15)	8193.6 (13)	15.7 (3)
C7	3477.7 (11)	2495.9 (14)	7835.1 (14)	15.1 (3)
C8	2039.4 (12)	428.4 (17)	6411.5 (16)	24.9 (4)
C9	2246.5 (11)	4679.9 (15)	5372.1 (14)	18.5 (3)
C10	1572.6 (11)	3902.4 (17)	6839.7 (14)	21.1 (3)
C11	1504.2 (11)	5599.3 (16)	5491.9 (15)	21.3 (3)
C12	1109.6 (11)	5137.3 (17)	6379.8 (15)	23.1 (4)
C13	418.2 (12)	5813 (2)	6729.0 (17)	31.8 (4)
C14	136.5 (13)	6967 (2)	6142 (2)	38.6 (5)
C15	521.8 (14)	7409.5 (19)	5233 (2)	36.9 (5)
C16	1220.3 (13)	6734.3 (17)	4888.5 (18)	29.2 (4)
O7	6104.2 (9)	1784.5 (13)	5855.6 (12)	29.6 (3)
C17	6828.8 (14)	2087 (2)	6986.8 (19)	37.3 (5)

Table 3 Anisotropic Displacement Parameters ($\text{\AA}^2 \times 10^3$) for don2b4. The Anisotropic displacement factor exponent takes the form: $-2\pi^2[h^2a^{*2}U_{11}+\dots+2hka \times b \times U_{12}]$

Atom	U_{11}	U_{22}	U_{33}	U_{23}	U_{13}	U_{12}
O1	26.2 (6)	29.6 (6)	12.5 (5)	2.7 (4)	9.6 (4)	-1.1 (5)
O2	29.0 (6)	29.0 (7)	13.5 (5)	4.9 (5)	10.1 (5)	10.9 (5)
O3	24.5 (6)	22.9 (6)	10.7 (5)	1.0 (4)	4.0 (4)	-2.2 (5)
O4	25.3 (6)	16.9 (6)	13.3 (5)	-1.7 (4)	8.7 (4)	-2.6 (4)
O5	30.2 (6)	27.7 (7)	21.6 (6)	7.1 (5)	15.3 (5)	5.7 (5)
O6	23.6 (6)	48.0 (8)	19.2 (6)	5.8 (5)	12.0 (5)	2.0 (5)
N1	19.1 (6)	23.2 (7)	13.5 (6)	1.0 (5)	8.7 (5)	3.4 (5)
C1	18.4 (7)	18.5 (8)	13.4 (7)	0.5 (6)	7.4 (6)	2.8 (6)
C2	20.0 (7)	24.7 (9)	14.6 (7)	-2.1 (6)	3.9 (6)	0.5 (6)
C3	27.4 (8)	21.7 (8)	15.9 (7)	-4.9 (6)	7.0 (6)	-3.0 (7)
C4	27.2 (8)	18.7 (8)	14.3 (7)	-1.1 (6)	10.4 (6)	-0.1 (6)
C5	21.8 (7)	18.6 (8)	13.5 (7)	1.9 (6)	8.7 (6)	2.6 (6)
C6	19.1 (7)	19.7 (8)	9.2 (7)	0.8 (5)	5.6 (5)	-0.8 (6)
C7	19.1 (7)	15.4 (7)	12.2 (7)	-0.9 (5)	7.0 (6)	-1.7 (6)
C8	22.6 (8)	27.8 (9)	25.5 (8)	-5.1 (7)	9.4 (7)	-8.3 (7)
C9	20.2 (7)	20.3 (8)	14.9 (7)	-1.4 (6)	5.1 (6)	1.8 (6)
C10	17.0 (7)	33.7 (10)	13.7 (7)	-3.6 (6)	6.5 (6)	0.6 (7)
C11	18.6 (7)	22.8 (8)	20.6 (8)	-6.0 (6)	3.3 (6)	2.0 (6)
C12	17.6 (7)	31.3 (9)	19.1 (7)	-8.8 (7)	3.9 (6)	2.7 (7)
C13	20.2 (8)	47.9 (12)	26.7 (9)	-14.5 (8)	6.7 (7)	5.1 (8)
C14	23.0 (9)	42.4 (12)	44.1 (12)	-22.4 (9)	1.3 (8)	10.5 (8)
C15	29.8 (10)	27.3 (10)	44.8 (12)	-10.4 (8)	-1.0 (8)	8.5 (8)
C16	26.7 (8)	24.2 (9)	32.0 (9)	-2.0 (7)	2.6 (7)	3.2 (7)
O7	30.5 (6)	34.9 (7)	21.4 (6)	2.6 (5)	5.4 (5)	-0.5 (5)
C17	30.9 (9)	43.5 (12)	31.6 (10)	-11.0 (9)	1.4 (8)	7.7 (8)

Table 4 Bond Lengths for don2b4.

Atom	Atom	Length/ \AA	Atom	Atom	Length/ \AA
O1	C4	1.4328 (19)	C3	C8	1.510 (2)
O2	C5	1.4334 (19)	C4	C5	1.517 (2)
O3	C6	1.4317 (17)	C5	C6	1.529 (2)
O4	C7	1.4324 (18)	C6	C7	1.540 (2)
O5	C9	1.205 (2)	C9	C11	1.492 (2)
O6	C10	1.208 (2)	C10	C12	1.492 (2)

N1	C1	1.4791 (19)	C11	C12	1.381 (2)
N1	C9	1.399 (2)	C11	C16	1.382 (2)
N1	C10	1.3912 (19)	C12	C13	1.386 (2)
C1	C2	1.514 (2)	C13	C14	1.393 (3)
C1	C7	1.545 (2)	C14	C15	1.385 (3)
C2	C3	1.502 (2)	C15	C16	1.391 (3)
C2	C8	1.508 (2)	O7	C17	1.401 (2)
C3	C4	1.504 (2)			

Table 5 Bond Angles for don2b4.

Atom	Atom	Atom	Angle/°	Atom	Atom	Atom	Angle/°
C9	N1	C1	122.95 (12)	O4	C7	C1	107.90 (12)
C10	N1	C1	125.43 (13)	O4	C7	C6	107.85 (12)
C10	N1	C9	111.63 (13)	C6	C7	C1	116.23 (12)
N1	C1	C2	107.72 (12)	C2	C8	C3	59.69 (11)
N1	C1	C7	108.70 (12)	O5	C9	N1	125.41 (14)
C2	C1	C7	118.14 (13)	O5	C9	C11	128.35 (15)
C3	C2	C1	122.52 (13)	N1	C9	C11	106.24 (13)
C3	C2	C8	60.23 (11)	O6	C10	N1	126.02 (16)
C8	C2	C1	123.60 (14)	O6	C10	C12	128.09 (15)
C2	C3	C4	121.97 (14)	N1	C10	C12	105.89 (14)
C2	C3	C8	60.08 (11)	C12	C11	C9	107.67 (15)
C4	C3	C8	124.15 (14)	C12	C11	C16	122.27 (16)
O1	C4	C3	110.40 (13)	C16	C11	C9	130.05 (16)
O1	C4	C5	106.50 (12)	C11	C12	C10	108.52 (14)
C3	C4	C5	117.23 (13)	C11	C12	C13	121.08 (18)
O2	C5	C4	104.91 (12)	C13	C12	C10	130.38 (17)
O2	C5	C6	107.67 (12)	C12	C13	C14	117.21 (19)
C4	C5	C6	116.50 (13)	C15	C14	C13	121.24 (17)
O3	C6	C5	104.03 (12)	C14	C15	C16	121.51 (19)
O3	C6	C7	107.13 (11)	C11	C16	C15	116.67 (19)
C5	C6	C7	119.08 (13)				

Table 6 Torsion Angles for don2b4.

A	B	C	D	Angle/°	A	B	C	D	Angle/°
O1	C4	C5	O2	-69.45 (15)	C3	C4	C5	C6	-74.66 (18)
O1	C4	C5	C6	49.49 (17)	C4	C3	C8	C2	110.36 (17)
O2	C5	C6	O3	-62.81 (14)	C4	C5	C6	O3	179.76 (12)
O2	C5	C6	C7	178.09 (11)	C4	C5	C6	C7	60.66 (17)
O3	C6	C7	O4	62.94 (14)	C5	C6	C7	O4	-
O3	C6	C7	C1	175.82 (12)	C5	C6	C7	C1	-58.33 (18)
O5	C9	C11	C12	179.10 (16)	C7	C1	C2	C3	-56.3 (2)
O5	C9	C11	C16	-1.9 (3)	C7	C1	C2	C8	17.2 (2)
O6	C10	C12	C11	177.52 (17)	C8	C2	C3	C4	-
O6	C10	C12	C13	4.0 (3)	C8	C3	C4	O1	136.50 (16)
N1	C1	C2	C3	179.88 (13)	C8	C3	C4	C5	-14.4 (2)
N1	C1	C2	C8	106.35 (16)	C9	N1	C1	C2	104.18 (16)
N1	C1	C7	O4	-45.32 (15)	C9	N1	C1	C7	126.71 (14)
N1	C1	C7	C6	166.54 (12)	C9	N1	C10	O6	177.23 (16)
N1	C9	C11	C12	-0.39 (17)	C9	N1	C10	C12	-2.21 (17)
N1	C9	C11	C16	178.66 (16)	C9	C11	C12	C10	-0.92 (18)
N1	C10	C12	C11	1.91 (17)	C9	C11	C12	C13	177.71 (15)
N1	C10	C12	C13	176.55 (17)	C9	C11	C16	C15	177.93 (17)
C1	N1	C9	O5	2.3 (2)	C10	N1	C1	C2	75.95 (17)
C1	N1	C9	C11	178.21 (13)	C10	N1	C1	C7	-53.16 (19)
C1	N1	C10	O6	-2.9 (3)	C10	N1	C9	O5	177.84 (15)
C1	N1	C10	C12	177.67 (13)	C10	N1	C9	C11	1.67 (17)
C1	C2	C3	C4	-0.8 (2)	C10	C12	C13	C14	178.70 (17)
C1	C2	C3	C8	113.04 (17)	C11	C12	C13	C14	0.4 (2)
C1	C2	C8	C3	111.32 (16)	C12	C11	C16	C15	1.0 (3)
C2	C1	C7	O4	168.38 (12)	C12	C13	C14	C15	1.0 (3)

C2 C1 C7 C6	70.41 (17)	C13 C14 C15 C16	-1.4 (3)
C2 C3 C4 O1	-63.19 (18)	C14 C15 C16 C11	0.4 (3)
C2 C3 C4 C5	59.0 (2)	C16 C11 C12 C10	179.94 (15)
C3 C4 C5 O2	166.41 (13)	C16 C11 C12 C13	-1.4 (3)

Table 7 Hydrogen Atom Coordinates ($\text{\AA} \times 10^4$) and Isotropic Displacement Parameters ($\text{\AA}^2 \times 10^3$) for don2b4.

Atom	<i>x</i>	<i>y</i>	<i>z</i>	U(eq)
H1	4141 (17)	790 (20)	4980 (30)	48 (7)
H2	5316 (19)	-540 (20)	8960 (30)	53 (8)
H3	5159 (16)	2060 (20)	9800 (20)	28 (6)
H4	4132 (17)	3990 (20)	7920 (20)	39 (7)
H1A	3412	2818	5975	19
H2A	1837	1729	4917	24
H3A	2513	-221	4909	26
H4A	3963	-921	6251	23
H5	3793	-175	8215	21
H6	4879	1988	7877	19
H7	3012	2190	8268	18
H8A	1383	67	6028	30
H8B	2274	430	7347	30
H13	148	5501	7343	38
H14	-329	7460	6369	46
H15	304	8192	4836	44
H16	1489	7038	4269	35
H7A	5580 (20)	1240 (30)	6050 (30)	74 (9)
H17A	6540	2154	7669	56
H17B	7127	2890	6890	56
H17C	7326	1428	7192	56

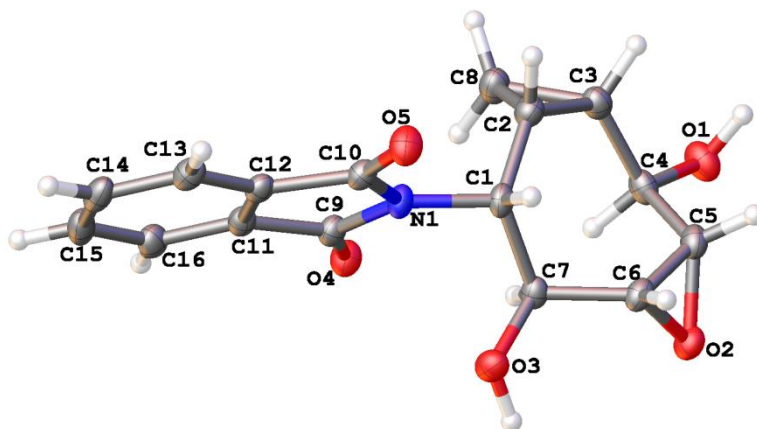


Table 1 Crystal data and structure refinement for (±)-II-57.

Identification code	don1y5
Empirical formula	C ₁₆ H ₁₅ NO ₅
Formula weight	301.29
Temperature/K	100.00(10)
Crystal system	triclinic
Space group	P-1
a/Å	7.40297(16)
b/Å	10.1453(2)
c/Å	18.2027(3)
α/°	82.2109(16)
β/°	85.4289(16)
γ/°	84.8574(17)
Volume/Å ³	1345.90(5)
Z	4
ρ _{calc} /mg/mm ³	1.487
m/mm ⁻¹	0.934
F(000)	632.0
Crystal size/mm ³	0.32 × 0.15 × 0.03
2θ range for data collection	8.82 to 141.9°
Index ranges	-9 ≤ h ≤ 9, -12 ≤ k ≤ 12, -22 ≤ l ≤ 22
Reflections collected	9087
Independent reflections	9087[R(int) = 0.0000]
Data/restraints/parameters	9087/0/414
Goodness-of-fit on F ²	1.067
Final R indexes [I ≥ 2σ(I)]	R ₁ = 0.0507, wR ₂ = 0.1441
Final R indexes [all data]	R ₁ = 0.0516, wR ₂ = 0.1452

Largest diff. peak/hole / e Å⁻³ 0.34/-0.29

Table 2 Fractional Atomic Coordinates ($\times 10^4$) and Equivalent Isotropic Displacement Parameters ($\text{\AA}^2 \times 10^3$) for don1y5. U_{eq} is defined as 1/3 of the trace of the orthogonalised U_{IJ} tensor.

Atom	x	y	z	U(eq)
O1	535.8 (16)	1754.9 (11)	-2247.3 (6)	29.5 (3)
O2	4886.3 (14)	1517.9 (11)	-1877.0 (6)	24.3 (2)
O3	5698.3 (14)	1575.8 (11)	-122.0 (6)	25.1 (2)
O4	2030.7 (14)	512.8 (10)	751.5 (6)	23.7 (2)
O5	3459.2 (15)	4778.7 (10)	881.5 (6)	27.5 (2)
N1	2778.9 (17)	2713.6 (12)	617.0 (7)	20.4 (3)
C1	2985.1 (19)	3027.4 (14)	-195.5 (7)	19.8 (3)
C2	1133.3 (19)	3443.3 (15)	-504.3 (8)	22.7 (3)
C3	415 (2)	3002.8 (15)	-1188.9 (8)	23.3 (3)
C4	1493 (2)	2011.7 (15)	-1643.0 (8)	22.9 (3)
C5	3335 (2)	2506.1 (15)	-1893.9 (8)	23.4 (3)
C6	4674 (2)	2462.2 (14)	-1342.2 (8)	21.4 (3)
C7	4156.8 (19)	1917.5 (14)	-545.5 (8)	19.7 (3)
C8	-395 (2)	2539.0 (17)	-423.6 (9)	27.5 (3)
C9	2345.1 (19)	1497.3 (14)	1017.2 (8)	20.1 (3)
C10	3081.0 (19)	3644.8 (14)	1087.5 (8)	20.1 (3)
C11	2355.0 (18)	1667.6 (14)	1815.4 (8)	19.8 (3)
C12	2814.3 (19)	2955.1 (15)	1859.2 (8)	19.8 (3)
C13	2965.5 (19)	3402.6 (16)	2533.4 (8)	23.9 (3)
C14	2647 (2)	2501.7 (17)	3172.1 (8)	27.0 (3)
C15	2180 (2)	1216.7 (17)	3125.2 (8)	27.6 (3)
C16	2021 (2)	769.6 (15)	2442.9 (8)	24.4 (3)
O1A	9365.3 (16)	3924.7 (11)	6819.5 (6)	25.8 (2)
O2A	5165.6 (14)	4214.3 (11)	6336.3 (6)	25.9 (2)
O3A	4439.5 (15)	3475.8 (12)	4691.4 (7)	27.8 (2)
O4A	6342.8 (16)	28.7 (11)	4020.7 (6)	28.7 (2)
O5A	8522.3 (14)	4147.8 (10)	3838.9 (6)	23.2 (2)
N1A	7456.3 (17)	2053.7 (12)	4124.1 (7)	19.9 (3)
C1A	7148 (2)	1992.4 (15)	4936.8 (8)	20.6 (3)
C2A	8912 (2)	1632.0 (15)	5318.4 (8)	22.4 (3)
C3A	9561 (2)	2283.9 (15)	5945.2 (8)	22.5 (3)
C4A	8518 (2)	3501.0 (14)	6222.1 (8)	21.4 (3)
C5A	6624 (2)	3169.9 (14)	6492.1 (8)	22.6 (3)

C6A	5344 (2)	3045.1 (15)	5937.1 (8)	22.9 (3)
C7A	5978.2 (19)	3264.1 (15)	5125.0 (8)	20.6 (3)
C8A	10565 (2)	2429.6 (17)	5188.5 (8)	27.3 (3)
C9A	6912.9 (19)	1068.0 (14)	3731.7 (8)	20.4 (3)
C10A	8017.8 (18)	3146.6 (14)	3644.6 (8)	18.6 (3)
C11A	7195.8 (18)	1584.8 (14)	2930.5 (8)	19.5 (3)
C12A	7844.6 (18)	2840.5 (14)	2877.2 (8)	18.9 (3)
C13A	8172 (2)	3604.7 (15)	2197.3 (8)	23.8 (3)
C14A	7828 (2)	3058.2 (17)	1563.6 (9)	27.7 (3)
C15A	7191 (2)	1793.5 (17)	1616.3 (8)	26.9 (3)
C16A	6861 (2)	1034.2 (15)	2306.9 (8)	23.7 (3)

Table 3 Anisotropic Displacement Parameters ($\text{\AA}^2 \times 10^3$) for don1y5. The Anisotropic displacement factor exponent takes the form: $-2\pi^2[h^2a^{*2}U_{11}+\dots+2hka \times b \times U_{12}]$

Atom	U_{11}	U_{22}	U_{33}	U_{23}	U_{13}	U_{12}
O1	37.1 (6)	28.3 (6)	25.3 (5)	-3.7 (5)	-12.9 (5)	-4.4 (5)
O2	26.7 (5)	27.8 (5)	19.3 (5)	-8.0 (4)	-0.2 (4)	-1.6 (4)
O3	21.4 (5)	31.9 (6)	23.2 (5)	-7.2 (4)	-4.5 (4)	-0.4 (4)
O4	28.0 (5)	22.1 (5)	22.2 (5)	-5.0 (4)	0.2 (4)	-7.6 (4)
O5	36.4 (6)	22.6 (5)	24.9 (5)	-5.3 (4)	0.2 (5)	-8.6 (4)
N1	24.7 (6)	22.0 (6)	15.2 (6)	-3.8 (5)	0.9 (5)	-5.5 (5)
C1	24.1 (7)	20.9 (6)	14.9 (6)	-1.8 (5)	1.0 (5)	-7.0 (5)
C2	22.7 (7)	24.9 (7)	20.4 (7)	-4.3 (6)	0.3 (6)	-1.0 (6)
C3	21.4 (7)	27.0 (7)	21.2 (7)	-0.5 (6)	-3.7 (6)	-3.3 (6)
C4	27.0 (7)	24.2 (7)	18.6 (7)	-1.2 (5)	-7.3 (6)	-4.7 (6)
C5	31.1 (8)	22.2 (7)	16.8 (6)	-2.9 (5)	0.0 (6)	-2.6 (6)
C6	23.7 (7)	21.8 (7)	19.5 (7)	-5.4 (6)	3.0 (5)	-5.1 (5)
C7	19.1 (6)	24.4 (7)	16.7 (6)	-3.1 (5)	-1.9 (5)	-5.7 (5)
C8	23.1 (7)	36.1 (8)	22.7 (7)	-0.5 (6)	-1.1 (6)	-4.9 (6)
C9	18.6 (7)	23.7 (7)	18.3 (7)	-3.4 (5)	1.1 (5)	-4.2 (5)
C10	18.3 (6)	23.0 (7)	19.9 (7)	-6.1 (5)	0.7 (5)	-3.6 (5)
C11	16.1 (6)	25.6 (7)	18.1 (7)	-2.8 (5)	-0.8 (5)	-3.2 (5)
C12	15.1 (6)	25.2 (7)	19.5 (7)	-5.0 (6)	0.1 (5)	-2.2 (5)
C13	19.5 (7)	31.1 (8)	22.9 (7)	-9.1 (6)	-0.6 (5)	-4.1 (6)
C14	19.7 (7)	43.7 (9)	18.5 (7)	-8.0 (6)	0.4 (5)	-3.7 (6)
C15	22.0 (7)	40.0 (9)	19.2 (7)	2.3 (6)	0.9 (6)	-5.3 (6)
C16	21.6 (7)	27.7 (8)	23.0 (7)	0.5 (6)	1.3 (6)	-4.5 (6)

O1A	31.9 (6)	27.5 (5)	19.4 (5)	-1.3 (4)	-5.4 (4)	-9.2 (4)
O2A	26.2 (5)	29.2 (6)	22.8 (5)	-8.1 (4)	-0.2 (4)	1.3 (4)
O3A	23.2 (5)	34.6 (6)	26.0 (5)	-3.7 (5)	-5.2 (4)	-2.9 (4)
O4A	40.9 (6)	21.2 (5)	25.7 (5)	-3.2 (4)	-0.5 (5)	-12.0 (5)
O5A	26.4 (5)	21.9 (5)	22.8 (5)	-4.8 (4)	0.6 (4)	-8.4 (4)
N1A	25.4 (6)	19.4 (6)	15.6 (6)	-2.3 (5)	0.3 (5)	-7.1 (5)
C1A	25.6 (7)	22.0 (7)	14.6 (6)	-2.0 (5)	0.8 (5)	-6.8 (6)
C2A	25.5 (7)	23.0 (7)	17.9 (7)	-2.4 (5)	0.5 (6)	0.4 (6)
C3A	22.2 (7)	27.4 (7)	17.7 (7)	-2.2 (5)	-1.3 (5)	-2.1 (5)
C4A	24.8 (7)	23.2 (7)	16.8 (6)	-0.9 (5)	-3.6 (5)	-5.4 (6)
C5A	29.1 (8)	21.3 (7)	17.7 (6)	-3.1 (5)	0.2 (6)	-4.0 (6)
C6A	21.5 (7)	24.2 (7)	24.0 (7)	-6.5 (6)	1.8 (6)	-4.9 (5)
C7A	19.1 (7)	24.9 (7)	18.5 (7)	-4.4 (5)	-2.0 (5)	-3.1 (5)
C8A	20.8 (7)	39.9 (9)	19.8 (7)	-0.8 (6)	-0.9 (6)	-0.4 (6)
C9A	22.5 (7)	20.1 (7)	19.6 (7)	-5.3 (5)	-2.7 (5)	-2.7 (5)
C10A	17.6 (6)	20.2 (7)	18.2 (6)	-2.2 (5)	-0.7 (5)	-3.5 (5)
C11A	16.8 (6)	22.2 (7)	20.0 (7)	-4.7 (5)	-1.2 (5)	-1.5 (5)
C12A	16.6 (6)	22.3 (7)	18.0 (7)	-3.4 (5)	-0.7 (5)	-2.1 (5)
C13A	21.9 (7)	27.3 (8)	21.6 (7)	-0.5 (6)	1.0 (6)	-4.7 (6)
C14A	24.9 (7)	37.6 (9)	19.2 (7)	-0.3 (6)	0.1 (6)	-1.2 (6)
C15A	22.6 (7)	40.4 (9)	19.1 (7)	-9.7 (6)	-3.9 (6)	0.3 (6)
C16A	21.9 (7)	27.2 (7)	23.9 (7)	-9.2 (6)	-2.4 (6)	-2.8 (6)

Table 4 Bond Lengths for don1y5.

Atom	Atom	Length/Å	Atom	Atom	Length/Å
O1	C4	1.4197 (17)	O1A	C4A	1.4298 (17)
O2	C5	1.4543 (18)	O2A	C5A	1.4598 (18)
O2	C6	1.4461 (17)	O2A	C6A	1.4637 (17)
O3	C7	1.4191 (17)	O3A	C7A	1.4213 (17)
O4	C9	1.2149 (18)	O4A	C9A	1.2086 (18)
O5	C10	1.2110 (18)	O5A	C10A	1.2177 (17)
N1	C1	1.4688 (17)	N1A	C1A	1.4724 (17)
N1	C9	1.3952 (18)	N1A	C9A	1.4084 (18)
N1	C10	1.4014 (18)	N1A	C10A	1.3880 (18)
C1	C2	1.526 (2)	C1A	C2A	1.520 (2)
C1	C7	1.5354 (19)	C1A	C7A	1.5506 (19)

C2	C3	1.528 (2)	C2A	C3A	1.523 (2)
C2	C8	1.505 (2)	C2A	C8A	1.513 (2)
C3	C4	1.519 (2)	C3A	C4A	1.520 (2)
C3	C8	1.504 (2)	C3A	C8A	1.508 (2)
C4	C5	1.511 (2)	C4A	C5A	1.500 (2)
C5	C6	1.460 (2)	C5A	C6A	1.464 (2)
C6	C7	1.5124 (19)	C6A	C7A	1.508 (2)
C9	C11	1.4869 (19)	C9A	C11A	1.4865 (19)
C10	C12	1.489 (2)	C10A	C12A	1.4890 (18)
C11	C12	1.393 (2)	C11A	C12A	1.3899 (19)
C11	C16	1.382 (2)	C11A	C16A	1.380 (2)
C12	C13	1.381 (2)	C12A	C13A	1.385 (2)
C13	C14	1.396 (2)	C13A	C14A	1.396 (2)
C14	C15	1.394 (2)	C14A	C15A	1.395 (2)
C15	C16	1.396 (2)	C15A	C16A	1.398 (2)

Table 5 Bond Angles for don1y5.

Atom	Atom	Atom	Angle/°	Atom	Atom	Atom	Angle/°
C6	O2	C5	60.43 (9)	C5A	O2A	C6A	60.09 (9)
C9	N1	C1	126.54 (12)	C9A	N1A	C1A	122.32 (12)
C9	N1	C10	111.75 (12)	C10A	N1A	C1A	125.45 (12)
C10	N1	C1	121.68 (12)	C10A	N1A	C9A	111.44 (12)
N1	C1	C2	110.07 (11)	N1A	C1A	C2A	111.34 (12)
N1	C1	C7	111.15 (12)	N1A	C1A	C7A	109.18 (11)
C2	C1	C7	116.76 (11)	C2A	C1A	C7A	117.62 (12)
C1	C2	C3	126.85 (12)	C1A	C2A	C3A	126.93 (13)
C8	C2	C1	123.39 (13)	C8A	C2A	C1A	125.13 (13)
C8	C2	C3	59.44 (9)	C8A	C2A	C3A	59.56 (10)
C4	C3	C2	122.50 (12)	C4A	C3A	C2A	121.61 (12)
C8	C3	C2	59.53 (10)	C8A	C3A	C2A	59.89 (10)
C8	C3	C4	120.10 (13)	C8A	C3A	C4A	119.24 (13)
O1	C4	C3	111.98 (12)	O1A	C4A	C3A	111.72 (12)
O1	C4	C5	112.22 (12)	O1A	C4A	C5A	108.49 (12)
C5	C4	C3	109.38 (12)	C5A	C4A	C3A	109.37 (12)
O2	C5	C4	117.18 (12)	O2A	C5A	C4A	116.90 (12)
O2	C5	C6	59.51 (9)	O2A	C5A	C6A	60.09 (9)

C6	C5	C4	118.55 (12)	C6A	C5A	C4A	118.03 (12)
O2	C6	C5	60.06 (9)	O2A	C6A	C7A	116.89 (12)
O2	C6	C7	116.76 (12)	C5A	C6A	O2A	59.82 (9)
C5	C6	C7	118.52 (12)	C5A	C6A	C7A	118.87 (13)
O3	C7	C1	107.48 (11)	O3A	C7A	C1A	109.62 (12)
O3	C7	C6	112.19 (11)	O3A	C7A	C6A	109.18 (12)
C6	C7	C1	107.34 (11)	C6A	C7A	C1A	108.00 (12)
C3	C8	C2	61.03 (10)	C3A	C8A	C2A	60.56 (10)
O4	C9	N1	125.76 (13)	O4A	C9A	N1A	124.42 (13)
O4	C9	C11	128.17 (13)	O4A	C9A	C11A	129.57 (13)
N1	C9	C11	106.07 (12)	N1A	C9A	C11A	106.01 (12)
O5	C10	N1	124.98 (13)	O5A	C10A	N1A	124.87 (13)
O5	C10	C12	128.95 (13)	O5A	C10A	C12A	128.63 (13)
N1	C10	C12	106.07 (12)	N1A	C10A	C12A	106.49 (11)
C12	C11	C9	108.26 (12)	C12A	C11A	C9A	108.05 (12)
C16	C11	C9	129.81 (13)	C16A	C11A	C9A	130.37 (13)
C16	C11	C12	121.93 (14)	C16A	C11A	C12A	121.54 (14)
C11	C12	C10	107.85 (13)	C11A	C12A	C10A	108.00 (12)
C13	C12	C10	130.40 (14)	C13A	C12A	C10A	130.25 (13)
C13	C12	C11	121.75 (14)	C13A	C12A	C11A	121.72 (13)
C12	C13	C14	116.94 (14)	C12A	C13A	C14A	117.12 (14)
C15	C14	C13	121.08 (14)	C15A	C14A	C13A	121.19 (14)
C14	C15	C16	121.82 (14)	C14A	C15A	C16A	121.08 (14)
C11	C16	C15	116.48 (14)	C11A	C16A	C15A	117.35 (14)

Table 6 Hydrogen Bonds for don1y5.

D	H	A	d(D-H)/Å	d(H-A)/Å	d(D-A)/Å	D-H-A/°
O1	H1	O1A ¹	0.96 (2)	1.79 (2)	2.7132 (16)	161 (2)
O3	H3	O4 ²	0.91 (3)	1.98 (3)	2.8883 (15)	179 (2)
O1A	H1AA	O5A ³	0.96 (3)	1.76 (3)	2.7056 (15)	171 (3)
O3A	H3AA	O2A ⁴	0.88 (3)	1.94 (3)	2.8150 (16)	176 (2)

¹-1+X,+Y,-1+Z; ²1-X,-Y,-Z; ³2-X,1-Y,1-Z; ⁴1-X,1-Y,1-Z

Table 7 Torsion Angles for don1y5.

A	B	C	D	Angle/°	A	B	C	D	Angle/°
---	---	---	---	---------	---	---	---	---	---------

O1	C4	C5	O2	-94.95	(15)	O1A	C4A	C5A	O2A	95.88	(14)
O1	C4	C5	C6	163.23	(12)	O1A	C4A	C5A	C6A	164.57	(12)
O2	C5	C6	C7	106.17	(14)	O2A	C5A	C6A	C7A	106.08	(14)
O2	C6	C7	O3	94.26	(14)	O2A	C6A	C7A	O3A	-94.77	(15)
O2	C6	C7	C1	147.89	(12)	O2A	C6A	C7A	C1A	146.09	(12)
O4	C9	C11	C12	179.08	(14)	O4A	C9A	C11A	C12A	178.84	(15)
O4	C9	C11	C16	0.2	(3)	O4A	C9A	C11A	C16A	1.1	(3)
O5	C10	C12	C11	178.61	(14)	O5A	C10A	C12A	C11A	179.30	(14)
O5	C10	C12	C13	-1.7	(3)	O5A	C10A	C12A	C13A	-1.3	(3)
N1	C1	C2	C3	136.32	(14)	N1A	C1A	C2A	C3A	135.43	(14)
N1	C1	C2	C8	-61.81	(18)	N1A	C1A	C2A	C8A	59.68	(19)
N1	C1	C7	O3	-45.62	(15)	N1A	C1A	C7A	O3A	49.05	(15)
N1	C1	C7	C6	166.49	(11)	N1A	C1A	C7A	C6A	167.91	(11)
N1	C9	C11	C12	-0.85	(15)	N1A	C9A	C11A	C12A	-1.22	(15)
N1	C9	C11	C16	179.78	(14)	N1A	C9A	C11A	C16A	178.92	(14)
N1	C10	C12	C11	-0.55	(15)	N1A	C10A	C12A	C11A	-0.15	(15)
N1	C10	C12	C13	179.12	(14)	N1A	C10A	C12A	C13A	177.84	(14)
C1	N1	C9	O4	-1.7	(2)	C1A	N1A	C9A	O4A	-8.5	(2)
C1	N1	C9	C11	178.23	(13)	C1A	N1A	C9A	C11A	171.53	(12)
C1	N1	C10	O5	2.9	(2)	C1A	N1A	C10A	O5A	8.5	(2)
C1	N1	C10	C12	177.84	(12)	C1A	N1A	C10A	C12A	170.66	(12)
C1	C2	C3	C4	2.5	(2)	C1A	C2A	C3A	C4A	-5.3	(2)
C1	C2	C3	C8	110.86	(16)	C1A	C2A	C3A	C8A	113.16	(17)
C1	C2	C8	C3	116.42	(15)	C1A	C2A	C8A	C3A	116.02	(16)
C2	C1	C7	O3	173.00	(11)	C2A	C1A	C7A	O3A	177.15	(12)
C2	C1	C7	C6	66.13	(15)	C2A	C1A	C7A	C6A	-63.99	(16)
C2	C3	C4	O1	179.57	(13)	C2A	C3A	C4A	O1A	179.07	(12)
C2	C3	C4	C5	-55.38	(17)	C2A	C3A	C4A	C5A	58.94	(17)
C3	C4	C5	O2	140.15	(12)	C3A	C4A	C5A	O2A	142.04	(12)
C3	C4	C5	C6	71.86	(16)	C3A	C4A	C5A	C6A	-73.35	(16)

C4 C3 C8 C2	112.31 (15)	C4A C3A C8A C2A	111.70 (15)
C4 C5 C6 O2	106.45 (14)	C4A C5A C6A O2A	106.56 (14)
C4 C5 C6 C7	0.3 (2)	C4A C5A C6A C7A	-0.5 (2)
C5 O2 C6 C7	109.06 (14)	C5A O2A C6A C7A	109.34 (14)
C5 C6 C7 O3	163.03 (12)	C5A C6A C7A O3A	163.42 (13)
C5 C6 C7 C1	-79.11 (15)	C5A C6A C7A C1A	77.44 (16)
C6 O2 C5 C4	108.72 (14)	C6A O2A C5A C4A	108.43 (14)
C7 C1 C2 C3	-8.4 (2)	C7A C1A C2A C3A	8.4 (2)
C7 C1 C2 C8	66.10 (18)	C7A C1A C2A C8A	-67.38 (19)
C8 C2 C3 C4	108.36 (15)	C8A C2A C3A C4A	107.82 (15)
C8 C3 C4 O1	108.58 (15)	C8A C3A C4A O1A	110.24 (14)
C8 C3 C4 C5	126.38 (14)	C8A C3A C4A C5A	129.64 (14)
C9 N1 C1 C2	84.47 (17)	C9A N1A C1A C2A	107.20 (15)
C9 N1 C1 C7	-46.48 (18)	C9A N1A C1A C7A	121.27 (14)
C9 N1 C10 O5	179.20 (14)	C9A N1A C10A O5A	178.54 (13)
C9 N1 C10 C12	0.01 (15)	C9A N1A C10A C12A	-0.66 (16)
C9 C11 C12 C10	0.86 (15)	C9A C11A C12A C10A	0.84 (15)
C9 C11 C12 C13	178.85 (13)	C9A C11A C12A C13A	177.36 (13)
C9 C11 C16 C15	178.38 (14)	C9A C11A C16A C15A	177.06 (14)
C10 N1 C1 C2	-98.01 (15)	C10A N1A C1A C2A	-83.82 (17)
C10 N1 C1 C7	131.04 (13)	C10A N1A C1A C7A	47.71 (18)
C10 N1 C9 O4	179.43 (14)	C10A N1A C9A O4A	178.90 (14)
C10 N1 C9 C11	0.50 (15)	C10A N1A C9A C11A	1.15 (16)
C10 C12 C13 C14	179.27 (14)	C10A C12A C13A C14A	177.97 (14)
C11 C12 C13 C14	0.4 (2)	C11A C12A C13A C14A	-0.2 (2)
C12 C11 C16 C15	-0.4 (2)	C12A C11A C16A C15A	-0.4 (2)
C12 C13 C14 C15	-0.7 (2)	C12A C13A C14A C15A	-0.3 (2)
C13 C14 C15 C16	0.4 (2)	C13A C14A C15A C16A	0.5 (2)
C14 C15 C16 C11	0.1 (2)	C14A C15A C16A C11A	-0.2 (2)

C16 C11 C12 C10 179.89 (13)
 C16 C11 C12 C13 0.2 (2)

C16A C11A C12A C10A 178.78 (13)
 C16A C11A C12A C13A 0.6 (2)

Table 8 Hydrogen Atom Coordinates ($\text{\AA}\times 10^4$) and Isotropic Displacement Parameters ($\text{\AA}^2\times 10^3$) for don1y5.

Atom	<i>x</i>	<i>y</i>	<i>z</i>	U(eq)
H1	210 (30)	2630 (20)	-2501 (13)	47 (6)
H3	6420 (30)	930 (20)	-327 (14)	50 (6)
H1A	3689	3836	-298	24
H2	698	4384	-437	27
H3A	-358	3708	-1484	28
H4	1692	1151	-1309	28
H5	3368	3259	-2309	28
H6	5522	3190	-1419	26
H7	3446	1121	-532	24
H8A	-123	1593	-219	33
H8B	-1629	2922	-279	33
H13	3272	4283	2561	29
H14	2750	2769	3646	32
H15	1963	629	3570	33
H16	1700	-106	2412	29
H1AA	10220 (40)	4550 (30)	6614 (17)	78 (9)
H3AA	4600 (30)	4180 (30)	4359 (15)	56 (7)
H1AB	6376	1231	5099	25
H2A	9254	649	5374	27
H3AB	10188	1656	6334	27
H4A	8457	4247	5803	26
H5A	6488	2576	6975	27
H6A	4423	2377	6083	28
H7A	6718	4054	5023	25
H8AA	11771	1933	5133	33
H8AB	10445	3312	4881	33
H13A	8611	4464	2164	29
H14A	8031	3557	1088	33
H15A	6978	1442	1176	32
H16A	6425	173	2345	28

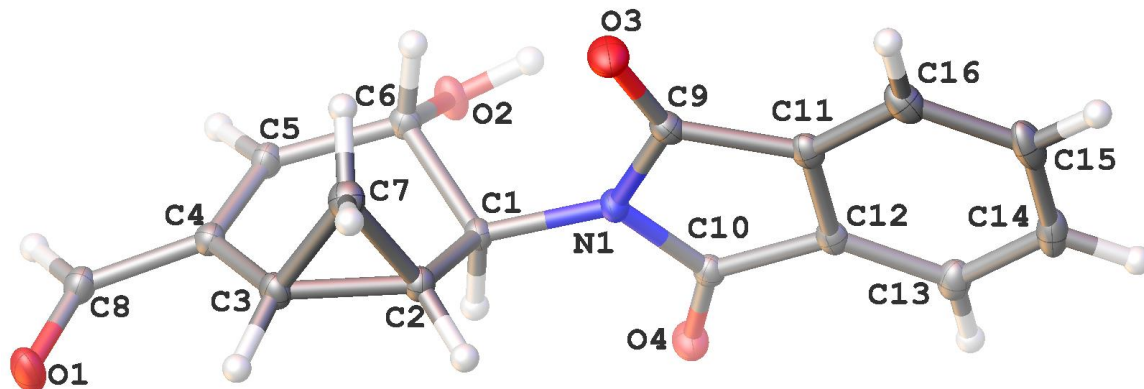


Table 1 Crystal data and structure refinement for (±)-II-58.

Identification code	don1z
Empirical formula	C ₁₆ H ₁₃ NO ₄
Formula weight	283.27
Temperature/K	100.00(10)
Crystal system	monoclinic
Space group	C2/c
a/Å	14.7396(2)
b/Å	8.13114(12)
c/Å	21.9186(3)
α/°	90.00
β/°	104.2876(16)
γ/°	90.00
Volume/Å ³	2545.69(7)
Z	8
ρ _{calc} /mm ³	1.478
m/mm ⁻¹	0.107
F(000)	1184.0
Crystal size/mm ³	0.2983 × 0.1942 × 0.1143
2θ range for data collection	6.04 to 58°
Index ranges	-19 ≤ h ≤ 20, -10 ≤ k ≤ 10, -29 ≤ l ≤ 29
Reflections collected	14590
Independent reflections	3106[R(int) = 0.0264]
Data/restraints/parameters	3106/0/195
Goodness-of-fit on F ²	1.085
Final R indexes [I ≥ 2σ (I)]	R ₁ = 0.0404, wR ₂ = 0.0942
Final R indexes [all data]	R ₁ = 0.0466, wR ₂ = 0.0982

Largest diff. peak/hole / e Å⁻³ 0.38/-0.24

Table 2 Fractional Atomic Coordinates ($\times 10^4$) and Equivalent Isotropic Displacement Parameters ($\text{\AA}^2 \times 10^3$) for don1z. U_{eq} is defined as 1/3 of the trace of the orthogonalised U_{IJ} tensor.

Atom	x	y	z	U(eq)
O1	1235.1 (7)	2548.0 (15)	3312.2 (5)	23.8 (3)
O2	4301.5 (7)	-1803.5 (13)	3186.5 (5)	17.7 (2)
O3	6019.3 (7)	2399.6 (14)	3282.7 (5)	21.7 (3)
O4	5646.3 (7)	-1276.0 (13)	4788.5 (5)	17.3 (2)
N1	5571.9 (8)	612.2 (15)	3984.1 (5)	12.5 (2)
C1	4546.9 (9)	746.4 (17)	3792.9 (6)	12.2 (3)
C2	4234.2 (9)	2498.5 (17)	3839.7 (7)	13.7 (3)
C3	3216.2 (10)	2852.6 (18)	3530.6 (7)	15.2 (3)
C4	2669.8 (10)	1476.8 (18)	3180.5 (6)	14.5 (3)
C5	3076.7 (10)	151.0 (18)	2994.9 (6)	15.4 (3)
C6	4122.6 (9)	-80.2 (17)	3153.3 (7)	14.1 (3)
C7	3995.1 (10)	3626.0 (18)	3282.8 (7)	17.3 (3)
C8	1644.6 (10)	1505.7 (19)	3082.8 (7)	17.3 (3)
C9	6212 (1)	1533.6 (17)	3746.1 (7)	14.3 (3)
C10	6027.4 (9)	-326.4 (17)	4506.4 (6)	12.9 (3)
C11	7149.4 (10)	1208.0 (17)	4178.9 (7)	14.5 (3)
C12	7035.7 (9)	100.8 (17)	4635.7 (7)	13.5 (3)
C13	7779.1 (10)	-422.8 (19)	5112.8 (7)	17.6 (3)
C14	8658.9 (10)	224.1 (19)	5119.2 (8)	21.0 (3)
C15	8778.8 (10)	1323.9 (19)	4660.1 (8)	21.4 (3)
C16	8020.3 (10)	1836.2 (18)	4177.4 (7)	18.9 (3)

Table 3 Anisotropic Displacement Parameters ($\text{\AA}^2 \times 10^3$) for don1z. The Anisotropic displacement factor exponent takes the form: $-2\pi^2[h^2a^*2U_{11}+...+2hka \times b \times U_{12}]$

Atom	U_{11}	U_{22}	U_{33}	U_{23}	U_{13}	U_{12}
O1	15.0 (5)	28.5 (6)	27.2 (6)	-7.8 (5)	3.8 (4)	5.6 (4)
O2	13.2 (5)	13.6 (5)	25.8 (6)	-4.2 (4)	3.9 (4)	2.6 (4)
O3	20.5 (5)	25.3 (6)	20.3 (5)	7.9 (5)	7.1 (4)	0.2 (4)
O4	15.6 (5)	17.7 (5)	19.1 (5)	5.2 (4)	5.1 (4)	0.1 (4)
N1	10.1 (5)	13.9 (6)	13.5 (6)	0.9 (4)	2.7 (4)	-0.2 (4)

C1	9.4 (6)	13.9 (6)	12.9 (6)	0.1 (5)	2.3 (5)	0.6 (5)
C2	12.4 (6)	13.3 (7)	14.5 (6)	-0.5 (5)	1.9 (5)	0.8 (5)
C3	13.5 (6)	14.4 (7)	17.3 (7)	-1.7 (5)	3.1 (5)	3.1 (5)
C4	13.2 (6)	17.4 (7)	12.3 (6)	-0.4 (5)	1.7 (5)	2.5 (5)
C5	12.1 (6)	18.4 (7)	14.2 (6)	-2.5 (5)	0.6 (5)	0.3 (5)
C6	13.4 (6)	14.2 (7)	14.5 (6)	-2.3 (5)	3.1 (5)	2.0 (5)
C7	17.5 (7)	14.8 (7)	19.1 (7)	2.6 (6)	3.6 (5)	1.5 (5)
C8	14.5 (6)	20.5 (7)	15.2 (7)	-1.8 (6)	0.1 (5)	2.1 (6)
C9	13.5 (6)	13.9 (7)	16.6 (7)	-1.6 (5)	5.7 (5)	-0.7 (5)
C10	12.7 (6)	12.5 (6)	13.5 (6)	-1.7 (5)	2.8 (5)	1.7 (5)
C11	13.7 (6)	12.5 (6)	17.5 (7)	-3.6 (5)	4.4 (5)	0.7 (5)
C12	12.4 (6)	11.6 (6)	16.6 (7)	-3.7 (5)	3.8 (5)	0.2 (5)
C13	15.6 (7)	16.3 (7)	18.8 (7)	-3.3 (6)	0.7 (5)	2.4 (5)
C14	13.9 (7)	18.7 (7)	26.9 (8)	-7.6 (6)	-1.8 (6)	2.9 (6)
C15	11.6 (6)	18.3 (7)	34.0 (9)	-8.7 (6)	5.3 (6)	-2.2 (6)
C16	16.7 (7)	14.8 (7)	26.7 (8)	-3.6 (6)	8.5 (6)	-2.0 (6)

Table 4 Bond Lengths for don1z.

Atom	Atom	Length/Å	Atom	Atom	Length/Å
O1	C8	1.2187 (18)	C3	C7	1.522 (2)
O2	C6	1.4243 (17)	C4	C5	1.345 (2)
O3	C9	1.2107 (18)	C4	C8	1.4732 (19)
O4	C10	1.2107 (17)	C5	C6	1.5061 (19)
N1	C1	1.4689 (17)	C9	C11	1.4941 (19)
N1	C9	1.4023 (17)	C10	C12	1.4839 (19)
N1	C10	1.4015 (17)	C11	C12	1.387 (2)
C1	C2	1.5087 (19)	C11	C16	1.382 (2)
C1	C6	1.5413 (19)	C12	C13	1.382 (2)
C2	C3	1.5139 (19)	C13	C14	1.396 (2)
C2	C7	1.4975 (19)	C14	C15	1.390 (2)
C3	C4	1.478 (2)	C15	C16	1.400 (2)

Table 5 Bond Angles for don1z.

Atom	Atom	Atom	Angle/°	Atom	Atom	Atom	Angle/°
C9	N1	C1	126.38 (12)	C2	C7	C3	60.17 (9)
C10	N1	C1	121.68 (11)	O1	C8	C4	123.08 (14)
C10	N1	C9	111.36 (11)	O3	C9	N1	125.65 (13)
N1	C1	C2	111.14 (11)	O3	C9	C11	128.64 (13)
N1	C1	C6	112.65 (11)	N1	C9	C11	105.70 (12)
C2	C1	C6	114.29 (11)	O4	C10	N1	125.13 (12)
C1	C2	C3	115.78 (12)	O4	C10	C12	128.38 (13)
C7	C2	C1	122.49 (12)	N1	C10	C12	106.49 (11)
C7	C2	C3	60.72 (9)	C12	C11	C9	108.42 (12)
C2	C3	C7	59.11 (9)	C16	C11	C9	130.30 (14)
C4	C3	C2	116.19 (12)	C16	C11	C12	121.28 (13)
C4	C3	C7	119.33 (12)	C11	C12	C10	107.92 (12)
C5	C4	C3	122.51 (13)	C13	C12	C10	129.95 (13)
C5	C4	C8	119.14 (13)	C13	C12	C11	122.13 (13)
C8	C4	C3	118.12 (12)	C12	C13	C14	116.90 (14)
C4	C5	C6	122.54 (13)	C15	C14	C13	121.27 (14)
O2	C6	C1	110.74 (11)	C14	C15	C16	121.21 (14)
O2	C6	C5	107.49 (11)	C11	C16	C15	117.20 (14)
C5	C6	C1	108.53 (11)				

Table 6 Hydrogen Bonds for don1z.

D	H	A	d(D-H)/Å	d(H-A)/Å	d(D-A)/Å	D-H-A/°
O2	H2	O1 ¹	0.91 (2)	1.94 (2)	2.8442 (14)	174 (2)

¹1/2+X,-1/2+Y,+Z**Table 7 Torsion Angles for don1z.**

A	B	C	D	Angle/°	A	B	C	D	Angle/°
O3	C9	C11	C12	178.35 (15)	C4	C5	C6	C1	31.07 (19)
O3	C9	C11	C16	2.4 (3)	C5	C4	C8	O1	169.66 (14)
O4	C10	C12	C11	178.34 (14)	C6	C1	C2	C3	38.99 (16)
O4	C10	C12	C13	-2.3 (3)	C6	C1	C2	C7	-31.36 (18)
N1	C1	C2	C3	167.85 (11)	C7	C2	C3	C4	109.99 (14)

N1 C1 C2 C7	97.51 (15)	C7 C3 C4 C5	50.1 (2)
N1 C1 C6 O2	63.26 (15)	C7 C3 C4 C8	135.43 (14)
N1 C1 C6 C5	178.97 (11)	C8 C4 C5 C6	171.63 (13)
N1 C9 C11 C12	1.52 (15)	C9 N1 C1 C2	-53.34 (17)
N1 C9 C11 C16	177.76 (14)	C9 N1 C1 C6	76.40 (17)
N1 C10 C12 C11	-2.35 (15)	C9 N1 C10 O4	177.24 (13)
N1 C10 C12 C13	177.00 (14)	C9 N1 C10 C12	3.43 (15)
C1 N1 C9 O3	-11.9 (2)	C9 C11 C12 C10	0.51 (15)
C1 N1 C9 C11	168.21 (12)	C9 C11 C12 C13	178.91 (13)
C1 N1 C10 O4	11.0 (2)	C9 C11 C16 C15	178.41 (14)
C1 N1 C10 C12	168.36 (11)	C10 N1 C1 C2	117.14 (14)
C1 C2 C3 C4	-4.41 (18)	C10 N1 C1 C6	113.11 (14)
C1 C2 C3 C7	114.40 (14)	C10 N1 C9 O3	176.77 (14)
C1 C2 C7 C3	103.53 (14)	C10 N1 C9 C11	-3.10 (15)
C2 C1 C6 O2	168.63 (11)	C10 C12 C13 C14	178.84 (14)
C2 C1 C6 C5	-50.86 (15)	C11 C12 C13 C14	0.4 (2)
C2 C3 C4 C5	-17.6 (2)	C12 C11 C16 C15	-0.8 (2)
C2 C3 C4 C8	156.90 (13)	C12 C13 C14 C15	-0.9 (2)
C3 C4 C5 C6	2.8 (2)	C13 C14 C15 C16	0.6 (2)
C3 C4 C8 O1	-5.0 (2)	C14 C15 C16 C11	0.3 (2)
C4 C3 C7 C2	104.70 (14)	C16 C11 C12 C10	179.86 (13)
C4 C5 C6 O2	150.88 (13)	C16 C11 C12 C13	0.4 (2)

Table 8 Hydrogen Atom Coordinates ($\text{\AA} \times 10^4$) and Isotropic Displacement Parameters ($\text{\AA}^2 \times 10^3$) for don1z.

Atom	x	y	z	U(eq)
H2	4921 (15)	-1960 (30)	3207 (9)	33 (5)
H1	4309	109	4112	15
H2A	4488	3046	4255	16
H3	2879	3595	3765	18

H5	2690	-672	2754	18
H6	4388	427	2819	17
H7A	4090	3213	2878	21
H7B	4117	4815	3358	21
H8	1286	673	2829	21
H13	7695	-1187	5422	21
H14	9186	-94	5444	25
H15	9387	1736	4674	26
H16	8101	2584	3862	23